DISSERTATION

GEOGRAPHICALLY-RESOLVED LIFE CYCLE ASSESSMENT AND TECHNO-ECONOMIC ANALYSIS OF ENGINEERED CLIMATE SOLUTIONS WITH AN INNOVATIVE FRAMEWORK FOR DECISION SUPPORT

Submitted by

Jonah Michael Greene

Department of Systems Engineering

In partial fulfillment of the requirements

For the Degree of Doctor of Philosophy

Colorado State University

Fort Collins, Colorado

Fall 2024

Doctoral Committee:

Advisor: Jason C. Quinn

Kenneth Reardon
Tim Coburn
Daniel Baker

ABSTRACT

GEOGRAPHICALLY-RESOLVED LIFE CYCLE ASSESSMENT AND TECHNO-ECONOMIC ANALYSIS OF ENGINEERED CLIMATE SOLUTIONS WITH AN INNOVATIVE FRAMEWORK FOR DECISION SUPPORT

The urgent challenge of addressing climate change requires a thorough evaluation of engineered solutions to ensure they are both economically viable and environmentally sustainable. This dissertation performs a comprehensive assessment of two key climate technologies: microalgae biorefineries for biofuel production and anaerobic digestion (AD) systems for reducing greenhouse gas (GHG) emissions on dairy farms. Using high-resolution life cycle assessment (LCA) and techno-economic analysis (TEA), it provides detailed insights into the sustainability performance of these technologies. In addition, this work goes further by introducing a decision-support framework that improves the interpretation of LCA and TEA results, enhancing decision-makers' ability to form sustainable policies and implement actionable outcomes that drive the transition to green energy solutions.

The first segment of this dissertation integrates high-resolution thermal and biological modeling with LCA and TEA to evaluate and compare two different microalgae biorefinery configurations targeting renewable diesel (RD) and sustainable aviation fuel (SAF) production in the United States. A dynamic engineering process model captures mass and energy balances for biomass growth, storage, dewatering, and conversion with hourly resolution. These configurations support facilities in remote areas and cultivation on marginal lands, enabling

large-scale biofuel production. The two pathways under examination share identical biomass production and harvesting assumptions but differ in their conversion processes. The first pathway evaluates hydrothermal liquefaction (HTL) to produce RD, while the second explores the Hydroprocessed Esters and Fatty Acids (HEFA) process to produce SAF. Results indicate that the Minimum Fuel Selling Price (MFSP) for RD could decrease from \$3.70-\$7.30 to \$1.50-\$4.10 per liter of gasoline equivalent, and for SAF from \$9.90-\$19.60 to \$2.20-\$7.30 per liter under future scenarios with increased lipid content and reduced CO_2 delivery costs. Optimization analyses reveal pathways to achieve an MFSP of \$0.75 per liter and 70% GHG emissions reductions compared to petroleum fuels for both pathways. Additional analysis covers the water footprint, land-use change emissions, and other environmental impacts, with a focus on strategic research and development investments to reduce production costs and environmental burdens from microalgae biofuels.

Beyond renewable transportation fuels, achieving a sustainable energy future will require innovations in the circular economy, such as waste-to-energy systems that reduce GHG emissions while simultaneously producing renewable energy. Accordingly, the second segment of this dissertation examines the GHG reduction potential of adopting AD technology on large-scale dairy farms across the contiguous United States. Regional and national GHG reduction estimates were developed through a robust life cycle modeling framework paired with sensitivity and uncertainty analyses. Twenty dairy configurations were modeled to capture key differences in housing and manure management practices, applicable AD technologies, regional climates, storage cleanout schedules, and land application methods. Monte Carlo uncertainty bounds suggest that AD adoption could reduce GHG emissions from the large-scale dairy industry by 2.45-3.52 million metric tons (MMT) of CO_2-equivalent (CO_2-eq) per year when biogas is used

solely in renewable natural gas programs, and as much as 4.53-6.46 MMT of CO_2-eq per year when combined heat and power is implemented as an additional biogas use case. At the farm level, AD technology may reduce GHG emissions from manure management systems by 58.1-79.8%, depending on the region. The study highlights the regional variations in GHG emissions from manure management strategies, alongside the challenges and opportunities surrounding broader AD adoption.

It is vital to confirm that engineered climate solutions offer real improvements and to identify key enhancements needed to replace existing technologies. This process hinges on effective policy and decision-making. To address these challenges, the final segment of this dissertation introduces the Environmental Comparison and Optimization Stakeholder Tool for Evaluating and Prioritizing Solutions (ECO-STEPS). ECO-STEPS offers a decision-support framework that utilizes outputs from LCA and TEA to help decision-makers evaluate and prioritize engineered climate solutions based on economic viability, environmental impacts, and resource use. The tool's framework combines stakeholder rankings for key sustainability criteria with diverse statistical weighting methods, offering decision support aligned with long-term sustainability goals across various technology sectors. Applied to a biofuels case study, ECO-STEPS compares algae-based RD, soybean biodiesel (BD), corn ethanol, and petroleum diesel, using an expert survey to determine criteria rankings. Results indicate that soybean BD is a strong near-term solution for the biofuels sector, given its economic viability and relatively low environmental impacts. In contrast, corn ethanol, while economically competitive, demonstrates poor environmental performance across multiple sustainability themes. Algae-based RD emerges as a promising long-term option as ongoing research and development reduce costs. The results of this case study illustrate that ECO-STEPS provides a flexible and comprehensive framework

for stakeholders to navigate complex decision-making processes in the pursuit of sustainable climate solutions.

In conclusion, the integration of high-resolution LCA, TEA, and a stakeholder-driven decision-support framework in this dissertation presents a comprehensive approach to evaluating engineered climate solutions. The results from these studies provide geographically resolved insights into the sustainability performance of key climate technologies, offering actionable pathways for optimizing biofuel production, reducing GHG emissions, and supporting sustainable decision-making to advance the transition to a green economy.

ACKNOWLEDGEMENTS

First, I would like to extend my deepest gratitude to my advisor, Dr. Jason Quinn, for giving me this opportunity and for being an invaluable mentor and friend throughout my journey in both research and life. I am also deeply thankful to my other committee members for their time, support, and guidance during my education and research. In particular, I would like to thank Dr. Kenneth Reardon for our thought-provoking discussions, insightful feedback, and his compliments on my work, which greatly enhanced my understanding of algae systems. I also want to express my gratitude to Dr. Daniel Baker for being an inspiring professor, igniting my passion for engineering, and offering both personal and professional guidance over the years. My thanks also go to Dr. Tim Coburn, who broadened my perspective on the energy transition and helped me consider this field's vital environmental and social justice aspects.

A heartfelt thanks to my incredible research colleagues—Jack Smith, Dr. Braden Limb, Dr. Noah Horesh, Garrett Cole, Brooke Silagy, Dr. Hailey Summers, Ashley Ryland, Dr. Evan Sproul, and Dr. Peter Chen—for their friendship, countless hours of presentations, and invaluable feedback. Together, you have strengthened our research group. A special thanks to Dr. David Quiroz, whose contributions to the modeling work were pivotal in completing our comprehensive algae biorefinery assessment. I would also like to acknowledge my collaborators, including the various researchers and institutions involved in the research projects that have contributed to the development of the models and data informing this work.

I am deeply grateful to my wife, Tara, my parents, David and Donna, and my brother Josh for their unwavering support and encouragement throughout this journey, as well as to all

my incredible friends. Each of you has played a vital role in shaping the person I am today and has given me the strength to pursue my dreams.

Finally, I would like to thank the Department of Energy's Bioenergy Technologies Office (BETO) and Dairy Management Inc. for funding my research. None of this work would have been possible without their support.

TABLE OF CONTENTS

CHAPTER 1: INTRODUCTION

The escalating climate change crisis stands as the defining challenge of our time, urgently demanding coordinated global action to avert catastrophic consequences. From intensifying heatwaves to unprecedented natural disasters, the ongoing rise in greenhouse gas (GHG) emissions is already wreaking havoc on ecosystems and human societies alike [1]. To avoid breaching the 1.5°C threshold set by the Paris Agreement, it is not only imperative to curb carbon dioxide (CO_2) emissions but also to tackle powerful, short-lived climate pollutants like methane [1]. Achieving this will require transformative decarbonization efforts across critical sectors such as road transportation, aviation, and agriculture. This dissertation focuses on two specific solutions to address emissions in these sectors: the production of renewable fuels from microalgae and the adoption of anaerobic digestion (AD) technology on dairy farms. These solutions are evaluated through detailed, geographically-resolved systems modeling integrated with techno-economic analysis (TEA), life cycle assessment (LCA), and optimization. Furthermore, a novel decision-support framework is introduced to guide the strategic deployment of climate solutions considering economic viability, environmental impacts, and resource consumption.

The transportation sector is responsible for approximately 28.5% of total U.S. GHG emissions, with medium- to heavy-duty trucks and aviation contributing 23.1% and 8.6% of transportation-related emissions, respectively [2]. Given the sector's reliance on petroleum-based fuels, transitioning to renewable alternatives is essential to achieving significant emissions reductions. Sustainable biofuels, including renewable diesel (RD) and sustainable aviation fuel (SAF), are particularly promising for decarbonizing transportation due to their compatibility with

existing infrastructure. Among the various biofuel feedstocks, microalgae offer several advantages, including high productivity, the ability to grow on non-arable land, and the potential to recycle nutrients [3–6]. However, significant challenges remain, particularly in achieving economic viability and reducing the environmental impacts of large-scale algae cultivation and fuel production. Through high-resolution spatiotemporal modeling integrated with TEA, LCA, and optimization, this dissertation offers a robust evaluation of two distinct microalgae-to-fuel pathways targeting the production of RD and SAF. By doing so, this work provides a detailed understanding of the trade-offs between fuel cost, environmental impact, and scalability while also identifying key areas for future research and development to improve the economic and environmental sustainability of algae-derived biofuels.

Beyond the transportation sector, the agricultural industry, particularly livestock farming, significantly contributes to global methane emissions. Methane, a GHG with a global warming potential 25 times greater than CO_2 over a 100-year period [7], is emitted in large quantities from manure management systems on dairy farms. In 2021, methane emissions from dairy manure management in the U.S. totaled 35.9 million metric tons (MMT) of CO_2-equivalent, accounting for over 54.4% of all methane emissions from livestock manure and 4.9% of total U.S. methane emissions [2]. Reducing methane emissions from this sector is essential to achieving national and international climate targets. AD technology offers a proven solution for capturing methane emissions from dairy manure and converting them into biogas, which can be used to produce renewable natural gas (RNG) or combined heat and power (CHP) [8–15]. Despite its potential, AD adoption in the U.S. dairy industry is shaped by regional variations in farm size, manure management practices, and economic feasibility. This dissertation comprehensively analyzes the GHG reduction potential of adopting AD technologies on large-scale dairy farms across the

contiguous United States. By modeling 20 different dairy configurations and capturing variations in manure management, climate, and biogas use, this research offers a robust, geographically-resolved assessment of the environmental and economic benefits of AD adoption while also highlighting the challenges and opportunities for scaling up its deployment nationwide.

In addition to these two climate solutions, this dissertation introduces the Environmental Comparison and Optimization Stakeholder Tool for Evaluating and Prioritizing Solutions (ECO-STEPS), a decision-support framework designed to assist stakeholders in selecting the most sustainable and economically viable technologies. The complexity of balancing multiple sustainability criteria—such as GHG emissions, resource use, and economic cost—makes it difficult for policymakers and industry leaders to determine the optimal path forward. ECO-STEPS addresses this challenge by integrating the outputs of LCA and TEA with stakeholder rankings for key sustainability criteria, providing a flexible and transparent framework for decision-making. In a case study comparing algae-based RD, soybean biodiesel, and corn ethanol, the tool demonstrates its utility in guiding biofuel technology choices, revealing trade-offs between economic performance, environmental impact, and long-term sustainability. By applying ECO-STEPS, stakeholders can make more informed decisions about which technologies to prioritize based on a comprehensive assessment of their environmental and economic impacts.

This dissertation aims to provide a geographically-resolved and multi-faceted evaluation of key engineered climate solutions, offering insights into the economic viability and environmental sustainability of technologies that can drive decarbonization in the transportation and agricultural sectors. Through the integration of high-resolution thermal and biological modeling, LCA, and TEA, this work not only advances the understanding of key climate

solutions but attempts to assist stakeholders in navigating the complex trade-offs involved in adopting these technologies. By addressing the need for high-resolution data and comprehensive sustainability assessments, this research contributes to the development of climate solutions that balance economic viability with environmental integrity, helping to pave the way toward a sustainable, low-carbon future.

CHAPTER 2: GEOGRAPHICALLY-RESOLVED TECHNO-ECONOMIC AND LIFE CYCLE ASSESSMENT COMPARING MICROALGAE-BASED RENEWABLE DIESEL AND SUSTAINABLE AVIATION FUEL IN THE UNITED STATES[1]

2.1. Introduction

In 2021, the transportation sector accounted for 28.5% of total U.S. greenhouse gas (GHG) emissions, with medium-to-heavy duty trucks and aviation contributing 23.1% and 8.6% of transportation-related emissions, respectively [2]. Transitioning these vehicles to sustainable fuels like renewable diesel (RD) and sustainable aviation fuel (SAF) is crucial. Major airlines such as Alaska Airlines, American Airlines, British Airways, Finnair, Japan Airlines, and Qatar Airways have announced initiatives to invest in SAF production to reduce dependence on petroleum-based jet fuel and meet company climate goals [16].

Renewable fuels can be produced using various feedstocks and technologies. First-generation biofuels rely on food crops like soybeans and corn, while second-generation biofuels use non-food biomass such as woody materials, energy grasses, and crop residues. However, both demand significant land and water, potentially causing deforestation and ecosystem damage with minor reductions in GHG emissions [17]. Third-generation biofuels from microalgae offer a sustainable alternative by thriving on marginal lands with higher oil yields per hectare and the ability to recycle water [3]. Microalgae's adaptability allows for optimized growth conditions and enhanced lipid production for fuels [18].

[1]This chapter was submitted for publication as a peer-reviewed journal article: Greene JM, Quiroz D, Limb BJ, Quinn JC. Geographically-Resolved Techno-Economic and Life Cycle Assessment Comparing Microalgae-Based Renewable Diesel and Sustainable Aviation Fuel in the United States (Manuscript in Review at Environmental Science and Technology)

Literature on techno-economic analysis (TEA) and life cycle assessment (LCA) of RD and SAF from microalgae is comprehensive yet fragmented. Many studies focus solely on either economic performance [19–23] or environmental life cycle impacts [24–28]. Integrated TEA and LCA studies exist, using advanced models and providing detailed results, but often focus on a single fuel type [3,4,29–32] or location [33–35]. Findings emphasize feedstock production and site selection [36,37], the impact of algal composition on sustainability [38], and the need for broader environmental metrics beyond global warming potential (GWP) [39–41]. Previous studies often ignore the economic implications of CO_2 sourcing and utilization in open raceway ponds, assuming seamless integration with CO_2 point sources like flue gas [5,6,42]. Microalgae cultivation can utilize CO_2 from Direct Air Capture (DAC) technology, which is more scalable [43]. Understanding the economic and environmental impacts of this transition is crucial [44]. A gap remains in the literature for integrated TEA and LCA studies with detailed spatiotemporal modeling offering geographically resolved sustainability results for multiple algae-to-fuel pathways considering available resources and critical performance parameters.

This study introduces a multi-layered modeling framework to analyze the life cycle of converting algal biomass into transportation fuels, addressing both economic and environmental dimensions. Cultivation modeling utilizes a spatiotemporal growth model, validated against experimental data, with a 3-stage dewatering process and long-term storage to ensure a consistent biomass supply. Two downstream pathways are evaluated including conversion of algae into biocrude via hydrothermal liquefaction (HTL) with upgrading to RD and naphtha, and an alternative pathway with lipid extraction followed by SAF production through the Hydroprocessed Esters and Fatty Acids (HEFA) process. The impacts of algae composition and process efficiencies on sustainability are evaluated through two scenarios. The “Current

Scenario" addresses challenges in algae cultivation, including low carbon utilization efficiencies (CUE) and nutrient recycle rates, high carbon capture costs, and productivity losses from nutrient depletion. The "Future Scenario" targets improvements in CUE, reduced DAC costs, increased nutrient recovery, and lipid accumulation without nitrogen starvation. Optimization algorithms reveal pathways to reduce costs and emissions, focusing on improvements with the greatest returns. Additionally, water footprint, direct Land Use Change (dLUC) emissions, total fuel production potential, and environmental impact categories from the Tool for the Reduction and Assessment of Chemical and other Environmental Impacts (TRACI) [45] are explored. This integrated approach offers a granular perspective on the sustainability of key algae-to-fuel pathways.

2.2 Methods

A modular engineering process model was constructed providing the foundation for subsequent TEA and LCA. Within the process model a robust mass and energy balance quantifies the material inputs, energy use, and product outputs for all upstream and downstream processes including algae cultivation, dewatering, long-term anaerobic storage, and conversion to fuel via HTL or HEFA. A process flow diagram illustrating the modeled pathways is provided in Figure 1.

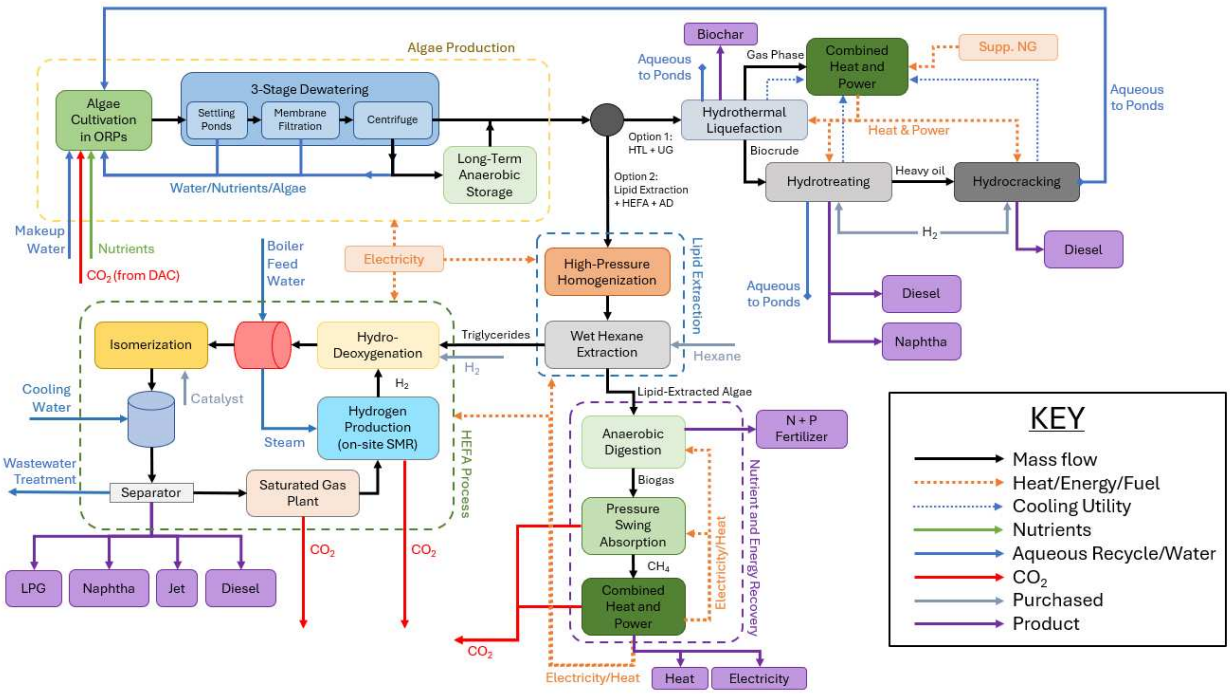

Figure 1: Process flow diagram showing the modeled pathways including Hydrothermal Liquefaction to produce renewable diesel and naphtha or lipid extraction with the Hydroprocessed Esters and Fatty Acids Process for the production of sustainable aviation fuel (ORP: Open Raceway Pond, DAC: Direct Air Capture, HTL: Hydrothermal Liquefaction, UG: Upgrading, HEFA: Hydroprocessed Esters and Fatty Acids, AD: Anaerobic Digestion, NG: Natural Gas, SMR: Steam Methane Reforming).

2.2.1 Facility Size and Layout

The facility size and layout were determined by adhering to benchmarks established in previous large-scale modeling studies. The facility encompasses 2023 wetted hectares (5000 acres), segmented into 4-hectare ponds, each measuring 670 m in length, 60 m in width, with a 20 cm depth as specified by Davis et al. [5]. The total area of the facility, including roadways, facilities, offices, on-site storage, and conversion facilities, extends to 3075 hectares [5]. The layout of water pipelines, the CO_2 storage sphere and delivery system, as well as harvesting channels and dewatering equipment, were also adopted from Davis et al. [5]. Consistent with other studies of a similar scale [3–5,46], the model assumes 330 operational days per year.

2.2.2 Spatiotemporal Growth Modeling

Algal cultivation was modeled in open-raceway ponds, chosen for their lower capital costs and energy demands compared to closed photobioreactors [6,47]. The biological growth model developed by Greene et al. [48] was used to simulate bulk algal growth rates, accounting for an hourly carbon fixation rate influenced by light, temperature, and dark respiration. The strain *Scenedesmus obliquus* (UTEX 393) was selected, due to its demonstrated performance in outdoor cultivation trails and potential for biofuels applications [49]. The model was validated against experimental data for UTEX 393 with an average error of -4.6 ± 8.1% over 12 harvests in a 30-day trial at the Arizona Center for Algal Innovation [49]. Following validation, algae productivity was evaluated across a weather grid covering 5,626 locations across the U.S., drawing weather data from the NREL National Solar Radiation Database (NSRDB) [50]. Correlations determining the decrease in productivity from nutrient starvation were developed using outdoor cultivation data for UTEX 393 from the Development of Integrated Screening, Cultivar Optimization, and Verification Research (DISCOVR) consortia [18]. The model captures hourly flowrates across the facility, estimating the consumption of energy and materials including media pumping, paddlewheel mixing, and the use of freshwater, ammonia, diammonium phosphate (DAP), and CO_2. Further details on the growth model construction and validation can be found in the works of Greene et al. [48] and Quiroz et al. [51].

2.2.3 Open-Raceway Pond Thermal Model

The pond temperature, a crucial factor in the biological growth model, was estimated on an hourly basis using the thermal pond model developed by Quiroz et al. [51]. The model performs an energy balance of the system by accounting for direct and diffuse radiation, long-wave radiation, pond re-radiation, convection at the pond surface, evaporation and evaporative

cooling, and thermal inflow from makeup water. These factors are influenced by the hourly weather conditions, the depth of the culture, and the wetted surface area of the facility. The thermal model has demonstrated temperature predictions with an accuracy of −0.96 ± 2.72 °C and evaporation rates with 1.46 ± 5.92% accuracy [51]. For a more comprehensive understanding and validation of this thermal model, readers are directed to the works of both Greene et al. [48] and Quiroz et al. [51].

2.2.4 Dewatering and Long-Term Anaerobic Storage

Dewatering to 20% total suspended solids was modeled based on the three-stage process outlined in Davis and Wiatrowski [52] which utilizes low-energy settling ponds followed by hollow fiber membrane filtration and centrifugation. In some locations, large variations in seasonal biomass productivity result in problematic fluctuations in the total flowrate exiting the dewatering facility and entering the biorefinery. Long-term (up to 6 months) anaerobic storage was utilized as a mechanism to adjust for seasonal variability and provide a constant year-round flowrate to the biorefinery with minimal biomass losses. The number of anaerobic tanks required, degradation losses, and compositional changes associated with long-term storage were modeled based on previous work from Wendt et al. [53]. Additional information regarding the anaerobic storage module is provided in Appendix A.

2.2.5 Algae Composition

Algae biomass compositions for the Current and Future scenarios were based on *Scenedesmus acutus* (LRB-AP 0401) compositions corresponding to medium and high nitrogen starvation levels from Davis et al. [5]. The Current Scenario assumes a biomass composition of 13.2 wt% proteins, 52.8 wt% carbohydrates, 27.4 wt% lipids (as Fatty Acid Methyl Esters or FAME), and 6.6% ash based on the mid-harvest *Scenedesmus* composition from Davis et al. [5]

and assumes a decrease in productivity resulting from nutrient starvation to achieve this composition. The Future Scenario assumes advancements in genetic engineering could enable high lipid content without compromising productivity. The composition for the Future scenario was based on the late-harvest *Scenedesmus* composition from Davis et al. [42] and assumes 9 wt% proteins, 42.1 wt% carbohydrates, 41.2 wt% lipids (FAME), and 7.7 wt% ash without any losses in biomass productivity. In all scenarios, the algae composition was adjusted to account for the loss of carbohydrates during anaerobic storage [53]. The content of nitrogen (N), phosphorus (P), and carbon (C) in the algae were obtained from previous modeling studies [3,5,18,42,54] and used to estimate the consumption of ammonia, DAP, and CO_2 during cultivation.

2.2.6 CO_2 Sourcing

This study critically examines assumptions in large-scale modeling studies regarding CO_2 sourcing and utilization. Previous studies [3,5,6,42,55] often assume CO_2 from industrial point sources, but the microalgae industry typically transports CO_2 as compressed liquid, leading to significant environmental impacts [56]. While previous studies [3–5] assume high CO_2 utilization efficiencies (up to 90%), real-world efficiencies range from 7% to 90%, with a median of 66% [57,58]. Lower efficiencies increase GHG burdens and costs when CO_2 is captured and compressed or sourced from underground reservoirs. The Current and Future Scenarios assume 65% and 90% CO_2 utilization efficiencies, respectively.

Scalability is another issue with point source CO_2 Quinn et al. [59] show reliance on point source CO_2 limits production volumes and fails to meet national fuel production targets. To align with future GHG and fuel production targets, CO_2 must be sourced from DAC, either with on-site DAC modules feeding directly into algal cultures, off-site DAC with short-distance

pipeline delivery, or direct capture in ponds [60]. The Current Scenario assumes a DAC CO_2 cost of \$230 tonne^{-1}, reflecting the average cost of DAC under the current state of technology [61], while the Future Scenario considers cost reductions to \$50 tonne^{-1}.

2.2.7 Water Conditions for Cultivation

Sustainable algae cultivation requires careful consideration of water sources. While freshwater use can be reduced through saline or wastewater cultivation, these configurations have substantial energy demands for water pumping and conditioning and may limit site selection and scalability [59,62]. This study assumes freshwater cultivation to avoid the energy requirements for seawater pumping, support industry scaleup, and provide flexibility in facility siting to maximize the utilization of marginal lands.

2.2.8 Hydrothermal Liquefaction and Fuel Upgrading

Conversion of algae biomass into biocrude via HTL and upgrading of biocrude to RD via hydrotreating and hydrocracking were modeled using the open-source HTL model from Chen and Quinn [4]. Algal composition was used to estimate HTL phase yields yield with the additive phase-yield model from Leow et al. [63]. The total outflow RD and naphtha was converted to liters of gasoline equivalent (LGE) based on the energy content of each fuel product (LHV basis) in relation to the energy content of gasoline [4]. In addition to the four main HTL phases, the model from Chen and Quinn [4] estimates the recovery of ammonia and DAP in the aqueous phase, which can be recycled to algae ponds to reduce nutrient inputs. HTL solids are treated as zero-burden biochar and assumed to be sold at a low value (\$0.10 per kg) to be used as soil amendments. The recovery efficiencies for nutrients and biochar (HTL solids) were set at 60% and 90% for Current and Future Scenarios, respectively.

2.2.9 Sustainable Aviation Fuel Pathway

A pathway was developed for converting algal biomass into SAF, focusing on three stages: lipid extraction, lipid conversion with the HEFA process, and recovery of energy and nutrients from Lipid-Extracted Algae (LEA). The initial stage involved high-pressure homogenization (HPH), modeled after Kang et al. [64], incorporating insights from their study on pressure settings and the number of passes needed to rupture the cell wall. The Current Scenario assumes two passes at high pressure (1500 psi), and the Future Scenario assumes one pass at low pressure (400 psi).

Lipids were extracted through wet hexane extraction based on Frank et al. [65], assuming a solvent-to-biomass ratio of 1.8 and a hexane loss of 5.2 g per kg of oil, with extraction efficiencies of 90% and 99% for the Current and Future Scenarios, respectively. Capital costs for wet hexane extraction were based on Delrue et al. [66]. The HEFA process was modeled based on Pearlson et al. [23], assuming similar requirements for algae oil as soybean oil [67]. Hydrogen was assumed to be purchased externally. Pearlson et al. [23] provided two yield profiles with the "Maximum Jet" profile assumed for SAF production. Equipment sizing and costing for the hydrotreater, isomerizer, gas processing plant, and storage were based on Gary et al. [68] and supplemented by Chen and Quinn [4] with further details in Appendix A.

2.2.10 Nutrient and Energy Recovery from Lipid-Extracted Biomass

The LEA remaining after lipid extraction was sent through anaerobic digestion (AD) to recover nutrients and energy. The AD model, informed by Frank et al. [65], assumed a methane yield of 0.3 L CH_4/g of total solids with a 67% methane composition. Costs for the AD process were derived from Frank et al. [65] and Zamalloa et al. [69]. Nitrogen and phosphorus recovered from AD digestate were considered for sale as fertilizers, earning co-product revenue and GHG

credits. The biogas was cleaned and upgraded through a pressure-swing absorption (PSA) process, with emissions accounted for based on Börjesson and Berglund [70]. The cleaned biogas was directed to an on-site combined heat and power (CHP) unit, providing process electricity and heat for AD, with performance and emissions parameters from Frank et al. [65] and costs from Zamalloa et al. [69]. Critical inputs and costing functions are provided in Appendix A.

2.2.11 Techno-Economic Analysis

TEA was used to evaluate the economic viability of each fuel conversion pathway by quantifying all capital and operational costs for each simulation location and integrating them into a 30-year discounted cash flow rate of return (DCFROR) model. Capital costs for cultivation, dewatering, anaerobic storage, HTL, HEFA, AD, PSA, and CHP were sourced from previous studies [3–5,23,52,53,64,68,69]. Operational costs were calculated using the dynamic process model, with commodity costs informed by Quiroz et al. [3]. The Bioenergy Technology Office's Nth Plant assumptions were applied, including a 10% Internal Rate of Return (IRR) and modified accelerated cost recovery system (MACRS) 7-year depreciation [3–5]. The model determined the minimum selling prices of biomass, lipids, and fuels for a net-present value of zero and a 10% IRR over 30 years. For HTL, the Minimum Fuel Selling Price (MFSP) was expressed in 2019 USD per LGE, and for SAF, fuel co-products were sold at market values [71] with the MFSP for SAF expressed in 2019 USD per liter SAF.

2.2.12 Life Cycle Assessment

LCA was used to evaluate the environmental impacts of each algae-to-fuel pathway following ISO standards 14040 and 14044 [72]. The LCA utilized a well-to-wheels (W2W)

system boundary for RD and a well-to-wake boundary for SAF, covering all processes from feedstock cultivation to end-use. Main results illustrate impacts with this W2W boundary, while the provided open-source models offer cradle-to-gate boundaries for independent feedstock and lipid production comparisons. LCI data was sourced from the EcoInvent Database (version 3.9.1) [73] and accessed via OpenLCA [74]. The TRACI method [45] was used for impact assessment, quantifying ten different environmental impacts at the county level. Biogenic carbon accounting credited CO_2 uptake during algae growth and counted all biogenic CO_2 releases as burdens. For the HTL pathway, fuel production was combined into LGE units based on naphtha and diesel energy content. For the SAF pathway, SAF (bio-kerosene) was the main product from the HEFA process, with energy allocation used for fuel co-products. Fuel energy contents and electricity grid region boundaries obtained from EcoInvent are provided in Appendix A.

2.2.13 Water Footprint Analysis

The methodology detailed by Quiroz et al. [62] was used to assess the blue water footprint (BWF) and water scarcity footprint (WSF) of algae cultivation and conversion processes. The BWF encompasses all freshwater usage within the W2W system boundary including water replenishment for pond evaporation, water lost to media recycling inefficiencies and blowdown, and water for cooling, washing, and other conversion processes. Indirect water usage for the production process consumables like ammonia, DAP, and electricity was also considered within the system boundary. WSF was quantified by applying a county-specific characterization factor from the Available Water Remaining (AWARE) methodology [75] to scale BWF based on geospatial water scarcity metrics. For the SAF pathway, bio-kerosene was treated as the main product from the HEFA process, with an energy allocation used to allocate a fraction of the BWF and WSF to the fuel co-products of diesel, naphtha, LNG, and propane.

2.2.14 Direct Land Use Change Emissions and Total Fuel Production Potential

To evaluate land in the Contiguous United States (CONUS) for algal cultivation and subsequent fuel production potential, CONUS land was divided into a 200 m by 200 m grid. This grid size was selected to balance the tradeoffs between high spatial resolution and computation times. To be considered as a possible cultivation location, the land plot needed to contain only land that fell into the National Land Cover Database (NLCD) categories of barren land, deciduous forest, evergreen forest, mixed forest, shrub/scrub, Grassland/Herbaceous, Pasture/Hay, or Cultivated Cropland currently being used for bioenergy production [76]. Additionally, potential land plots must have a maximum slope at any point of 2% [77], exclude protected lands [78], and exclude Key Biodiversity Areas [79]. Further details are provided in Appendix A.

2.2.15 Optimization Algorithm

An optimization algorithm was integrated with the model to identify process improvements to reduce the MFSP and GWP. Webb County, TX, was chosen as a case study location for its favorable productivity and fuel production potential on non-arable land. For each fuel pathway, the algorithm started with assumptions for the Current Scenario and iteratively tested improvements, implementing those with the greatest reductions in MFSP or GWP.

The RD pathway considered increasing lipid content (with a correlated decrease in carbohydrates) and areal productivity, enhancing CUE, decreasing CO_2 cost, recovering algal proteins for revenue, and improving ammonia, DAP, and biochar recovery. Similarly, the SAF pathway focused on increasing lipid content and areal productivity, enhancing CUE, decreasing CO_2 cost, recovering algal proteins for revenue, increasing lipid extraction efficiency, and reducing HPH passes. Recovered proteins were assumed to generate a profit of \$2.00 kg protein^{-1}

based on a previous work from Davis et al. [58]. The option to recover proteins was purely an economic exercise for the MFSP optimization and the GHG emissions from protein extraction and purification were not quantified or considered in the GWP optimization. The algorithm was designed to shift to different improvements at the point of diminishing returns. However, in the optimization analysis for GWP, the algorithm was given the option to reduce emissions for electricity (simulating the transition to a renewable grid) only after all other potential improvements had reached their respective limits.

2.2.16 Sensitivity Analysis

Model sensitivity was evaluated using single-factor sensitivity analysis on 25 input parameters, each varied by ±20% from the assumed values in both the Current and Future Scenarios. This assessment measured the impacts on key sustainability metrics, including MFSP, GWP, and BWF. Additional details on the sensitivity analysis are available in the Appendix A.

2.3 Results

2.3.1 Minimum Fuel Selling Price

Results for the MFSP for the two different conversion pathways under the Current and Future Scenarios are presented in Figure 2. The results in Figure 2 illustrate a close relationship between MFSP and the annual average microalgae productivity (presented in Figures A7-A9 in Appendix A). The lowest MFSPs occur in southern latitudes, including counties in southern California, Arizona, Texas, Louisiana, Mississippi, Alabama, Georgia, Florida, and Hawaii, where productivities under nutrient-replete conditions range from 20-24.7 g ash free dry weight (AFDW) m^{-2} day^{-1}. Conversely, the highest MFSPs occur in northern latitudes and high-elevation areas, such as the Rocky Mountains, with significantly lower productivity. Under the

Current Scenario, the MFSP for RD ranges from \$3.70 to \$7.30 LGE^{-1}. High production costs for RD under the Current Scenario are driven by a high cost of CO_2 from DAC at \$230 $tonne^{-1}$, a 65% CO_2 utilization efficiency, lower lipid content (27.4 wt% lipids), and reduced productivity due to nutrient depletion.

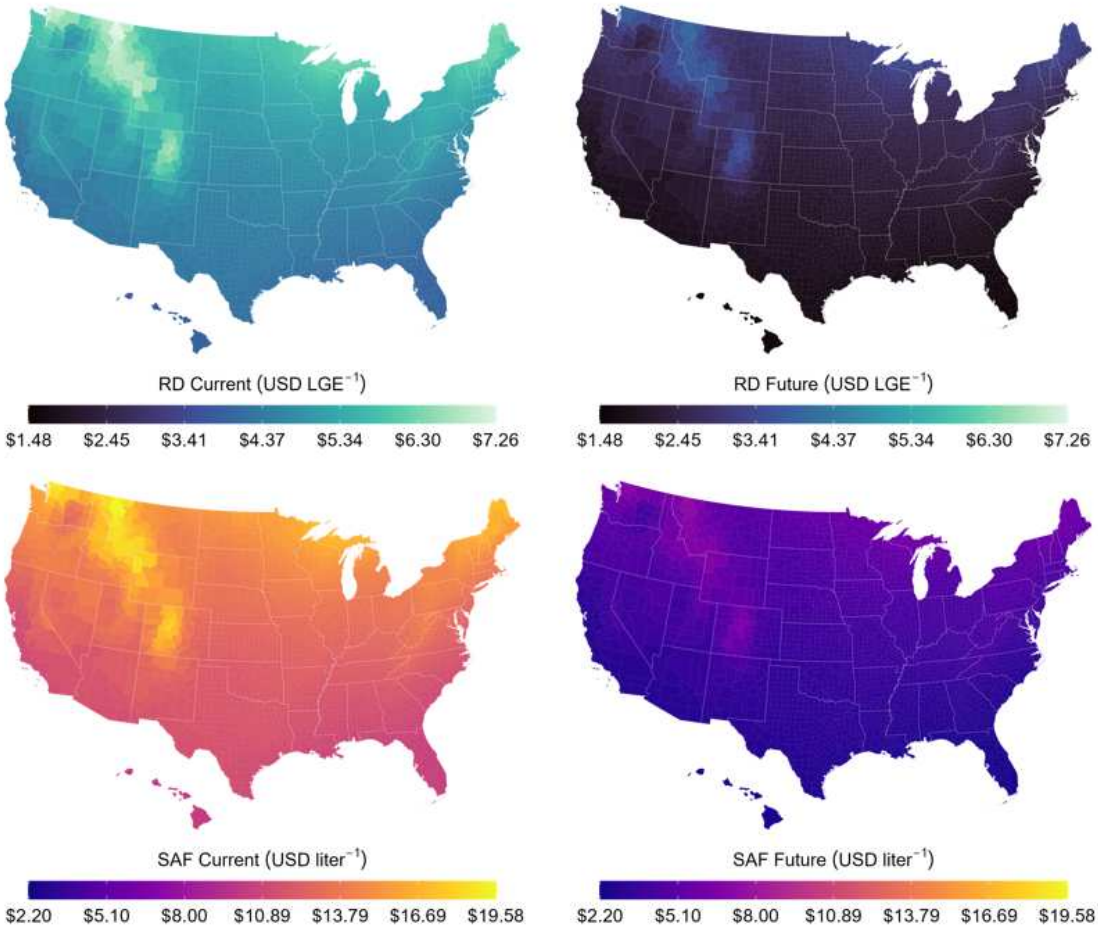

Figure 2: Minimum Fuel Selling Price for Renewable Diesel produced through Hydrothermal Liquefaction and Sustainable Aviation Fuel produced through the Hydroprocessed Esters and Fatty Acids process for the Current and Future Scenarios.

The Future Scenario explores several improvements including a DAC CO_2 cost of \$50 $tonne^{-1}$, 90% CO_2 utilization efficiency, a lipid content of 41.2 wt% with no productivity losses, and 90% nutrient recovery efficiency from the HTL aqueous phase. These improvements lead to a decreased MFSP for RD ranging from \$1.50 to \$4.10 LGE^{-1}. Under the Future Optimistic

scenario, the MFSP in the Southern U.S. approaches economic viability, but would still require further improvements, policy advances, or subsidies to reach economic parity with conventional petroleum fuels which are heavily subsidized [80].

In the analysis of SAF production from microalgae shown in Figure 2, the MFSP exhibits a substantial sensitivity to the lipid content of the biomass. Under the Current Scenario, with 27.4 wt% lipids, the MFSP ranges from \$9.90 to \$19.60 liter^{-1}. In contrast, the Future scenario, where lipid content rises to 41.2 wt%, shows large reductions in MFSP with a range of \$2.20 to \$7.30 liter^{-1}. Cultivation assumptions are consistent across both fuel pathways, with the HTL pathway showing less sensitivity to changes in biomass composition. The HTL pathway exhibits higher biomass utilization by converting whole-algal biomass to bio-oil, achieving biocrude yields of 43 wt% AFDW algae and 50 wt% AFDW algae with lipid contents of 27.4% and 41.2%, respectively. This can be compared to the SAF pathway where bio-oil yields are, at best, equivalent to the lipid content of the algae, with additional losses (10% and 1% losses for the Current and Future Scenarios, respectively) during the lipid extraction process. This cost sensitivity is also shaped by the specific fuel outputs of each conversion pathway, with the HTL process yielding only RD and naphtha. In contrast, the HEFA process achieves a 52% SAF yield in the Maximum Jet profile.

2.3.2 Global Warming Potential

County-level results for the GWP for each fuel production pathway under the Current and Future Scenarios are presented in Figure 3. Due to significant variations in dLUC emissions based on the assumed land type, these emissions are excluded from Figure 3. Detailed dLUC emissions for non-arable and arable land types are provided separately in Figures A4 and A5 in Appendix A.

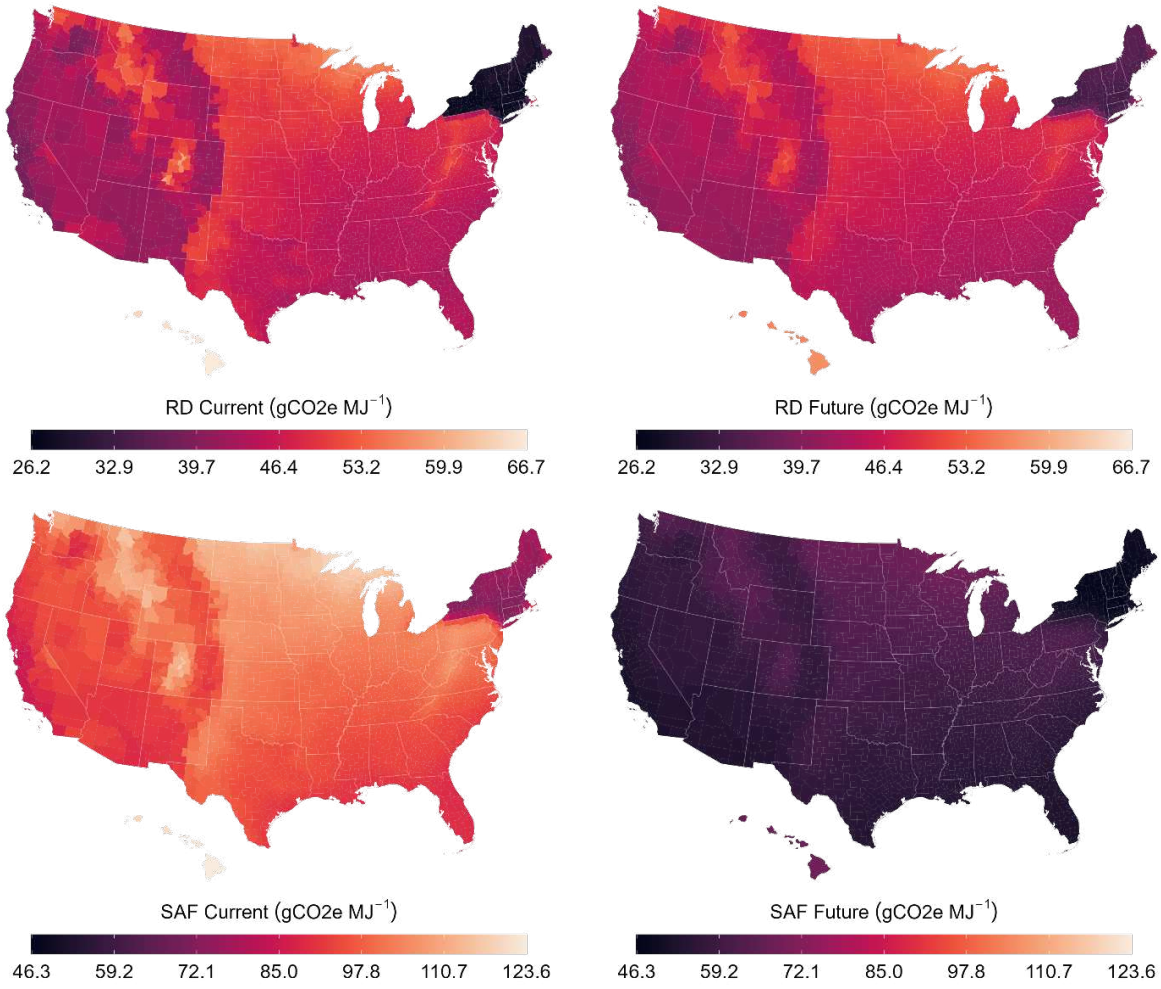

Figure 3: Global Warming Potential for Renewable Diesel produced through Hydrothermal Liquefaction and Sustainable Aviation Fuel produced through the Hydroprocessed Esters and Fatty Acids process for the Current and Future Scenarios.

The results in Figure 3 indicate that GWP is heavily influenced by the carbon intensity of the regional electricity grid with less dependence on areal productivity. In the Current scenario, the GWP of RD spans from 26.2 to 66.7 gCO_2-eq MJ Fuel^{-1}, with the lowest emissions for counties in the Northeast Power Coordinating Council (NPCC) grid region due to the abundance of hydropower resources. A map illustrating grid region boundaries is provided in Figure A6 in Appendix A. As the consumption of GHG-intensive commodities is correlated with biorefinery output, GWP remains the lowest in the Northeastern U.S. despite lower biomass productivity and high MFSPs in these areas. Locations under the Western Electricity Coordinating Council grid

region and in southern latitudes exhibit the second-lowest emissions in the U.S., due to abundant renewables in the grid mix. The majority of modeled locations meet the Renewable Fuel Standard (RFS) [81] for RD of 45 gCO_2-eq MJ $Fuel^{-1}$ even under the Current Scenario. The GWP of RD under the Future Scenario ranges from 32.7 to 57.3 gCO_2-eq MJ $Fuel^{-1}$, with most locations satisfying the RFS. The unexpected GWP increase in the NPCC region is due to higher nutrient demands from increased biomass yields under the Future Scenario. While emissions from electricity remain low, emissions from nutrient consumption are independent of the grid region used for cultivation. In other grid regions, decreases in GWP are due to improved lipid content boosting biocrude yields, higher CO_2 utilization efficiency reducing energy demands, and 90% nutrient and biochar recovery from HTL phases providing GHG displacement credits. The discrepancy between locations with low MFSP and low GWP underscores a critical trade-off between economic viability and environmental sustainability, emphasizing the impact of geospatial factors. This tradeoff is notable in Hawaii, where MFSPs are the lowest in the country due to high algae yields and grid emissions are the highest due to heavy fossil-fuel use.

Life cycle emissions for petroleum jet fuel range between 81.1 and 94.8 gCO_2-eq per MJ Fuel [82], setting the RFS for SAF between 40.6 and 47.4 gCO_2-eq MJ^{-1}. Under the Current Scenario, the GWP of algae-based SAF poses a significant challenge, with values between 70.5 and 185.3 gCO_2-eq MJ^{-1}, and many locations surpassing the GWP of petroleum jet fuel. These figures contrast with the Future Scenario, where the GWP ranges from 46.3 to 69.3 gCO_2-eq MJ^{-1}. The results for SAF follow the spatiotemporal trends observed in the RD pathway, with the lowest emissions in the NPCC grid region, second lowest in the WECC, and highest emissions in Hawaii. There is a 34%-44% reduction in emissions between the Current and Future Scenarios, indicating a pronounced sensitivity to algae lipid content compared to the RD pathway. LCA

results suggest that the net GWP is heavily influenced by the carbon intensity of local electricity grids followed by spatiotemporal variations in algal productivity.

This increased GWP of SAF relative to RD can also be attributed to the consumption of natural gas, hydrogen, and electricity for the HEFA conversion process. Under the Future Scenario, many U.S. locations, especially in the productive southern latitudes, approach the RFS for SAF. However, Hawaii remains an exception due to its fossil fuel-dependent electricity grid.

2.3.3 Cost and Emissions Optimization

Under the Current Scenario, the MFSP of RD and SAF are not economically competitive against existing petroleum counterparts. To achieve economic targets of \$0.75 liter^{-1} (\$3.00 gallon^{-1}), advancements are necessary in biomass productivity and composition, CO_2 delivery and utilization, and valorization of under-utilized biomass fraction through co-product recovery. Figure 4 presents the results from the optimization algorithm targeting reductions in MFSP for both fuel production pathways.

Figure 4: Minimum Fuel Selling Price optimization for a) Renewable Diesel, and b) Sustainable Aviation Fuel in Webb County, Texas.

The results in Figure 4 illustrate that both fuel production pathways benefit dramatically from increasing lipid composition up to 62% (upper limit set within the optimization analysis), increasing productivity to 22.36 g m^{-2} day^{-1}, and increasing the CUE to 95%. These improvements show the greatest benefits and represent the steepest slopes in the optimization curve, indicating the highest returns across all possible improvements. Through these three improvements alone, the MFSP for RD and SAF decreases by 63% and 78%, respectively. For RD, the next highest returns come from reducing the cost of DAC CO_2 down to \$40 $tonne^{-1}$ (fixed lower limit), further reducing the MFSP by 29% to \$1.15 LGE^{-1}. Prior to reducing CO_2 costs, the HEFA pathway sees greater returns from increasing the lipid extraction efficiency of the wet hexane extraction process to 98%, highlighting the sensitivity of the HEFA pathway to lipid production and recovery. Increased lipid recovery and reduced CO_2 costs lower the MFSP of SAF by another 55% to \$1.25 $liter^{-1}$. To hit the \$0.75 $liter^{-1}$ target for RD, the productivity is further increased to 35 g m^{-2} day^{-1} (fixed upper limit), followed by the extraction of 40% of algal proteins, earning a profit of \$2.00 kg $protein^{-1}$. To hit the \$0.75 $liter^{-1}$ target for SAF, the HEFA pathway sees greater returns from recovering a protein co-product than further increasing productivity and hits the target at 55% of proteins recovered. This distinction highlights the loss of intrinsic biomass value when LEA is sent through AD rather than further fractionated and valorized.

The optimization analysis was also performed specifically targeting reduction in GWP for both fuel pathways with the results presented in Figure 5. The results in Figure 5 suggest the RFS for RD can be satisfied by increasing algal productivity to ~11 g m^{-2} day^{-1} without any additional improvements relative to the Current Scenario assumptions. A 70% reduction over

petroleum diesel is achieved by increasing productivity to ~28 g m^{-2} day^{-1}, increasing CUE to 75%, and increasing ammonia recovery from the HTL aqueous phase to 70%.

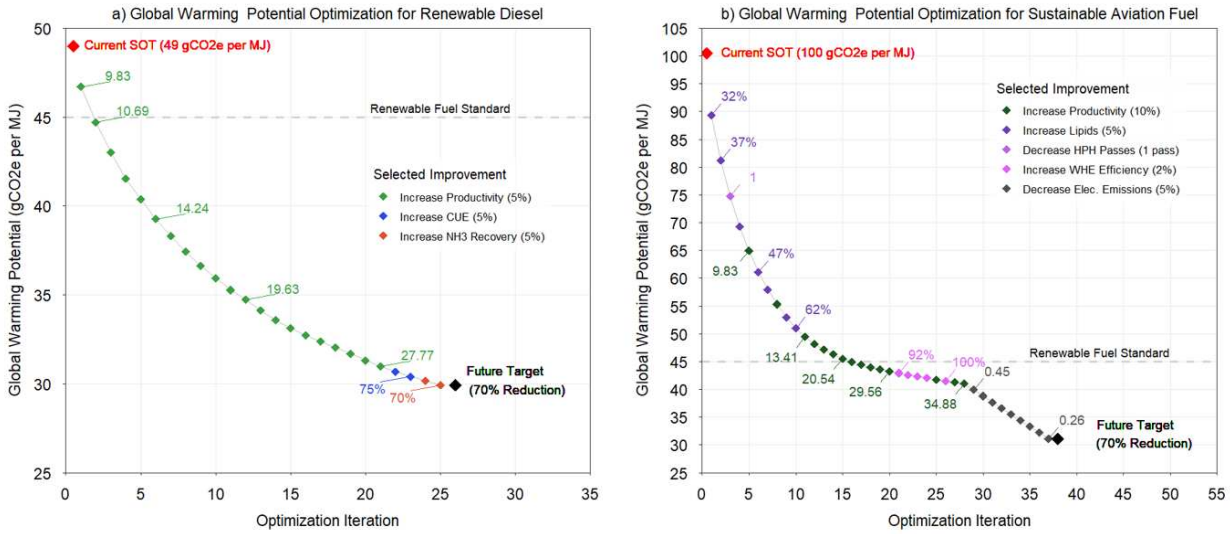

Figure 5: *Global Warming Potential optimization for a) Renewable Diesel, and b) Sustainable Aviation Fuel in Webb County, Texas.*

Under the Current Scenario, the GWP of SAF in Webb County, TX is equivalent to the GWP of petroleum jet fuel. The RFS for SAF can be satisfied by increasing algae lipid content to 62% and increasing productivity to 20.5 g m^{-2} day^{-1}. These improvements yield a 50% reduction in GWP, with 45% attributed to increased lipids and only 5% attributed to increased productivity, highlighting a pronounced sensitivity to lipid content over productivity in the HEFA pathway. The GWP can be further reduced to 40 gCO_2-eq MJ^{-1} by recovering 100% of lipids through wet hexane extraction and further increasing productivity to 35 g m^{-2} day^{-1}. Simultaneously achieving 62 wt% lipids and 35 g m^{-2} day^{-1} presents a significant challenge, as current lipid accumulation methods rely on nutrient deprivation. This goal will necessitate substantial advancements in genetic engineering or other innovative techniques. In contrast to the HTL pathway, the HEFA pathway is unable to achieve a 70% reduction in GWP through

performance improvements and relies on a 42% reduction in emissions associated with electricity consumption (from 0.45 to 0.26 $gCO_{2\text{-}eq}$ kWh^{-1}) to achieve this target.

2.3.4 Direct Land Use Change and Other Environmental Impacts

A broad range of economic and environmental sustainability metrics were obtained as a part of this study and are offered in Appendix A. The annual average and seasonal areal productivities were determined at the county level for both nutrient-replete and deplete conditions and are presented in Figures A7-A9. dLUC emissions were determined for non-arable and arable land types at the county level and are offered in Figures A13 and A14. Total fuel production potential on non-arable and arable land types are presented in Figures A15-A16. The Minimum Biomass Selling Price (MBSP) and Minimum Lipid Selling Price (MLSP) under the Current and Future Scenarios are provided in Figures A10 and A11. The BWF and WSF for both fuel production pathways are offered in Figures A17 and A18. Ternary diagrams illustrating the impacts of composition on the MFSP, GWP, BWF, and biocrude yield are presented in Figures A19-A25. Results from the sensitivity analysis are in Figures A26-A29. Finally, results for the TRACI impact categories are presented for 5 case study locations in Figures A30-A33.

2.3.5 Recommendations

This study, though comprehensive, has several limitations. The HEFA pathway modeling assumes algae oil properties are similar to soybean oil, which does not fully capture the unique characteristics of algae oil. Additionally, the HEFA conversion model lacks a full kinetic model, resulting in uncertainties in the mass balance. Another significant limitation is the gap between lab-scale performance and large-scale commercial demonstration. Despite decades of R&D, algal systems still face challenges like pest invasion, culture crashes, equipment malfunctions, and environmental fluctuations [83]. Carbon uptake credits from biomass growth depend on effective

CO_2 utilization, which has not yet been demonstrated at scale. This study attempts to address these uncertainties through scenario analysis and recent research-based assumptions.

Based on the findings of this study, several actionable recommendations are proposed for stakeholders and policymakers to advance the economic and environmental viability of microalgae-derived biofuels. R&D investments in genetic engineering and innovative techniques to enhance lipid content and biomass productivity without nutrient deprivation should be prioritized. Collaborative efforts between academic institutions, industry, and government agencies can accelerate this development. Additionally, policy measures should focus on reducing the cost and improving the efficiency of CO_2 delivery from DAC technology. Financial incentives, subsidies, and grants for DAC technology can facilitate its adoption and integration into large-scale algae cultivation systems. Promoting renewable energy sources for powering algae biorefineries can further enhance environmental sustainability. Stakeholders should advocate for comprehensive TEA and LCA frameworks in biofuel projects, emphasizing detailed spatiotemporal modeling to capture important trade-offs between economic and environmental sustainability. Policymakers should support high-resolution data repositories and modeling tools to optimize biofuel production pathways. Adopting these recommendations can drive the transition towards sustainable transportation fuels from microalgae and make strides towards global GHG emissions reduction targets.

CHAPTER 3: NATIONAL GREENHOUSE GAS EMISSIONS REDUCTION POTENTIAL FROM ADOPTING ANAEROBIC DIGESTION ON LARGE-SCALE DAIRY FARMS IN THE UNITED STATES[2]

3.1 Introduction

Reducing global greenhouse gas (GHG) emissions is crucial to mitigate the effects of climate change. The Intergovernmental Panel on Climate Change (IPCC) has identified the need to reduce GHG emissions by about 45% from 2010 levels by 2030 and reach net-zero emissions by 2050 to limit warming to 1.5°C, with the current global trajectory falling far short of these critical targets [84]. In 2021, methane (CH_4) emissions from dairy manure management totaled 35.9 MMT CO_2-eq, accounting for 54.4% of CH_4 emissions from livestock manure management, 4.9% of total CH_4 emissions, and 0.57% of gross annual GHG emissions in the United States [2]. Nitrous oxide (N_2O) emissions from dairy manure management totaled 5.5 MMT CO_2-eq in 2021, accounting for 31.6% of N_2O emissions from livestock manure management, 1.4% of total N_2O emissions, and 0.08% of gross GHG emissions in the United States [2]. Previous studies have shown that anaerobic digestion (AD) of dairy manure can effectively reduce emissions and provide environmental and economic benefits while displacing fossil fuels [8–15]. While enteric fermentation was the largest source of CH_4 emissions in the U.S. in 2021, totaling 195 MMT CO_2-eq (26.4% of total CH_4 emissions and 3.1% of gross GHG emissions), these emissions cannot be mitigated through AD technologies [2].

[2] This chapter was published as a peer-reviewed journal article: Greene JM, Wallace J, Williams RB, Leytem AB, Bock BR, McCully M, et al. National Greenhouse Gas Emission Reduction Potential from Adopting Anaerobic Digestion on Large-Scale Dairy Farms in the United States. Environ Sci Technol 2024;58:12409–19. https://doi.org/10.1021/acs.est.4c00367.

Previous studies of AD have focused on specific aspects of the technology [15,85–87], provided location-specific results [12,14,88–90], or offered broad reviews of AD technologies and industry practices [11,91]. National assessments by agencies like the EPA [9] and USDA [92] have offered insights into regional manure management practices and potential CH_4 emissions reductions from AD adoption. However, these studies primarily addressed CH_4 emissions reduction and have often overlooked critical factors like N_2O emissions from certain livestock housing types, solid manure storage, and land application of residual solids and digestate. Moreover, these analyses heavily relied on census data, which limited their scope to historical and current observations without considering future scenarios. Understanding the dairy industry's trajectory concerning regionally-appropriate AD adoption is vital for determining national GHG emission trends and adjusting strategies for GHG mitigation and fossil fuel phase-out.

This study aimed to determine the potential reduction in CH_4 and N_2O emissions from adopting AD technologies on applicable large-scale dairy farms in the contiguous United States considering regional differences in climate and manure management strategies. Applicable dairy farms were identified as the large-scale operations most likely to adopt AD technology in the near term based on scale, logistics, and economic estimates. The study examines emissions reduction under current incentives for renewable natural gas (RNG) production and explores the impact of incentivizing combined heat and power (CHP) as an additional biogas use case. Additionally, this study offers a robust modeling framework that can be used to evaluate farm-level emissions reduction opportunities and explore alternative AD adoption scenarios.

3.2 Materials and Methods

This study employs a systematic mass balance approach combined with Life Cycle Assessment (LCA) methodology to quantify emissions of CH_4, N_2O, and anthropogenic CO_2 (resulting from non-biological processes like diesel fuel combustion) across manure management systems (MMS), AD systems, and land application of residual manure and digestate. Regional manure management practices are represented through a detailed collection of baseline and adoption scenarios, which are integrated with future technology adoption projections to quantify the national GHG emissions reduction potential. Furthermore, modeling methodologies and region-specific modeling assumptions have been thoroughly reviewed and informed by the Manure Technology Team (MTT), a panel of experts assembled by the Innovation Center for U.S. Dairy [93] with representatives from key dairy regions. The MTT Members and their affiliations are provided in Table B35 in Appendix B.

3.2.1 Goal and Scope

The objective of this study is to conduct a detailed evaluation of a distinct segment within the U.S. dairy industry, specifically focusing on large-scale dairy farms. These farms are notable for their considerable GHG emissions and their dominant contributions to national milk production. The analysis zeroes in on large-scale dairies that have yet to implement AD technologies and are prime candidates for AD adoption. Accordingly, the research delineates baseline scenarios to document the existing GHG emissions profile of these operations, while also quantifying the potential for emissions reduction through the adoption of AD technology by this segment of the dairy industry. The analysis begins at the point of dairy cow feces and urine excretion and includes all downstream CH_4 and N_2O emissions. Baseline scenarios encompass emissions from animal housing, MMS, long-term storages, and land application of residual

Volatile Solids (VS) and Nitrogen (N). Adoption scenarios also include emissions from AD, biogas upgrading, and biogas end-use. The model comprises 10 baseline and 10 adoption scenarios spanning six U.S. dairy regions (Northwest, California, Southwest, Midwest, Northeast, and Southeast). Dairy regions were delineated by clustering states that share similar manure management practices and climates. California was evaluated as its own dairy region due to its large dairy industry, particularly in the San Joaquin Valley. Details on the contribution of manure from states within each of the five remaining regions can be found in Appendix B. Figure 6 presents a general process flow diagram outlining the modeled pathways for baseline and AD scenarios. Detailed diagrams for each modeled scenario and definitions of each manure management sub-system are available in Appendix B.

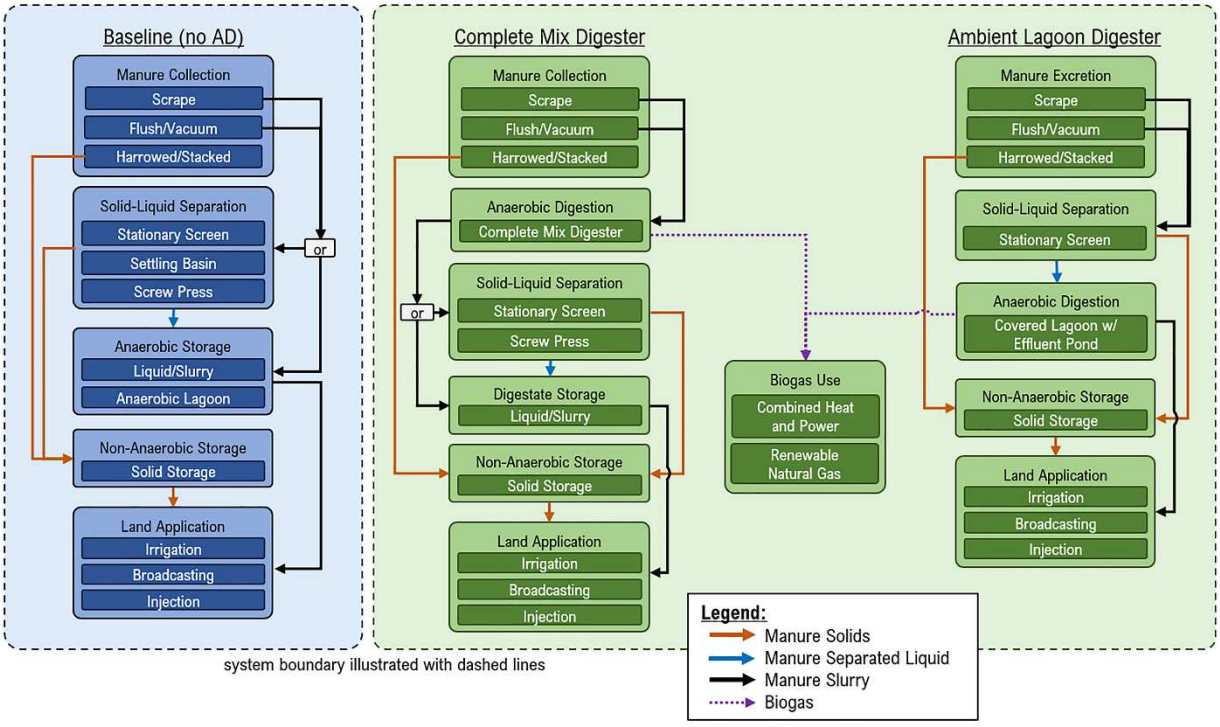

Figure 6: Process flow diagram illustrating the system boundary of the study, and the various pathways captured by the 10 baseline scenarios and 10 anaerobic digestion (AD) scenarios.

Baseline scenarios are defined by the chosen methods for manure collection, solid-liquid separation, and long-term storage, while the chosen AD technology and biogas application further differentiates AD adoption scenarios. Five manure collection configurations were considered and are described here. For open lots, 90% of manure is stacked in dry solid storage and 10% is flushed from the milking parlor to treatment. For open lots with concrete feed alleys, 60% of manure is stacked in solid storage and 40% is vacuumed to treatment. For confined scrape and confined flush scenarios, 100% of manure is scraped or flushed to treatment. For the confined flush scenario specific to CA, 23% of manure is collected from exercise pens and stacked in solid storage and 77% of manure is flushed from barns/milking parlors to subsequent systems. Table 1 summarizes the key characteristics of each baseline and AD adoption scenario.

Table 1: Descriptions of baseline (1A-3C) and anaerobic digestion (4A-6D) scenarios modeled.

Scenario	% of Manure Collected				Solid-Liquid Separation[1]	Anaerobic Digestion[2]	Biogas Use[3]	Long-Term Storage[4]	Regions[5]
	Stacked	Flushed	Vacuumed	Scraped					
1A	90%	10%	-	-	SS	None	NA	UCL	NW, SW
1B	90%	10%	-	-	SB	None	NA	UCL	NW, SW
1C	60%	-	40%	-	SS	None	NA	UCL	NW, SW
1D	60%	-	40%	-	SB	None	NA	UCL	SW
2A	-	-	-	100%	SS	None	NA	LS	NW, SW
2B	-	-	-	100%	SP	None	NA	LS	MW, NE
2C	-	-	-	100%	None	None	NA	LS	NW, MW, NE
3A	-	100%	-	-	SS	None	NA	UCL	SE
3B	23%	77%	-	-	SS	None	NA	UCL	CA
3C	23%	77%	-	-	SB	None	NA	UCL	CA
4A	60%	-	40%	-	SS	CMAD	CHP	LS	NW, SW
4B	60%	-	40%	-	SS	CMAD	RNG	LS	NW, SW

5A	-	-	-	100%	SS	CMAD	CHP	LS	NW, SW
5B	-	-	-	100%	SP	CMAD	CHP	LS	MW, NE
5C	-	-	-	100%	SS	CMAD	RNG	LS	NW, SW
5D	-	-	-	100%	SP	CMAD	RNG	LS	MW, NE
6A	-	100%	-	-	SS	CL-EP	CHP	CL-EP	SE
6B	-	100%	-	-	SS	CL-EP	RNG	CL-EP	SE
6C	23%	77%	-	-	SS	CL-EP	CHP	CL-EP	CA
6D	23%	77%	-	-	SS	CL-EP	RNG	CL-EP	CA

[1]SS: Stationary Screen; SB: Settling Basin; SP: Screw Press
[2]CMAD: Complete Mix Anaerobic Digester; CLEP: Covered Lagoon with Effluent Pond
[3]NA: Not Applicable; CHP: Combined Heat and Power; RNG: Renewable Natural Gas
[4]UCL: Uncovered Anaerobic Lagoon, LS: Liquid/Slurry; CL-EP: Covered Anaerobic Lagoon with Effluent Pond
[5]NW: Northwest; SW: Southwest; MW: Midwest; NE: Northeast; SE: Southeast; CA: California

For baseline scenarios 1A-3C, long-term liquid manure storage occurs in Uncovered Anaerobic Lagoons (UCL) or Liquid/Slurry (LS) systems. For AD adoption scenarios 4A-5D, solid-liquid separation occurs after AD and long-term digestate storage occurs in LS systems. For AD adoption scenarios 6A-6D, solid-liquid separation occurs prior to the covered lagoon with an effluent pond (CLEP) which serves as the method of both AD and long-term storage. All modeled scenarios assume land application as the end-fate for stored manure (solid and liquid) and digestate.

3.2.2 Functional Unit

LCA results for regional manure management scenarios are presented using the functional unit of a Wet Cow Equivalent (WCE). The functional unit inherently incorporates regional and temporal variations in milk and VS production, thereby enabling the results to serve effectively in both detailed regional and national assessments of dairy-related GHG emissions. This functional unit was chosen to represent realistic dairy operations which contain a dynamic

mix of lactating (wet) and non-lactating (dry) dairy cows. This study assumes that an average dairy cow is lactating 305 days out of the year or roughly 85% of the time based on inventory data from the USDA National Agriculture Statistics Service (NASS) [94]. Daily VS excretion is dependent on dairy cow mass, milk production, and caloric intake [2]. Thus, there is a significant difference in the daily VS excretion rates between wet and dry dairy cows [2,95]. The VS excretion rate of one WCE in a specific state can be calculated by equation 1:

$$VS_{WCE,i} = 0.85\left(\frac{TAM_L}{1000}\right)VS_{L,i} + 0.15\left(\frac{TAM_{NL}}{1000}\right)VS_{NL,i} \quad \text{(Eq. 1)}$$

where TAM_L is the typical average mass of a lactating dairy cow, TAM_{NL} is the typical average mass of a non-lactating or "dry" dairy cow, $VS_{L,i}$ is the VS excretion per 1000 kg animal mass for lactating dairy cows in state i, and $VS_{NL,i}$ is the VS excretion per 1000 kg animal mass for non-lactating dairy cows in state i. Regional VS and N excretion rates were derived using a weighted average of state-level data [2,95], weighted by each state's share of cows in a region. These rates, along with state-level VS and N excretion data, are detailed in Tables B12 and B13 of Appendix B. Results for manure management scenarios and emissions reductions are based on Holstein cows, which made up 79.9% of the U.S. dairy herd in 2020 [96]. The analysis also considers the impact of increasing Jersey and mixed breed populations by incorporating TAM variability in the Monte Carlo uncertainty analysis. Replacement stock were excluded from the analysis due to a lack of uniform management practices throughout the defined dairy regions.

3.2.3 Life Cycle Assessment Methodology

LCA methodology following ISO 14040 and 14044 standards [72] was used to determine the global warming potential (GWP) of each baseline and adoption scenario, with the delta between scenarios representing the potential GHG reduction. GHG emissions are reported with

the units of "CO_2 equivalents" (CO_2-eq) which include emissions of CO_2 (anthropogenic only), CH_4 (non-fossil), CH_4 (fossil), and N_2O multiplied by their respective impact factors of 1, 27, 29.8, and 273 kg CO_2-eq/kg gas and summed [97]. Total GHG emissions were normalized by the number of cows and time over which emissions occurred to determine the GWP in kg CO_2-eq per WCE per year (kg CO_2-eq WCE^{-1} yr^{-1}).

This study's system boundary comprehensively includes direct and indirect GHG emissions related to manure management and biogas generation, upgrading, and end-use. Notably, it does not account for biogenic CO_2 - neither recognizing CO_2 capture through photosynthesis in feed production and grazing nor considering CO_2 emissions from the combustion of RNG. The analysis specifically covers biogenic CH_4 emissions from manure management, fugitive CH_4 leaks, N_2O emissions across all stages, and anthropogenic CO_2 emissions from diesel machinery. Additionally, anthropogenic CO_2 emissions resulting from the consumption of grid energy (both electricity and natural gas) and consumables for biogas upgrading are incorporated as indirect emissions within this study's framework.

Life Cycle Inventory (LCI) data were collected from various sources. State-level emissions data for grid energy consumption and grid energy displacement credits CHP using captured biogas were sourced from the EPA's Emissions and Generation Resource Integrated Database (eGRID) [98]. Average emissions for each of the 6 dairy regions were determined from this state-level data, as detailed in Appendix B. Owing to uncertainties in AD adoption timelines and the predominance of biological CH_4 and N_2O emissions over GHG emissions from grid energy consumption, a dynamic LCA framework addressing changing grid emissions was considered beyond the scope of the study. CH_4 and N_2O emissions related to CHP were sourced from Zamalloa et al. [69], while CH_4 and N_2O tailpipe emissions from CNG vehicles were

obtained from the EPA [99]. Emissions associated with diesel combustion for manure collection, tanker injection, and manure broadcasting were directly obtained from Aguirre-Villegas and Larson [10]. LCI data for consumables in biogas upgrading, heat generation with a natural gas boiler, and RNG pipeline transport were sourced from the EcoInvent Life Cycle Inventory Database (version 3.9.1) [73] through cutoff analysis and accessed via openLCA 1.11.0 [100], with additional details provided in Appendix B.

3.2.4 Regional Data

Region-specific inputs required for the modeling work included ambient temperature, VS and N excretion rates, and emissions associated with the electricity grid (described in section 3.2.3). Monthly average temperatures (5-year averages from 2018-2022) for each state in the contiguous U.S. were obtained from the National Oceanic and Atmospheric Administration (NOAA) [101] and used to determine average monthly temperatures for each region. Average temperatures were used throughout the analysis to calculate the temperature-dependent Arrhenius factor, the temperature-dependent methane conversion factor (MCF) for solid storages, as well as the sensible heat input for heating anaerobic digesters. For California, the average temperature used in the analysis only included counties in the San Joaquin Valley as over 90% of the California dairy industry is located there. All state-level and regional average data are presented in Appendix B.

3.2.5 Methane Emissions from Baseline Scenarios

Baseline scenarios to characterize GHG profiles of current large-scale dairy operations were established across six regions, following two pathways: 1) manure flushed or vacuumed into uncovered anaerobic lagoons for storage and land application; or 2) manure scraped or vacuumed into liquid/slurry storage for eventual land application. Variations include the ratio of

dry to wet storage, the use of settling basins or solid-liquid separation, and land application methods. Table 1 details each of the modeled baseline configurations (1A-3C).

3.2.5.1 Methane Emissions from Non-Anaerobic Storage

All modeled scenarios aside from 2C include non-anaerobic solid storage of VS removed through solid-liquid separation. Furthermore, non-anaerobic solid storage is the method of long-term storage assumed for the portion of manure collected from open lots in scenarios 1A-1D, 3B-3C, 4A-4B, and 6C-6D. Details on where these scenarios occur can be found in Table 1, while the number of cows considered under each scenario are available in Tables B29 and B31 in Appendix B. For estimating monthly methane emissions from solid storage, calculations followed the IPCC protocol [102] using temperature-dependent monthly MCF values for solid storage obtained from the "Reference" tab in the California Air Resource Board (CARB) version of the Greenhouse Gases, Regulated Emissions, and Energy Use in Transportation (GREET) Model [95]. The portion of VS removed through solid-liquid separation was dependent on the selected separation technology, with separation efficiencies obtained from the "Reference" tab in the CARB GREET model [95] and the separation efficiency of sloped screen separators was updated to 30% based on the work of Williams et al. [103]. Appendix B provides detailed equations, solid-liquid separation efficiencies, and temperature-dependent MCF values for solid storage.

3.2.5.2 Liquid/Slurry Storages

In the Northwest, Southwest, Midwest, and Northeast, baseline configurations with scrape manure collection delivered manure to liquid/slurry storages. These storages hold manure as excreted or with minimal water addition, for durations up to 4 years. Mechanical agitation ensured that specified monthly cleanout percentages corresponded to equivalent VS removal

[102]. MTT recommendations informed regionally-specific cleanout schedules, with some regions requiring 4 years for complete emptying. A monthly time step was used for VS input, regional cleanout schedules, and temperature-dependent Arrhenius factors. The Arrhenius factor was used to determine the portion of VS that was biologically available to degrade, and methane formation was determined by multiplying degraded VS by maximum specific methane formation (B_0) [95]. This monthly time step aligns with IPCC recommendations [102] and is essential for emissions accounting in regions with significant temperature variations and variable VS loading. All baseline scenarios aside from 2C incorporated solid-liquid separation before long-term liquid/slurry storage, with emissions from separated solids covered in section 3.2.5.1 and reduced VS loading accounted for in the VS mass balance.

When solids are not removed through solid-liquid separation prior to liquid/slurry storages, natural crust covers can develop and may reduce methane emissions by up to 40% [102]. IPCC recommendations state that this 40% reduction may be applied when a thick and dry crust cover is present [102]. This 40% reduction was not applied to scenario 2C in this study based on a unanimous decision from the MTT informed by first-hand observation suggesting that the majority of crust covers in liquid-slurry systems are cracked and bubbling rather than thick and dry. However, the MTT supported that bottom load slurry tanks often used by small dairies in the Northeast could apply this reduction.

3.2.5.3 Methane Emissions from Uncovered Ambient Lagoons

Ambient lagoons have lower depth, larger surface area, and lower total solids compared to liquid/slurry storages [102]. Manure was delivered to ambient anaerobic lagoons for long-term storage in baseline scenarios across the Northwest, California, Southwest, and Southeast. Unlike liquid/slurry systems, lagoons involve sequential VS flow from covered lagoons to uncovered

effluent ponds, requiring a unique modeling approach. In the mass balance, degradable and non-degradable VS were separated to determine residual VS carried over each month, potentially degrading to produce CH_4. The degradable VS fraction entering the system was 51.7%, based on the maximum specific methane formation (B_0) for manure-separated liquid [104] and reported biogas formation values per kg VS destroyed [105].

Ambient lagoon systems provide flush water and irrigation water enriched by manure nitrogen [102]. VS used for flush water was assumed to return to the lagoon with minimal loss but using lagoon liquid for irrigation resulted in VS outflow from the system. Irrigation schedules reflecting regional practices were incorporated in the model and are presented in Appendix B. The model estimated VS leaving the lagoon in irrigation water by tracking monthly lagoon volume and using measured VS concentrations in lagoon flush water [105–107] to account for VS settling and the dynamic degradable vs. non-degradable VS fraction. Published VS concentrations for CA were used in calculations for CA, the SW, and SE, while values for VS concentrations in Idaho were used for the NW. The possibility of additional regional variation was addressed by including these parameters in the Monte Carlo analysis of uncertainty. Degradable VS was multiplied by the temperature-dependent Arrhenius factor to determine monthly VS degradation. Total degraded VS was multiplied by 0.505 m^3 CH_4 kg VS $degraded^{-1}$ to calculate monthly methane formation from lagoons [105]. Detailed equations for the mass balance, constants used for the Arrhenius factor, and calculations for lagoon volume approximations are provided in Appendix B.

Several baseline scenarios incorporated settling basins before lagoon storage to enable gravity settling and reduce lagoon system VS loading. The assumed 50% VS removal efficiency in these scenarios was based on work from Chastain and Henry [108]. Methane emissions from

the 50% of VS retained in the settling basin were calculated using the same approach for ambient lagoons. Mechanical agitation was assumed before settling basin cleanout. For baseline scenarios with settling basins preceding lagoons, the measured VS exit concentration of the lagoon [105–107] was multiplied by 50% to account for the VS retained in the settling basin.

3.2.5.4 Land Application of Residual Manure Solids

Following cleanout of solid and liquid storages, all residual manure solids and any accompanying liquids were assumed to be land applied through irrigation, tanker injection, or broadcasted in fields. Land application procedures defined for each region are provided in Appendix B. In general, this study assumed that the potential to produce methane would be significantly reduced once manure solids were removed from the anaerobic storage environment. This study assumed that any residual land-applied carbon would be broken down by soil microbes and released to the atmosphere as biogenic CO_2 [95]. Biogenic CO_2 emissions resulting from land application of residual manure solids were not counted as burdens to the system. However, emissions of N_2O following land application were considered burdens with the accounting methodology described in section 3.2.8.

3.2.6 Anaerobic Digestion Adoption Scenarios

The AD technology chosen for regional adoption scenarios depended on the corresponding baseline scenario. Baseline scenarios with anaerobic lagoon storage were transformed into AD scenarios by installing a lagoon cover to capture 95% of produced biogas [95,102], which was then directed to one of two biogas utilization scenarios detailed in section 3.2.7. For scenarios involving covered lagoons, the monthly volume entering the effluent pond was assumed to equal the volume entering the lagoon, with flush and irrigation water sourced from the effluent pond. Methane emissions from effluent ponds were estimated using the same

method applied to liquid/slurry storages. The total VS in the effluent pond for any given month was calculated as the balance between incoming VS (equivalent to the difference between VS entering the lagoon and VS destroyed through biogas formation) and VS leaving through effluent pond cleanout. Agitation was assumed before effluent pond cleanout. Methane emissions from effluent ponds were determined by multiplying the total VS in the system for a given month by the monthly Arrhenius factor, then by the maximum specific methane formation for manure separated liquid [104].

Regions employing scrape collection and liquid/slurry storage were assumed to adopt an engineered complete-mix anaerobic digester (CMAD). CMAD systems were assumed to operate in the mesophilic range at a fixed temperature of 36 °C requiring a sensible heat source to maintain this temperature throughout the year [109–111]. For CHP scenarios, waste heat was utilized for digester heating, supplemented by a natural gas boiler. In scenarios producing RNG, a natural gas boiler was used as a heat source. Detailed calculations for temporally-resolved sensible heat input are available in Appendix B. CMAD units were assumed to achieve 85% of the maximum specific methane formation (B_0) due to constant reactor temperature and consistent VS loading throughout the year [110,112]. A sensitivity analysis exploring reactor efficiencies ranging from 30-100% is presented in Appendix B. CMAD reactors were assumed to leak 2% of produced biogas to the atmosphere based on prior studies [95,102]. Digestate containing the remaining 15% of VS was directed to liquid/slurry storage, with methane emissions calculated using the method described in section 3.2.5.2. In all CMAD scenarios, digestate was subject to solid-liquid separation before long-term storage in liquid/slurry systems, resulting in reduced VS loading to long-term storage. Methane emissions from solid storage of separated VS from AD digestate were determined following the methodology described in 3.2.5.1.

3.2.7 Biogas Use

Two pathways were modeled for biogas use: 1) direct use in combined heat and power; 2) biogas upgrading, compression, and pipeline transport for use in CNG vehicles. Thermal and electrical efficiencies for combined heat and power were informed by Zamalloa et al. [69] and the "Reference" tab in the CARB GREET model [95]. Heat generated through CHP was assumed to be used onsite to heat CMAD systems, with any excess heat considered a burden-free waste product. Electricity generated through CHP was assumed to be sold directly to the local grid, with the system earning a grid emissions avoidance credit equal to the carbon intensity (kg CO_2-eq kWh^{-1}) of the regional grid.

In the second biogas-use scenario, raw biogas was upgraded to vehicle-ready CNG based on the process described by Skorek-Osikowska et al. [113] for biogas produced through anaerobic digestion of dairy manure. Indirect emissions for consumables used in the biogas upgrading process, including iron (II) chloride, calcium hydroxide, monoethanolamine (MEA), tap water, waste-water treatment, and process electricity, were included. The model included 3% parasitic consumption of biogas for process heat and 2% loss to fugitive emissions based on Skorek-Osikowska et al. [113]. Furthermore, the CNG pathway included emissions for pipeline transport of 1000 km [73]. Biogenic CO_2 captured in the upgrading process was assumed to be vented to the atmosphere with no burden to the system. Once delivered to a CNG station, the model assumed 90% use in CNG buses with an assumed average fuel economy of 4 miles per diesel gallon equivalent (DGE) and 10% use in CNG passenger vehicles with an assumed average fuel economy of 25 miles per DGE. Miles driven by each type of vehicle were used to determine tailpipe emissions of CH_4 and N_2O [114]. The total production of DGE from captured biogas was determined by multiplying the energy content of RNG [113] expressed in DGE by an

adjustment factor of 0.9 to account for the difference in engine efficiency between diesel and CNG vehicles [95]. For every diesel gallon equivalent of CNG delivered to the station, the system received a diesel displacement credit equal to the well-to-wheels emissions for petroleum-based diesel of 92 g CO_2-eq MJ $fuel^{-1}$ obtained from the GREET Life Cycle Inventory model [115]. Further details for both biogas-use pathways are included in Appendix B.

3.2.8 N_2O Emissions Accounting

This study includes both direct and indirect emissions of N_2O resulting from the various manure management scenarios considering the impacts of solid-liquid separation, the method of manure storage or digestion, and the land application method for residual manure solids. State-level nitrogen excretion data for dairy cows were obtained from the EPA [2] and used as the starting point of the nitrogen mass balance for each scenario. Next, nitrogen losses and resulting N_2O emissions from each sub-process were determined using the protocol outlined in the IPCC 2019 Refinement to the 2006 Guidelines for Greenhouse Gas Inventories [102]. Appendix B provides the fraction of manure nitrogen volatilized and lost to leaching and all applicable N2O emissions factors for the various manure management strategies in the regional scenarios.

Results from previous studies [116–119] were used to estimate the nitrogen removed through solid-liquid separation with screw press and stationary screen separators. A total nitrogen removal of 15% of incoming nitrogen was assumed for solid-liquid separation scenarios. Furthermore, storage of separated solids was assumed to ocurr in an aerobic environment, resulting in negligible N_2O emissions from storage and land application. Emissions factors were developed for each land application method considering the impacts of manure digestion on N_2O formation, and the full assessment and resulting N_2O emission factors are provided in Appendix B.

3.2.9 Anthropogenic Emissions from Manure Management Energy

GHG emissions associated with diesel consumption for equipment used for manure scraping, vacuuming, and tanker trucks used for manure broadcasting and injection were obtained directly from Aguirre-Villegas and Larson [10]. Estimates for grid electricity consumption for flush water pumping, manure pumping, mechanical agitation of manure storage systems, irrigation, and solid-liquid separation were obtained from Aguirre-Villegas and Larson [10] and multiplied by the carbon intensity of regional electricity grids to determine total indirect GHG emissions for each scenario. Energy consumption values for mechanical mixing of CMAD systems were based on previous studies [13,116,120].

3.2.10 Regional Adoption Projections

Two AD adoption cases were developed in this study. The Status Quo adoption case reflects the current landscape of AD adoption on largescale dairy farms. In this scenario, adoption is primarily driven by the economics of producing RNG for the California Low Carbon Fuel Standard (LCFS) market, the U.S. EPA Renewable Fuel Standard (RFS) D3 RINs, and renewable CNG sales. The Opportunity Case expands on this and considers future incentive programs like the EPA RFS eRIN Program via CHP for electricity production, which requires less capital and operational complexity, providing opportunities for smaller dairy farms.

Forecasting AD adoption for dairy farms is complicated by existing practices, farm dynamics, RNG pipeline access, and changing policy. A full techno-economic analysis was considered outside the scope of the study. Instead, a high-level economic analysis was developed, leveraging input from digester developers and industry experts to assess the economic viability of AD adoption. Capital cost, operating cost, farm configuration, and revenue were used to estimate the required number of mature cows to ensure economic viability for

large-scale digester facilities. The Status Quo Case considered the number of cows in the 2,500 - 4,999 and 5,000+ NASS categories with an estimated threshold of 3,500 mature cows required for AD adoption. The Opportunity Case augmented the Status Quo case by adding cows in the 1000 - 2,499 NASS category and an estimated threshold of 1,750 mature cows. Where the average number of cows per farm fell short of the threshold for a given region, a simplifying assumption was made that smaller farms could form clusters to achieve the total number of cows predicted for each region. In these scenarios, a central digester processes manure from several farms, or a central biogas upgrading facility collects and processes biogas from multiple farms.

First-order economic estimates considered the top ten milk-producing states plus Florida and Arizona, resulting in 76% of the U.S. dairy herd and giving the estimates a built-in safety factor. Florida was chosen as the representative state for the Southeast and has the largest number of mature cows in the 1000+ NASS category in the region. Arizona was selected based on significant state-wide efforts to adopt AD technology with 84,514 cows currently contributing to digesters. Furthermore, it ranks 14th in total milk production and has the second-largest average herd size in the United States. Further details on the economic estimates can be found in the Supporting Document titled “Economic_Analysis_StatusQuo_and_Opportunity_V5.xlsx.” Table 2 summarizes the participating cows considered for each adoption scenario at the regional level. A detailed explanation of the adoption estimation approach is provided in Appendix B.

Table 2: Summary of Anaerobic Digestion Adoption Estimates by State and Region

Region	State	Participating Cows (Status Quo)	Participating Cows (Opportunity)
Northwest	Washington	70,000	109,900
	Idaho	45,500	112,000
California	California	309,091	515,909
Southwest	Arizona	35,280	75,800
	New Mexico	0	65,757
	Texas	114,720	207,362
Midwest	Michigan	70,000	111,580
	Minnesota	17,500	50,260
	Wisconsin	38,500	129,063
Southeast	Florida	31,500	54,250
Northeast	New York	42,000	110,040
	Pennsylvania	10,500	21,840

3.2.11 Sensitivity Analysis

Model sensitivity was analyzed using single-factor sensitivity analysis across 128 parameters, each altered by ±20% from baseline to assess impacts on emissions reductions, both regionally and nationally, for each adoption case. Parameters affecting emissions reductions by >10% (21 in total) were then used in a Monte Carlo uncertainty analysis, with detailed results in Appendix B.

3.2.12 Monte Carlo Analysis of Uncertainty

Model uncertainty was evaluated via Monte Carlo analysis in JMP Statistical Software [121], focusing on 21 key parameters identified through sensitivity analysis. Parameter distributions, informed by published data and expert input, are detailed in Appendix B. The analysis examined regional and national emissions reduction under the Status Quo and Opportunity scenarios, running 5000 iterations per scenario and randomly selecting parameter

values within the defined distributions. Results, including uncertainty bounds for emissions reductions, are analyzed at the regional and national level for both adoption scenarios.

3.3. Results and Discussion

Net GHG emissions per WCE per year for 10 baseline scenarios (1A through 3A) and 10 AD adoption scenarios (4A through 6B) are shown in Figure 7. Regional differences in climate and storage practices lead to varying net GHG emissions in both baseline and adoption scenarios. Reduction in direct farm-level emissions from manure management through AD adoption ranged from 58.2% in the Southwest to 78.8% in the Northeast.

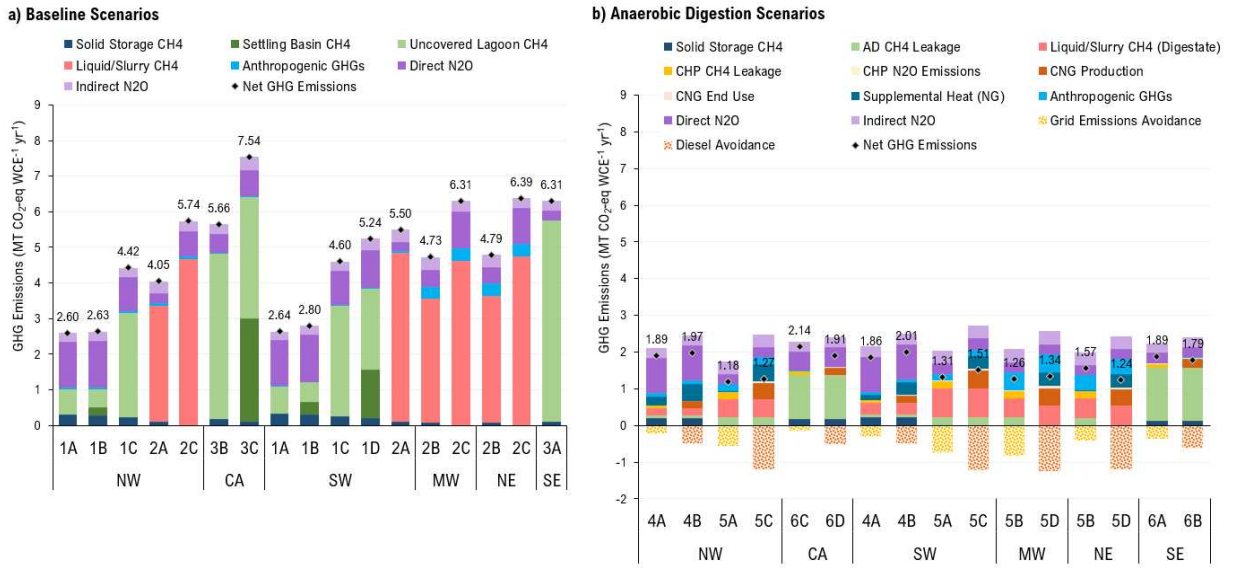

Figure 7: Greenhouse gas emissions per wet cow equivalent per year for each of the regional baseline (a) and anaerobic digestion (b) scenarios in the system engineering model (AD: Anaerobic Digestion; CHP: Combined Heat and Power; CNG: Compressed Natural Gas; NG: Natural Gas; GHG: Greenhouse Gas) Scenario descriptions are presented in Table 1.

The highest emissions among baseline scenarios occur in California (scenario 3C), with significant methane emissions from settling basins and uncovered lagoons, totaling 7.54 MT CO_2-eq WCE^{-1} yr^{-1}. Following is scenario 2C, with 6.39, 6.31, and 5.74 MT CO_2-eq WCE^{-1} yr^{-1} in the Northeast, Midwest, and Northwest, respectively. Scenario 2C employs liquid/slurry

storage without upfront VS removal through solid-liquid separation, resulting in higher emissions compared to scenarios 2A and 2B, which remove 30% of VS before storage. The VS removed through solid-liquid separation is stored in non-anaerobic solid storage prior to land application with negligible emissions from manure broadcasting (please see Table B26 for more details). Use of solid-liquid separation reduces emissions by 29.4% in the Northwest (2C vs. 2A) and 25% in the Midwest and Northeast (2C vs. 2B). The percentage of VS removed pre-storage correlates closely with emission reduction, emphasizing the potential benefits of technologies like centrifugation with higher VS removal rates.

Baseline scenarios using ambient lagoons for long-term storage without settling basins (3A and 3B) exhibit emissions similar to 2A, 2B, and 2C, ranging from 5.66 MT CO_2-eq WCE^{-1} yr^{-1} in California to 6.31 MT CO_2-eq WCE^{-1} yr^{-1} in the Southeast. Open lot scenarios 1A and 1B, storing 90% of manure in non-anaerobic solid storage, display the lowest emissions, indicating anaerobic storage conditions significantly affect methane formation. Emissions from 1A range from 2.60 to 2.64 MT CO_2-eq WCE^{-1} yr^{-1}, while 1B varies from 2.63 to 2.80 MT CO_2-eq WCE^{-1} yr^{-1}. Increased non-anaerobic storage reduces methane but raises N_2O emissions, contributing 56-59% of net GHG emissions in 1A and 1B in the Northwest and Southwest, compared to 14.5% in the highest methane emitting scenario, 3C.

For the various AD adoption scenarios (Figure 7b) the highest emissions result from scenario 6C which utilizes a covered lagoon digester. Net emissions for these lagoon digester scenarios range from 1.79 MT CO_2-eq WCE^{-1} yr^{-1} in the Southeast to 2.14 MT CO_2-eq WCE^{-1} yr^{-1} in California. The increased emissions for covered lagoon systems relative to other adoption scenarios can be attributed to higher methane leakage rates from lagoons (5% as opposed to 2% in CMAD systems). Scenarios 4A and 4B show the next highest emissions ranging from 1.86 to

2.01 MT CO_2-eq WCE^{-1} yr^{-1}. These scenarios are representative of open lot scenarios with manure on concrete, resulting in 40% of manure sent the CMAD and 60% of manure managed in non-anaerobic storage. These collection percentages result in unfavorable conditions in which the potential diesel and grid emissions avoidance credits are not maximized, and N_2O emissions dominate the emissions profile due to the majority of manure managed in non-anaerobic solid storage. In scenarios 4A-4B, the contribution of N_2O to the total GHG burdens ranges from 50-58%. The lowest emissions among the AD adoption scenarios are from confined scrape systems (scenarios 5A, 5B, 5C, and 5D) in which 100% of manure is collected and sent through the CMAD, maximizing diesel and grid emissions avoidance credits while minimizing methane leaks and N_2O emissions from non-anaerobic solid storage. Net GHG emissions for scenarios 5A-5D range from 1.18 MT CO_2-eq WCE^{-1} yr^{-1} in the Northwest to 1.57 MT CO_2-eq WCE^{-1} yr^{-1} in the Northeast, with N2O emissions contributing 24 - 36% of total GHG burdens.

The regional GHG emissions reduction potential as well as the total national GHG emissions reduction potential from adopting AD technologies on large-scale dairy farms in the U.S. are shown in Figure 8.

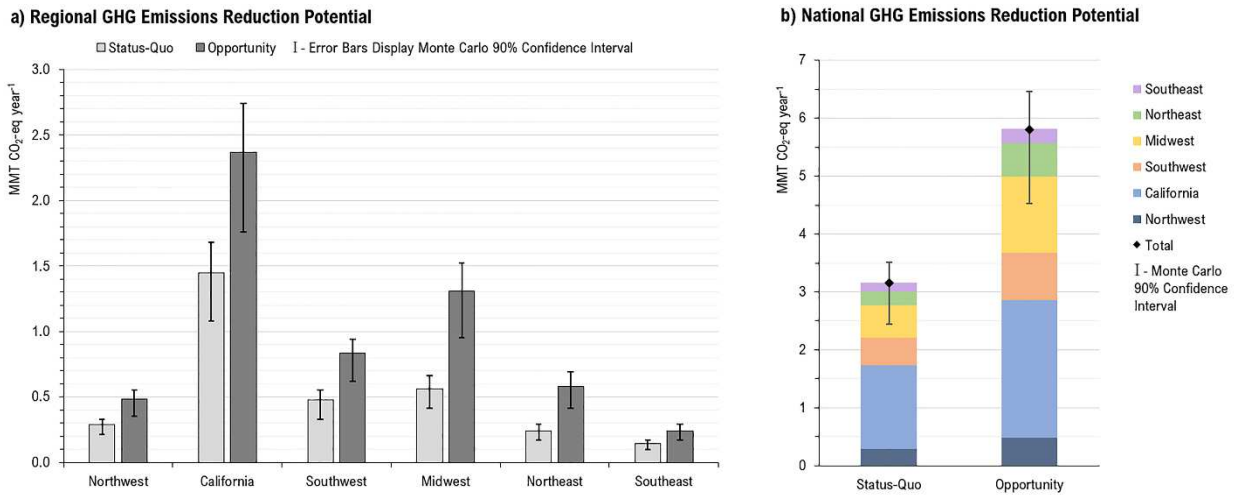

Figure 8: Regional greenhouse gas emissions (GHG) reduction potential from adopting anaerobic digestion technology for the status-quo and opportunity adoption cases (a) and contribution of each region to the total national GHG reduction potential under both adoption cases (b). Error bars display the uncertainty bounds derived from the 5000 simulation outputs from the Monte Carlo analysis of uncertainty.

Regional reductions under Status-Quo assumptions range from as little as 0.14 MMT CO_2-eq per year in the Southeast to as high as 1.45 MMT CO_2-eq per year in California. Status Quo adoption correlates to a total national GHG reduction potential of 3.15 MMT CO_2-eq per year. Under the opportunity adoption case, these figures increase to 0.24 MMT CO_2-eq per year in the Southeast, 2.37 MMT CO_2-eq per year in California, and a national GHG emission reduction of 5.82 MMT CO_2-eq per year, highlighting the improved emissions reduction opportunity for the dairy industry throughout the U.S. from incentivizing CHP on smaller farms. From a regional perspective, the greatest emissions reduction opportunities from AD adoption are in California (1.45 to 2.37 MMT CO_2-eq per year), the Midwest (0.56 to 1.31 MMT CO_2-eq per year), and the Southwest (0.47 to 0.83 MMT CO_2-eq per year).

These values can be compared to other national GHG assessments. The Status Quo and Opportunity adoption scenarios yield reductions of 7.6% and 14.1%, respectively, in total GHG emissions from all U.S. dairy manure [2]. The entire life cycle GHG emissions associated with

U.S. milk production is approximately 97 MMT CO_2-eq per year [122]. Accounting for 15% of manure emissions allocated to beef cattle in the farmgate life cycle assessment, [122] these reductions translate to a 3.8% and 7.1% reduction in total GHG emissions from all U.S. milk production for the Status Quo and Opportunity adoption scenarios, respectively. The reductions quantified in this study represent a smaller portion of overall industry emissions. However, farm-level emissions reductions between baseline and AD scenarios range from 58.1% to 78.8%, depending on the region. These farm-level reductions surpass the IPCC's 45% target by 2030 [84], underscoring the need for faster AD adoption across all industry levels to achieve greater emissions reductions and mitigate climate change impacts.

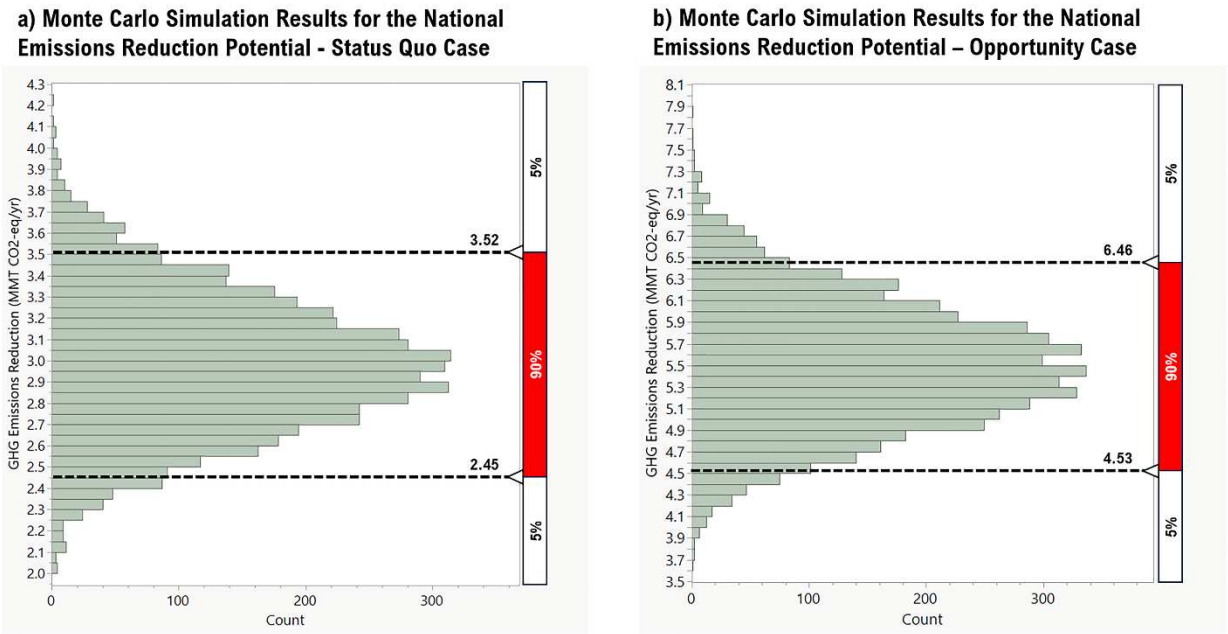

Figure 9: Monte Carlo simulation output summary showing the national emissions reduction potential under the Status Quo (a) and Opportunity (b) adoption case. Each figure presents an uncertainty bound, indicating the range encompassing 90% of the simulation outcomes.

Figure 9 displays the Monte Carlo analysis results, outlining the uncertainty bounds for estimated emissions reductions due to variability in key model inputs. For national emissions

reduction estimates, 90% of simulated estimates were between 2.45 to 3.52 MMT CO_2-eq annually under the Status Quo case, accounting for a 5.9-8.5% reduction in U.S. dairy manure management emissions. For the Opportunity case, 90% of simulated reductions were between 4.53 to 6.46 MMT CO_2-eq per year, or 10.9-15.6%. The sensitivity analysis reveals that activation energy and bioassay temperature, key factors in calculating the Arrhenius factor, significantly influence these estimates. Detailed regional results and further sensitivity analysis data are provided in Appendix B.

For another point of comparison, carbon intensity (CI) scores are offered in Appendix B for electricity and RNG per MJ of energy when going from each baseline scenario to each adoption scenario in each respective region.

3.3.3 Other Potential Environmental Impacts

In discussing the environmental ramifications of land applying digestate from the AD of dairy manure, it's crucial to consider a spectrum of potential impacts beyond the primary goal of GHG emissions reduction. While digestate application can enrich soil nutrients and reduce the need for synthetic fertilizers, it also presents challenges. For instance, the high nutrient content, particularly nitrogen and phosphorus, can lead to nutrient runoff into water bodies, potentially exacerbating eutrophication in aquatic ecosystems [123]. Moreover, the application of digestate must be carefully managed to prevent the leaching of nitrates into groundwater, posing risks to water quality and public health. Additionally, the presence of pathogens and pharmaceutical residues in digestate requires attention, as improper handling and application can affect soil health and biodiversity. As the anaerobic digestion process converts organic matter into more stable forms, there is also a potential impact on soil carbon sequestration capacities, which

warrants further investigation to fully understand the balance between emissions reductions and potential trade-offs in soil carbon dynamics. Therefore, while the land application of digestate offers a sustainable waste management solution, it necessitates a holistic assessment of environmental impacts to optimize benefits and mitigate adverse effects.

3.3.4 Recommendations

There are several limitations in this modeling approach. The monthly time step used for methane calculations and the annual time step for N_2O emissions could benefit from increased temporal resolution. Thermal modeling to estimate the actual temperature of ambient lagoons and liquid/slurry storages was not included, relying on ambient temperature data. Expanding the system boundary to include feed production and including biogenic carbon accounting in the framework could further enhance accuracy of the results. Further validation of study results with farm-level data is imperative to confirm the reliability and accuracy of the identified emissions reduction potential. Actual AD adoption will depend heavily on economic viability, which relies on dynamic factors such as carbon markets, government subsidies, milk production, and other economic influences. The preliminary economic modeling performed in this study does not consider these dynamic factors in adoption estimates and introduces uncertainty into the emissions reduction estimates. Lastly, this study considered larger-scale dairy, however the combination of technical innovation coupled with policy has the potential to reduce the size of dairy farms adopting anaerobic digestion. Despite these limitations, this study offers valuable insights from the expanded system boundary and inclusion of N_2O emissions. Additionally, extensive peer review and discussion from the MTT has ensured that regional modeling assumptions are aligned with actual industry practices.

Several strategic recommendations emerge from this study to enhance GHG reduction through AD adoption in the U.S. dairy industry. Scenario specific results highlight the promise of AD adoption in confined scrape systems with 100% manure collection. These systems benefit from reduced N_2O emission and maximized diesel or grid emissions avoidance credits. In lagoon systems, increasing the biogas collection efficiency of installed liners can yield further GHG reductions. Additionally, enhancing solid-liquid separation processes with technologies that achieve higher VS removal rates can provide further reductions in life cycle emissions. The introduction of targeted policy incentives, such as subsidies or tax incentives, is recommended to encourage adoption among smaller farms and support transitions to more efficient manure management systems. A comprehensive environmental assessment of digestate application is crucial to ensure that GHG reduction benefits are not offset by other environmental risks such as nutrient runoff and groundwater contamination. These recommendations aim to guide industry stakeholders in implementing strategies that align with national and global sustainability goals.

CHAPTER 4: ECO-STEPS: A MULTI-CRITERIA DECISION SUPPORT TOOL FOR EVALUATING THE SUSTAINABILITY OF ENGINEERED CLIMATE SOLUTIONS

4.1 Introduction

The emission of greenhouse gases (GHGs) from human activities has unequivocally caused global warming, resulting in a global surface temperature rise of approximately 1.1°C above pre-industrial levels [1]. Since 1970, the rate of warming has accelerated more rapidly than in any other 50-year period in the last 2000 years, leading to extensive and far-reaching changes in the atmosphere, oceans, cryosphere, and biosphere [1]. This increase in GHG emissions is driven by unsustainable energy use, land-use changes, and shifting patterns of consumption and production. These changes have disproportionately affected vulnerable communities, particularly those who have historically contributed the least to climate change, while the accumulation of GHGs continues to drive unprecedented levels of warming [1].

The impacts of this warming are severe and multifaceted, ranging from the loss of human lives and property to the degradation of ecosystems. Extreme weather events, such as heatwaves, floods, and storms, have become more frequent and intense, leading to significantly higher mortality rates, especially in vulnerable regions where climate-related disasters were 15 times more deadly between 2010 and 2020 [1]. Beyond immediate loss of life, climate change exacerbates public health crises through increased heat-related illnesses, respiratory conditions due to worsening air quality, and the spread of vector-borne diseases. Ecosystems are suffering irreversible damage, with the retreat of glaciers, thawing permafrost, and widespread loss of biodiversity, leading to substantial economic losses in sectors dependent on natural resources [1].

These profound impacts underscore the urgent need for immediate and sustained reductions in GHG emissions to prevent further damages and protect both natural and human systems.

Effectively reducing GHG emissions requires robust methods to quantify and evaluate potential solutions, and Life Cycle Assessment (LCA) serves as a powerful tool in this effort. By assessing and comparing a wide range of environmental impacts across every phase of a product or system's value chain, LCA provides the comprehensive perspective essential for guiding decisions in both the public and private sectors. As policies and regulations increasingly demand more rigorous environmental assessments [124]. LCA offers the critical framework needed to drive meaningful progress and support the development of effective and sustainable emission reduction strategies.

In addition to environmental sustainability, economic viability is a crucial factor in developing and implementing effective climate solutions. Techno-Economic Analysis (TEA) serves as a valuable tool for evaluating the economic aspects of potential technologies and strategies. By systematically analyzing the costs, benefits, and financial feasibility of various options, TEA provides a clear understanding of the economic trade-offs involved in reducing GHG emissions. This method not only helps to identify the most cost-effective solutions but also ensures that they are scalable. TEA and LCA are often integrated to provide a comprehensive framework for addressing both environmental and economic sustainability [3,4,125–128]. These integrated studies ensure that climate solutions are not only ecologically sound and economically viable but also optimized for real-world impact and rapid adoption.

While TEA and LCA provide powerful tools for evaluating the sustainability of potential solutions, it is important to recognize potential pitfalls in their application, particularly the risk of developing "tunnel vision." This term refers to the narrow focus on reducing costs and carbon

emissions as the primary or sole indicators of economic and environmental sustainability, respectively [129]. Although reducing carbon emissions is vital, this singular focus can lead to burden shifting, where efforts to mitigate one environmental impact inadvertently exacerbate another. For instance, a strategy solely focused on lowering carbon emissions might lead to excessive water consumption, habitat destruction, or social inequity, ultimately undermining its environmental sustainability and social license to operate. For example, efforts to reduce methane emissions from dairy manure management through anaerobic digestion may be a cost-effective solution for reducing GHG emissions while inadvertently increasing eutrophication potential or impacting water quality in nearby communities [123,130,131]. By broadening the scope of sustainability assessments beyond carbon emissions and costs, stakeholders can avoid the pitfalls of tunnel vision and develop strategies that address the complexity of environmental challenges in a more holistic manner.

The recognition and avoidance of burden shifting represents a critical aspect of the environmental justice movement. Emerging in the 1980s, this movement addresses the disproportionate environmental burdens faced by marginalized communities, focusing on equitable distribution of environmental burdens and benefits, inclusive decision-making, and the rectification of past injustices [132]. The environmental justice movement has laid the foundation for various forms of activism including climate justice, energy justice, food justice, and water justice and is intertwined with other sustainability frameworks such as the triple bottom line and the water-energy-food (WEF) nexus [133]. The WEF nexus, which emphasizes the interconnectedness of water, energy, and food systems, highlights the trade-offs and synergies between these vital resources. These resources are not only essential for sustaining human life but are also often at the center of environmental justice issues, where access and

availability can be starkly inequitable. Recent advances in the field of LCA have resulted in the creation of integrated assessment models that aim to integrate social and political dimensions into traditional LCA frameworks [134–137]. While these models provide valuable scientific insights, they are often based on numerous assumptions and subjective value judgments, making them challenging for policymakers to interpret or rely upon [45,138]. Similarly, recent attempts to quantify the synergies and trade-offs within the WEF nexus [139] have proven to be highly complex, requiring sophisticated methodologies that can be difficult for non-experts to grasp. Striking a balance between a comprehensive analysis of these trade-offs and presenting findings in a clear, accessible way for stakeholders is essential for effective decision-making.

A significant opportunity exists to enhance LCA results interpretation by leveraging existing output metrics to achieve actionable outcomes without relying on complex midpoint-to-endpoint models. This study introduces a user-friendly decision-making tool designed to support the development and implementation of effective climate solutions: the Environmental Comparison and Optimization Stakeholder Tool for Evaluating and Prioritizing Solutions (ECO-STEPS). ECO-STEPS is engineered to address the complexities and trade-offs of climate solution projects while providing actionable insights. It offers a comprehensive platform that integrates environmental and economic criteria with stakeholder priorities, enabling the holistic evaluation and prioritization of various climate strategies. The tool's capabilities are demonstrated through a case study on biofuels, comparing algae-based renewable diesel (RD), soybean biodiesel (BD), corn ethanol, and petroleum diesel. ECO-STEPS incorporates typical outputs from TEA and LCA studies, including economic viability (characterized by the minimum product selling price), 10 environmental impact categories from the Tool for the Reduction and Assessment of Chemicals and Other Environmental Impacts (TRACI) [45], as

well as water footprint, land use, and land value. ECO-STEPS streamlines the decision-making process by enabling decision-makers to pinpoint the most sustainable and effective solutions aligned with specific project goals and stakeholder priorities. By balancing simplicity with analytical depth, the tool serves as an essential resource for advancing long-term sustainability and climate resilience.

4.2 Methods

This study introduces ECO-STEPS, a user-friendly decision-making tool designed to support the development and implementation of effective climate solutions. The underlying framework utilizes standard outputs from TEA and LCA studies, stakeholder priorities, and statistical weighting methods to guide decision making for engineered climate solutions. The tool's capabilities are demonstrated through a case study evaluating various biofuel options, including algae-based RD, soybean BD, and corn ethanol, in comparison with conventional petroleum-based diesel.

4.2.1 Inputs Required for the ECO-STEPS Tool

The ECO-STEPS tool evaluates climate solutions using 14 key inputs derived from TEA and LCA studies, ensuring a comprehensive assessment of economic viability, environmental impacts, and resource use. These inputs are standardized to a common functional unit to ensure comparability across technologies. For the biofuel systems case study presented here, the chosen functional unit is 1 megajoule (MJ) of fuel.

Technology cost is determined through TEA and is characterized by the Minimum Fuel Selling Price (MFSP), expressed in dollars per MJ of fuel. Environmental impacts are calculated using the TRACI method, which quantifies ten midpoint metrics: respiratory effects,

acidification, ecotoxicity, non-carcinogenics, carcinogenics, global warming potential (including direct land use change emissions), smog formation, ozone depletion, eutrophication, and fossil fuel depletion [140]. Each impact is measured in specific units as defined by the TRACI methodology and is standardized to the chosen functional unit of 1 MJ of fuel. While the TRACI method covers a broad spectrum of environmental impacts relevant to stakeholders, it does not specifically address water or land use, which are key factors in the overall sustainability of engineered climate solutions [140].

To address this gap, water footprint and land use metrics are integrated into the analysis framework. While these may not be standard outputs directly reported from TEA and LCA studies, they are often quantified within the underlying process models, making them accessible additions for more comprehensive decision-making. The analysis considers both blue and grey water footprints, measured in cubic meters of freshwater per MJ of fuel. The blue water footprint reflects the volume of surface and groundwater consumed during the production process, whereas the grey water footprint indicates the amount of freshwater needed to assimilate pollutants and maintain water quality standards [62]. Land use inputs encompass both the total land footprint (in m^2 per MJ) and the land classification. This dual consideration allows for an assessment of the total land requirements as well as the broader economic implications of utilizing land with higher value.

4.2.2 Land Value Index

Land types within the US are categorized according to the National Land Cover Database (NLCD) [141] and include cultivated cropland, pasture/hay, barren, forest, shrubland, and grassland/herbaceous. While the NLCD also includes developed areas, wetlands, and water, these categories were excluded as they are unsuitable for large-scale biofuel production, which

relies on land types that can support biomass production and conversion infrastructure. The economic value of each land type was derived from a combination of official agricultural statistics and a detailed analysis of property listings. Values for cultivated cropland and pasture/hay were obtained from the USDA National Agricultural Statistics Service [94], with averages of $5,460 per acre for cropland and $1,760 per acre for pasture/hay. Meanwhile, economic values for land categories such as barren, mixed forest, shrub, and grassland/herbaceous were determined through a more comprehensive approach to account for their diverse uses and market conditions.

To determine the average cost per acre for the categories of barren, forest, shrubland, and grassland/herbaceous, a comprehensive property listing analysis was conducted using Zillow.com [142]. This analysis focused on the top four states with the largest shares of each respective land type, as identified by Wentland et al. [143]. Five property listings were obtained for each state, resulting in 20 listings per land type. Listings included details such as location, total acreage, and cost per acre, ensuring diverse representation across different regions.

From this dataset, the average cost per acre for each land type was calculated and is presented in Table 3. These values were normalized to develop a Land Value Index, providing a standardized measure (ranging from 0 to 1) to compare the economic value of different land types evaluated by the ECO-STEPS tool. This approach grounds the tool's land use considerations in current economic realities while capturing the unique characteristics of each land type. Detailed listings and analyses, including specific property data and market values, are provided in Appendix C to ensure transparency and reproducibility.

Table 3: Land type, average value per acre, and normalized Land Value Index used in ECO-STEPS.

Land Type	Average Value ($/acre)	Land Value Index (0-1)
Cultivated Crops	$5,460	0.71
Pasture/Hay	$1,760	0.23
Barren	$777	0.10
Forest	$7,732	1.00
Shrub	$3,248	0.42
Grassland/Herbaceous	$4,229	0.55

The required land type for each fuel production system is determined by the specific characteristics and demands of its production process. For biofuel crops such as corn and soybean, cultivated cropland is necessary due to the agricultural requirements for planting and harvesting these crops [125]. In contrast, algae-based fuels offer greater flexibility in land use by utilizing marginal or low-value lands, such as barren land and shrubland, which are less suitable for conventional agriculture but ideal for algae cultivation in open raceway ponds [3,4,144]. For petroleum diesel, shrubland is assumed to be the primary land type, reflecting the typical use of land associated with oil extraction infrastructure, such as well pads and supporting facilities [145].

The ECO-STEPS tool integrates land footprint and land value into a single "High-Value Land Use" impact criterion to comprehensively evaluate the economic and environmental trade-offs associated with different fuel production systems. This metric is obtained by multiplying the land use required per functional unit by the Land Value Index (Table 3). By applying this approach, the High-Value Land Use impact metric provides a weighted measure of land use that reflects both the quantity of land required and its relative economic value. For example, if a fuel production system requires large amounts of high-value cropland (as is the case for soybean BD

or corn ethanol), the impact on high-value land use will be more significant due to the higher economic value assigned to cultivated crops in the Land Value Index. Conversely, if a system predominantly utilizes low-value land types like barren land or shrubland (as with algae-based biofuels), the resulting impact on high-value land use will be lower, reflecting the lesser economic value of these land types. This metric helps highlight the potential opportunity costs of different fuel production systems and supports more informed decision-making that aligns with sustainability goals and economic realities.

4.2.3 Data Collection for Biofuels Systems and Conventional Diesel

Data were collected for three renewable fuels: algae-based RD, soybean BD, and corn ethanol, as well as petroleum diesel, to demonstrate the application of the ECO-STEPS tool. The assessed pathway for algae-based RD assumes large-scale microalgae cultivation in open raceway ponds, followed by a three-stage dewatering process, anaerobic storage to manage seasonal variability, and conversion to RD and naphtha via hydrothermal liquefaction. All required ECO-STEPS metrics for algae-based RD were sourced from Greene et al. (currently under review at Environmental Science and Technology). The spatiotemporal model developed by Greene et al. provides county-level TEA and LCA results enabling performance evaluation across the US. Five case study locations were chosen to capture a diverse range of algal productivities, water footprints, and grid emissions. Polk County, Florida was selected for its high productivity and low water footprint; San Diego County, California for its high productivity and low grid emissions; Pima County, Arizona for its high water footprint and abundance of non-arable land; Honolulu County, Hawaii for its high productivity paired with elevated grid emissions; and Webb County, Texas for its balanced water footprint, productivity, and moderate grid emissions.

For soybean BD and corn ethanol, TRACI metrics, MFSP, and land use data were sourced from the county-level biofuels assessment conducted by Smith et al. [125]. McClean County, Illinois, was selected as a representative location for soybean BD due to its status as a top producer of soybeans in the United States, while Kossuth County, Iowa, was chosen for corn ethanol due to its high corn production. Regional average water footprint metrics for these biofuels were sourced from Quiroz et al. [62]. For petroleum diesel, land use metrics and direct land use change emissions were based on data from Yeh et al. [146] with TRACI impacts obtained from Chen and Quinn [4] and water footprint data from Staples [147]. The cost of petroleum diesel was derived from the U.S. Energy Information Administration (EIA) [148]. All data used as case study inputs to the ECO-STEPS tool are summarized in Table 4.

Table 4: Summary of data inputs for the biofuels case study using ECO-STEPS

Parameter	Units	Algae Renewable Diesel					Soybean Biodiesel	Corn Ethanol	Petroleum Diesel
		San Diego County, CA	Pima County, AZ	Honolulu County, HI	Webb County, TX	Polk County, FL	McClean County, Il	Kossuth County, IA	US Average
Land Use	m2 per MJ	1.43E-02	1.49E-02	1.04E-02	1.44E-02	1.22E-02	6.71E-02	3.04E-02	1.39E-05
Land Type	Classification	Barren	Shrub	Shrub	Shrub	Shrub	Cultivated Crops	Cultivated Crops	Shrub
Land Index	Index	0.10	0.42	0.42	0.42	0.42	0.71	0.71	0.42
High Value Land Use	m2 per MJ	1.44E-03	6.24E-03	4.38E-03	6.05E-03	5.14E-03	4.74E-02	2.15E-02	5.82E-06
Water Footprint	m3 water per MJ	1.41E-02	1.72E-02	8.62E-03	1.30E-02	8.83E-03	9.00E-03	3.55E-02	2.09E-04
Respiratory Effects	kg PM2.5-eq per MJ	5.23E-05	5.49E-05	6.67E-05	5.51E-05	2.38E-05	2.71E-05	4.47E-05	1.62E-05
Acidification	kg SO2-eq per MJ	8.12E-02	8.51E-02	2.57E-01	8.85E-02	8.47E-02	6.77E-05	2.47E-04	1.44E-04
Ecotoxicity	CTUe per MJ	2.06E-01	2.17E-01	2.15E-01	2.20E-01	1.52E-01	3.82E-01	8.17E-01	1.94E-02
Non-Carcinogenics	CTUh per MJ	5.28E-09	5.57E-09	5.39E-09	5.37E-09	4.06E-09	1.57E-08	1.93E-08	7.71E-10
Carcinogenics	CTUh per MJ	2.09E-09	2.20E-09	2.05E-09	2.20E-09	1.60E-09	1.98E-09	3.19E-09	3.67E-10
Global Warming Potential*	kg CO2-eq per MJ	4.13E-02	4.37E-02	5.80E-02	4.48E-02	4.38E-02	1.87E-02	4.04E-02	8.84E-02
Smog Formation	kg O3-eq per MJ	9.49E-04	9.92E-04	2.65E-03	8.21E-04	8.66E-04	1.23E-03	2.59E-03	2.02E-03
Ozone Depletion	kg CFC-11 per MJ	6.48E-10	6.92E-10	8.27E-10	6.44E-10	6.73E-10	1.78E-09	3.79E-09	2.01E-08
Eutrophication	kg N-eq per MJ	1.32E-04	1.39E-04	1.38E-04	1.37E-04	7.87E-05	5.56E-05	2.15E-04	4.05E-05
Fossil Fuel Depletion	MJ per MJ	6.74E-02	6.87E-02	9.40E-02	7.54E-02	7.26E-02	2.55E-02	6.82E-02	1.67E-01
Minimum Fuel Selling Price	$ per MJ	$0.06	$0.06	$0.05	$0.06	$0.05	$0.03	$0.02	$0.03

**Global Warming Potential includes direct land use change (dLUC) emissions*

4.2.4 Criteria Ranking and Weighting in ECO-STEPS

To ensure comparability, all required input data must first be harmonized to the common functional unit of 1 MJ of fuel. Then, values are normalized across competing technologies for each sustainability criterion. Following data collection and normalization, stakeholders are asked to rank each of the 13 criteria from most important (rank 1) to least important (rank 13) and indicate their confidence level in these rankings (high, medium, or low). Based on this input, the tool employs different statistical weighting methods to assign overall importance to each criterion according to stakeholder priorities. Combining stakeholder rankings with the most appropriate weighting method, the tool calculates an overall impact score for each technology. This score is determined by the product sum of normalized economic and environmental criteria with their assigned weights. The technology option with the lowest total impact score is identified as the most favorable solution, aligned with stakeholder priorities.

4.2.4.1 Exponential Decay Weighting Method

For stakeholders who express high confidence in their rankings, the ECO-STEPS tool utilizes an exponential decay model to assign weights. This approach places significant emphasis on the highest-ranked criteria, with exponential decay rapidly diminishing the weight of lower-ranked criteria. The first two criteria receive weights of 0.78 and 0.17, respectively, while subsequent criteria have significantly lower weights, nearing zero past the third criterion. The formula for exponential decay weighting is given by Equations 2 and 3:

$$W_{i,raw} = e^{-k(i-1)} \qquad \text{(Eq.2)}$$

where $W_{i,raw}$ is the raw exponential weight of the i-th criterion, and k is the decay constant, which approximately equals 1.21 for the ECO-STEPS tool, which considers 13 criteria. Raw weighting factors are then normalized to ensure they sum to 1 by Equation 3:

$$W_i = \frac{W_{i,raw}}{\sum_i^j W_{i,raw}} \qquad \text{(Eq. 3)}$$

The exponential weighting method has the advantage of providing a clear focus on the top-ranked criteria, which can be particularly beneficial when the decision-making process hinges on a few key factors. This sharp differentiation allows stakeholders to prioritize their most critical concerns effectively. However, the rapid decline in weighting for lower-ranked criteria may overlook potentially important but lower-priority considerations, making it less suitable in scenarios where a more balanced assessment across all criteria is desired. This method is most effective when stakeholders have strong confidence in their rankings and the primary objective is to concentrate on the highest-priority factors.

4.2.4.2 Rank Order Centroid Weighting Method

The tool employs the Rank Order Centroid (ROC) statistical weighting method if stakeholders indicate a medium degree of confidence in their rankings. This method offers a more balanced distribution of weights, starting with 0.24 for the highest-ranked criterion, followed by 0.17 for the second, 0.13 for the third, and 0.10 for the fourth, with weights gradually decreasing to a minimum of 0.006 for the 13th criterion. The ROC weighting is calculated with Equation 4:

$$W_i = \frac{1}{n}\sum_{j=i}^{n}\frac{1}{j} \qquad \text{(Eq. 4)}$$

where W_i is the weight of the i-th criterion and n is the total number of criteria.

The ROC method provides a moderate approach to weighting, suitable for situations where stakeholders have medium confidence in their rankings. While it still places more emphasis on the top criteria, it does so with less intensity than exponential decay, which heavily prioritizes the first and second criteria. In the ROC method, weights decrease more gradually, offering diminishing returns after the fourth criterion. This allows the top-ranked criteria to be emphasized, but not to the extent that lower-ranked criteria lose relevance entirely. This characteristic makes the ROC method advantageous for scenarios where decision-makers want to maintain focus on the most important criteria while still considering the broader range of factors. The ROC method is also widely utilized in other multicriteria decision analyses (MCDA), such as the framework for assessing technology appropriateness developed by Bauer and Brown [149], demonstrating its broad applicability in various contexts.

4.2.4.3 Rank Sum Weighting Method

For stakeholders with low confidence in their rankings, the Rank Sum method is used, which offers a more equal weighting across criteria. This method provides a relatively uniform distribution of weights, with the highest-ranked criterion receiving a weight of 0.14, followed by 0.12 for the second, and 0.11 for the third, with weights decreasing linearly as the rank lowers. By the 10th criterion, the weight drops to 0.04, and it reaches a minimum of 0.01 by the 13th criterion. Weighting factors for the rank sum method are determined by Equation 5:

$$W_i = \frac{\frac{1}{R_i}}{\sum_{j=1}^{n} \frac{1}{R_j}} \qquad \text{(Eq. 5)}$$

where W_i is the weight of the i-th criterion and n is the total number of criteria.

The advantage of the Rank Sum method is that it prevents any single criterion from dominating the overall evaluation, making it suitable for situations where there is uncertainty or

limited consensus on the relative importance of criteria. However, the downside is that it may dilute the influence of more critical criteria, as the weighting is less sensitive to priority differences compared to the exponential decay or ROC methods. The Rank Sum method is applicable in decision-making frameworks that require an equitable approach, providing a way to account for all criteria without heavily favoring the top-ranked ones. This makes it particularly useful when stakeholders have diverse opinions or when a balanced evaluation of multiple criteria is desired. Curves showing the distribution of criteria weights for each weighting method are shown in Figure 10.

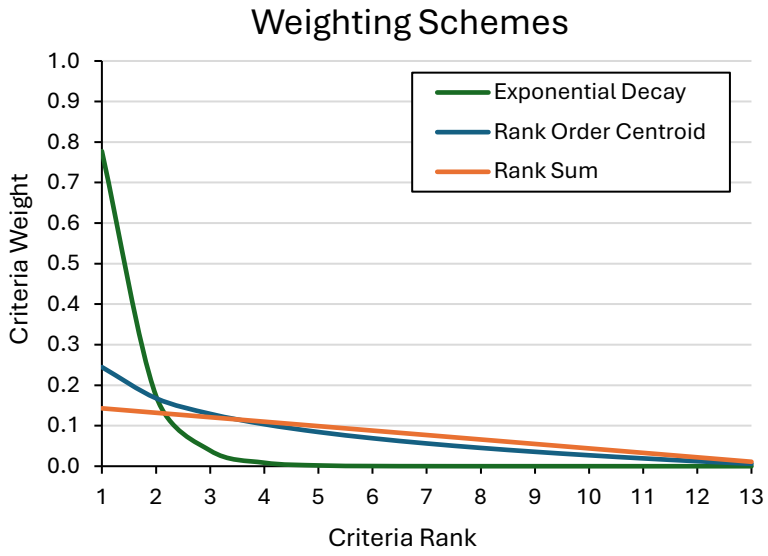

Figure 10: Distribution of criteria weights for the exponential decay, rank order centroid, and rank sum weighting methods used in ECO-STEPS.

4.2.5 Permutation Analysis

To enhance decision-making, ECO-STEPS features a permutation analysis tool that examines the user's top six criteria and recalculates impact scores for all possible permutations of these criteria. This allows stakeholders to explore how different combinations affect the

performance and ranking of each technology, providing insights into potential trade-offs and dependencies between criteria.

Permutation analysis helps stakeholders understand the robustness of selected technologies under varying priorities, revealing which solutions remain consistently optimal and which are sensitive to specific criteria. By systematically exploring various arrangements of the top-ranked criteria, stakeholders can see how different perspectives influence technology rankings, offering a comprehensive view of potential outcomes.

This analysis can also uncover scenarios where less favored options perform better under certain conditions. For example, a technology that ranks lower when considering environmental impacts might excel when prioritizing economic factors. This capability provides a nuanced understanding of how shifting priorities affect technology choices, supporting a more transparent and inclusive decision-making process. By highlighting alternative scenarios, permutation analysis allows stakeholders to see the strengths and weaknesses of each option, encouraging a balanced approach to selecting climate solutions that align with diverse stakeholder values and objectives.

4.2.6 Stakeholder Input and Surveys

For the biofuels case study, a survey was conducted with 9 experts (7 external respondents plus both authors of this study) in the field to capture diverse perspectives on sustainable biofuel development. Respondents were asked to rank each of the 13 criteria from most to least important, thereby reflecting their priorities and considerations for evaluating biofuel technologies. This survey approach mimics a decision-making room, where stakeholders from different backgrounds and expertise collaboratively assess and prioritize criteria that align with broader sustainability goals.

By simulating this decision-making environment, the survey results provide a valuable representation of how experts might negotiate and compromise on criteria rankings when selecting the most viable climate solutions. The data collected from these expert rankings serve as a foundation for the initial impact scores calculated in this study. These results, summarized in Appendix C, offer a starting point for further analysis using the ECO-STEPS tool, enabling the exploration of how different weighting methods and stakeholder priorities can influence technology rankings and recommendations.

4.2.7 Pre-Made Sustainability Themes

When stakeholders cannot reach a consensus on the top decision priorities, ECO-STEPS provides pre-made categorical rankings that order the 13 technology criteria in relation to specific sustainability themes. These pre-made categories include human health, terrestrial biodiversity, aquatic biodiversity, economic viability, food and water supply, energy supply, and global impacts.

These predefined themes can be evaluated using the standard statistical weighting methods described earlier or through an alternative approach employing the geometric mean. In this process, criteria are not only ranked by their overall importance but are also assigned levels of influence—direct, indirect, peripheral, or marginal—reflecting their specific relevance to the theme. Appendix C includes the criteria ranking and their influence levels for each of the seven pre-made sustainability themes. The geometric mean method provides a systematic way to assess the relative importance of each criterion within a theme by making pairwise comparisons.

For each pairwise comparison, the assigned levels of influence are compared to determine the relative weight of one criterion against another. The geometric mean is then calculated to provide a composite score that reflects the cumulative importance of each criterion

within the sustainability theme. This approach captures the multiplicative relationships between criteria, offering a refined weighting system highlighting subtle stakeholder priority differences. The geometric mean for each criterion is determined by Equation 6:

$$GM_i = \left(\prod_{j=1}^{n} M_{ij}\right)^{1/n} \qquad \text{(Eq. 6)}$$

Where GM_i is the geometric mean for criterion i, n is the total number of criteria, and M_{ij} is the pairwise comparison value representing the relative influence of criterion i compared to criterion j defined by Equation 7:

$$M_{ij} = \begin{cases} 5 \text{ if } I_i > I_j \\ 1 \text{ if } I_i = I_j \\ 0.2 \text{ if } I_i < I_j \end{cases} \qquad \text{(Eq. 7)}$$

where I_i and I_j are the level of influence of criterion i and j, respectively.

The values of 5 and 0.2 were chosen for the pairwise comparison to maintain an appropriate level of sensitivity in the weighting calculations. This selection allows for a clear differentiation between levels of influence among the criteria while keeping the weighting factors within a meaningful range for decision-making. The resulting weights for criteria with direct influence fall between 0.1 and 0.2, ensuring these criteria are prioritized more heavily in the overall assessment. Criteria with indirect influence receive weights between 0.05 and 0.1, reflecting their moderate importance without overshadowing the most critical factors. Criteria with peripheral influence are assigned weights between 0.02 and 0.05, while criteria with marginal influence are given weights of less than 0.02. This structured weighting scheme ensures that the most relevant criteria are appropriately emphasized, while those with less impact are proportionately scaled down, providing a balanced and interpretable framework for stakeholders to assess trade-offs among multiple factors. Following the calculation of the geometric mean, the

geometric means for each criteria are normalized to determine the final weighting factor by Equation 8:

$$W_i = \frac{GM_i}{\sum_{j=1}^{n} GM_j} \qquad \text{(Eq. 8)}$$

This method provides a nuanced assessment of the criteria's importance and enables stakeholders to compare technology performance across a wide array of contexts, even when consensus on priorities is lacking.

Technologies are evaluated across each sustainability theme and with each of the four weighting methods: exponential decay, ROC, Rank Sum, and geometric mean. For each theme and weighting method, the ECO-STEPS tool calculates an overall impact score for every technology option. Technologies are then assigned a "number of wins," indicating how often a technology achieves the lowest impact score across different sustainability themes and weighting approaches.

This "number of wins" metric enables stakeholders to easily identify which technologies perform best under specific sustainability themes, such as human health or energy security, and under various weighting scenarios that emphasize different priorities. The results highlight the strengths and weaknesses of each technology in relation to diverse sustainability goals and provide a clear picture of their sensitivity to different criteria. This comprehensive analysis helps stakeholders understand not only the overall performance of each technology but also how performance shifts depending on the weighting method and criteria rankings. By visualizing these results, stakeholders can more effectively balance trade-offs and make informed decisions that align with their unique sustainability objectives.

ECO-STEPS incorporates comprehensive and flexible evaluation methods to support decision-making, whether stakeholder preferences are aligned or diverge. By offering insights across multiple weighting methods and sustainability themes, the tool enables a deeper understanding of trade-offs and technology performance under various scenarios. This flexibility allows stakeholders to make informed decisions when there is strong agreement on priorities and high confidence in criteria rankings. At the same time, it offers a valuable approach for situations where consensus is lacking by using pre-made environmental themes to evaluate potential impacts across areas such as biodiversity, the WEF nexus, and global sustainability. The following results section demonstrates the application of these methods to assess the comparative performance of various biofuels against petroleum diesel, highlighting their relative sustainability and identifying the most effective solutions based on stakeholder priorities and sector goals.

4.3 Results and Discussion

The results in Figure 11 illustrate the impact scores for each technology derived from expert survey rankings of the 13 sustainability criteria, evaluated under three distinct weighting methods: exponential decay, ROC, and rank sum. These methods provide different perspectives on the relative performance of each technology, revealing the influence of prioritization on sustainability outcomes.

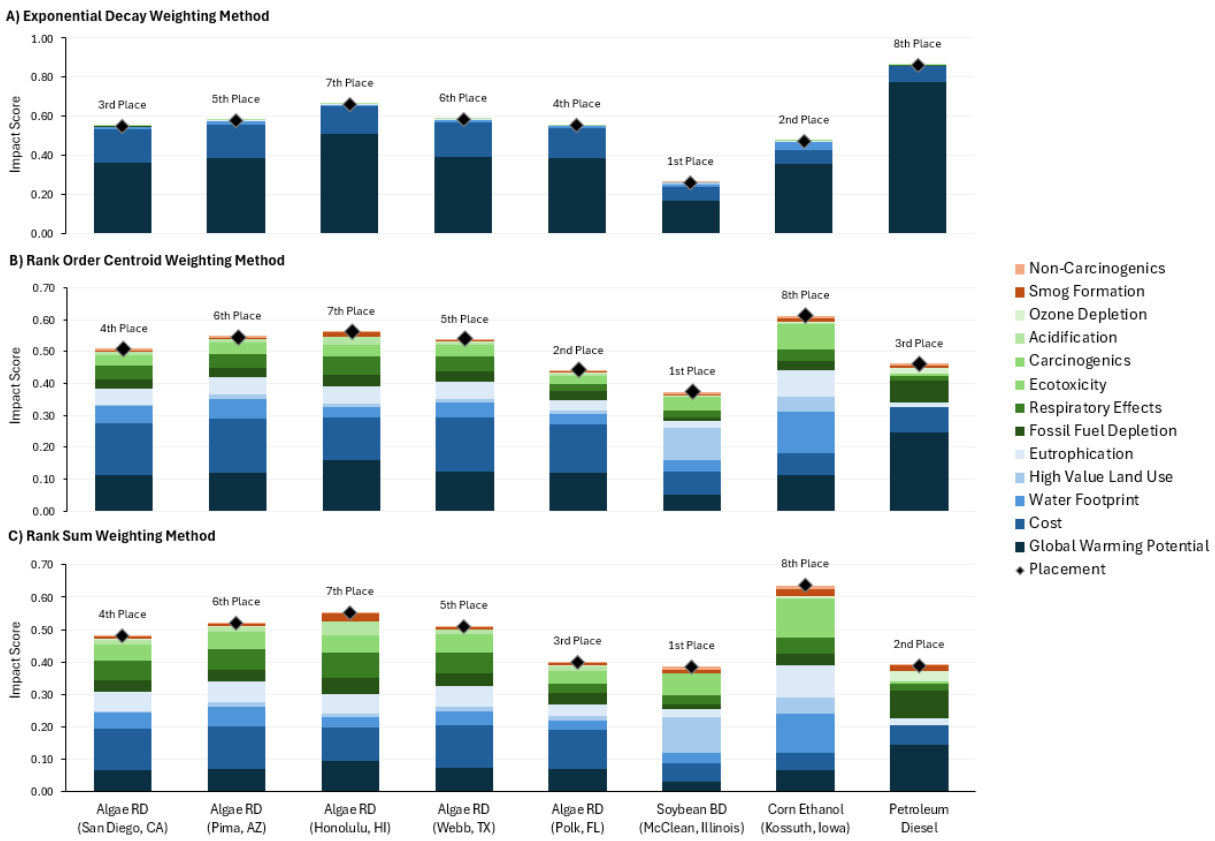

Figure 11: Resulting impact score of each technology under three different weighting methods: A) Exponential Decay, B) Rank Order Centroid, and C) Rank Sum using criteria rankings from the expert survey.

Under the exponential decay weighting method, the impact score for each fuel scenario is heavily influenced by the two highest-ranked criteria: GWP and cost, which receive weights of 0.78 and 0.17, respectively. This strong emphasis on GWP and cost results in soybean BD, corn ethanol, and algae RD in San Diego County emerging as the top three performers, ranked first, second, and third, respectively. With the lowest GWP and second lowest cost across fuel types, soybean BD secures the first-place position under the exponential decay method. Corn ethanol follows in second place, driven by the second-lowest GWP and lowest overall cost. Despite the high cost of algae RD in San Diego County (third highest among all scenarios), the low carbon intensity of the California electricity grid results in the third lowest GWP across fuel scenarios and secures its third-place position under the exponential decay weighting method. Petroleum

diesel has the highest GWP across fuel types coming in last place despite having the second lowest overall cost. The remaining algae RD scenarios rank between fourth and seventh place due to high production costs which can be attributed to the low technology readiness level (TRL) of algae biofuels [150]. The exponential decay method's strong focus on the top-ranked criteria—GWP and cost, identified as the highest priorities in the expert survey—minimizes the impact of lower-priority factors like water footprint or high-value land use on the final impact scores. This narrow emphasis effectively marginalizes other important sustainability criteria that significantly alter technology rankings under more balanced weighting methods.

Under the ROC weighting method, a more balanced influence of different impacts is observed on the overall scores. For example, corn ethanol drops from second to eighth place, mainly due to its large water footprint, high-value land use, and ecotoxicity, which outweigh the benefits of low cost and GWP seen in the exponential decay method. Soybean BD remains in first place, driven by its low impact across the top-weighted criteria of cost, GWP, water footprint, and high-value land use. With a higher emphasis on water footprint under the ROC weighing method (weighting factor of 0.12) the low water use of algae RD in Polk County, FL secures the second-place ranking. An interesting trend is observed with petroleum diesel moving into third place. Despite its high GWP (the highest weighted criterion), its low cost, water footprint, and impact score for high-value land use make petroleum diesel competitive under the ROC weighting method. The remaining algae RD scenarios show mixed performance, ranking between fourth and seventh place across the remaining counties.

Under the rank sum weighting method, a notable shift occurs as this method provides a more even distribution of weights across all criteria. Here, later-ranked categories, such as high-value land use (ranked fourth) and eutrophication (ranked fifth), gain more influence. As a result,

petroleum diesel achieves a lower total impact score than algae RD in Polk County, FL shifting from third to second place. Soybean BD maintains its first-place ranking, while corn ethanol remains in last place due to high impacts across multiple criteria. Contrary to the exponential decay weighting method, which magnifies the low GWP and cost of corn ethanol, rank sum considers a broader range of impacts, revealing its higher overall environmental burden.

An intriguing trend emerges when comparing the performance of algae RD across different locations. For instance, despite having the highest productivity and lowest cost across algae RD scenarios, the heavy reliance on fossil fuels in the Hawaiian electricity grid adversely affects several impact categories, including GWP, eutrophication, respiratory effects, ecotoxicity, and acidification. These impacts make algae RD in Honolulu County the worst-performing algae scenario under all three weighting methods. Similarly, increased evaporation rates in the Desert Southwest increase the impact scores for San Diego County, CA, Webb County, TX, and Pima County, AZ, under the ROC and Rank Sum weighting methods, resulting in fourth-, fifth-, and sixth-place rankings, respectively. Conversely, the low water footprint of algae RD in Polk County propels it to first place across algae scenarios and second place across all technologies under the ROC method, despite its higher cost. This demonstrates the sensitivity of algae-based biofuels to regional grid emissions and water footprint and emphasizes the importance of location-specific assessments.

Overall, these results illustrate the importance of carefully selecting weighting methods when evaluating climate solutions, as different methods can significantly impact the perceived sustainability of a technology. The exponential decay method offers a clear view of the highest-priority criteria but may overlook other relevant factors. ROC provides a moderate balance, allowing a broader perspective while still emphasizing key criteria. Rank sum, with its more

even distribution, ensures a holistic evaluation across all criteria but may dilute the impact of the most critical concerns. Seven of the nine survey respondents expressed medium confidence in the rankings, while two indicated high confidence, suggesting that the ROC method reflects stakeholder input most accurately. Based on these rankings and confidence levels, soybean BD and algae RD stand out as the most sustainable alternatives to petroleum diesel.

The flexibility of ECO-STEPS in applying various weighting methods allows stakeholders to explore multiple perspectives, providing valuable insights into the trade-offs, robustness, and sensitivities of different technologies. This capability supports more nuanced decision-making by highlighting how changes in stakeholder priorities can shift the ranking and overall sustainability performance of the evaluated technologies. Figure 12 presents the results of the permutation analysis, which explores the impact scores for each technology under every possible permutation of the top six criteria from the expert survey (GWP, cost, water footprint, high-value land use, eutrophication, and fossil fuel depletion) using each of the three weighting methods: exponential decay, ROC, and rank sum.

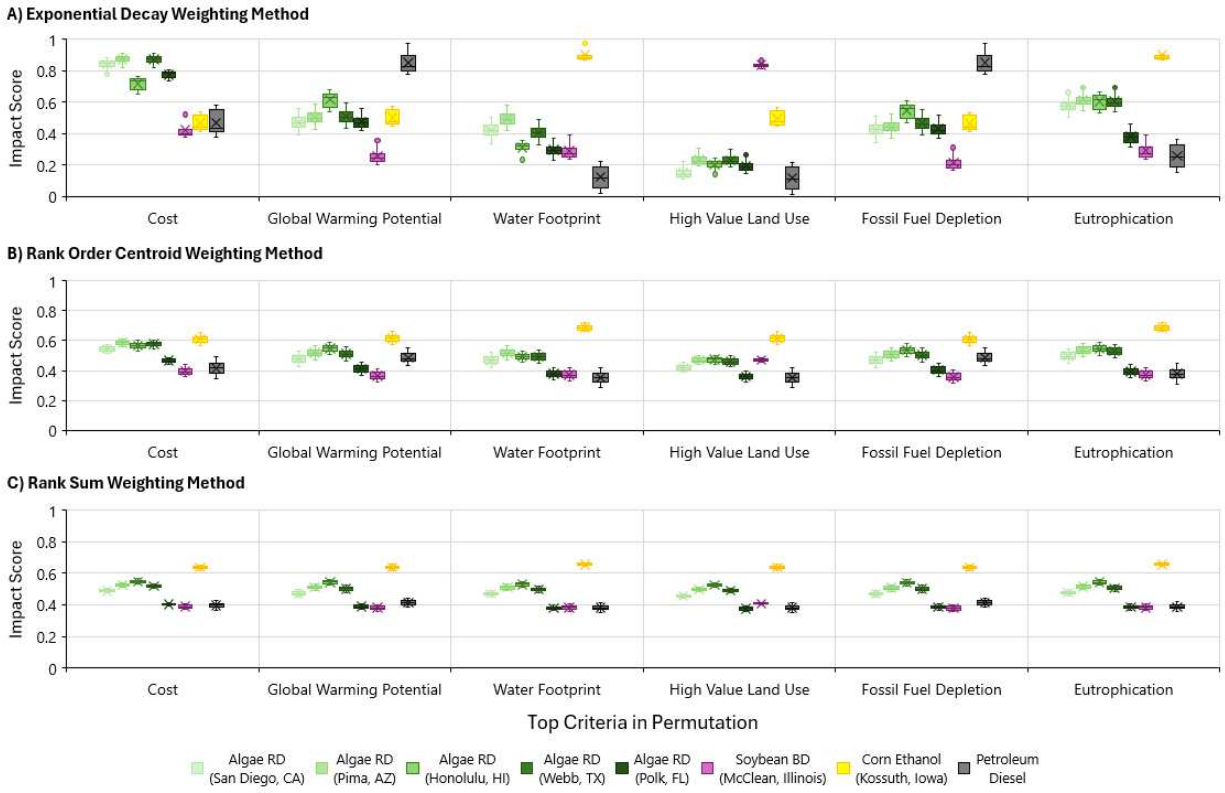

Figure 12: Results of the permutation analysis showing the impact scores for each technology across all possible permutations of the top six criteria identified by the expert survey, under three weighting methods: exponential decay, rank order centroid, and rank sum. Each box plot represents the distribution of impact scores for a technology under a given weighting method, illustrating how technology rankings change depending on criteria ordering.

Under the exponential decay weighting method, technology performance is highly sensitive to the criteria ordering, as this method places significant emphasis on the top-ranked criteria. For example, all algae scenarios have the highest impact scores (worst performance) in permutations where cost is the top criterion, reflecting the high costs associated with algae-based RD due to its low TRL. In contrast, in cost-driven permutations, soybean BD and corn ethanol show economic parity with petroleum diesel. Conversely, petroleum diesel exhibits the highest impact scores under permutations where GWP and fossil fuel depletion are prioritized, highlighting its poor environmental performance. Corn ethanol scores poorly when water footprint is prioritized, while algae RD in Polk County, which has the lowest water footprint

among the algae scenarios, remains competitive against soybean BD. Corn ethanol shows the highest impact for eutrophication, and both corn ethanol and soybean BD have the greatest impacts for high-value land use, while algae scenarios perform more competitively with petroleum diesel on this criterion. The permutation analysis under exponential decay highlights the strengths and weaknesses of each technology and their sensitivity to the criteria weighting. For example, the wide distribution of impact scores for petroleum diesel, as shown by the box and whisker plots, reflects the trade-offs between its strong performance in cost, water footprint, and land use and its poor performance in criteria like fossil fuel depletion and GWP. Similarly, certain algae scenarios can outperform petroleum diesel in permutations where high-value land use is the top criterion, notably when criteria like GWP or fossil fuel depletion are ranked second. Conversely, petroleum diesel can outperform algae when cost or land use is ranked second.

Under the ROC weighting method, differences between technologies are less pronounced, and more general trends emerge. Corn ethanol consistently performs the worst across all permutations due to its poor scores in several environmental categories. Soybean BD performs best in permutations where cost, GWP, and fossil fuel depletion are among the top-weighted criteria, while petroleum diesel excels in permutations prioritizing cost, water footprint, high-value land use, and eutrophication. Algae scenarios generally fall in the middle range; however, algae RD in Polk County can outperform soybean BD and petroleum diesel under permutations where criteria like GWP, water footprint, high-value land use, fossil fuel depletion, and eutrophication are more heavily weighted. This analysis also reveals that under ROC, algae across all five locations can outperform corn ethanol in cost-driven permutations, underscoring

the significant environmental impacts of corn ethanol. However, soybean BD and petroleum diesel consistently outperform algae in all cost-forward permutations under this method.

When applying the rank sum method, these trends are further reinforced. Corn ethanol remains the worst performer in all permutations. Algae RD in Polk County, Florida, emerges as a strong performer, surpassing petroleum diesel and becoming competitive with soybean BD in permutations where GWP, fossil fuel depletion, and eutrophication are top criteria. Moreover, algae RD in Polk County takes the top spot in permutations where water footprint and high-value land use are prioritized and even becomes competitive with soybean BD and petroleum diesel in permutations where cost is the top criterion.

As the weighting method becomes less extreme—from exponential decay to rank order centroid to rank sum—it offers a more balanced view of sustainability and technology performance, placing greater emphasis on criteria beyond the top two ranked criteria. This balanced perspective allows for a more comprehensive assessment of each technology's overall impacts, capturing a wider range of factors beyond the major strengths and weaknesses emphasized under more extreme weighting methods.

Figure 13 illustrates the performance of each technology across the seven pre-made sustainability themes—human health, terrestrial biodiversity, aquatic biodiversity, economic viability, food and water supply, energy supply, and global impacts—under four weighting methods: Exponential Decay, ROC, Rank Sum, and Geometric Mean. The "number of wins" metric identifies the technology with the lowest impact score within each theme and weighting method, providing insights into how different technologies align with varied sustainability priorities.

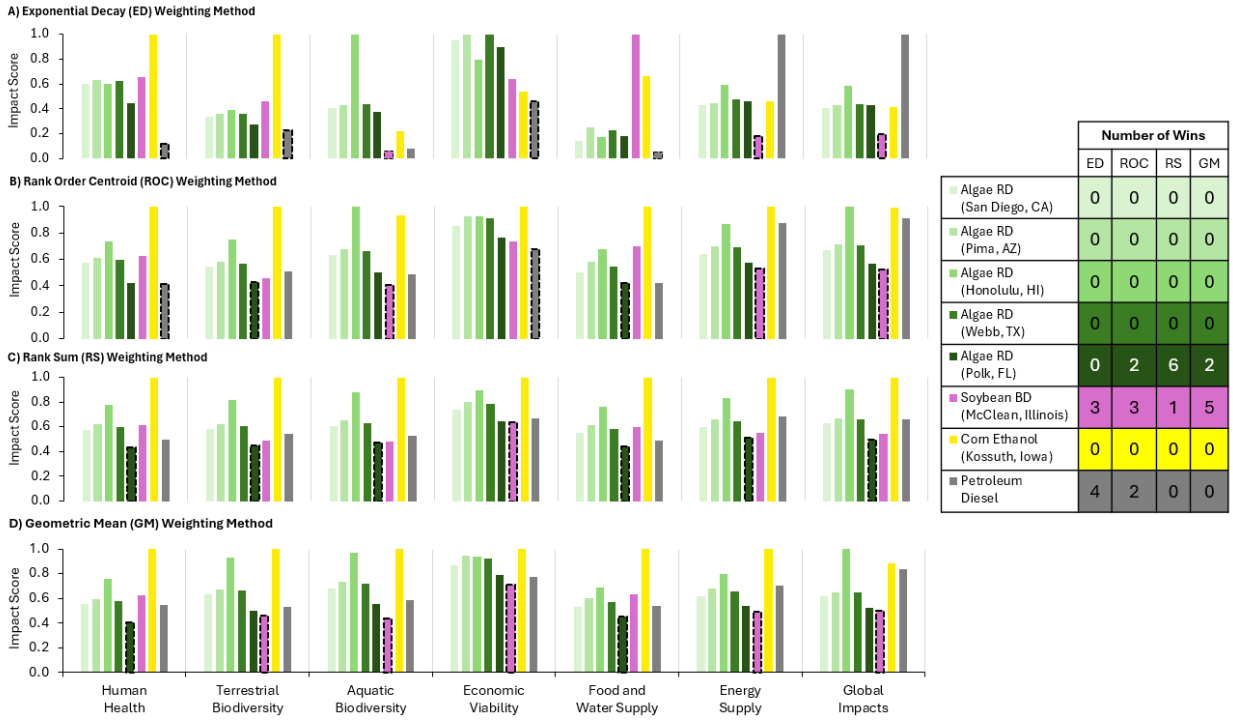

Figure 13: Technology performance in relation to the seven sustainability themes across four criteria weighting methods including A) Exponential Decay (ED), B) Rank Order Centroid (ROC), C) Rank Sum (RS), and D) Geometric Mean (GM). The total number of wins across sustainability themes for each technology is also provided.

The results in Figure 13 indicate that soybean BD is a consistently strong performer across different sustainability themes and weighting methods, securing three wins under exponential decay, three under rank order centroid, one under rank sum, and five under geometric mean. This demonstrates soybean BD's versatility and robustness in balancing economic viability with environmental impacts. Its wins in numerous sustainability themes under both extreme weighting methods (exponential decay) and more balanced approaches (ROC and geometric mean) highlight its ability to perform well across various sustainability scenarios. This suggests that soybean BD is an effective choice in contexts where both cost and environmental criteria are crucial, making it a broadly adaptable technology option.

Algae RD in Polk County, FL, performs well under more balanced weighting methods like ROC, rank sum, and geometric mean due to its favorable impact profile across various

sustainability themes. Under ROC, it secures wins in terrestrial biodiversity and food and water supply, owing to its low ecotoxicity, emissions, and water footprint, which are critical factors in these themes. Under rank sum, algae RD in Polk County, FL demonstrates even stronger competitiveness, winning in all themes except economic viability, which remains closely competitive with soybean BD. The more even distribution of weights in rank sum favors technologies with strong, balanced performance across multiple criteria. Algae RD in Polk County, FL benefits from this holistic approach, particularly excelling in themes like human health, aquatic biodiversity, and global impacts, where low water footprint, efficient land use, and lower fossil fuel depletion are prioritized. This underscores the potential of algae-based biofuels in sustainability contexts that demand comprehensive evaluations of resource use and environmental impacts.

Petroleum diesel demonstrates strong performance under exponential decay, achieving four wins, and secures additional wins under ROC in the human health and economic viability themes. However, its success is significantly reduced under more balanced weighting methods like rank sum and geometric mean, where it secures no wins. This pattern indicates that while petroleum diesel may perform well in themes that prioritize economic aspects or specific environmental impacts, it is less competitive when broader sustainability concerns are considered. The decline in performance under rank sum and geometric mean reflects the technology's higher impact scores in themes related to global impacts and energy supply, where GWP and fossil fuel depletion become more critical.

Corn ethanol consistently fails to secure any wins across all weighting methods and sustainability themes. This outcome reflects its overall weaker performance profile, particularly in themes related to food and water supply and aquatic biodiversity, where corn ethanol's high-

value land use, water footprint, and eutrophication potential are detrimental. The consistent lack of wins suggests that corn ethanol is less favorable when sustainability assessments consider a wide range of ecological and resource-related impacts beyond cost or GWP.

4.4. Recommendations

The biofuels case study using the ECO-STEPS tool highlights a strategic approach to biofuel adoption. Soybean BD stands out as a strong near-term solution due to its economic benefits and balanced environmental performance across key criteria such as GWP, eutrophication, and fossil fuel depletion, making it well-suited for immediate deployment where cost-effectiveness and emissions reduction are priorities. In contrast, algae RD demonstrates significant potential to become the preferred sustainable biofuel as its technology matures and production costs decrease. Algae RD, particularly in regions like Polk County, FL, excels under balanced sustainability assessments that evenly weigh environmental and resource impacts. Its favorable performance across various sustainability themes, especially where water footprint and land use are critical, suggests it could be a viable option in areas facing high water stress or constraints on valuable cropland.

Based on these insights, stakeholders should pursue a dual strategy: leverage the immediate advantages of soybean BD while investing in the development of algae-based biofuels. This could involve targeted R&D to optimize production methods and increase the TRL of algae RD, aiming for cost competitiveness with established technologies like soybean BD and petroleum diesel. Moreover, the sensitivity of algae RD to regional grid emissions underscores the need to align biofuel production with cleaner grids or renewable energy sources. This approach allows for a flexible transition to more sustainable biofuels over time, ensuring that biofuel strategies adapt to evolving sustainability goals and technological progress.

4.5. Limitations and Future Work

While the ECO-STEPS tool offers a robust framework for decision support and sustainability assessment, several limitations should be considered. One primary concern is data quality, as the inputs for the tool are sourced from various studies, each with different levels of data uncertainty and reliability [151]. These inconsistencies can influence the tool's outcomes and potentially skew decision-making. Additionally, the extensive use of multiple weighting methods and criteria ranking requirements, while intended to provide flexibility and insight, could lead to decision fatigue and complicate the decision-making process, particularly when consensus is difficult to achieve. Another limitation is the focus on midpoint metrics for decision-making, which may not fully address the endpoint metrics that many stakeholders prioritize, such as specific health outcomes or ecosystem damage [138]. The tool's emphasis on broader sustainability impacts could also overlook local environmental justice issues, such as water and air quality, that are crucial in specific regions or contexts.

Several areas for future development are proposed to enhance the ECO-STEPS tool's utility and address current limitations. First, the tool could incorporate additional metrics to enable comparison across a broader range of climate solution technologies. For example, to assess electric vehicles (EVs) against internal combustion (IC) vehicles, the tool could include impact categories related to using rare and valuable critical minerals. Expanding the tool to account for location-specific impacts, such as those captured by the Available Water Remaining (AWARE) methodology [75], could provide more accurate assessments for water-stressed regions. Another potential enhancement is the inclusion of metrics for resource availability, utilizing market-based restrictions to evaluate the scalability of climate solutions relative to alternatives. Additionally, integrating metrics for waste toxicity or environmental risks would

provide a more comprehensive assessment of environmental impacts. Finally, expanding the tool to consider social and political factors, such as job creation, economic resilience, policy alignment, or public acceptance, would enhance its relevance for stakeholders considering broader societal implications in their decision-making processes.

4.6 Conclusion

The ECO-STEPS tool offers significant strengths in decision support, particularly in situations where multiple sustainability criteria need to be balanced. Its flexibility in applying various weighting methods allows stakeholders to explore the relative importance of different criteria and evaluate technology performance across diverse scenarios, making it particularly valuable when there is uncertainty or disagreement about priorities. The tool enhances inclusivity and transparency in multi-stakeholder environments by providing robust decision support that accommodates diverse stakeholder perspectives. Additionally, the availability of pre-made sustainability themes enables decision-makers to focus on specific areas of concern, such as human health or economic viability, without requiring consensus on individual criteria rankings. ECO-STEPS also improves the interpretation of LCA results by integrating traditional LCA outputs, like TRACI metrics, with additional considerations such as water footprint and high-value land use. This holistic approach prevents tunnel vision and avoids decision-making that overly focuses on a few impacts, such as GWP or cost. By enabling a comprehensive evaluation of both environmental and economic factors, ECO-STEPS helps prevent burden-shifting and ensures that prioritized strategies promote long-term sustainability.

CHAPTER 5: CONCLUSIONS AND RECOMMENDATIONS

The work presented in this dissertation addresses critical challenges in decarbonizing key sectors of the U.S. economy—namely transportation and agriculture—through the evaluation and optimization of engineered climate solutions. By employing geographically-resolved life cycle assessment (LCA) and techno-economic analysis (TEA), this research provides a comprehensive assessment of two promising climate solutions: microalgae biorefineries for renewable diesel (RD) and sustainable aviation fuel (SAF) production, and anaerobic digestion (AD) for reducing methane emissions on large-scale dairy farms. Additionally, the development of the Environmental Comparison and Optimization Stakeholder Tool for Evaluating and Prioritizing Solutions (ECO-STEPS) offers a novel framework to guide decision-making in the adoption of sustainable technologies.

The first major finding of this research is the significant potential of microalgae biorefineries to produce RD and SAF, especially in regions with favorable climatic conditions such as the high solar irradiance and high humidity in the Southeastern United States. High-resolution modeling of algal productivity and fuel conversion pathways shows that RD from algae could achieve a minimum fuel selling price (MFSP) as low as $1.50 per liter gasoline equivalent and SAF as low as $2.20 per liter given anticipated technological advancements. Further optimization analyses indicate that both fuels could reduce costs below $0.75 per liter, while reducing GHG emissions 70% compared to petroleum-based fuels. However, achieving these favorable outcomes depends heavily on improving key process efficiencies, such as CO_2 utilization and lipid extraction, and reducing the costs of direct air capture (DAC) technology for CO_2 sourcing. While these results highlight the long-term promise of algae-based fuels, they also

underscore the current economic barriers to their widespread adoption. The economic models used in this study are based on current technologies, meaning that future technological advancements could significantly alter the cost dynamics. This analysis reveals that advancements in algal strain engineering and investments in carbon capture technologies are essential to making algae biofuels cost-competitive with petroleum-based fuels. The environmental benefits of algae biorefineries, including their ability to utilize non-arable land and recycle nutrients, further enhance their appeal as a sustainable fuel option, particularly in regions with limited freshwater resources or agricultural capacity.

In the agricultural sector, this dissertation demonstrates the potential for anaerobic digestion (AD) technology to significantly reduce methane emissions from dairy manure management systems, contributing to national and global climate mitigation efforts. Detailed modeling of 20 different dairy configurations across the contiguous United States suggests that adopting AD could reduce GHG emissions by up to 6.46 million metric tons (MMT) of CO_2-equivalent annually when biogas is utilized for renewable natural gas (RNG) production or combined heat and power (CHP) generation. Even in more conservative scenarios where biogas is solely upgraded to RNG, AD could still achieve reductions of 2.45–3.52 MMT of CO_2-equivalent annually. These findings highlight the importance of AD technology in reducing methane emissions from the agricultural sector, particularly in regions where dairy farms are concentrated and where methane emissions from manure management are most pronounced. However, the analysis also reveals significant regional variability in the economic feasibility of AD adoption, with some regions facing higher capital and operational costs due to climatic conditions and manure management practices. Policymakers should therefore consider targeted subsidies or incentives to promote AD adoption in regions where it is most cost-effective and

where emissions reductions can be maximized. Additionally, further research is needed to explore the long-term management of digestate, particularly with respect to land application and its potential impacts on soil health and water quality.

The introduction of the ECO-STEPS decision-support framework represents a major contribution to the sustainable technology assessment field, providing a flexible and transparent tool for stakeholders to evaluate and prioritize climate solutions. By integrating LCA and TEA results with stakeholder rankings for key sustainability criteria, ECO-STEPS allows for a more nuanced comparison of technologies based on their economic viability, environmental impact, and alignment with long-term sustainability goals. The case study application of ECO-STEPS in this dissertation demonstrates its utility in comparing biofuel technologies, revealing important trade-offs between algae-based RD, soybean biodiesel (BD), and corn ethanol. Specifically, algae-based RD emerges as a highly promising long-term solution, offering the scalability needed to meet future energy demands while enabling substantial reductions in GHG emissions and production costs through technological innovations. Meanwhile, soybean BD proves to be a viable near-term alternative, with lower costs and reduced environmental impacts compared to petroleum diesel. However, its scalability is limited by its dependence on high-value agricultural land. Corn ethanol, while economically competitive, performs poorly across multiple environmental metrics, highlighting the need for continued investment in more sustainable farming practices and conversion technologies.

A key limitation of ECO-STEPS is the subjectivity of stakeholder input, as the rankings and weightings assigned to sustainability criteria are influenced by the individual preferences of the stakeholders involved. This introduces the potential for varying outcomes depending on the specific participants in the decision-making process, potentially affecting the consistency and

objectivity of the results. Additionally, while the framework effectively integrates environmental and economic metrics, the social impacts of technologies—such as job creation or community acceptance—were not included in this iteration. Despite these limitations, the flexibility of ECO-STEPS makes it adaptable to a wide range of technology sectors beyond biofuels, offering a valuable tool for policymakers, industry leaders, and researchers looking to understand and prioritize climate solutions using comprehensive and holistic sustainability criteria.

Future Directions for Microalgae Biorefineries

While the results of this dissertation provide a clear path forward for optimizing algae-based biofuel production, significant challenges remain before these technologies can be commercially viable. Future research should focus on improving algae cultivation systems by enhancing productivity and lipid accumulation through genetic engineering and strain selection. Advances in CO_2 utilization are also crucial, particularly in reducing the cost and improving the efficiency of direct air capture technologies. Additionally, more efficient methods of harvesting and dewatering algae biomass will be necessary to further reduce energy consumption and costs. Another promising area of research is the development of new co-products from algae, such as edible proteins, bio-chemicals, and polyurethanes which could improve the overall economics of algae biorefineries. Finally, future studies should explore the potential for integrating algae cultivation with other industrial processes, such as wastewater treatment or carbon capture from power plants, to create more synergistic and economically viable systems.

Future Directions for AD on Dairy Farms

Adopting AD technology in the dairy industry offers substantial opportunities for reducing methane emissions and generating renewable energy. However, as this dissertation shows, regional variability in farm practices and economic barriers pose significant challenges to widespread AD adoption. Future research should focus on developing regionally-optimized AD systems that account for local manure management practices, climate, and energy markets. Improving the efficiency and scalability of AD technology, particularly for smaller farms, will be critical to achieving broader adoption. In addition, the environmental impacts of digestate management need further exploration, with a focus on optimizing nutrient recovery and reducing the potential for nutrient runoff or groundwater contamination. Policymakers and industry leaders should also explore the potential for incentives that integrating AD systems with other manure management technologies such as centrifugation to maximize methane emissions reductions. Finally, continued development of financial incentives and policy frameworks will be necessary to support the economic viability of AD projects, especially in regions where the upfront costs of AD systems remain prohibitive.

Future Directions for the ECO-STEPS Decision-Support Framework

The development of the ECO-STEPS framework marks a significant step forward in the field of decision support for sustainable technology adoption. However, there are several areas where the tool could be further refined and expanded. Future iterations of ECO-STEPS should incorporate a broader range of sustainability metrics, including social and political factors such as job creation, public health impacts, and community acceptance of new technologies. The framework could also be adapted to include more dynamic weighting methods, allowing stakeholders to adjust criteria rankings based on real-time data or evolving policy priorities.

Additionally, future research should explore the application of ECO-STEPS to a wider range of technology sectors beyond biofuels, such as renewable energy systems, electric vehicles, or carbon capture and storage. As the urgency of the climate crisis grows, tools like ECO-STEPS will play an increasingly important role in guiding stakeholders toward the most sustainable and impactful solutions.

Final Thoughts

The findings of this dissertation highlight the complexity and critical importance of tackling climate change through regionally optimized, engineered solutions that are specifically tailored to local conditions and needs. The geographically-resolved analyses presented here for microalgae biofuels and anaerobic digestion demonstrate the substantial potential of these technologies to contribute to global GHG reductions. However, they also highlight the nuanced challenges that arise from economic viability, geographic conditions, and technological barriers. This research emphasizes that a one-size-fits-all approach to climate mitigation will not suffice. Instead, solutions must be adapted to the specific environmental, economic, and social conditions of the regions in which they are implemented. As climate change continues to be one of the greatest challenges of our time, tools like ECO-STEPS will be invaluable in identifying the most effective pathways forward.

In conclusion, this dissertation contributes not only to the academic understanding of algae biofuels, AD, and decision-support frameworks but also to the practical advancement of solutions for achieving a low-carbon future. The work presented here provides key insights into how engineered climate solutions can be optimized and adopted on a larger scale, offering a roadmap for researchers, policymakers, and industry leaders committed to addressing climate change. As global efforts to mitigate climate impacts intensify, the research, frameworks, and

future directions outlined in this dissertation will be crucial in driving innovation and achieving sustainable development goals.

REFERENCES

[1] IPCC, 2023: Summary for Policymakers. In: Climate Change 2023: Synthesis Report. Contribution of Working Groups I, II and III to the Sixth Assessment Report of the Intergovernmental Panel on Climate Change. First. Geneva, Switzerland: IPCC; 2023. https://doi.org/10.59327/IPCC/AR6-9789291691647.

[2] US EPA O. Inventory of U.S. Greenhouse Gas Emissions and Sinks: 1990-2021 2023. https://www.epa.gov/ghgemissions/inventory-us-greenhouse-gas-emissions-and-sinks-1990-2021 (accessed November 16, 2023).

[3] Quiroz D, Greene JM, Limb BJ, Quinn JC. Global Life Cycle and Techno-Economic Assessment of Algal-Based Biofuels. Environ Sci Technol 2023. https://doi.org/10.1021/acs.est.3c02892.

[4] Chen PH, Quinn JC. Microalgae to biofuels through hydrothermal liquefaction: Open-source techno-economic analysis and life cycle assessment. Applied Energy 2021;289:116613. https://doi.org/10.1016/j.apenergy.2021.116613.

[5] Davis R, Markham J, Kinchin C, Grundl N, Tan ECD, Humbird D. Process Design and Economics for the Production of Algal Biomass: Algal Biomass Production in Open Pond Systems and Processing Through Dewatering for Downstream Conversion. 2016. https://doi.org/10.2172/1239893.

[6] Davis RE, Markham JN, Kinchin CM, Canter C, Han J, Li Q, et al. 2017 Algae Harmonization Study: Evaluating the Potential for Future Algal Biofuel Costs, Sustainability, and Resource Assessment from Harmonized Modeling. 2018. https://doi.org/10.2172/1468333.

[7] US EPA O. Understanding Global Warming Potentials. US EPA 2016. https://www.epa.gov/ghgemissions/understanding-global-warming-potentials (accessed April 22, 2019).

[8] Feng X, Smith W, VanderZaag AC. Dairy manure nutrient recovery reduces greenhouse gas emissions and transportation cost in a modeling study. Frontiers in Animal Science 2023;4.

[9] US EPA O. Anaerobic Digestion on Dairy Farms 2021. https://www.epa.gov/agstar/anaerobic-digestion-dairy-farms (accessed September 11, 2023).

[10] Aguirre-Villegas H, Larson R. Evaluating greenhouse gas emissions from dairy manure management practices using survey data and lifecycle tools. Journal of Cleaner Production 2016;143. https://doi.org/10.1016/j.jclepro.2016.12.133.

[11] Niles MT, Wiltshire S. Tradeoffs in US dairy manure greenhouse gas emissions, productivity, climate, and manure management strategies. Environ Res Commun 2019;1:075003. https://doi.org/10.1088/2515-7620/ab2dec.

[12] Anaerobic Digestion Implementation at Dairies in Colorado. National Renewable Energy Lab. (NREL), Golden, CO (United States); 2021.

[13] Williams Engineering Associates. Anaerobic Digestion on Dairy Farms for Electrical Generation 2018.

[14] Bishop CP, Shumway CR. The Economics of Dairy Anaerobic Digestion with Coproduct Marketing. Applied Economic Perspectives and Policy 2009;31:394–410. https://doi.org/10.1111/j.1467-9353.2009.01445.x.

[15] Usack JG, Van Doren LG, Posmanik R, Tester JW, Angenent LT. Harnessing anaerobic digestion for combined cooling, heat, and power on dairy farms: An environmental life cycle and techno-economic assessment of added cooling pathways. Journal of Dairy Science 2019;102:3630–45. https://doi.org/10.3168/jds.2018-15518.

[16] Which Airlines Are Embracing SAF? n.d. https://i6.io/blog/which-airlines-are-embracing-saf (accessed March 4, 2024).

[17] Biofuels - Energy System. IEA n.d. https://www.iea.org/energy-system/low-emission-fuels/biofuels (accessed February 5, 2024).

[18] Huesemann M, Gao S, Edmundson S, Laurens LML, Van Wychen S, Beirne N, et al. DISCOVR strain pipeline screening – Part II: Winter and summer season areal productivities and biomass compositional shifts in climate-simulation photobioreactor cultures. Algal Research 2023;70:102948. https://doi.org/10.1016/j.algal.2022.102948.

[19] Gu X, Yu L, Pang N, Martinez-Fernandez JS, Fu X, Chen S. Comparative techno-economic analysis of algal biofuel production via hydrothermal liquefaction: One stage versus two stages. Applied Energy 2020;259:114115. https://doi.org/10.1016/j.apenergy.2019.114115.

[20] Jiang Y, Jones SB, Zhu Y, Snowden-Swan L, Schmidt AJ, Billing JM, et al. Techno-economic uncertainty quantification of algal-derived biocrude via hydrothermal liquefaction. Algal Research 2019;39:101450. https://doi.org/10.1016/j.algal.2019.101450.

[21] Ranganathan P, Savithri S. Techno-economic analysis of microalgae-based liquid fuels production from wastewater via hydrothermal liquefaction and hydroprocessing. Bioresource Technology 2019;284:256–65. https://doi.org/10.1016/j.biortech.2019.03.087.

[22] Ou L, Thilakaratne R, Brown RC, Wright MM. Techno-economic analysis of transportation fuels from defatted microalgae via hydrothermal liquefaction and hydroprocessing. Biomass and Bioenergy 2015;72:45–54. https://doi.org/10.1016/j.biombioe.2014.11.018.

[23] Pearlson M, Wollersheim C, Hileman J. A techno-economic review of hydroprocessed renewable esters and fatty acids for jet fuel production. Biofuels, Bioprod Bioref 2013;7:89–96. https://doi.org/10.1002/bbb.1378.

[24] Nie Y, Bi X. Life-cycle assessment of transportation biofuels from hydrothermal liquefaction of forest residues in British Columbia. Biotechnol Biofuels 2018;11. https://doi.org/10.1186/s13068-018-1019-x.

[25] Sun C-H, Fu Q, Liao Q, Xia A, Huang Y, Zhu X, et al. Life-cycle assessment of biofuel production from microalgae via various bioenergy conversion systems. Energy 2019;171:1033–45. https://doi.org/10.1016/j.energy.2019.01.074.

[26] Marangon BB, Castro JS, Assemany PP, Couto EA, Calijuri ML. Environmental performance of microalgae hydrothermal liquefaction: Life cycle assessment and improvement insights for a sustainable renewable diesel. Renewable and Sustainable Energy Reviews 2022;155:111910. https://doi.org/10.1016/j.rser.2021.111910.

[27] Elgowainy A, Han J, Wang M, Carter N, Stratton R, Hileman J, et al. Life-cycle analysis of alternative aviation fuels in GREET. Argonne National Lab. (ANL), Argonne, IL (United States); 2012. https://doi.org/10.2172/1046913.

[28] Prussi M, Weindorf W, Buffi M, Sánchez López J, Scarlat N. Are algae ready to take off? GHG emission savings of algae-to-kerosene production. Applied Energy 2021;304:117817. https://doi.org/10.1016/j.apenergy.2021.117817.

[29] Carter NA. Environmental and economic assessment of microalgae-derived jet fuel. Thesis. Massachusetts Institute of Technology, 2012.

[30] Pipitone G, Zoppi G, Pirone R, Bensaid S. Sustainable aviation fuel production using in-situ hydrogen supply via aqueous phase reforming: A techno-economic and life-cycle greenhouse gas emissions assessment. Journal of Cleaner Production 2023;418:138141. https://doi.org/10.1016/j.jclepro.2023.138141.

[31] Farooq D, Thompson I, Ng KS. Exploring the feasibility of producing sustainable aviation fuel in the UK using hydrothermal liquefaction technology: A comprehensive techno-economic and environmental assessment. Cleaner Engineering and Technology 2020;1:100010. https://doi.org/10.1016/j.clet.2020.100010.

[32] Roles J, Yarnold J, Hussey K, Hankamer B. Techno-economic evaluation of microalgae high-density liquid fuel production at 12 international locations. Biotechnology for Biofuels 2021;14:133. https://doi.org/10.1186/s13068-021-01972-4.

[33] Neuling U, Kaltschmitt M. Techno-economic and environmental analysis of aviation biofuels. Fuel Processing Technology 2018;171:54–69. https://doi.org/10.1016/j.fuproc.2017.09.022.

[34] Klein-Marcuschamer D, Turner C, Allen M, Gray P, Dietzgen RG, Gresshoff PM, et al. Technoeconomic analysis of renewable aviation fuel from microalgae, Pongamia pinnata, and sugarcane. Biofuels, Bioproducts and Biorefining 2013;7:416–28. https://doi.org/10.1002/bbb.1404.

[35] Cox K, Renouf M, Dargan A, Turner C, Klein-Marcuschamer D. Environmental life cycle assessment (LCA) of aviation biofuel from microalgae, Pongamia pinnata, and sugarcane

molasses. Biofuels, Bioproducts and Biorefining 2014;8:579–93. https://doi.org/10.1002/bbb.1488.

[36] Fortier M-OP, Roberts GW, Stagg-Williams SM, Sturm BSM. Life cycle assessment of bio-jet fuel from hydrothermal liquefaction of microalgae. Applied Energy 2014;122:73–82. https://doi.org/10.1016/j.apenergy.2014.01.077.

[37] Mishra RK, kumar V, Kumar P, Mohanty K. Hydrothermal liquefaction of biomass for bio-crude production: A review on feedstocks, chemical compositions, operating parameters, reaction kinetics, techno-economic study, and life cycle assessment. Fuel 2022;316:123377. https://doi.org/10.1016/j.fuel.2022.123377.

[38] Guo F, Zhao J, A L, Yang X. Life cycle assessment of microalgae-based aviation fuel: Influence of lipid content with specific productivity and nitrogen nutrient effects. Bioresource Technology 2016;221:350–7. https://doi.org/10.1016/j.biortech.2016.09.044.

[39] W. Kolosz B, Luo Y, Xu B, M. Maroto-Valer M, M. Andresen J. Life cycle environmental analysis of 'drop in' alternative aviation fuels: a review. Sustainable Energy & Fuels 2020;4:3229–63. https://doi.org/10.1039/C9SE00788A.

[40] Martinez-Villarreal S, Breitenstein A, Nimmegeers P, Perez Saura P, Hai B, Asomaning J, et al. Drop-in biofuels production from microalgae to hydrocarbons: Microalgal cultivation and harvesting, conversion pathways, economics and prospects for aviation. Biomass and Bioenergy 2022;165:106555. https://doi.org/10.1016/j.biombioe.2022.106555.

[41] Giwa A, Adeyemi I, Dindi A, Lopez CG-B, Lopresto CG, Curcio S, et al. Techno-economic assessment of the sustainability of an integrated biorefinery from microalgae

and Jatropha: A review and case study. Renewable and Sustainable Energy Reviews 2018;88:239–57. https://doi.org/10.1016/j.rser.2018.02.032.

[42] Davis R, Kinchin C, Markham J, Tan ECD, Laurens LM. Process Design and Economics for the Conversion of Algal Biomass to Biofuels: Algal Biomass Fractionation to Lipid- and Carbohydrate-Derived Fuel Products. Renewable Energy 2014:110.

[43] Quinn JC, Davis R. The potentials and challenges of algae based biofuels: A review of the techno-economic, life cycle, and resource assessment modeling. Bioresource Technology 2015;184:444–52. https://doi.org/10.1016/j.biortech.2014.10.075.

[44] Wilcox J, Psarras PC, Liguori S. Assessment of reasonable opportunities for direct air capture. Environ Res Lett 2017;12:065001. https://doi.org/10.1088/1748-9326/aa6de5.

[45] Bare J. TRACI 2.0: the tool for the reduction and assessment of chemical and other environmental impacts 2.0. Clean Techn Environ Policy 2011;13:687–96. https://doi.org/10.1007/s10098-010-0338-9.

[46] Jones SB, Zhu Y, Anderson DB, Hallen RT, Elliott DC, Schmidt AJ, et al. Process Design and Economics for the Conversion of Algal Biomass to Hydrocarbons: Whole Algae Hydrothermal Liquefaction and Upgrading. 2014. https://doi.org/10.2172/1126336.

[47] Cruce JR, Beattie A, Chen P, Quiroz D, Somers M, Compton S, et al. Driving toward sustainable algal fuels: A harmonization of techno-economic and life cycle assessments. Algal Research 2021;54:102169. https://doi.org/10.1016/j.algal.2020.102169.

[48] Greene JM, Quiroz D, Compton S, Lammers PJ, Quinn JC. A validated thermal and biological model for predicting algal productivity in large scale outdoor cultivation systems. Algal Research 2021;54:102224. https://doi.org/10.1016/j.algal.2021.102224.

[49] McGowen J, Knoshaug EP, Laurens LML, Forrester J. Outdoor annual algae productivity improvements at the pre-pilot scale through crop rotation and pond operational management strategies. Algal Research 2023;70:102995. https://doi.org/10.1016/j.algal.2023.102995.

[50] NSRDB n.d. https://nsrdb.nrel.gov/ (accessed July 13, 2023).

[51] Quiroz D, Greene JM, McGowen J, Quinn JC. Geographical assessment of open pond algal productivity and evaporation losses across the United States. Algal Research 2021;60:102483. https://doi.org/10.1016/j.algal.2021.102483.

[52] Davis R, Wiatrowski M. Algal Biomass Conversion to Fuels via Combined Algae Processing (CAP): 2019 State of Technology and Future Research. National Renewable Energy Lab. (NREL), Golden, CO (United States); 2020. https://doi.org/10.2172/1659895.

[53] Wendt LM, Kinchin C, Wahlen BD, Davis R, Dempster TA, Gerken H. Assessing the stability and techno-economic implications for wet storage of harvested microalgae to manage seasonal variability. Biotechnology for Biofuels 2019;12:80. https://doi.org/10.1186/s13068-019-1420-0.

[54] Gao S, Edmundson S, Huesemann M, Gutknecht A, Laurens LML, Van Wychen S, et al. DISCOVR strain screening pipeline – Part III: Strain evaluation in outdoor raceway ponds. Algal Research 2023;70:102990. https://doi.org/10.1016/j.algal.2023.102990.

[55] Klein BC, Davis RE, Laurens LML. Quantifying the intrinsic value of algal biomass based on a multi-product biorefining strategy. Algal Research 2023:103094. https://doi.org/10.1016/j.algal.2023.103094.

[56] Summers HM, Sproul E, Quinn JC. The greenhouse gas emissions of indoor cannabis production in the United States. Nat Sustain 2021:1–7. https://doi.org/10.1038/s41893-021-00691-w.

[57] Eustance E, Lai Y-JS, Shesh T, Rittmann BE. Improved CO2 utilization efficiency using membrane carbonation in outdoor raceways. Algal Research 2020;51:102070. https://doi.org/10.1016/j.algal.2020.102070.

[58] Davis R, Hawkins T, Coleman A, Gao S, Klein B, Wiatrowski M, et al. Economic, Greenhouse Gas, and Resource Assessment for Fuel and Protein Production from Microalgae: 2022 Algae Harmonization Update. 2024. https://doi.org/10.2172/2318964.

[59] Quinn JC, Catton KB, Johnson S, Bradley TH. Geographical Assessment of Microalgae Biofuels Potential Incorporating Resource Availability. Bioenerg Res 2013;6:591–600. https://doi.org/10.1007/s12155-012-9277-0.

[60] Vadlamani A, Viamajala S, Pendyala B, Varanasi S. Cultivation of Microalgae at Extreme Alkaline pH Conditions: A Novel Approach for Biofuel Production. ACS Sustainable Chem Eng 2017;5:7284–94. https://doi.org/10.1021/acssuschemeng.7b01534.

[61] Executive summary – Direct Air Capture 2022 – Analysis - IEA n.d. https://www.iea.org/reports/direct-air-capture-2022/executive-summary (accessed May 11, 2023).

[62] Quiroz D, Greene JM, Quinn JC. Regionalized Life-Cycle Water Impacts of Microalgal-Based Biofuels in the United States. Environ Sci Technol 2022. https://doi.org/10.1021/acs.est.2c05552.

[63] Leow S, R. Witter J, R. Vardon D, K. Sharma B, S. Guest J, J. Strathmann T. Prediction of microalgae hydrothermal liquefaction products from feedstock biochemical composition. Green Chemistry 2015;17:3584–99. https://doi.org/10.1039/C5GC00574D.

[64] Kang S, Heo S, Lee JH. Techno-economic Analysis of Microalgae-Based Lipid Production: Considering Influences of Microalgal Species. Ind Eng Chem Res 2019;58:944–55. https://doi.org/10.1021/acs.iecr.8b03999.

[65] Frank ED, Han J, Palou-Rivera I, Elgowainy A, Wang MQ. Life-Cycle Analysis of Algal Lipid Fuels with the GREET Model. Argonne National Laboratory; 2011.

[66] Delrue F, Setier P-A, Sahut C, Cournac L, Roubaud A, Peltier G, et al. An economic, sustainability, and energetic model of biodiesel production from microalgae. Bioresource Technology 2012;111:191–200. https://doi.org/10.1016/j.biortech.2012.02.020.

[67] mkulwiec. Algae Oil. Cellana - Algae-Based Products for a Sustainable Future n.d. https://cellana.com/algae-oil/ (accessed January 26, 2024).

[68] Gary JH, Handwerk GE, Kaiser MJ. Petroleum refining: technology and economics. 5th ed. Boca Raton: CRC Press; 2007.

[69] Zamalloa C, Vulsteke E, Albrecht J, Verstraete W. The techno-economic potential of renewable energy through the anaerobic digestion of microalgae. Bioresource Technology 2011;102:1149–58. https://doi.org/10.1016/j.biortech.2010.09.017.

[70] Börjesson P, Berglund M. Environmental systems analysis of biogas systems—Part I: Fuel-cycle emissions. Biomass and Bioenergy 2006;30:469–85. https://doi.org/10.1016/j.biombioe.2005.11.014.

[71] Alternative Fuels Data Center: Fuel Prices n.d. https://afdc.energy.gov/fuels/prices.html (accessed January 26, 2024).

[72] Lee K-M, Inaba A. Life Cycle Assessment Best Practices of ISO 14040 Series 2004.

[73] Wernet G, Bauer C, Steubing B, Reinhard J, Moreno-Ruiz E, Weidema B. The ecoinvent database version 3 (part I): overview and methodology. The International Journal of Life Cycle Assessment 2016;21:1218–30. https://doi.org/10.1007/s11367-016-1087-8.

[74] openLCA.org | openLCA is a free, professional Life Cycle Assessment (LCA) and footprint software with a broad range of features and many available databases, created by GreenDelta since 2006 n.d. https://www.openlca.org/ (accessed September 20, 2023).

[75] What is AWARE (Available WAter REmaining)? WULCA n.d. https://wulca-waterlca.org/aware/what-is-aware/ (accessed January 26, 2024).

[76] Wickham J, Stehman SV, Sorenson DG, Gass L, Dewitz JA. Thematic accuracy assessment of the NLCD 2019 land cover for the conterminous United States. GIScience & Remote Sensing 2023;60:2181143. https://doi.org/10.1080/15481603.2023.2181143.

[77] LANDFIRE Program: Data Products - Topographic - Slope n.d. https://www.landfire.gov/slope.php (accessed February 12, 2024).

[78] Protected Planet | United States of America. Protected Planet n.d. https://www.protectedplanet.net/country/USA (accessed February 12, 2024).

[79] A global standard for the identification of Key Biodiversity Areas : version 1.0. IUCN; 2016.

[80] Fossil Fuel Subsidies n.d. https://www.imf.org/en/Topics/climate-change/energy-subsidies (accessed April 29, 2024).

[81] US EPA O. Renewable Fuel Standard Program 2015. https://www.epa.gov/renewable-fuel-standard-program (accessed July 18, 2022).

[82] Jing L, El-Houjeiri HM, Monfort J-C, Littlefield J, Al-Qahtani A, Dixit Y, et al. Understanding variability in petroleum jet fuel life cycle greenhouse gas emissions to inform aviation decarbonization. Nat Commun 2022;13:7853. https://doi.org/10.1038/s41467-022-35392-1.

[83] Echenique-Subiabre I, Greene JM, Ryan A, Martinez H, Balleza M, Gerber J, et al. Site-specific factors override local climatic conditions in determining microalgae productivity in open raceway ponds. Algal Research 2023;74:103235. https://doi.org/10.1016/j.algal.2023.103235.

[84] IPCC, 2018: Summary for Policymakers. In: Global Warming of 1.5°C. An IPCC Special Report on the impacts of global warming of 1.5°C above pre-industrial levels and related global greenhouse gas emission pathways, in the context of strengthening the global response to the threat of climate change, sustainable development, and efforts to eradicate poverty. Geneva, Switzerland: World Meteorological Organization; n.d.

[85] Demirer GN, Chen S. Two-phase anaerobic digestion of unscreened dairy manure. Process Biochemistry 2005;40:3542–9. https://doi.org/10.1016/j.procbio.2005.03.062.

[86] Flores-Orozco D, Patidar R, Levin DB, Sparling R, Kumar A, Çiçek N. Effect of mesophilic anaerobic digestion on the resistome profile of dairy manure. Bioresource Technology 2020;315:123889. https://doi.org/10.1016/j.biortech.2020.123889.

[87] Wang Y, Liang L, Liu J, Guo D, Zhu Z, Dong H. Impact of anaerobic digestion on reactive nitrogen gas emissions from dairy slurry storage. Journal of Environmental Management 2022;316:115306. https://doi.org/10.1016/j.jenvman.2022.115306.

[88] Sarah, Susilawati HL, Pramono A. Quantifying the potency of greenhouse gas emission from manure management through anaerobic digester in Central Java. IOP Conf Ser: Earth Environ Sci 2021;648:012111. https://doi.org/10.1088/1755-1315/648/1/012111.

[89] Techno-economic and life cycle analysis of a farm-scale anaerobic digestion plant in Iowa - ScienceDirect n.d. https://www.sciencedirect.com/science/article/abs/pii/S0956053X19302260 (accessed September 11, 2023).

[90] O'Connor S, Ehimen E, Pillai SC, Lyons G, Bartlett J. Economic and Environmental Analysis of Small-Scale Anaerobic Digestion Plants on Irish Dairy Farms. Energies 2020;13:637. https://doi.org/10.3390/en13030637.

[91] Bhatnagar N, Ryan D, Murphy R, Enright AM. A comprehensive review of green policy, anaerobic digestion of animal manure and chicken litter feedstock potential – Global and Irish perspective. Renewable and Sustainable Energy Reviews 2022;154:111884. https://doi.org/10.1016/j.rser.2021.111884.

[92] Liebrand CB, Ling KC. Cooperative Approaches for Implementation of Dairy Manure Digesters. United States Department of Agriculture; 2009.

[93] Innovation Center for U.S. Dairy n.d. https://www.usdairy.com/about-us/innovation-center (accessed December 18, 2023).

[94] USDA - National Agricultural Statistics Service - Census of Agriculture n.d. https://www.nass.usda.gov/AgCensus/ (accessed December 18, 2023).

[95] LCFS Life Cycle Analysis Models and Documentation | California Air Resources Board n.d. https://ww2.arb.ca.gov/resources/documents/lcfs-life-cycle-analysis-models-and-documentation (accessed September 5, 2023).

[96] Analysis of Jersey versus Holstein breed profitability on north central US dairies - PMC n.d. https://www.ncbi.nlm.nih.gov/pmc/articles/PMC10505770/ (accessed April 2, 2024).

[97] AR5 Synthesis Report: Climate Change 2014 — IPCC n.d. https://www.ipcc.ch/report/ar5/syr/ (accessed July 6, 2023).

[98] US EPA O. Emissions & Generation Resource Integrated Database (eGRID) 2020. https://www.epa.gov/egrid (accessed June 27, 2022).

[99] US EPA O. Inventory of U.S. Greenhouse Gas Emissions and Sinks: 1990-2012 2016. https://www.epa.gov/ghgemissions/inventory-us-greenhouse-gas-emissions-and-sinks-1990-2012 (accessed November 15, 2023).

[100] Di Noi C, Ciroth A, Srocka M. OpenLCA 1.7. Comprehensive User Manual. Berlin, Germany: GreenDelta GmbH; 2017.

[101] Temperature - US Monthly Average | NOAA Climate.gov n.d. http://www.climate.gov/maps-data/data-snapshots/data-source/temperature-us-monthly-average (accessed November 25, 2022).

[102] Calvo Buendia E, Tanabe K, Kranjc A, Baasansuren J, Fukuda M, Ngarize S, et al. IPCC 2019, 2019 Refinement to the 2006 Guidelines for National Greenhouse Gas Inventories; Chapter 10: Emissions from Livestock and Manure Management. Switzerland: IPCC; 2019.

[103] Williams RB, Elmashad H, Kaffka S. Research and Technical Analysis to Support and Improve the Alternative Manure Management Program Quantification Methodology. University of California, Davis; 2020.

[104] Labatut RA, Angenent LT, Scott NR. Biochemical methane potential and biodegradability of complex organic substrates. Bioresource Technology 2011;102:2255–64. https://doi.org/10.1016/j.biortech.2010.10.035.

[105] Summers M, Williams D. Energy and Environmental Performance of Six Dairy Digester Systems in California. California Energy Commission; 2013.

[106] Meyer D, Heguy J, Karle B, Robinson P. Characterize Physical and Chemical Properties of Manure in California Dairy Systems to Improve Greenhouse Gas Emission Estimates. University of California, Davis; 2019.

[107] Leytem AB, Dungan RS, Bjorneberg DL. Spatial and Temporal Variation in Physicochemical Properties of Dairy Lagoons in South-Central Idaho. American Society of Agricultural and Biological Engineers 2017. https://doi.org/10.13031.

[108] Chastain JP, Henry S. Management of Lagoons and Storage Structures For Dairy Manure. Clemson University; 2015.

[109] Lo KV, Liao PH, Whitehead AJ, Bulley NR. Mesophilic anaerobic digestion of screened and unscreened dairy manure. Agricultural Wastes 1984;11:269–83. https://doi.org/10.1016/0141-4607(84)90035-0.

[110] Moset V, Poulsen M, Wahid R, Højberg O, Møller HB. Mesophilic versus thermophilic anaerobic digestion of cattle manure: methane productivity and microbial ecology. Microb Biotechnol 2015;8:787–800. https://doi.org/10.1111/1751-7915.12271.

[111] Zhang X, Lopes IM, Ni J-Q, Yuan Y, Huang C-H, Smith DR, et al. Long-term performance of three mesophilic anaerobic digesters to convert animal and agro-industrial wastes into organic fertilizer. J Clean Prod 2021;307:1–8. https://doi.org/10.1016/j.jclepro.2021.127271.

[112] Mackie RI, Bryant MP. Anaerobic digestion of cattle waste at mesophilic and thermophilic temperatures. Appl Microbiol Biotechnol 1995;43:346–50. https://doi.org/10.1007/BF00172837.

[113] Skorek-Osikowska A, Martín-Gamboa M, Dufour J. Thermodynamic, economic and environmental assessment of renewable natural gas production systems. Energy Conversion and Management: X 2020;7:100046. https://doi.org/10.1016/j.ecmx.2020.100046.

[114] US EPA O. GHGRP Reported Data 2016. https://www.epa.gov/ghgreporting/ghgrp-reported-data (accessed April 14, 2022).

[115] Argonne GREET Publication : Summary of Expansions and Updates in GREET® 2021 n.d. https://greet.anl.gov/publication-greet-2021-summary (accessed June 24, 2024).

[116] Gooch C, Labatut R. FINAL REPORT "EVALUATION OF THE CONTINUOUSLY-MIXED ANAEROBIC DIGESTER SYSTEM AT SYNERGY BIOGAS - JUN 2012 TO MAY 2014. 2014. https://doi.org/10.13140/2.1.4277.9206.

[117] Fournel S, Godbout S, Ruel P, Fortin A, Généreux M, Côté C, et al. Production of recycled manure solids for bedding in Canadian dairy farms: I. Solid–liquid separation. Journal of Dairy Science 2019;102:1832–46. https://doi.org/10.3168/jds.2018-14966.

[118] Z. Wu. Phosphorus and Nitrogen Distribution of Screw Press Separated Dairy Manure with Recovery of Bedding Material. Applied Engineering in Agriculture 2007;23:757–62. https://doi.org/10.13031/2013.24059.

[119] Zhang R, Mashad HE, Edalati A, Chen Y, Barzee T, Lin XJ, et al. Effect of Solid Separation on Mitigation of Methane Emission in Dairy Manure Lagoons: Final Report to the California Department of Food and Agriculture. 2019.

[120] Commission CE. Construction and Operation of the ABEC #3 Covered Lagoon Digester and Electrical Generation System. California Energy Commission current-date. https://www.energy.ca.gov/publications/2020/construction-and-operation-abec-3-covered-lagoon-digester-and-electrical (accessed August 8, 2023).

[121] Jones B, Sall J. JMP statistical discovery software. WIREs Computational Statistics 2011;3:188–94. https://doi.org/10.1002/wics.162.

[122] Rotz A, Stout R, Leytem A, Feyereisen G, Waldrip H, Thoma G, et al. Environmental assessment of United States dairy farms. Journal of Cleaner Production 2021;315:128153. https://doi.org/10.1016/j.jclepro.2021.128153.

[123] Lamolinara B, Pérez-Martínez A, Guardado-Yordi E, Fiallos CG, Diéguez-Santana K, Ruiz-Mercado GJ. Anaerobic digestate management, environmental impacts, and techno-economic challenges. Waste Manag 2022;140:14–30. https://doi.org/10.1016/j.wasman.2021.12.035.

[124] SEC.gov | SEC Adopts Rules to Enhance and Standardize Climate-Related Disclosures for Investors n.d. https://www.sec.gov/newsroom/press-releases/2024-31 (accessed September 4, 2024).

[125] Smith JP, Limb BJ, Beal CM, Banta KR, Field JL, Simske SJ, et al. Evaluating the sustainability of the 2017 US biofuel industry with an integrated techno-economic analysis and life cycle assessment. Journal of Cleaner Production 2023;413:137364. https://doi.org/10.1016/j.jclepro.2023.137364.

[126] Cole G, Greene JM, Quinn J, McDaniel B, Kemp L, Simmons D, et al. Integrated Techno-Economic and Life Cycle Assessment of a Novel Algae-Based Coating for Direct Air Carbon Capture and Sequestration 2022. https://doi.org/10.2139/ssrn.4288154.

[127] DeRose K, DeMill C, Davis RW, Quinn JC. Integrated techno economic and life cycle assessment of the conversion of high productivity, low lipid algae to renewable fuels. Algal Research 2019;38:101412. https://doi.org/10.1016/j.algal.2019.101412.

[128] Umenweke GC, Pace RB, Santillan-Jimenez E, Okolie JA. Techno-economic and life-cycle analyses of sustainable aviation fuel production via integrated catalytic deoxygenation and hydrothermal gasification. Chemical Engineering Journal 2023;452:139215. https://doi.org/10.1016/j.cej.2022.139215.

[129] Deivanayagam TA, Osborne RE. Breaking free from tunnel vision for climate change and health. PLOS Glob Public Health 2023;3:e0001684. https://doi.org/10.1371/journal.pgph.0001684.

[130] Greene JM, Wallace J, Williams RB, Leytem AB, Bock BR, McCully M, et al. National Greenhouse Gas Emission Reduction Potential from Adopting Anaerobic Digestion on Large-Scale Dairy Farms in the United States. Environ Sci Technol 2024;58:12409–19. https://doi.org/10.1021/acs.est.4c00367.

[131] Paccanelli N, Teli A, Scaglione D, Insabato G, Casula A. Comparison based on environmental effects of nitrogen management techniques in a manure digestate case study. Environmental Technology 2015;36:3176–85. https://doi.org/10.1080/09593330.2015.1055820.

[132] Gonzalez C. The Environmental Justice Implications of Biofuels 2016:47.

[133] Middleton C, Allouche J, Gyawali D, Allen S. The Rise and Implications of the Water-Energy-Food Nexus in Southeast Asia through an Environmental Justice Lens. Water Alternatives 2015;8:627–54.

[134] GCAM: Global Change Analysis Model | Global Change Intersectoral Modeling System n.d. https://gcims.pnnl.gov/modeling/gcam-global-change-analysis-model (accessed September 4, 2024).

[135] van Beek L, Hajer M, Pelzer P, van Vuuren D, Cassen C. Anticipating futures through models: the rise of Integrated Assessment Modelling in the climate science-policy interface since 1970. Global Environmental Change 2020;65:102191. https://doi.org/10.1016/j.gloenvcha.2020.102191.

[136] Emmerling J, Tavoni M. Representing inequalities in integrated assessment modeling of climate change. One Earth 2021;4:177–80. https://doi.org/10.1016/j.oneear.2021.01.013.

[137] Integrated Assessment Models of Climate Change. NBER n.d. https://www.nber.org/reporter/2017number3/integrated-assessment-models-climate-change (accessed September 4, 2024).

[138] Bare JC, Gloria TP. Environmental impact assessment taxonomy providing comprehensive coverage of midpoints, endpoints, damages, and areas of protection. Journal of Cleaner Production 2008;16:1021–35. https://doi.org/10.1016/j.jclepro.2007.06.001.

[139] Frontiers | Quantifying interactions in the water-energy-food nexus: data-driven analysis utilizing a causal inference method n.d. https://www.frontiersin.org/journals/environmental-science/articles/10.3389/fenvs.2023.1328009/full (accessed September 4, 2024).

[140] Bare J. Tool for the Reduction and Assessment of Chemical and Other Environmental Impacts (TRACI) TRACI version 2.1 2012. https://nepis.epa.gov/Adobe/PDF/P100HN53.pdf (accessed January 8, 2020).

[141] National Land Cover Database Class Legend and Description | Multi-Resolution Land Characteristics (MRLC) Consortium n.d. https://www.mrlc.gov/data/legends/national-land-cover-database-class-legend-and-description (accessed December 29, 2023).

[142] Zillow: Real Estate, Apartments, Mortgages & Home Values n.d. https://www.zillow.com/ (accessed September 4, 2024).

[143] Wentland SA, Ancona ZH, Bagstad KJ, Boyd J, Hass JL, Gindelsky M, et al. Accounting for land in the United States: Integrating physical land cover, land use, and monetary valuation. Ecosystem Services 2020;46:101178. https://doi.org/10.1016/j.ecoser.2020.101178.

[144] Davis R, Laurens L. Algal Biomass Production via Open Pond Algae Farm Cultivation: 2019 State of Technology and Future Research. Renewable Energy 2020.

[145] Pocewicz A, Copeland H, Kiesecker J. Potential Impacts of Energy Development on Shrublands in Western North America. Natural Resources and Environmental Issues 2011;17.

[146] Yeh S, Jordaan S, Brandt A, Turetsky M, Spatari S, Keith D. Land Use Greenhouse Gas Emissions from Conventional Oil Production and Oil Sands. Environmental Science & Technology 2010;44:8766–72. https://doi.org/10.1021/es1013278.

[147] Staples MD. Water consumption footprint and land requirements of alternative diesel and jet fuel. Thesis. Massachusetts Institute of Technology, 2013.

[148] Gasoline and Diesel Fuel Update n.d. https://www.eia.gov/petroleum/gasdiesel/index.php (accessed August 8, 2022).

[149] Bauer AM, Brown A. Quantitative Assessment of Appropriate Technology. Procedia Engineering 2014;78:345–58. https://doi.org/10.1016/j.proeng.2014.07.076.

[150] Dębowski M, Świca I, Kazimierowicz J, Zieliński M. Large Scale Microalgae Biofuel Technology—Development Perspectives in Light of the Barriers and Limitations. Energies 2023;16:81. https://doi.org/10.3390/en16010081.

[151] Anber R. Understanding Uncertainty in Life Cycle Assessment (LCA): Navigating the Unknown. Carbon Leadership Forum 2024. https://carbonleadershipforum.org/understanding-uncertainty/ (accessed September 4, 2024).

[152] The Chemical Engineering Plant Cost Index - Chemical Engineering n.d. https://www.chemengonline.com/pci-home (accessed January 31, 2020).

[153] Davis R, Hawkins T, Coleman A, Gao S, Klein B, Wiatrowski M, et al. Economic, Greenhouse Gas, and Resource Assessment for Fuel and Protein Production from Microalgae: 2022 Algae Harmonization Update 2024. https://doi.org/10.2172/2318964.

[154] N Hexane Weekly Report 15 Aug, 2015 14 Aug 15, 04:50 pm - Global Chemical Price n.d. http://www.globalchemicalprice.com/chemical-market-reports/n-hexane-weekly-report-15-aug-2015 (accessed July 1, 2024).

[155] Combined Heat and Power – Finance A detailed guide for CHP developers – Part 5. Kew, London: Department for Business, Energy & Industrial Strategy; 2021.

[156] Statistics About The Average Cow Weight • Gitnux n.d. https://gitnux.org/average-cow-weight/ (accessed April 4, 2024).

[157] Mangino J, Bartram D, Brazy A. Development of a methane conversion factor to estimate emissions from animal waste lagoons. Paper Presented at US EPAs 17th Annual Emission Inventory Conference, Atlanta, GA, 16-18 April 2002 2001.

[158] Petersen SO, Olsen AB, Elsgaard L, Triolo JM, Sommer SG. Estimation of Methane Emissions from Slurry Pits below Pig and Cattle Confinements. PLOS ONE 2016;11:e0160968. https://doi.org/10.1371/journal.pone.0160968.

[159] Zhang J, Chen J, Ma R, Kumar V, Wah Tong Y, He Y, et al. Mesophilic and thermophilic anaerobic digestion of animal manure: Integrated insights from biogas productivity, microbial viability and enzymatic activity. Fuel 2022;320:123990. https://doi.org/10.1016/j.fuel.2022.123990.

[160] Barth C, Powers T, Rickman J. Part 651 Agricultural Waste Management Field Handbook; Chapter 4: Agricultural Waste Characteristics. United States Department of Agriculture Natural Resources Conservation Service; 2008.

[161] Pain BF, Phillips VR, West R. Mesophilic anaerobic digestion of dairy cow slurry on a farm scale: Energy considerations. Journal of Agricultural Engineering Research 1988;39:123–35. https://doi.org/10.1016/0021-8634(88)90135-7.

[162] Curt A. Gooch, Scott F. Inglis, Karl J. Czymmek. Mechanical Solid-Liquid Manure Separation: Performance Evaluation on Four New York State Dairy Farms - A Preliminary Report. 2005 Tampa, FL July 17-20, 2005, American Society of Agricultural and Biological Engineers; 2005. https://doi.org/10.13031/2013.19506.

[163] Mùller HB, Lund I, Sommer SG. Solid-liquid separation of livestock slurry: efficiency and cost. Bioresource Technology 2000.

[164] Möller K. Effects of anaerobic digestion on soil carbon and nitrogen turnover, N emissions, and soil biological activity. A review. Agron Sustain Dev 2015;35:1021–41. https://doi.org/10.1007/s13593-015-0284-3.

[165] Meisinger J. 1 Ammonia Volatilization from Dairy and Poultry Manure, 2005.

[166] Comfort SD, Kelling KA, Keeney DR, Converse JC. The Fate of Nitrogen from Injected Liquid Manure in a Silt Loam Soil. Journal of Environmental Quality 1988;17:317–22. https://doi.org/10.2134/jeq1988.00472425001700020027x.

[167] Markfoged R, Nielsen LP, Nyord T, Ottosen LDM, Revsbech NP. Transient N2O accumulation and emission caused by O2 depletion in soil after liquid manure injection. European Journal of Soil Science 2011;62:541–50. https://doi.org/10.1111/j.1365-2389.2010.01345.x.

[168] Dell CJ, Salon PR, Franks CD, Benham EC, Plowden Y. No-till and cover crop impacts on soil carbon and associated properties on Pennsylvania dairy farms. Journal of Soil and Water Conservation 2008;63:136–42. https://doi.org/10.2489/63.3.136.

[169] Herr C, Mannheim T, Müller T, Ruser R. Effect of Nitrification Inhibitors on N2O Emissions after Cattle Slurry Application. Agronomy 2020;10:1174. https://doi.org/10.3390/agronomy10081174.

[170] Vanderzaag A, Jayasundara S, Wagner-Riddle C. Strategies to mitigate nitrous oxide emissions from land applied manure. Fuel and Energy Abstracts 2011;166:464–79. https://doi.org/10.1016/j.anifeedsci.2011.04.034.

[171] Viscosity dependent dual-permeability modeling of liquid manure movement in layered, macroporous, tile drained soil - Frey - 2012 - Water Resources Research - Wiley Online Library n.d. https://agupubs.onlinelibrary.wiley.com/doi/full/10.1029/2011WR010809 (accessed December 20, 2023).

[172] Möller K, Stinner W. Effects of different manuring systems with and without biogas digestion on soil mineral nitrogen content and on gaseous nitrogen losses (ammonia,

nitrous oxides). European Journal of Agronomy 2009;30:1–16. https://doi.org/10.1016/j.eja.2008.06.003.

[173] Anaerobically digested dairy manure as an alternative nitrogen source to mitigate nitrous oxide emissions in fall-fertilized corn n.d. https://cdnsciencepub.com/doi/full/10.1139/cjss-2016-0097 (accessed December 20, 2023).

[174] Thomas BW, Hao X. Nitrous Oxide Emitted from Soil Receiving Anaerobically Digested Solid Cattle Manure. J Environ Qual 2017;46:741–50. https://doi.org/10.2134/jeq2017.02.0044.

[175] Verhoeven E, Pereira E, Decock C, Garland G, Kennedy T, Suddick E, et al. N 2 O emissions from California farmlands: A review. California Agriculture 2017;71:148–59. https://doi.org/10.3733/ca.2017a0026.

[176] Chastain JP. A Model to Estimate Ammonia Loss Following Application of Animal Manure 2006.

[177] Chastain JP. Ammonia Volatilization Losses during Irrigation of Liquid Animal Manure. Sustainability 2019;11:6168. https://doi.org/10.3390/su11216168.

[178] Chang, Harter T, Letey J, Meyer D, Meyer R, Campbell M, et al. Managing Dairy Manure in the Central Valley of California. ANR Publication 2006;9004.

[179] US EPA O. Livestock Anaerobic Digester Database 2014. https://www.epa.gov/agstar/livestock-anaerobic-digester-database (accessed December 20, 2023).

[180] FNR: Mediathek - LEITFADEN FÜR DAS EINREICHEN VON ANTRÄGEN im Rahmen der Richtlinie zur Förderung von Investitionen in emissionsmindernde

Maßnahmen bei der Vergärung von Wirtschaftsdüngern n.d. https://mediathek.fnr.de/leitfaden-fur-das-einreichen-von-antragen-forderung-von-investitionen-in-emissionsmindernde-massnahmen-bei-der-vergarung-von-wirtschaftsdungern.html (accessed January 10, 2024).

[181] Sarika J. Market Report: Germany. World Biogas Association; 2023.

APPENDIX A: SUPPORTING INFORMATION FOR CHAPTER 2

Critical Assumptions and Modeling Inputs

Critical modeling inputs and assumptions for the Current and Future Scenarios are provided in Tables A1 and A2. All commodity costs have been indexed to 2019 USD using the Chemical Engineering Plant Cost Index (CEPI) [152].

Table A1: Modeling constants use in both fuel production pathways and scenarios.

Parameter	Value	Units	Reference
Operational Days per Year	330	days/yr	Davis et al. [5]
Cultivation Area	5000	wetted acres	Davis et al. [5]
Pond Size	10	acres per pond	Davis et al. [5]
Pond Depth	0.20	m	Davis et al. [5]
Cultivated Strain	*Scenedesmus obliquus*	[strain]	Quiroz et al. [62]; Gao et al. [54]
Inoculation Concentration	0.1	g/L	Assumption
Harvesting Concentration	0.6	g/L	Assumption
Days to Automated Harvest	5	days	Assumption
P Content of DAP*	20%	dry wt%	Davis et al. [5]
N Content of DAP	18%	dry wt%	Davis et al. [5]
N Content of Ammonia	82%	dry wt%	Davis et al. [5]
Cost of Electricity	$0.07	$/kWh	Quiroz et al. [3]
Cost of Ammonia	$0.80	$/kg	Quiroz et al. [3]
Cost of DAP	$0.66	$/kg	Quiroz et al. [3]
Cost of Natural Gas	$0.22	$/kg	Quiroz et al. [3]
Cost of Hydrogen	$1.47	$/kg	Quiroz et al. [3]
Cost of Process Water	$0.20	$/m3	Quiroz et al. [3]
Value of Biochar	$0.10	$/kg	Assumption
Value of Recovered Ammonia	$0.80	$/kg	Quiroz et al. [3]
Value of Recovered DAP	$0.66	$/kg	Quiroz et al. [3]
Cost Year	2019	[year]	Assumption
Internal Rate of Return	10%	%	BETO**

*DAP: Diammonium Phosphate

**BETO: Bioenergy Technologies Office

Table A2: Modeling inputs for the Current and Future modeling scenarios.

Cultivation Parameters	**Current Scenario**	**Future Scenario**	**Units**	**Reference**
Carbon Utilization Efficiency	65%	90%	%	Davis et al. [153]
Cost of CO_2 (from DAC)	$230	$50	$/tonne CO_2	EIA [61]
Nutrient Surplus	0%	20%	% excess	Davis et al. [5]
Algae Carbon Content	54%	57.4%	wt% AFDW	Davis et al. [5]
Algae P Content	0.22%	0.20%	wt% AFDW	Davis et al. [5]
Algae N Content	1.8%	1.6%	wt% AFDW	Davis et al. [5]
Algae Protein Content	13.2%	9.0%	dry wt%	Davis et al. [5]
Algae Carbohydrate Content	52.8%	42.1%	dry wt%	Davis et al. [5]
Algae Lipid Content	27.4%	41.2%	dry wt%	Davis et al. [5]
Algae Ash Content	6.6%	7.7%	dry wt%	Assumption
Anaerobic Storage Losses	10%	5%	% dry matter loss	Wendt et al. [53]
Slurry Pump Efficiency	70%	70%	% (efficiency)	Wendt et al. [53]
HEFA[1] Parameters	**Current Scenario**	**Future Scenario**	**Units**	**Reference**
HPH[2] - Number of Passes	2	1	number of passes	Kang et al. [64]
HPH - Pressure Rating	1500	400	PSI	Kang et al. [64]
WHE[3] - Solvent to Biomass Ratio	1.8	1.8	g solvent:g wet biomass	Frank et al. [65]
WHE - Hexane Loss	5.2	5.2	g hexane per kg oil	Frank et al. [65]
WHE - Extraction Efficiency	90%	99%	% of lipids extracted	Frank et al. [65]
Cost of Hexane Solvent	$0.74	$0.74	$/kg	Gillarkar [154]
Propane Selling Price	$0.94	$0.94	$/liter	(AFDC[5]) [71]
LNG Selling Price	$0.96	$0.96	$/liter	(AFDC[5]) [71]
Naphtha Selling Price	$1.07	$1.07	$/liter	(AFDC[5]) [71]
Diesel Selling Price	$0.65	$0.65	$/liter	(AFDC[5]) [71]
HTL[4] Parameters	**Current Scenario**	**Future Scenario**	**Units**	**Reference**
Reactor Residence Time	15	15	minutes	Chen and Quinn [4]
Biochar (HTL solids) Recovery	60%	90%	% of input recovered	Assumption [4]
Ammonia Recovery	60%	90%	% of input recovered	Assumption [4]
DAP Recovery	60%	90%	% of input recovered	Assumption [4]

[1]HEFA: Hydroprocessed Esters and Fatty Acids
[2]HPH: High Pressure Homogenization
[3]WHE: Wet Hexane Extraction
[4]HTL: Hydrothermal Liquefaction
[5]AFDC: Alternative Fuels Data Center

Algae Cultivation and Dewatering

For more details on the thermal and biological growth model used to estimate algae productivity and other cultivation parameters the reader is referred to the works of Greene et al.

[48], Quiroz et al. [51] Quiroz et al. [62], and Quiroz et al. [3]. These publications and supporting information documents contain the equations and methodologies used for model construction as well as detailed results for various model validation studies.

Long-Term Anaerobic Storage

Long-term anaerobic storage was the assumed method of biomass storage to offset seasonal variability in biomass production and provide a continual supply of biomass to the conversion facility. Biomass was assumed to be stored in 1,000 m^3 belowground storage pits at 20% solids [53]. A 30-day dry matter loss rate of 10% was applied, based on experimental data from Wendt et al. [53] with losses applied to the carbohydrate fraction of the biomass and the resulting biomass composition for downstream conversion determined accordingly. Costs for gravity settlers were used as a proxy to estimate the capital expenses of the storage process [5,53].

Sustainable Aviation Fuel (SAF) Production Pathway

Additional information regarding the high-pressure homogenization (HPH) and wet hexane extraction (WHE) processes are provided in Table A3. Critical modeling inputs and assumptions surrounding the HEFA process are provided in Table A4-A5. Additional information regarding the recovery of nutrients and energy via anaerobic digestion (AD), pressure swing absorption (PSA), and combined heat and power (CHP) is provided in Table A6-A9.

Lipid Extraction

Table A3: Critical modeling inputs for the high-pressure homogenization (HPH) and wet hexane extraction (WHE) processes.

HPH Parameters	Value	Units	Reference
HPH Low Pressure Rating	400	bar	Kang et al. [64]
HPH High Pressure Rating	1500	bar	Kang et al. [64]
Number of passes (Tetraselmis)	1	pass (at low pressure)	Kang et al. [64]
Number of passes (Chlorella)	2	passes (at high pressure)	Kang et al. [64]
Number of passes (Nanno)	6	passes (at high pressure)	Kang et al. [64]
Flow Rate (low pressure)	23	m3/hour	Kang et al. [64]
Flow Rate (high pressure)	5	m3/hour	Kang et al. [64]
Capital Cost	$475,209	per unit	Kang et al. [64]
Install Factor	1	install factor	Assumption [5]
Scaling Exponent	0.7	scaling exponent	Assumption [5]
Electricity consumption	0.1784	kWh/kg dry biomass	Kang et al. [64]
Cell disruption efficiency	90%	% of cells disrupted	Kang et al. [64]
WHE Parameters	**Value**	**Units**	**Reference**
Natural Gas Input	1.7	kWh (thermal)/kg oil	Frank et al. [65]
Electricity Input	0.54	kWh (electric)/kg oil	Frank et al. [65]
Hexane Loss	5.2	g/kg oil	Frank et al. [65]
Extraction Efficiency	95%	% of lipid extracted	Frank et al. [65]
Solvent:Biomass Ratio	1.8	g solvent/g wet biomass	Frank et al. [65]
WHE Capital Cost	$84.51	2011 USD tonne DW^{-1} yr^{-1}	Delrue et al. [66]

Hydroprocessed Esters and Fatty Acids (HEFA) Process

Table A4: Product profiles for the hydroprocessed esters and fatty acids (HEFA) process from Pearlson et al. [23]

Product Profiles (wt%)	Maximum Distillate	Maximum Jet
Oil In	100	100
Hydrogen Input	2.7	4
Total In	**102.7**	**104**
Water	8.7	8.7
CO_2	5.5	5.4
Propane	4.2	4.2
LPG	1.6	6
Naphtha	1.8	7
Jet	12.8	49.4
Diesel	68.1	23.3
Total Out	**102.7**	**104**

Table A5: Utility usage for the hydroprocessed esters and fatty acids (HEFA) process based on the "Maximum Jet" profile from Pearlson et al. [23]*. All utilities are reported per kg of oil feed.*

Process	Boiler Feed Water (kg/hr)	Cooling Water (kg/hr)	Steam (kg/hr)	Power (kW)	NG (kg/hr)
Hydrotreater	0.25	0	-0.25	0.01	0.02
Isomerization	0	2.55	0	0	0.03
Gas Processing Unit	0	5.26	0	0.01	0
Hydrogen SMR	0.5	5.33	-0.25	0.02	0.06
Additional Inputs for "Max. Jet"	0	0	0	0	0.06

Costing Functions for HEFA Equipment

Costing equations for the hydrotreater, cooling water tower and pump, and firewater storage tank and pump were obtained from Chen and Quinn [4] and are presented in Equations A1-A4.

$$HT_{CAPEX} = \$27000000 * \left(\frac{BPD_{in}}{6524}\right)^{0.75} * \left(\frac{CEPI_{2019}}{CEPI_{2007}}\right) * 1.51 \qquad \text{(Eq. A1)}$$

In Equation A1, the hydrotreater capital cost (HT_{CAPEX}) was determined using the base cost of a hydrotreater (in 2007 USD) from Chen and Quinn [4] with a scaling flowrate of 6524 BPD of algae oil. The scaling exponent of 0.75 and install factor of 1.51 were also obtained from Chen and Quinn [4]. The installed capital cost was indexed to 2019 USD using the CEPI [152].

$$CWT_{CAPEX} = \$2000000 * \left(\frac{CW_{flow}}{16162253}\right)^{0.6} * \left(\frac{CEPI_{2019}}{CEPI_{2009}}\right) * 2.95 \qquad \text{(Eq. A2)}$$

$$CWP_{CAPEX} = \$445700 * \left(\frac{CW_{flow}}{16162253}\right)^{0.6} * \left(\frac{CEPI_{2019}}{CEPI_{2009}}\right) * 2.95 \qquad \text{(Eq. A3)}$$

In Equations A2 and A3, the cooling water tower capital cost (CWT_{CAPEX}) and cooling water pump capital cost (CWP_{CAPEX}) were determined using the base cost of each (in 2009 USD) from Chen and Quinn [4] with a scaling flowrate of 16162253 kg/hr. The scaling exponent of 0.6 and install factor of 2.95 were also obtained from Chen and Quinn [4]. The installed capital costs

were indexed to 2019 USD using the CEPI [152]. Capital costing equations for the firewater storage tank and pump are shown in Equations A4 and A5.

$$FWST_{CAPEX} = \$166100 * \left(\frac{TPD_{AFDW\ algae}}{2000}\right)^{0.51} * \left(\frac{CEPI_{2019}}{CEPI_{1997}}\right) * 2.95 \qquad \text{(Eq. A4)}$$

$$FWP_{CAPEX} = \$184000 * \left(\frac{TPD_{AFDW\ algae}}{2000}\right)^{0.79} * \left(\frac{CEPI_{2019}}{CEPI_{1997}}\right) * 2.95 \qquad \text{(Eq. A5)}$$

In Equations A4 and A5, the fire water storage tank capital cost ($FWST_{CAPEX}$) and fire water pump capital cost (FWP_{CAPEX}) were determined using the base cost of each (in 1997 USD) from Chen and Quinn [4] with a scaling flowrate of 2000 tonnes AFDW biomass per day through the biorefinery. The scaling exponent of 0.51 and 0.79 and install factor of 2.95 were also obtained from Chen and Quinn [4]. The installed capital costs were indexed to 2019 USD using the CEPI [152].

Costing functions for the isomerizer, hydrogen island (for on-site steam methane reforming), saturated gas plant were obtained from Gary et al. [68] and are presented in Figures A1-A3. Costing curves are shown in 2005 USD and installed equipment costs were indexed to 2019 USE using the CEPI [152]. Additionally, costs for crude oil storage (13 days) and liquid fuel products (25 days) were obtained from Gary et al. [68].

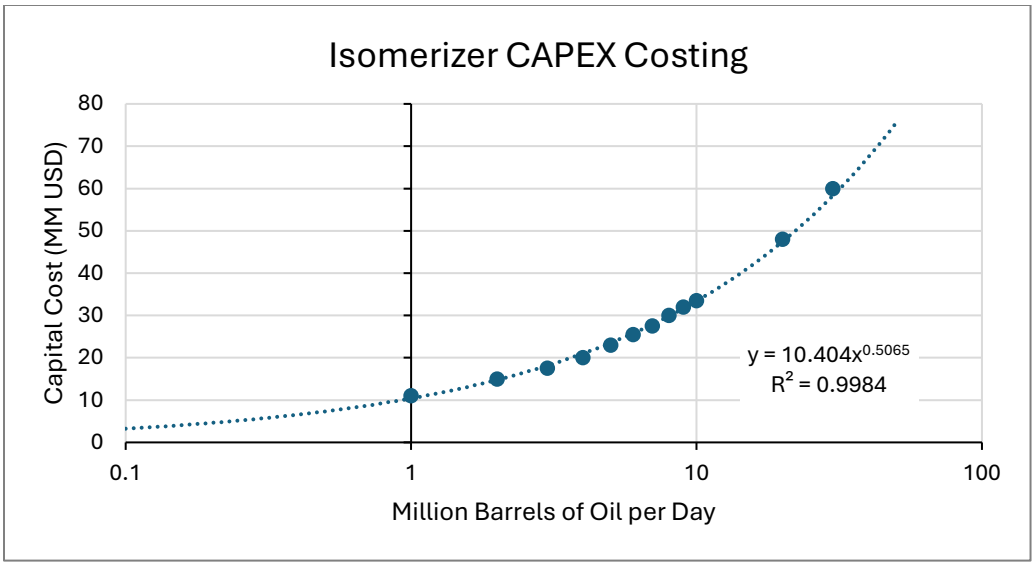

Figure A1: Costing curve for the isomerizer in 2005 USD [68].

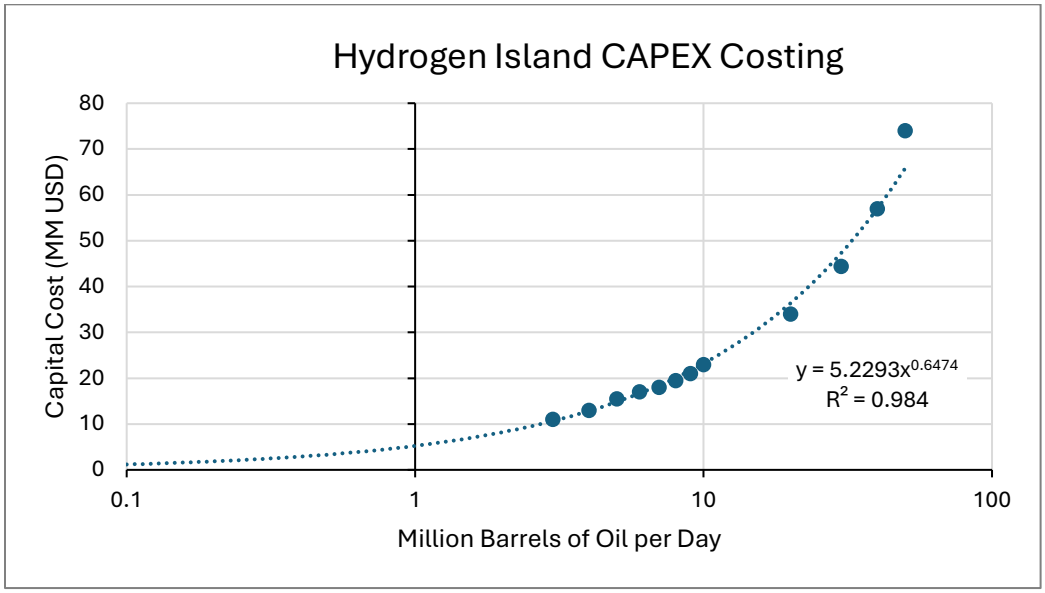

Figure A2: Costing curve for the hydrogen island in 2005 USD [68].

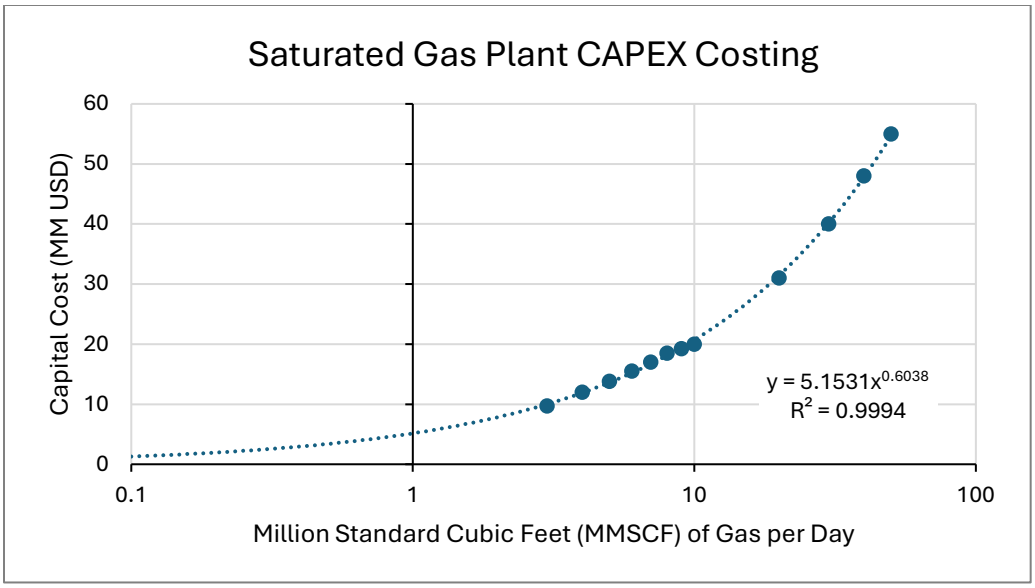

Figure A3: Costing curve for the saturated gas plant in 2005 USD [68].

Additional Capital Expenses and Fixed Operational Expenses

Additional direct capital costs for a warehouse, site development, and additional piping were assessed as 4%, 9%, and 4.5% of total installed capital costs, respectively [5]. A project contingency of 10% was applied to the fixed capital investment for all refinery equipment. Fixed operational costs for labor (12 employees at an average salary of $72,000 per year), maintenance 5.5% of the fixed capital investment), property insurance and tax (1.5% of the fixed capital investment), miscellaneous supplies (0.2% of the fixed capital investment), and a 10% contingency on fixed operational costs were obtained directly from Pearlson et al. [23].

Nutrient and Energy Recovery

Table A6: Critical modeling inputs for anaerobic digestion (AD) of lipid-extracted algae (LEA) [65]

Parameter	Value	Units
CH_4 Yield	0.3	L CH4/g-TS entering AD
Biogas CH_4 Content	67%	% of CH4 in biogas
Process Heat	0.68	kWh (thermal)/kg TS
Process Electricity	0.122	kWh/kg VS
Centrifuge Electricity	0.014	kWh/kg VS
Total AD Electricity	0.136	kWh/kg VS
Ratio of VS:TS	0.900	kg VS/kg TS

Table A7: Nutrient recovery from anaerobic digestion (AD) of lipid-extracted algae (LEA) [65]

Parameter	Value	Units
LEA Carbon Content	44%	wt% of dry solids
C in Supernatant	50%	% of C balance
C in Digestate	50%	% of C balance
C:N:P in Biomass	103:10:01	ratio
C in Biomass	50%	wt% C in whole biomass
C Sequestration in AD Residues	8%	% of C in digestate sequestered
N Retention in Supernatant	80%	% of N retained as NH_3
N Volatilization	5%	% of N volatilized
Resulting N Recovery	76%	% N recovery to algae cultures
N to Digestate (Solids)	20%	% of N to organic N in digestate
N Bioavailability in Digestate	40%	availability
N2O-N Emissions to Soil	0.01	kg N2O-N per kg N in residues
P to Supernatant	50%	% of P to supernatant
P to Digestate	50%	% of P to digestate
P Utilization	100%	availability

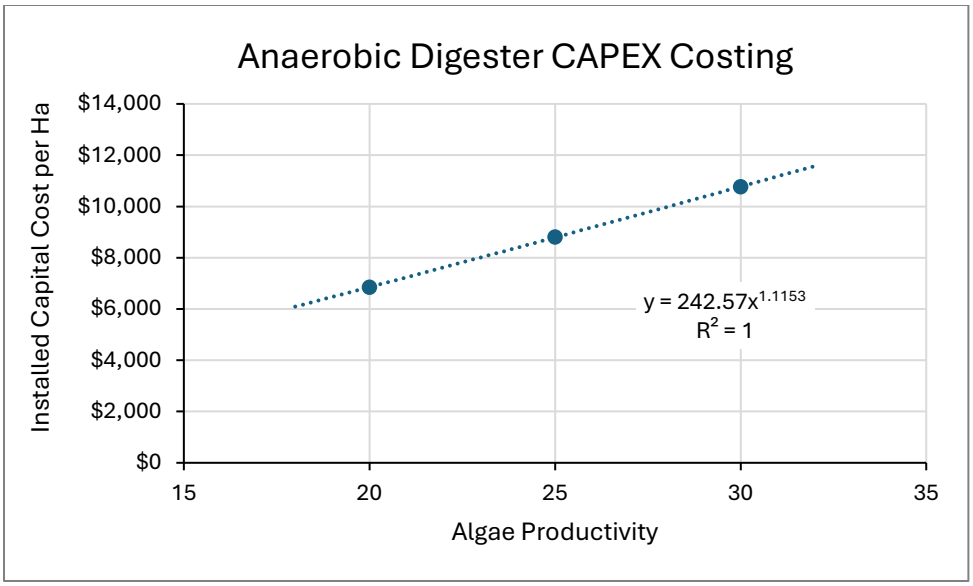

Figure A4: Costing curve for the anaerobic digester as a function of algae productivity based on costing data from Zamalloa et al. [69]

Table A8: Critical modeling inputs for pressure swing absorption [65]

Parameter	Value	Units
Exit pressure	200	psig
Electricity	0.25	kWh/Nm3-raw biogas
Potential fugitive CH_4 emissions	3%	% of CH_4 in

The capital expense of the pressure swing absorption (PSA) unit was determined with a costing function obtained from Chen and Quinn [4] presented in Equation A6.

$$PSA_{CAPEX} = \$1750000 * \left(\frac{V_{biogas}}{10}\right)^{0.8} * \left(\frac{CEPI_{2019}}{CEPI_{2004}}\right) * 2.47 \qquad \text{(Eq. A5)}$$

In Equation A5, the PSA unit capital cost (PSA_{CAPEX}) was determined using the base cost of a PSA unit (in 2004 USD) from Chen and Quinn [4] with a scaling flowrate of 10 MMSCF/day of biogas. The scaling exponent of 0.8 and install factor of 2.47 were also obtained from Chen and Quinn [4]. The installed capital cost was indexed to 2019 USD using the CEPI [152].

Table A9: Critical modeling parameters for combined heat and power [65]

Parameter	Value	Units
Electrical Efficiency	33%	% on LHV basis
Total CHP Efficiency	76%	% on LHV basis
VOC	1	g/mmBTU of fuel input
CO	24	g/mmBTU of fuel input
NOx	113	g/mmBTU of fuel input
PM10	3.1	g/mmBTU of fuel input
PM2.5	3.1	g/mmBTU of fuel input
SOx	0.269	g/mmBTU of fuel input
CH_4	4.26	g/mmBTU of fuel input
N_2O	1.5	g/mmBTU of fuel input
CO_2	59360	g/mmBTU of fuel input

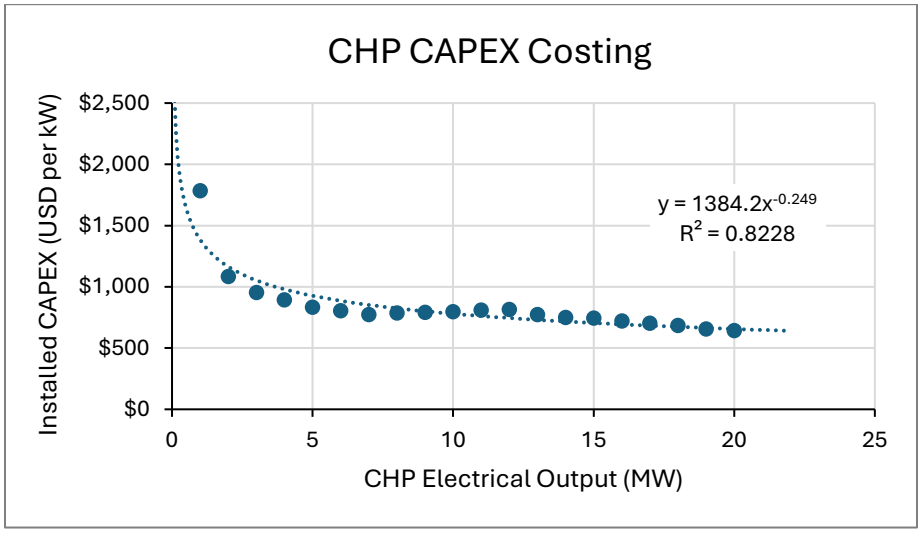

Figure A5: Capital costing curve for the combined heat and power unit (CHP) [155]

Life Cycle Assessment

Table A10: Fuel densities and energy contents used for the energy allocation for life cycle assessment results

Fuel	Density (kg/L) [4,23]	Lower Heating Value (LHV) in mmBTU per liter
Propane	0.4930	0.02227
Liquified Natural Gas (LNG)	0.5500	0.01974
Renewable Diesel	0.8366	0.03421
Bio-Kerosene (SAF)	0.8000	0.03165
Naphtha	0.7447	0.03089

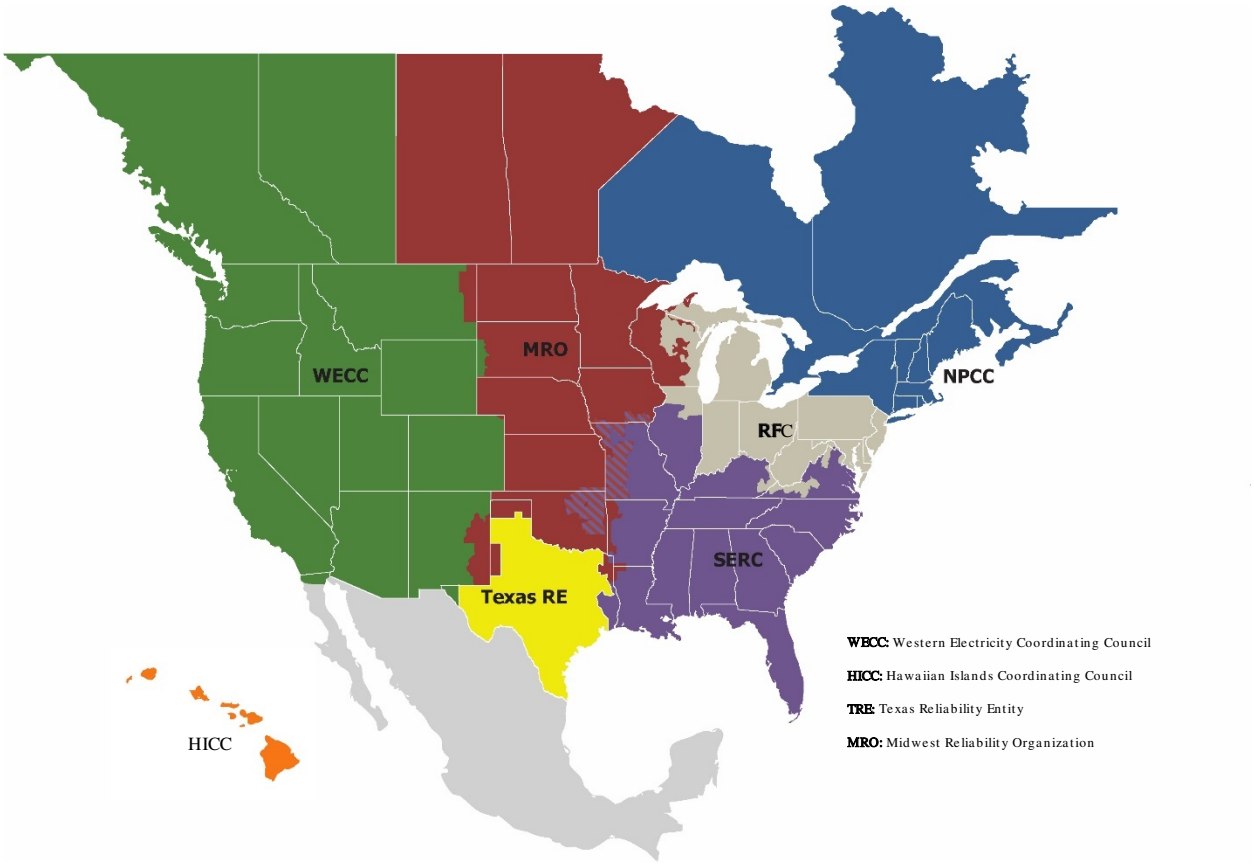

Figure A6: Electricity grid regions used to determine emissions associated with process electricity consumption throughout the United States [73].

Additional Model Outputs

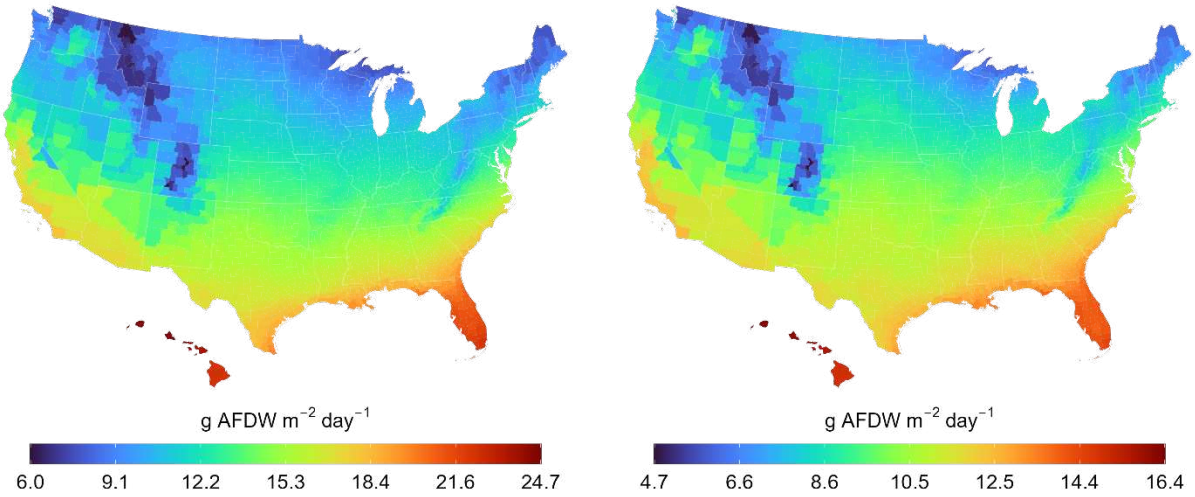

Figure A7: Annual average areal productivity under nutrient replete conditions (left) and nutrient depleted conditions (right).

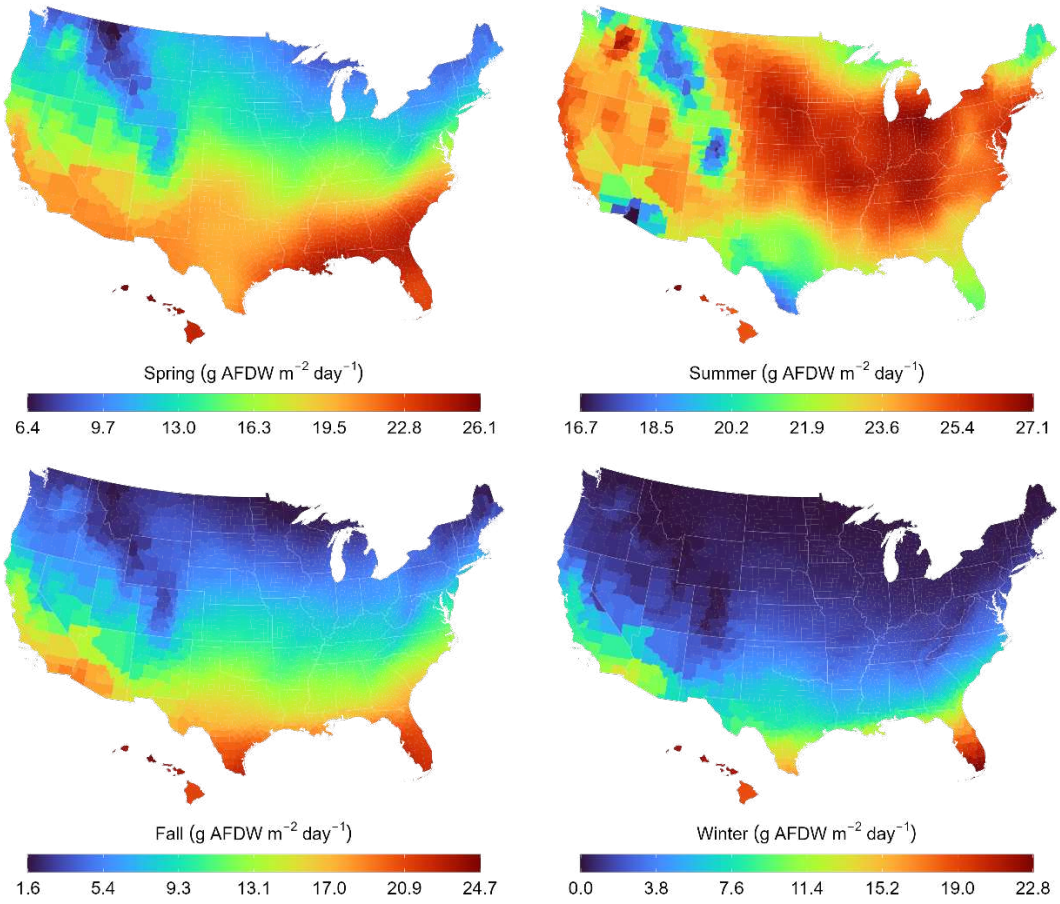

Figure A8: Seasonal areal productivity under nutrient replete conditions

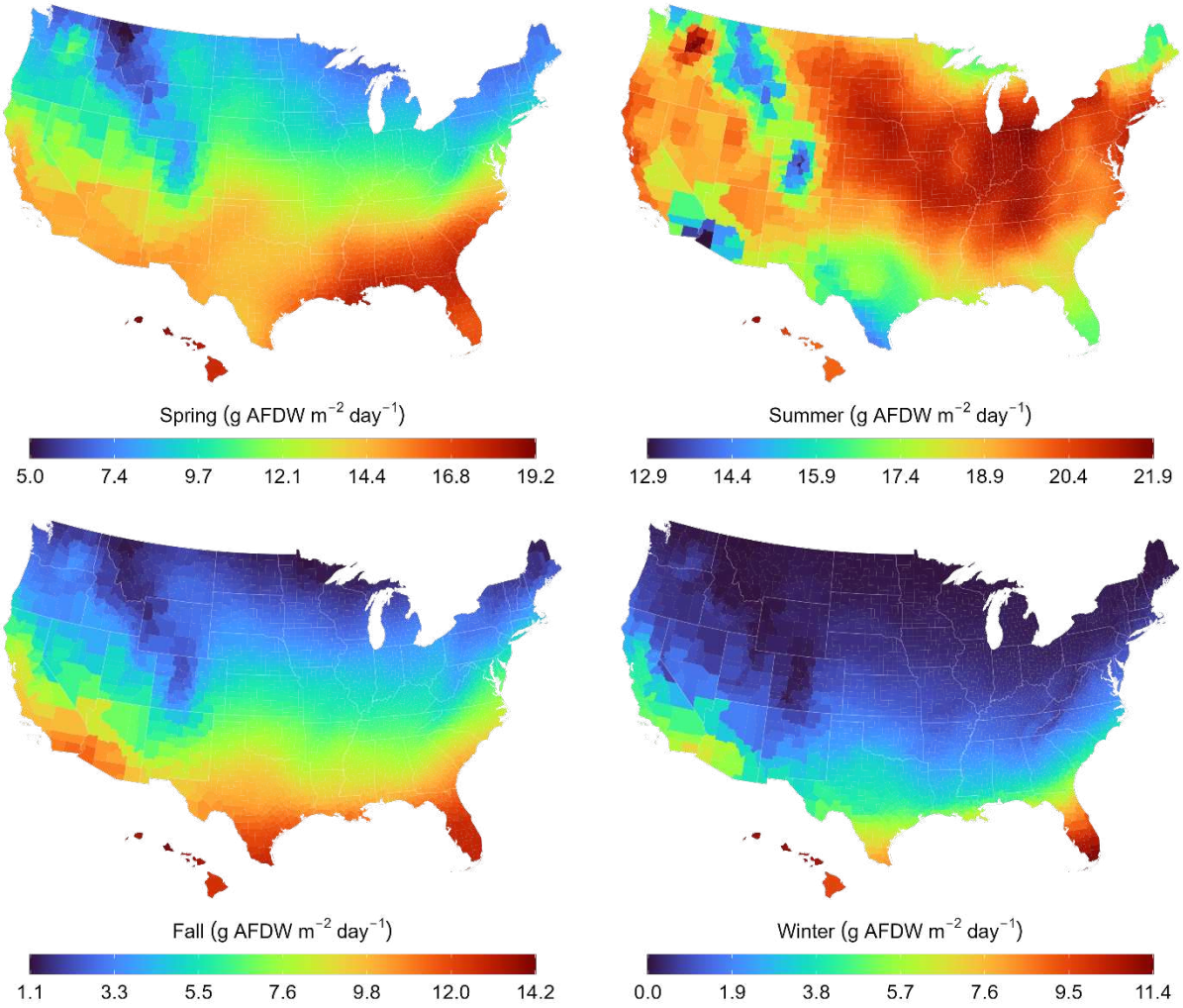

Figure A9: Seasonal areal productivity under nutrient depleted conditions to trigger lipid accumulation in algae biomass.

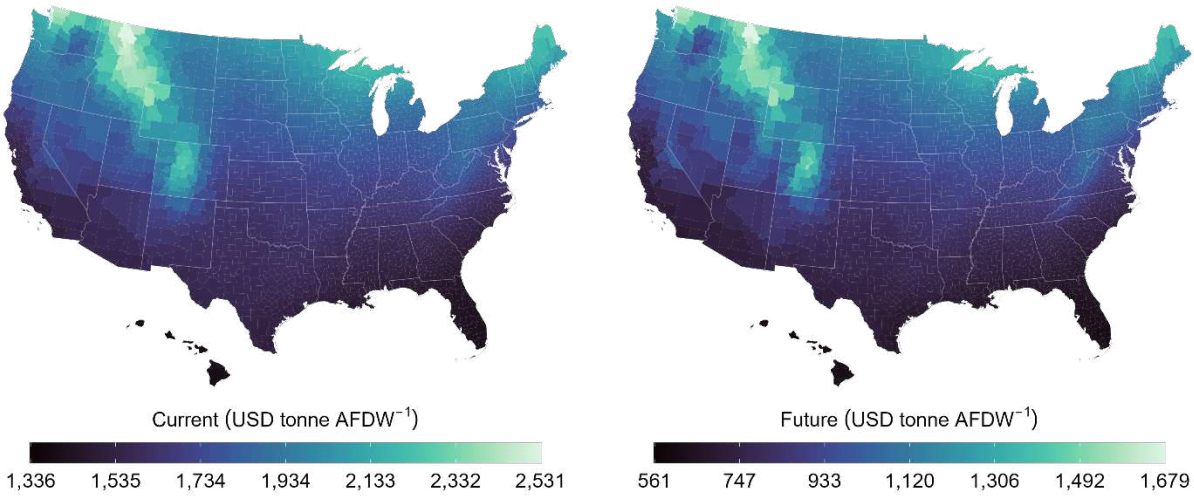

Figure A10: Minimum biomass selling price (MBSP) under the Current (left) and Future (right) scenario assumptions

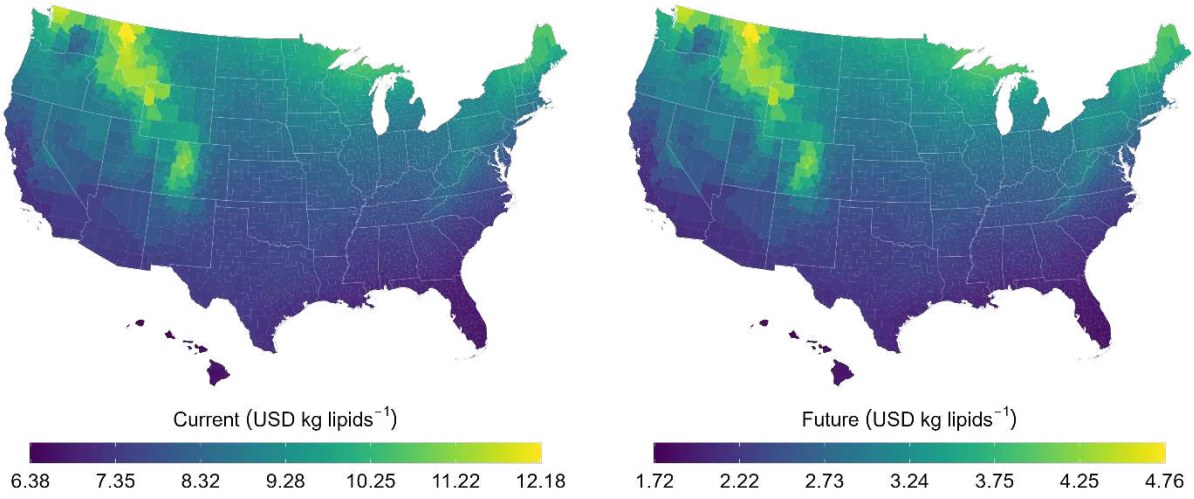

Figure A11: Minimum lipid selling price (MLSP) under the Current (left) and Future (right) scenario assumptions

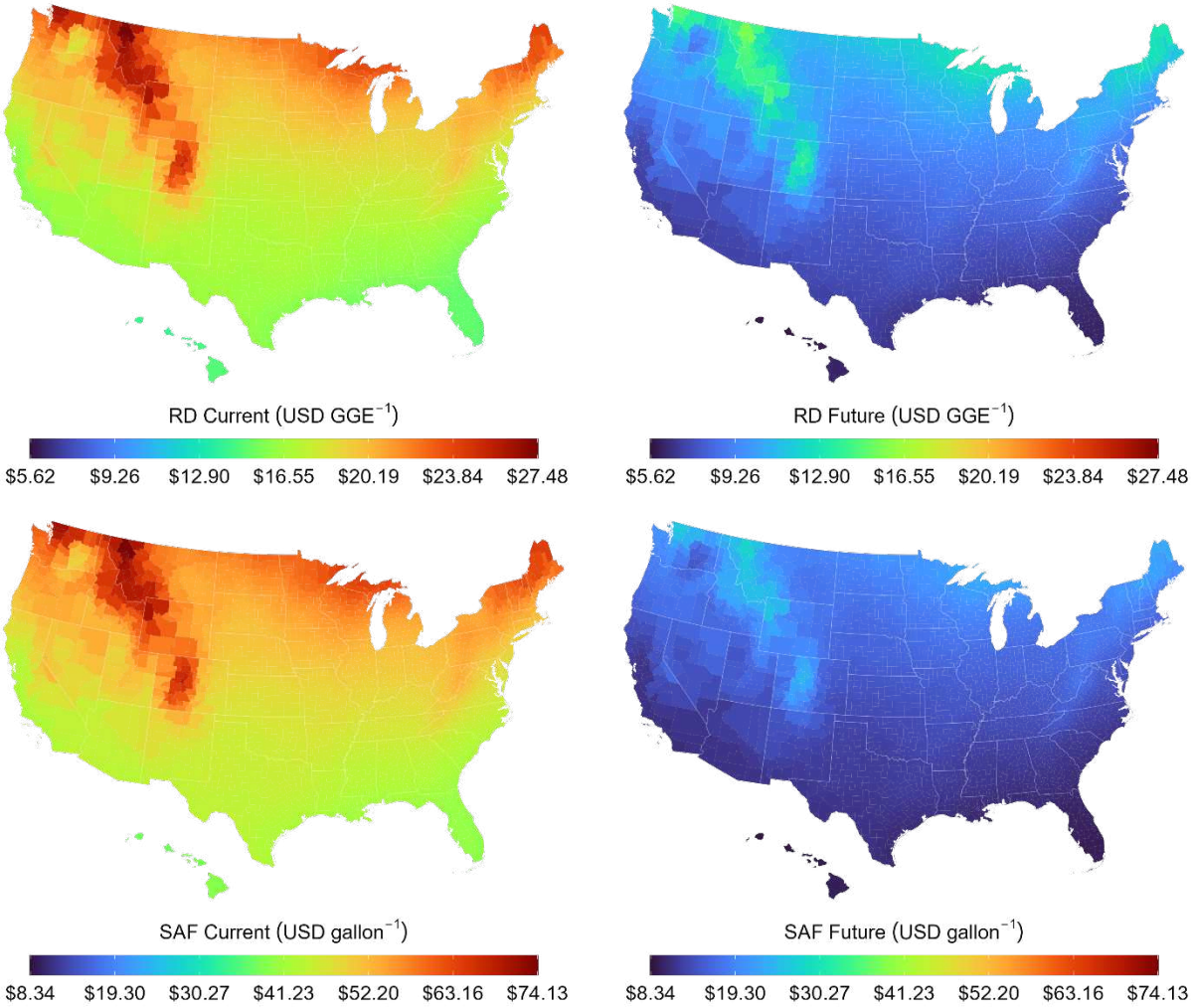

Figure A12: Minimum fuel selling price (in imperial units) for both fuel production pathways under the Current and Future scenarios.

Direct Land Use Change (dLUC) Emissions and Fuel Production Potential

For more details regarding the methodology and assumptions used to quantify dLUC emissions, the reader is referred to the Supporting Information document for Quiroz et al. [3]. In total, 32,801,500 grid cells (measuring 200 m by 200 m) were identified as feasible algae production locations. To account for the direct land use change (dLUC) effects when converting land to an algal biorefinery, dLUC emissions have been estimated using IPCC methodology [102] for each biorefinery location as detailed in Quiroz et al. [3]. In this study arable land types

included deciduous forest, evergreen forest, mixed forest, grasslands, pasture/hay, and cultivated crop lands, and the potential dLUC emissions from converting these areas into algae cultivation facilities was evaluated. The total potential fuel production was determined for each land type in each county based on the spatiotemporal fuel yield per facility area and used to estimate the corresponding dLUC emissions in gCO2-eq MJ Fuel^{-1}. The same approach was used for non-arable land types including barren and shrubland.

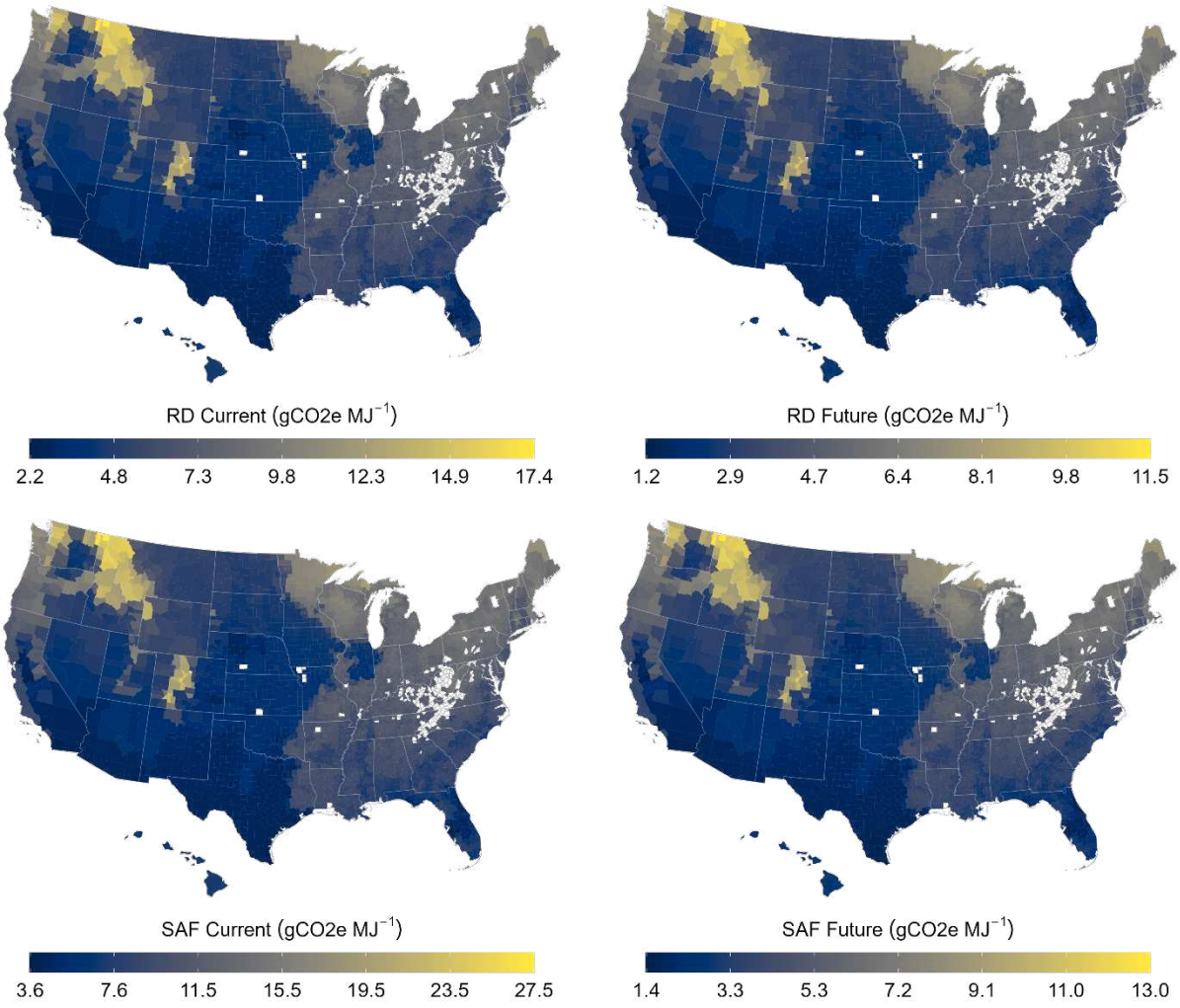

Figure A13: Direct land use change (dLUC) emissions for non-arable land types including barren and shrub land. Blank counties represent counties with zero acres of non-arable land suitable for algae cultivation.

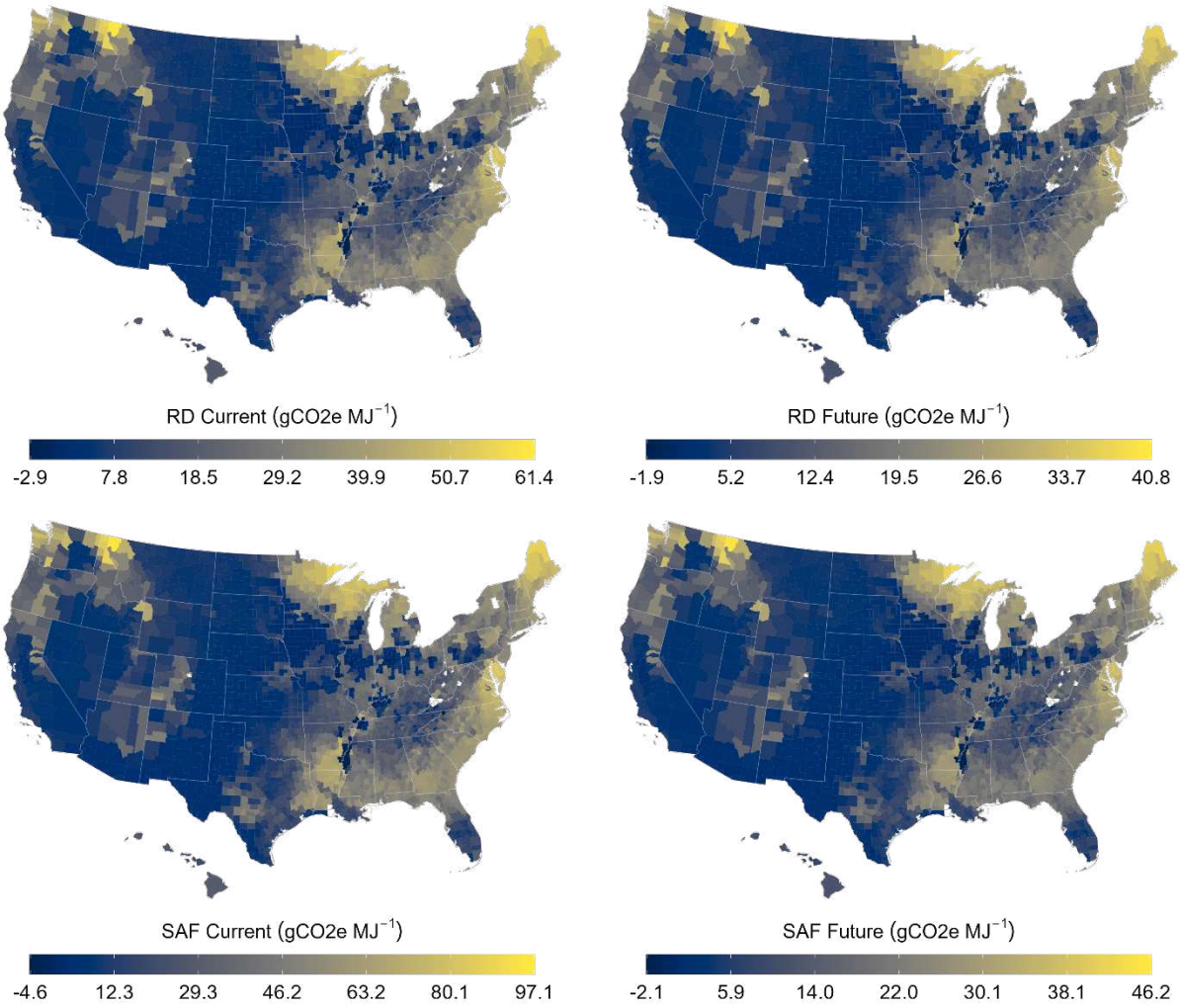

Figure A14: Direct land use change (dLUC) emissions for arable land types including deciduous forest, evergreen forest, mixed forest, grasslands, pasture/hay, and cultivated crop lands currently used for biofuel crops. Blank counties represent counties with zero acres of arable land suitable for algae cultivation.

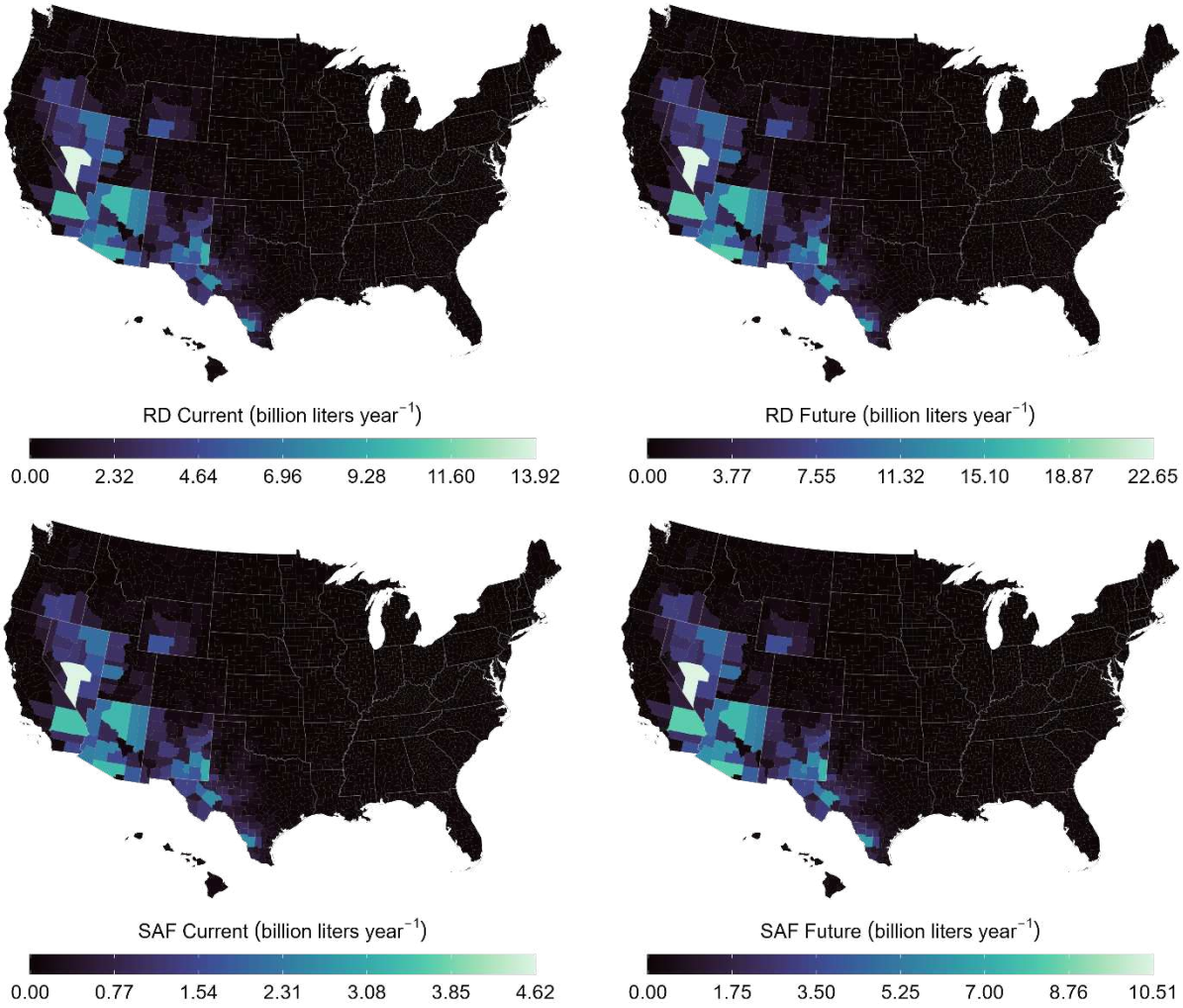

Figure A15: Total annual fuel production potential in billion liters per year on non-arable land types for both fuel production pathways under the Current and Future scenarios.

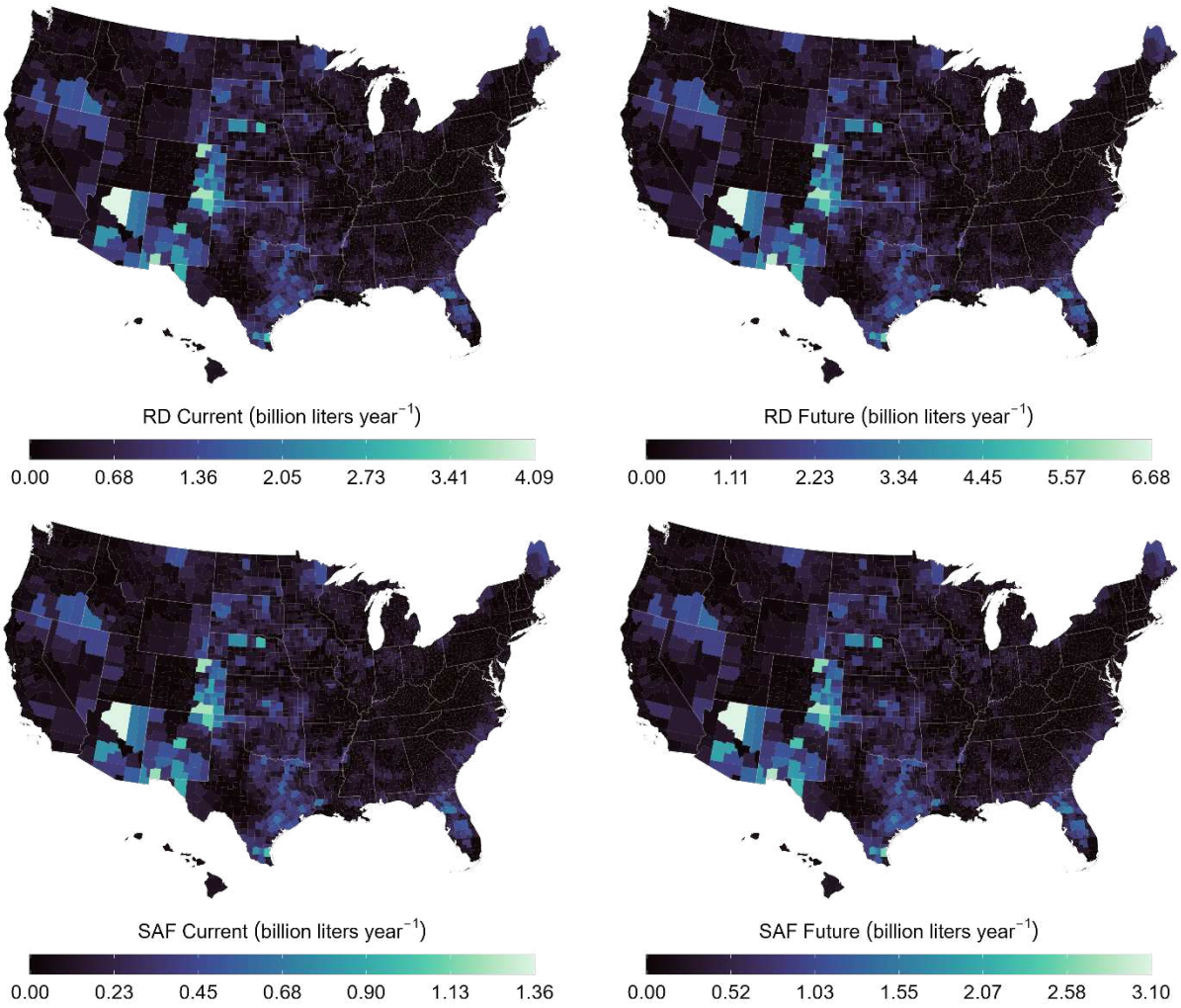

Figure A16: Total annual fuel production potential in billion liters per year on arable land types for both fuel production pathways under the Current and Future scenarios.

Blue Water Footprint and Water Scarcity Footprint

We adopted the methodology used by Quiroz et al. [62] to assess the BWF and water scarcity footprint (WSF) of algae cultivation and conversion processes. The BWF encompasses all freshwater usage within the W2W system boundary. This includes water replenishment for pond evaporation, water lost to media recycling inefficiencies and blowdown, and water for cooling, washing, and other conversion processes. Indirect water usage for the production process consumables like ammonia, DAP, and electricity was also considered within the system boundary. For the SAF pathway, bio-kerosene was treated as the main product from the HEFA process, with an energy allocation used to allocate a fraction of the BWF to the fuel co-products of diesel, naphtha, LNG, and propane.

For the Water Scarcity Footprint (WSF), the Available Water Remaining in the US (AWARE-US) model was employed [75]. This model calculates the WSF by multiplying the BWF by a county-specific characterization factor. These factors compare the freshwater availability of a particular county to the national average in the U.S., with the AWARE-US model offering monthly characterization factors for each U.S. County.

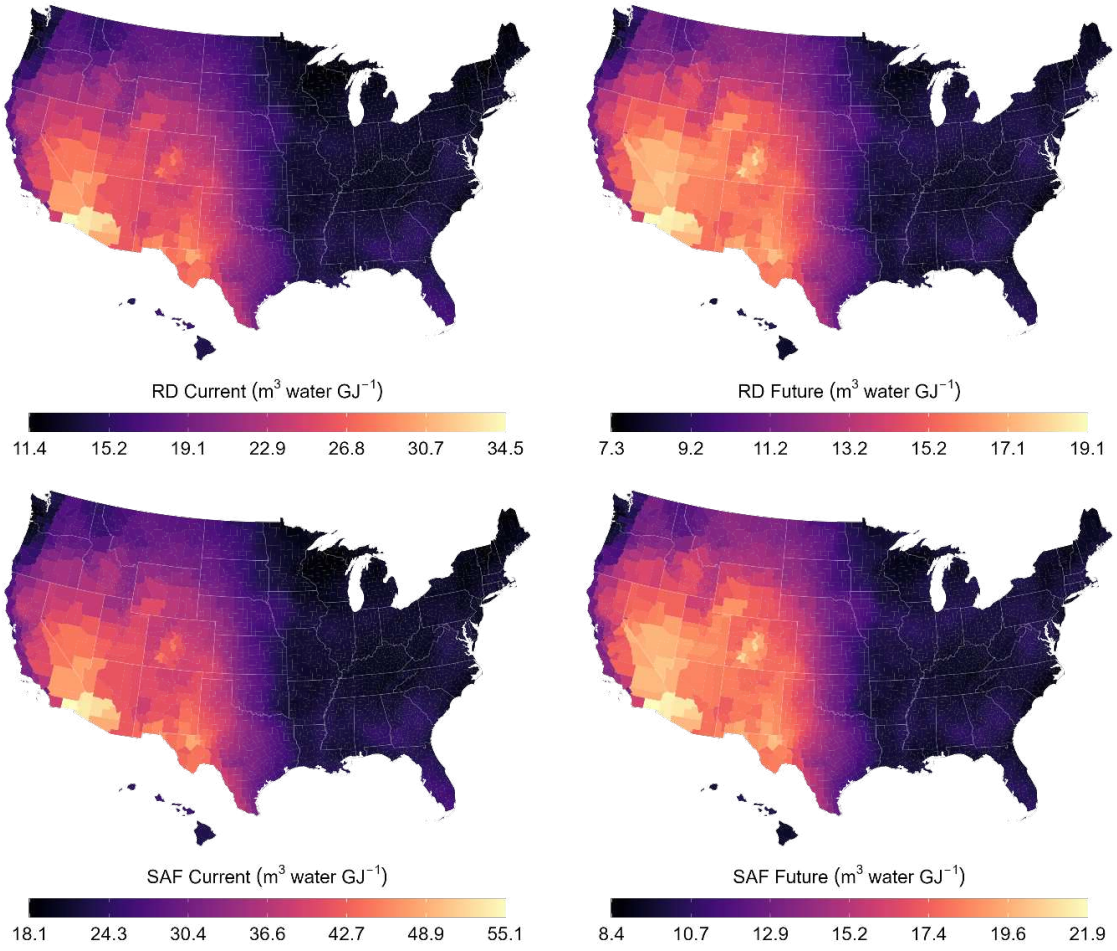

Figure A17: Bue water footprint (BWF) in m3 water per GJ fuel for both conversion pathways under the Current and Future scenarios.

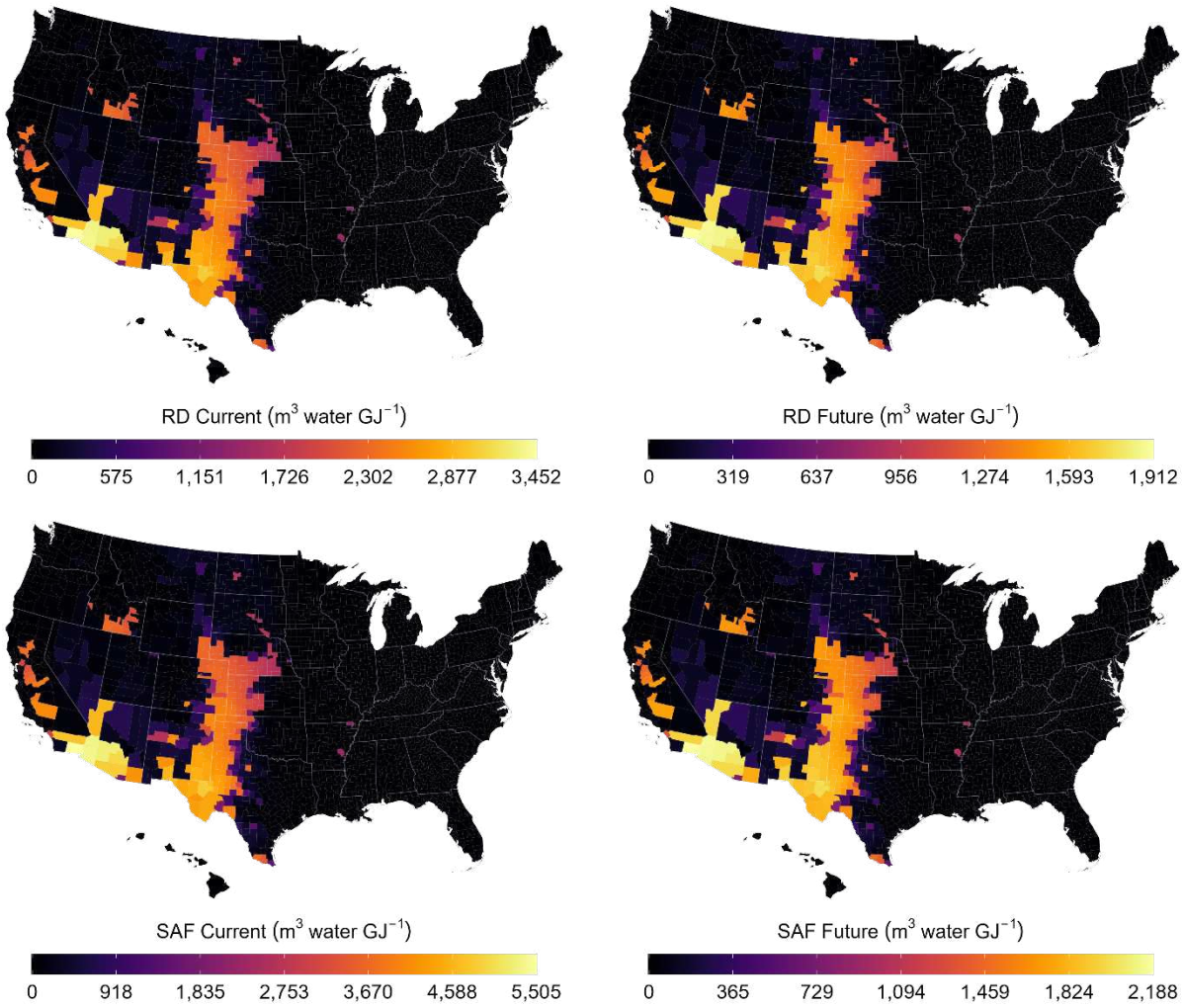

Figure A18: Water scarcity footprint (WSF) in m3 water per GJ fuel for both conversion pathways under the Current and Future scenarios.

Compositional Impacts

The impact of biomass composition on various sustainability and performance metrics was quantified through a ternary plot analysis. For each fuel pathway, the MFSP, GWP, BWF, and biocrude yield (for the HTL pathway) were evaluated at every possible combination of carbohydrates, proteins, and lipids in 5% increments (231 total compositions) under both the Current and Future scenario assumptions. The analysis was performed using Pima County, Arizona as a case study location. Results are plotted in Figures A19-A25.

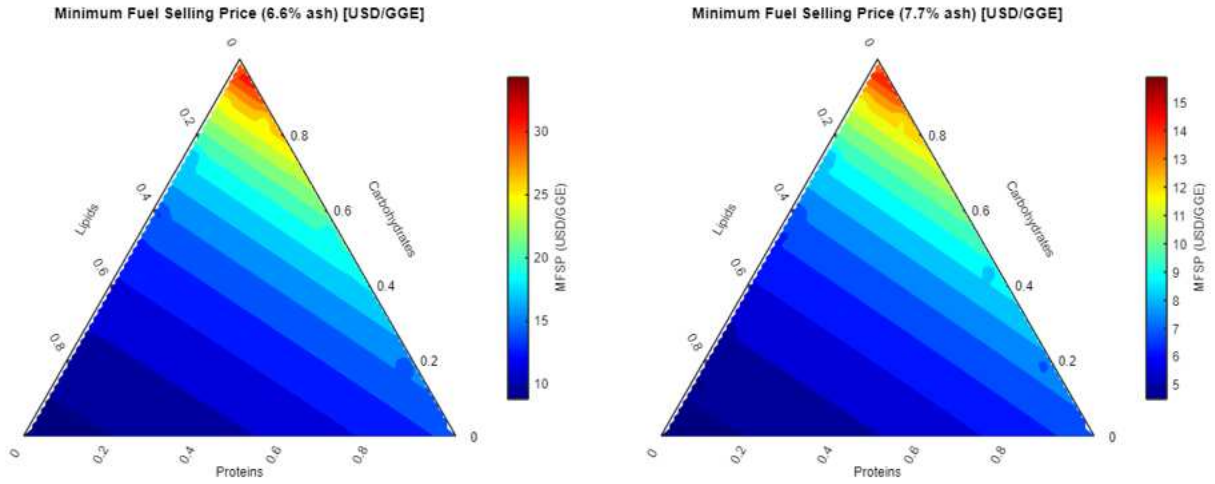

Figure A19: Impact of biomass composition on the minimum fuel selling price of renewable diesel produced through the HTL process under the Current (left) and Future (right) scenarios for Pima County, Arizona.

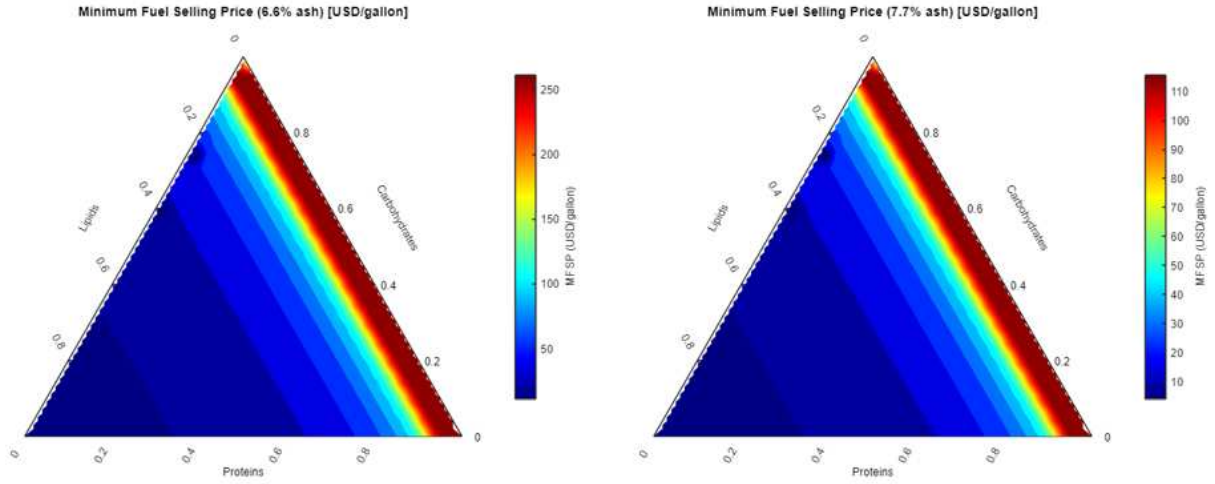

Figure A20: Impact of biomass composition on the minimum fuel selling price of sustainable aviation fuel produced through the HEFA process under the Current (left) and Future (right) scenarios for Pima County, Arizona.

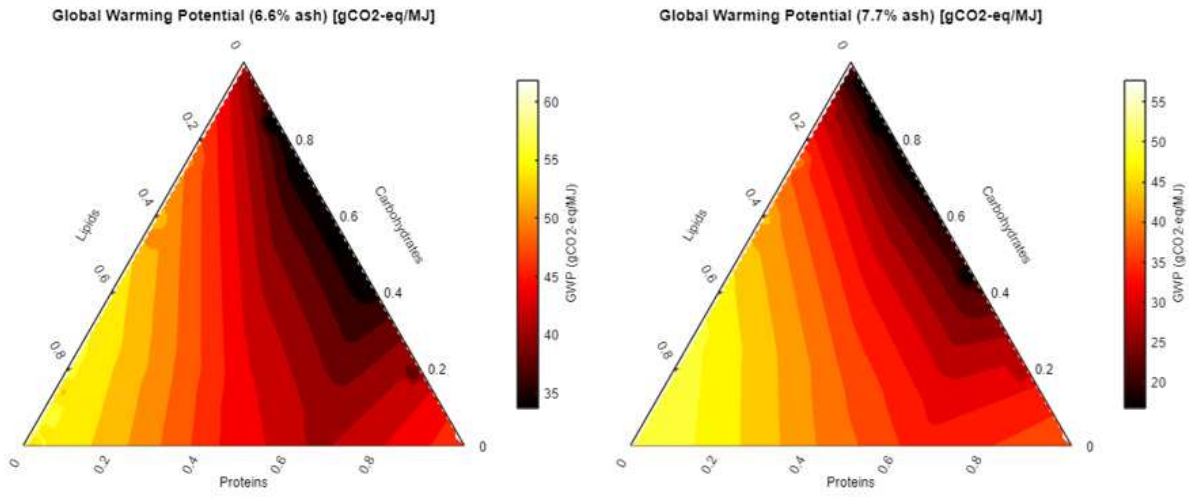

Figure A21: Impact of biomass composition on the global warming potential of renewable diesel produced through the HTL process under the Current (left) and Future (right) scenarios for Pima County, Arizona.

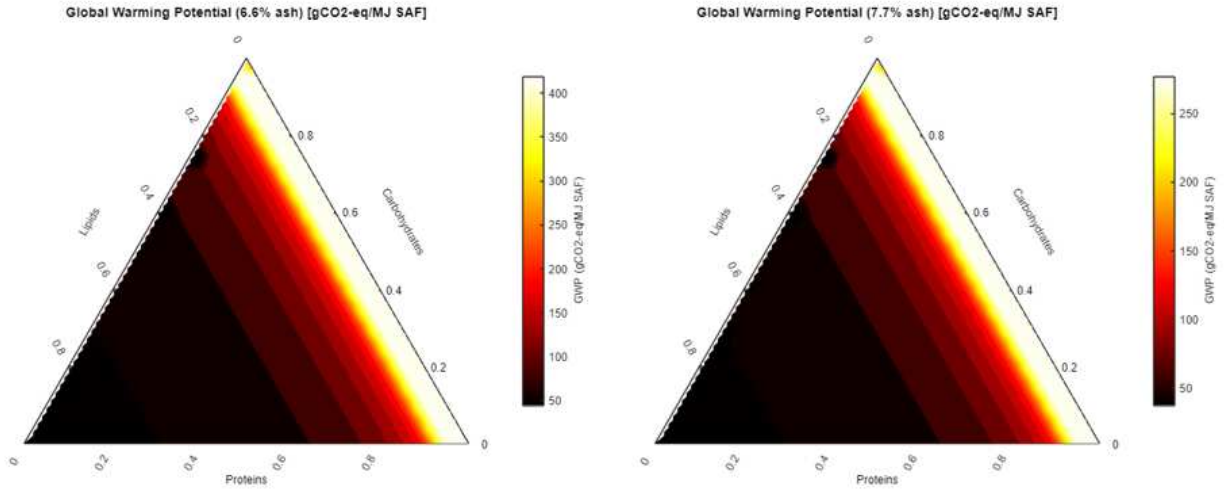

Figure A22: Impact of biomass composition on the global warming potential of sustainable aviation fuel produced through the HEFA process under the Current (left) and Future (right) scenarios for Pima County, Arizona.

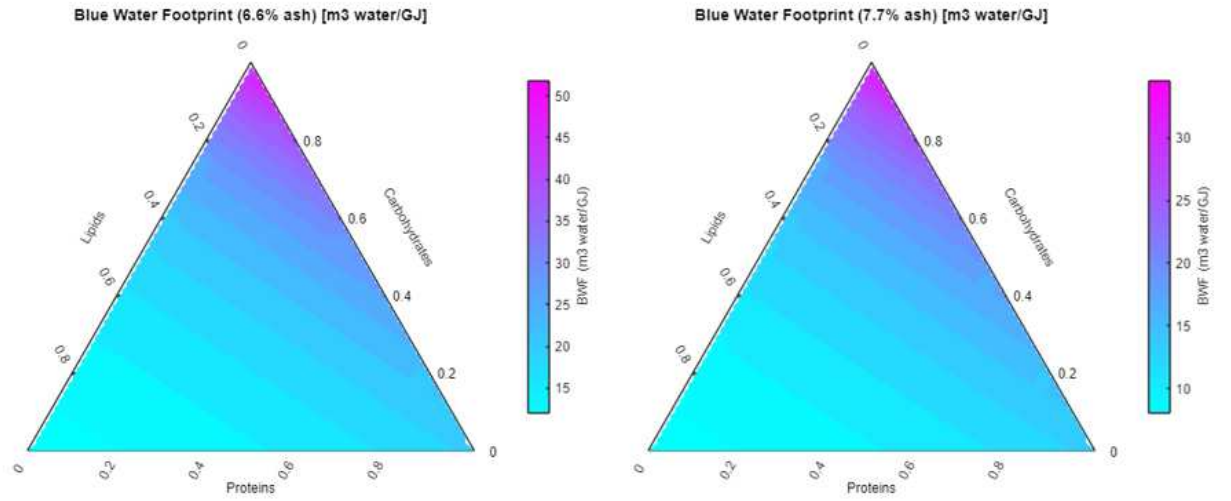

Figure A23: Impact of biomass composition on the blue water footprint of renewable diesel produced through the HTL process under the Current (left) and Future (right) scenarios for Pima County, Arizona.

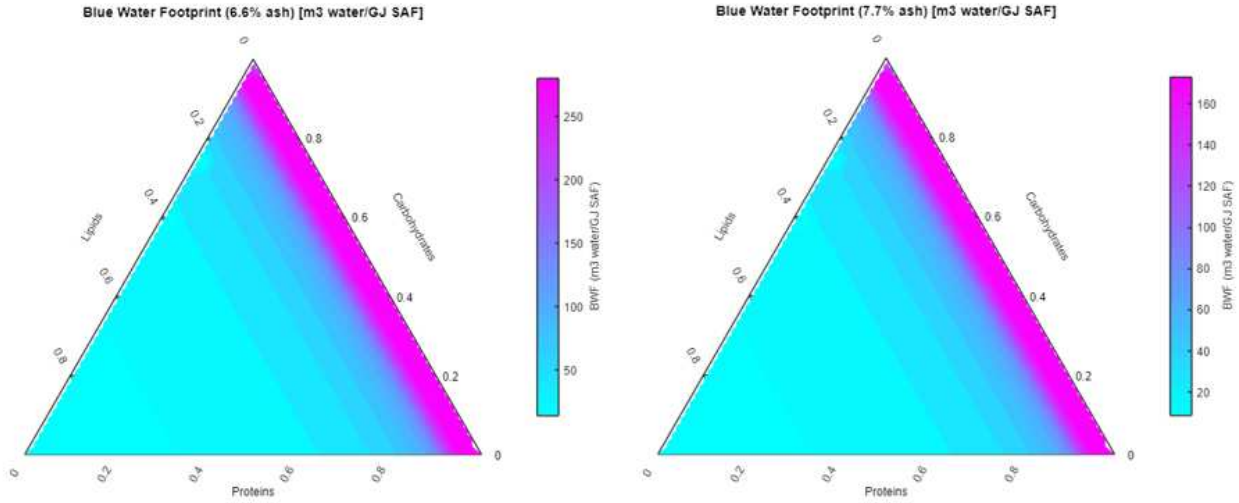

Figure A24: Impact of biomass composition on the blue water footprint of sustainable aviation fuel produced through the HEFA process under the Current (left) and Future (right) scenarios for Pima County, Arizona.

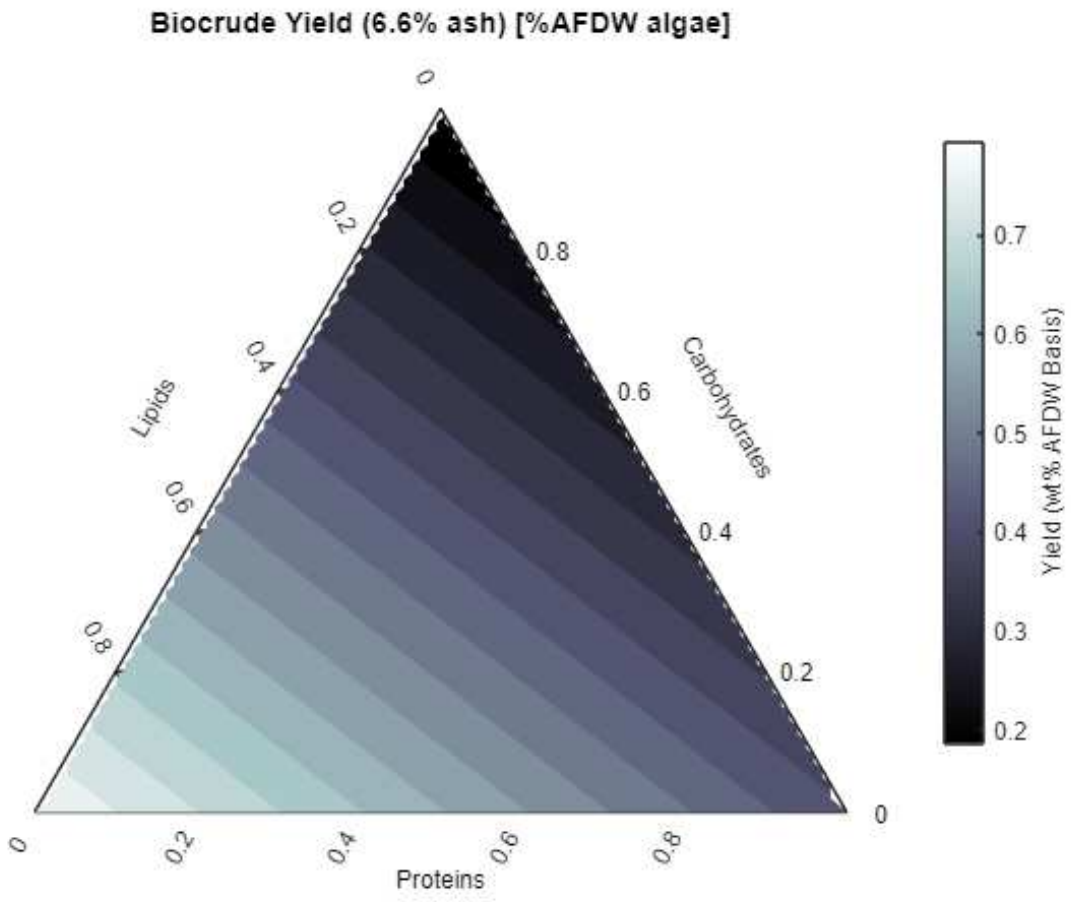

Figure A25: Impact of biomass composition on the biocrude yield from the HTL process.

Sensitivity Analysis

Results from the sensitivity analysis exploring the impacts of key modeling inputs on the MFSP and GWP for both fuel production pathways under the Current and Future scenarios are presented in Figures A26-A29.

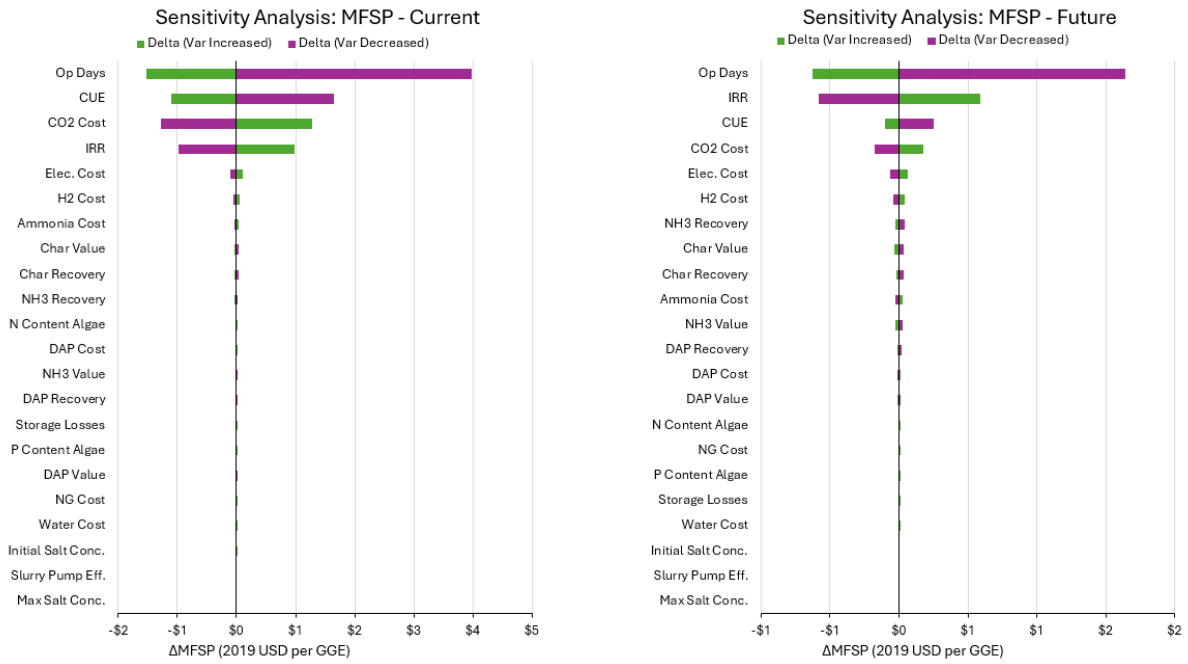

Figure A26: Minimum Fuel Selling Price sensitivity for the HTL pathway under the Current (left) and Future (right) scenarios.

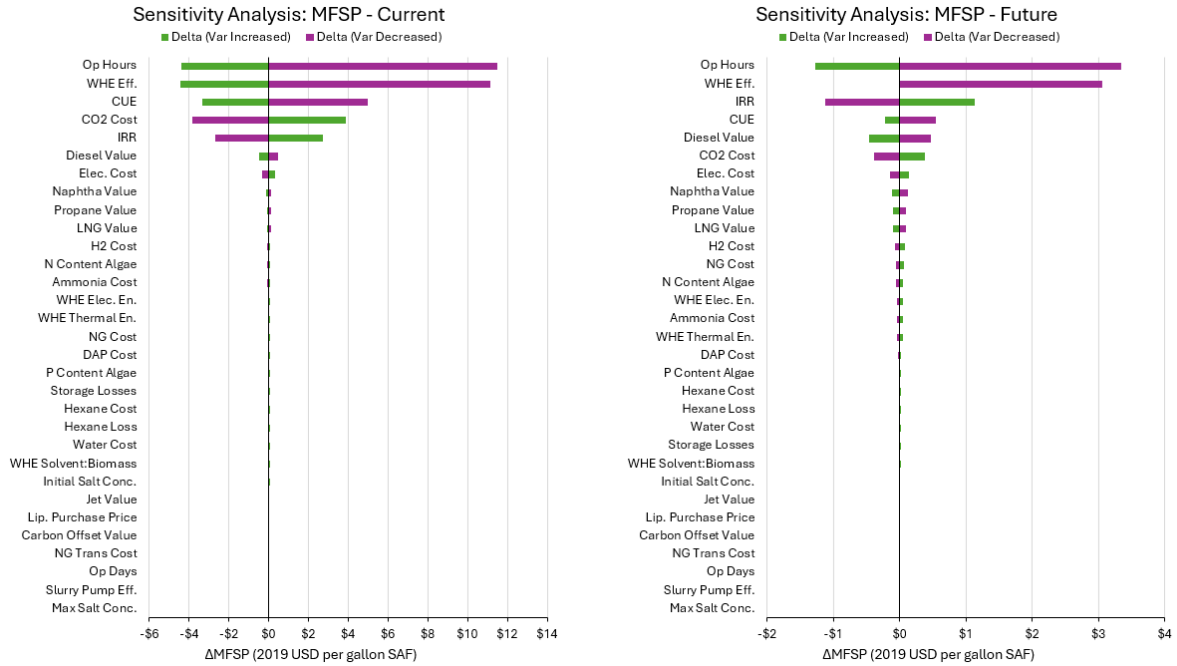

Figure A27: Minimum Fuel Selling Price sensitivity for the HEFA pathway under the Current (left) and Future (right) scenarios.

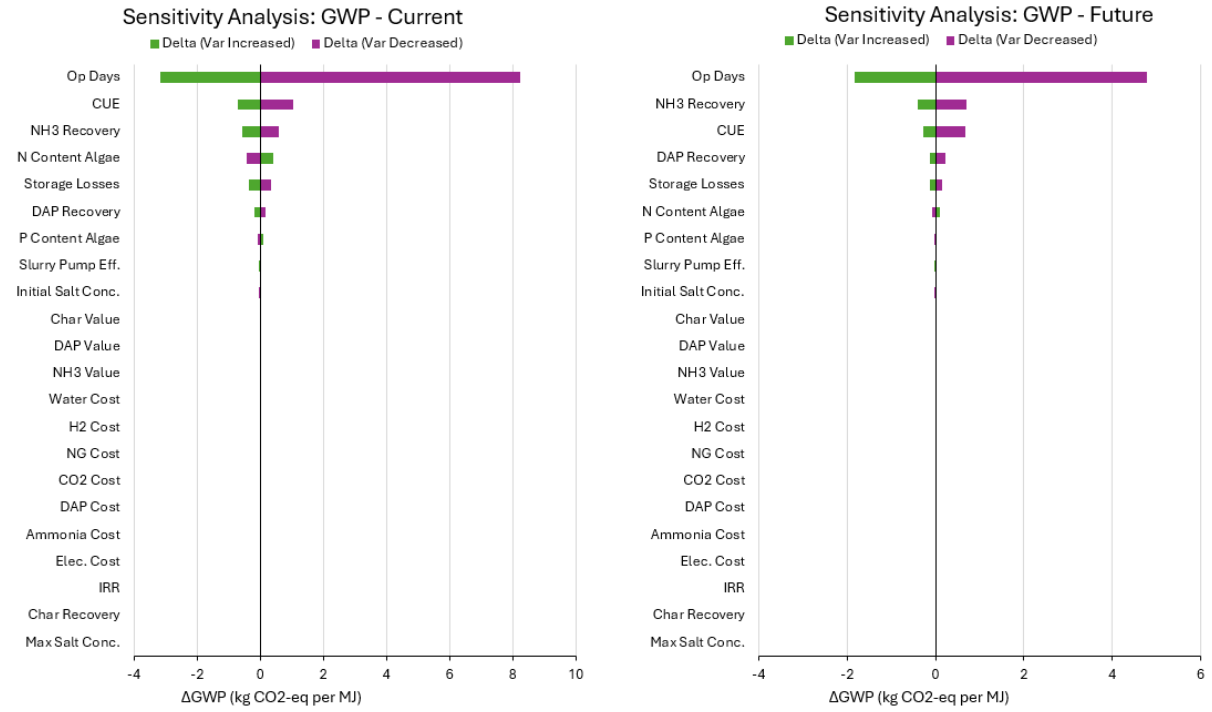

Figure A28: Global warming potential sensitivity for the HTL pathway under the Current (left) and Future (right) scenarios.

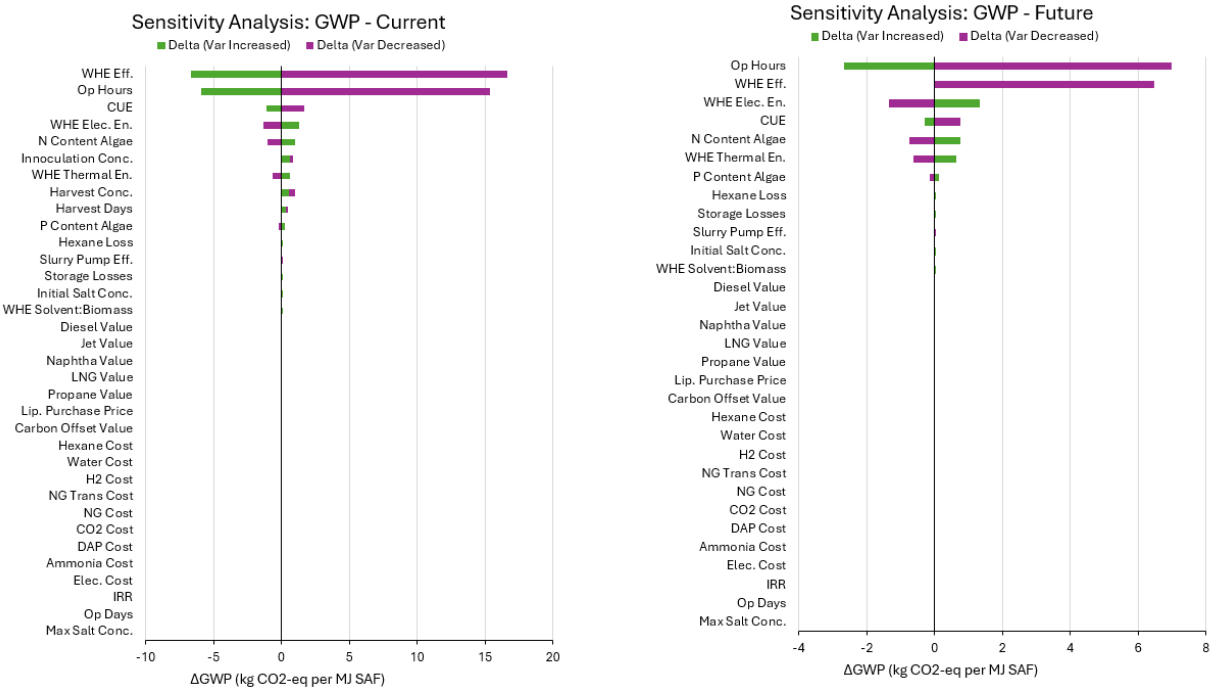

Figure A29: Global warming potential sensitivity for the HEFA pathway under the Current (left) and Future (right) scenarios.

Other Environmental Impacts

Each of the 10 environmental impact categories from the Tool for the Reduction and Assessment of Chemical and other Environmental Impacts (TRACI) [45] were quantified for both fuel production pathways under the Current and Future scenarios. To present the detailed breakout of each environmental impact based on the contribution from process consumables, five case study locations were chosen. Case study locations include Webb County, Texas, San Diego County, California, Polk County, Florida, Pima County, Arizona, and Honolulu County, Hawaii. Locations were chosen to capture geographical differences in grid emissions, evaporation rates, and algae productivities. Results from this analysis are presented in Figures A30-A33.

Figure A30: TRACI environmental impacts for renewable diesel production via HTL under the Current scenario. Results show the contribution of process consumables to each impact category for five case studly locations including (from top to bottom) Webb County, Texas, San Diego County, California, Polk County, Florida, Pima County, Arizona, and Honolulu County, Hawaii.

Figure A31: TRACI environmental impacts for renewable diesel production via HTL under the Future scenario. Results show the contribution of process consumables to each impact category for five case studly locations including (from top to bottom) Webb County, Texas, San Diego County, California, Polk County, Florida, Pima County, Arizona, and Honolulu County, Hawaii.

Figure A32: TRACI environmental impacts for sustainable aviation fuel production via the HEFA process under the Current scenario. Results show the contribution of process consumables to each impact category for five case studly locations including (from top to bottom) Webb County, Texas, San Diego County, California, Polk County, Florida, Pima County, Arizona, and Honolulu County, Hawaii.

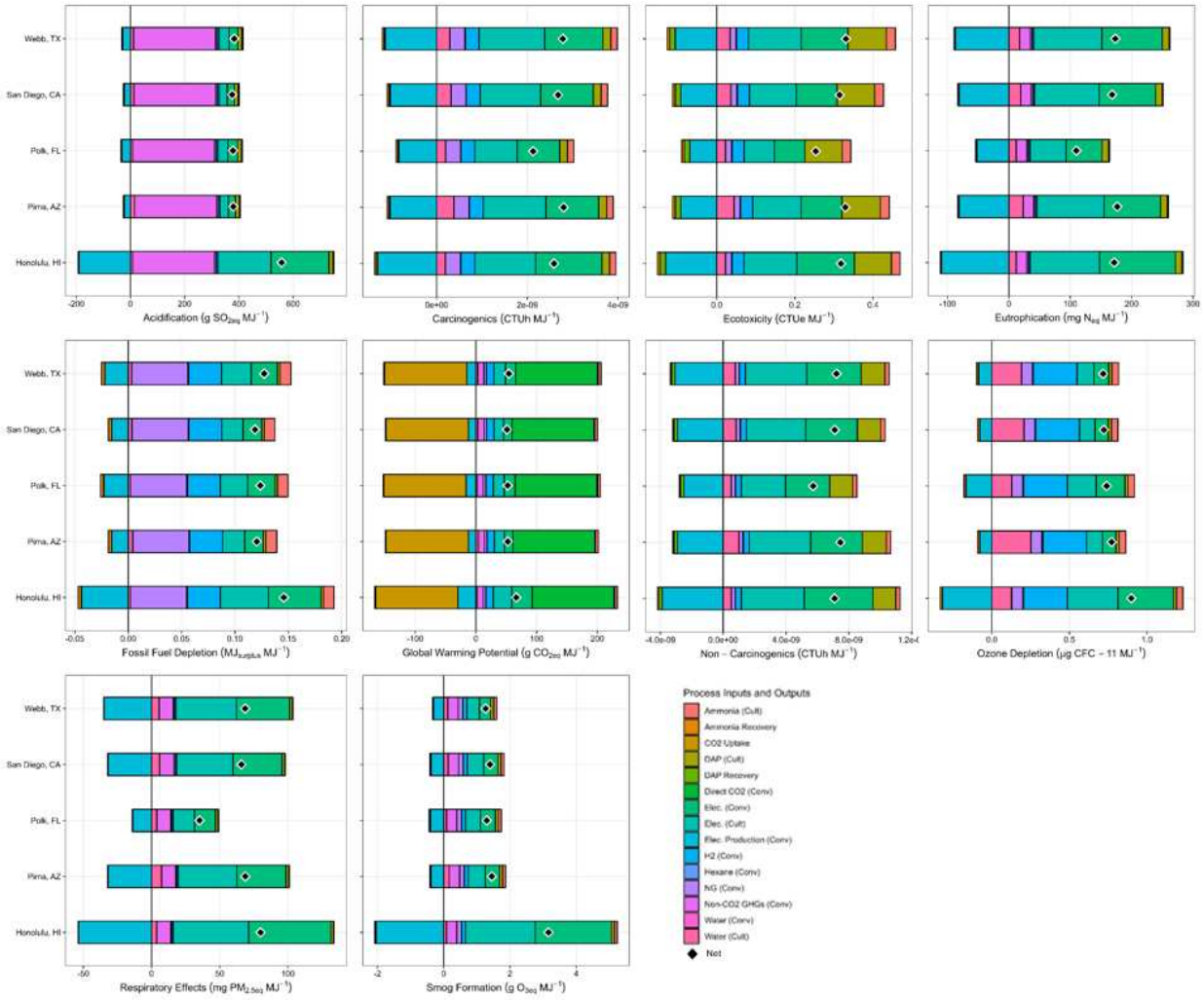

Figure A33: TRACI environmental impacts for sustainable aviation fuel production via the HEFA process under the Future scenario. Results show the contribution of process consumables to each impact category for five case studly locations including (from top to bottom) Webb County, Texas, San Diego County, California, Polk County, Florida, Pima County, Arizona, and Honolulu County, Hawaii.

APPENDIX B: SUPPORTING INFORMATION FOR CHAPTER 3

Process Flow Diagrams for Baseline and Anaerobic Digestion Scenarios

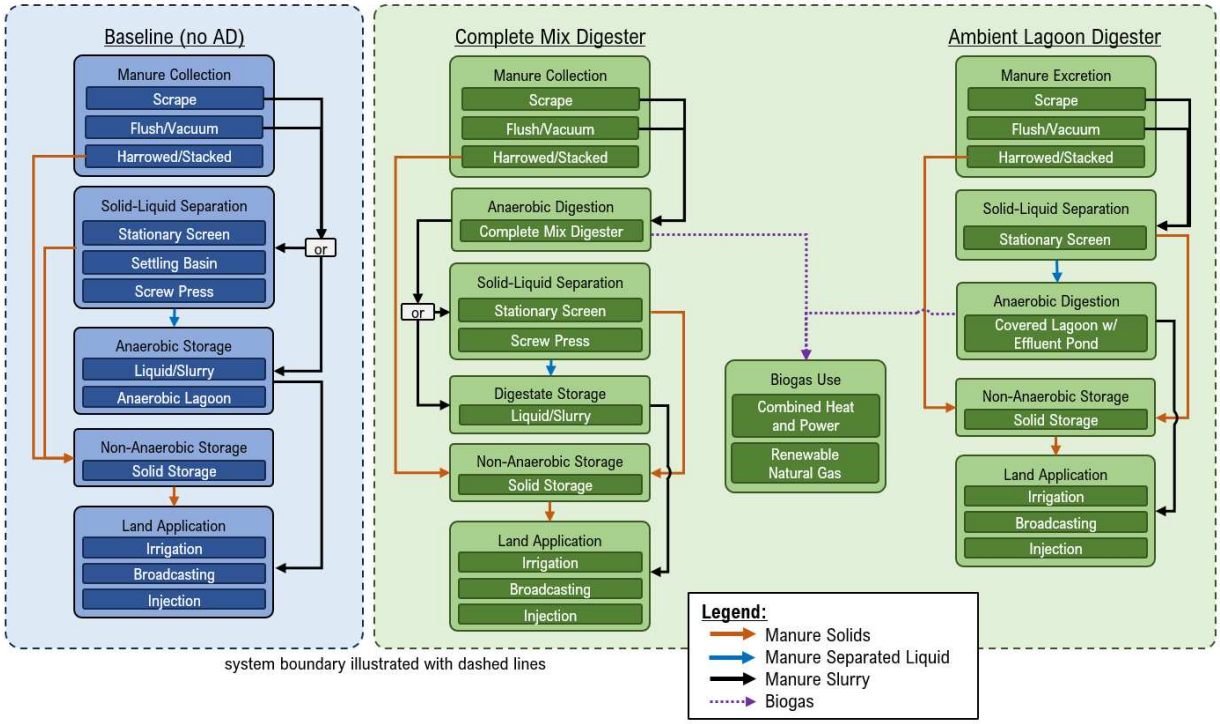

Figure B1: Process flow diagram illustrating the system boundary of the study and the various pathways captured in the 10 baseline scenarios and 10 anaerobic digestion scenarios (AD: Anaerobic digestion).

Table B1: Description of the modeled baseline and anaerobic digestion scenarios.

	Scenario	Description	Applicable Regions
Baseline Scenarios (1A – 3C)	1A	Open Lot (90% manure to solid storage; 10% manure flushed) → Stationary Screen → Uncovered Lagoon → Land Application	Northwest, Southwest
	1B	Open Lot (90% manure to solid storage; 10% manure flushed) → Settling Basin → Uncovered Lagoon → Land Application	Northwest, Southwest
	1C	Open Lot w/ MOC (60% manure to solid storage; 40% manure vacuumed) → Stationary Screen → Uncovered Lagoon → Land Application	Northwest, Southwest
	1D	Open Lot w/ MOC (60% manure to solid storage; 40% manure vacuumed) → Settling Basin → Uncovered Lagoon → Land Application	Southwest
	2A	Confined Scrape (100% manure scraped) → Stationary Screen → Liquid/Slurry Storage → Land Application	Northwest, Southwest
	2B	Confined Scrape (100% manure scraped) → Screw Press → Liquid/Slurry Storage → Land Application	Midwest, Northeast
	2C	Confined Scrape (100% manure scraped) → Liquid/Slurry Storage → Land Application	Northwest, Midwest, Northeast
	3A	Confined Flush (100% manure flushed) → Stationary Screen → Uncovered Lagoon → Land Application	Southeast
	3B	Confined Flush (CA) (23% manure to solid storage; 77% manure flushed) → Stationary Screen → Uncovered Lagoon → Land Application	California
	3C	Confined Flush (CA) (23% manure to solid storage; 77% manure flushed) → Settling Basin → Uncovered Lagoon → Land Application	California
Anaerobic Digestion Scenarios (4A – 6D)	4A	Open Lot w/ MOC (60% manure to solid storage; 40% manure vacuumed) → Mesophilic AD → CHP → Stationary Screen → Land Application	Northwest, Southwest
	4B	Open Lot w/ MOC (60% manure to solid storage; 40% manure vacuumed) → Mesophilic AD → RNG → Stationary Screen → Land Application	Northwest, Southwest
	5A	Confined Scrape (100% manure scraped) → Mesophilic AD → CHP → Stationary Screen → Liquid/Slurry Storage → Land Application	Northwest, Southwest
	5B	Confined Scrape (100% manure scraped) → Mesophilic AD → CHP → Screw Press→ Liquid/Slurry Storage → Land Application	Midwest, Northeast
	5C	Confined Scrape (100% manure scraped) → Mesophilic AD → RNG → Stationary Screen → Liquid/Slurry Storage → Land Application	Northwest, Southwest
	5D	Confined Scrape (100% manure scraped) → Mesophilic AD → RNG → Screw Press→ Liquid/Slurry Storage → Land Application	Midwest, Northeast
	6A	Confined Flush (100% manure flushed) → Stationary Screen → Covered Lagoon w/ Effluent Pond → CHP → Land Application	Southeast
	6B	Confined Flush (100% manure flushed) → Stationary Screen → Covered Lagoon w/ Effluent Pond → RNG → Land Application	Southeast
	6C	Confined Flush (CA) (23% manure to solid storage; 77% manure flushed) → Stationary Screen → Covered Lagoon w/ EP → CHP → Land Application	California
	6D	Confined Flush (CA) (23% manure to solid storage; 77% manure flushed) → Stationary Screen → Covered Lagoon w/ EP → RNG → Land Application	California

MOC: Manure on Concrete; CA: California; EP: Effluent Pond; CHP: Combined Heat and Power; RNG: Renewable Natural Gas

Figure B2: Process Flow Diagrams for Open Lot Scenarios 1A-1D:

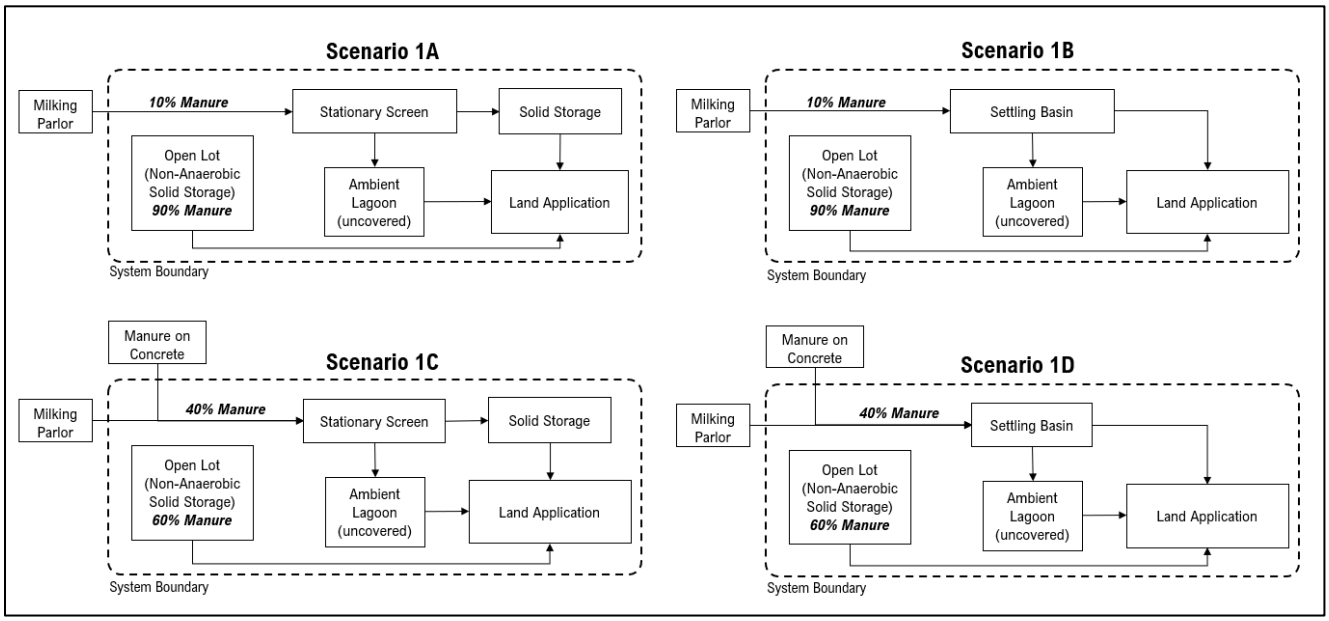

Figure B3: Process Flow Digarms for Confined Scrape Scenarios 2A-2C:

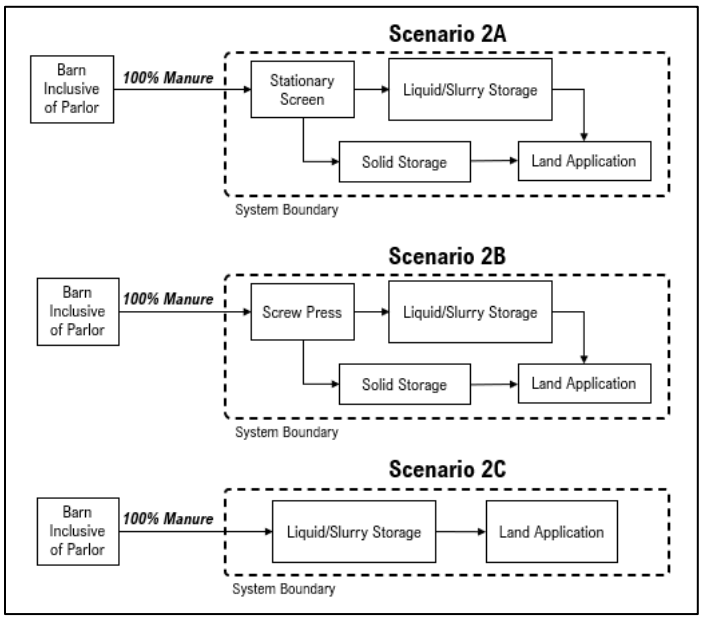

Figure B4: Process Flow Diagrams for Confined Flush Scenarios 3A-3C

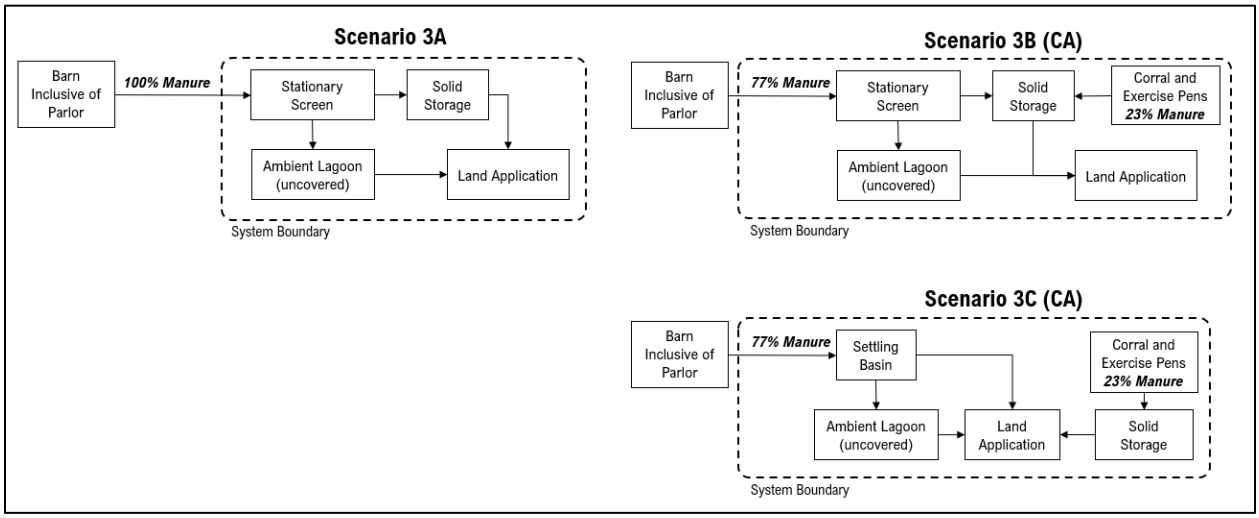

Figure B5: Process Flow Diagrams for Open Lot w/ Manure on Concrete Scenarios 4A-4D:

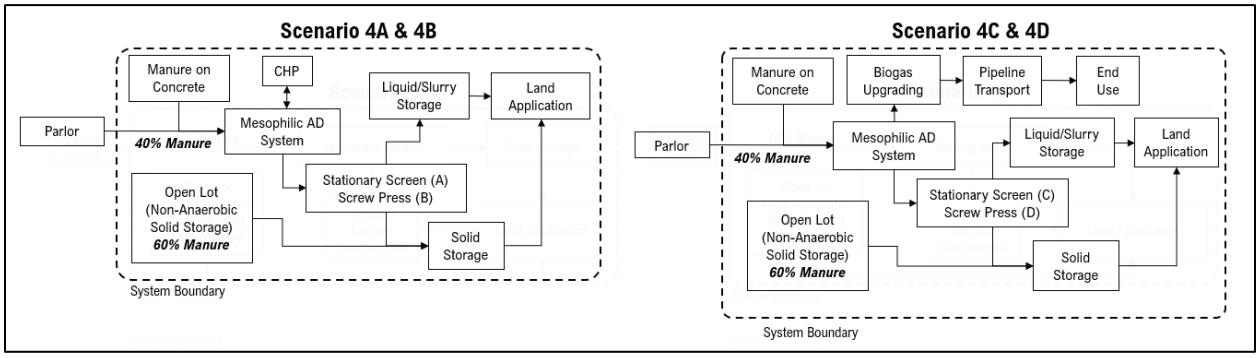

Figure B6: Process Flow Diagrams for Confined Scrape Scenarios 5A-5D:

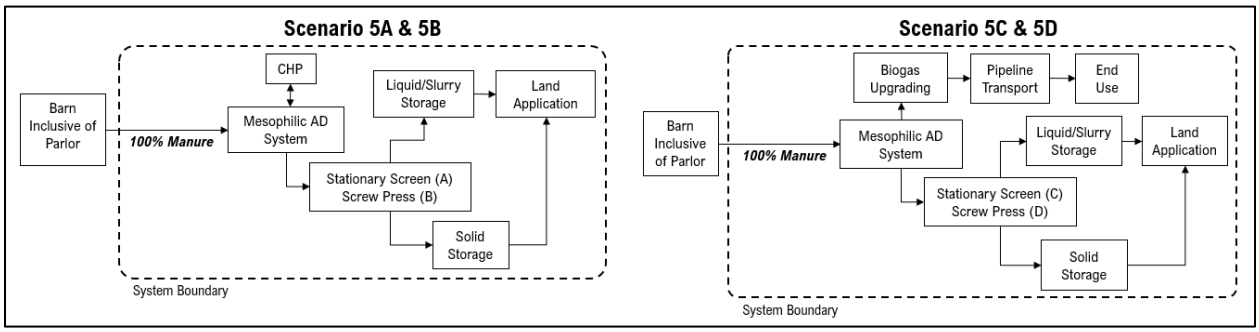

Figure B7: Process Flow Diagrams for Confined Flush Scenarios (6A-6D):

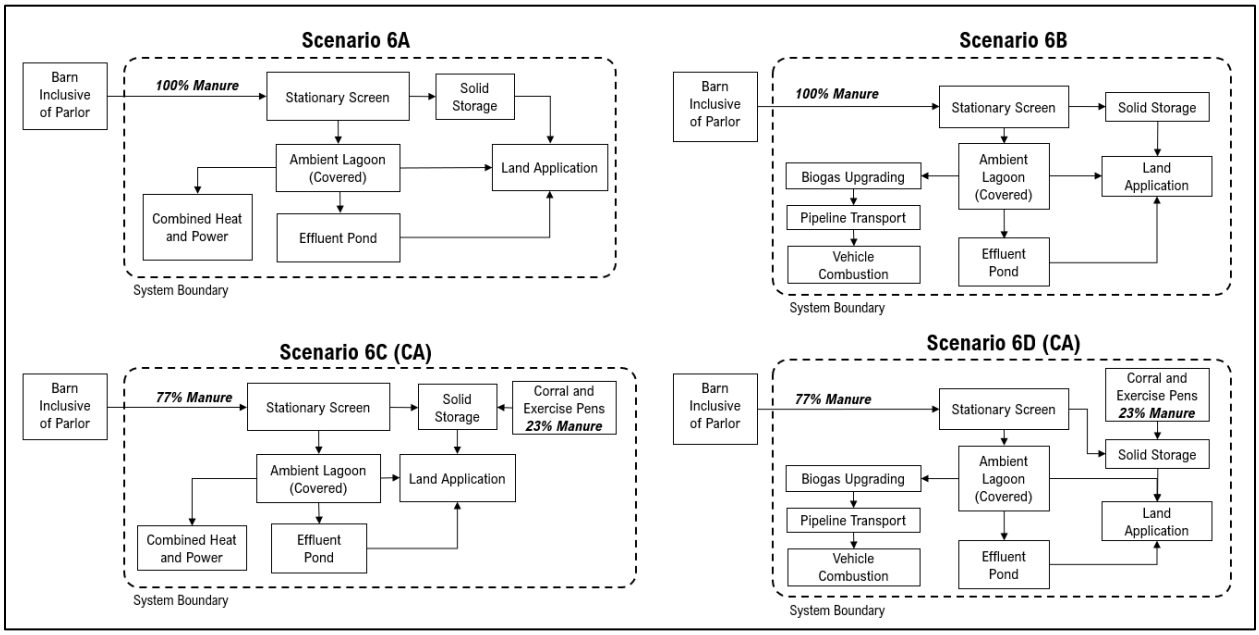

Table B2: Grid Emissions by State from 2021 eGRID data [98] *and Regional Average Emissions*

State	Dairy Region	lbs CO_2 per MWh	lbs CH_4 per MWh	lbs N_2O per MWh	lbs CO_2e per MWh
Alabama	Southeast	750.80	0.06	0.01	754.62
Arizona	Southwest	724.81	0.04	0.01	727.70
Arkansas	Southeast	1086.93	0.09	0.01	1093.19
California	California	479.01	0.03	0.00	480.57
Colorado	Southwest	1216.92	0.11	0.02	1224.65
Connecticut	Northeast	515.14	0.05	0.01	518.21
Delaware	Northeast	867.50	0.04	0.01	870.06
Florida	Southeast	834.14	0.05	0.01	837.60
Georgia	Southeast	758.08	0.06	0.01	762.45
Idaho	Northwest	271.34	0.01	0.00	271.88
Illinois	Midwest	653.05	0.06	0.01	657.38
Indiana	Midwest	1632.59	0.15	0.02	1643.13
Iowa	Midwest	768.93	0.08	0.01	774.62
Kansas	Southwest	838.19	0.10	0.01	844.84
Kentucky	Southeast	1727.09	0.19	0.03	1740.00
Louisiana	Southeast	826.04	0.04	0.01	828.87
Maine	Northeast	301.04	0.12	0.02	309.65
Maryland	Northeast	698.19	0.06	0.01	702.10
Massachusetts	Northeast	851.43	0.13	0.02	859.92
Michigan	Midwest	1003.76	0.10	0.01	1010.44
Minnesota	Midwest	825.97	0.08	0.01	831.69

Mississippi	Southeast	833.95	0.04	0.01	836.39
Missouri	Midwest	1636.06	0.19	0.03	1649.06
Montana	Northwest	1045.02	0.12	0.02	1053.15
Nebraska	Midwest	1124.84	0.13	0.02	1133.90
Nevada	Southwest	715.08	0.03	0.00	717.00
New Hampshire	Northeast	304.04	0.06	0.01	308.10
New Jersey	Northeast	480.92	0.04	0.00	483.05
New Mexico	Southwest	1134.31	0.10	0.01	1141.02
New York	Northeast	455.35	0.03	0.00	456.97
North Carolina	Southeast	669.48	0.05	0.01	672.89
North Dakota	Midwest	1340.69	0.15	0.02	1351.19
Ohio	Midwest	1208.18	0.10	0.01	1214.95
Oklahoma	Southwest	753.55	0.05	0.01	756.58
Oregon	Northwest	325.80	0.02	0.00	326.80
Pennsylvania	Northeast	726.43	0.05	0.01	729.80
Rhode Island	Northeast	832.72	0.02	0.00	833.75
South Carolina	Southeast	567.03	0.05	0.01	570.43
South Dakota	Midwest	302.92	0.03	0.00	304.76
Tennessee	Southeast	698.28	0.07	0.01	702.67
Texas	Southwest	856.44	0.06	0.01	860.32
Utah	Southwest	1560.50	0.16	0.02	1571.46
Vermont	Northeast	36.05	0.14	0.02	45.04
Virginia	Southeast	599.21	0.05	0.01	602.31
Washington	Northwest	201.83	0.02	0.00	202.88
West Virginia	Southeast	1944.15	0.22	0.03	1959.53
Wisconsin	Midwest	1267.12	0.12	0.02	1275.25
Wyoming	Northwest	1833.92	0.20	0.03	1847.74
Regional Average Grid Emissions					
Northeast		551.71	0.07	0.01	556.06
Midwest		1069.46	0.11	0.02	1076.94
Southeast		941.26	0.08	0.01	946.74
Southwest		974.97	0.08	0.01	980.45
California		479.01	0.03	0.00	480.57
Northwest		735.58	0.07	0.01	740.49

Life Cycle Inventory (LCI) Data

Table B3: Combined Heat and Power Efficiency and GHG Emissions – Zamalloa et al. [69]

Parameter	Value	Units
Electrical efficiency	33%	% on LHV basis
Total CHP efficiency	76%	% on LHV basis
CH4	4.26	g/mmBTU of fuel input
N2O	1.5	g/mmBTU of fuel input
CO2 (biogenic)	59360	g/mmBTU of fuel input

Table A4: RNG Production Yields – Skorek-Osikowska et al. [113]

Parameter	Value	Units
RNG Output Stream	95%	of CH4 input
Leaked Methane (Fugitive Emissions)	2%	of CH4 input
Methane Combusted for Process Heat	3%	of CH4 input (parasitic)
Total Energy Output (BTU)	44.71	mmBTU per MT RNG
Total Energy Output (MWh)	13.10	MWh per MT RNG
Total Energy Output (DGE)*	348.13	diesel gallon equivalents per MT RNG
**37.64 kWh/DGE*		

Table B5: RNG Production Consumables – Skorek-Osikowska et al. [113]

Consumable	kg per MWh RNG
Iron (II) Chloride	51.80
Calcium Hydroxide	10.22
Monoethanolamine (MEA)	5.75
Tap Water	2416.45
Wastewater (to be treated)	1024.71
Grid Electricity (kWh)	25.54

Table B6: CNG Vehicle Tailpipe Emissions – EPA [114]

Vehicle Type	CH4 (g/mile)	N2O (g/mile)
CNG Light-Duty Vehicles	0.737	0.050
CNG Buses	1.966	0.175

Table B7: Manure Management Electricity – Aguirre-Villegas and Larson [10]

Process	Energy	Units
Collection (Flush with Flumes)	1.29E-04	kWh day^{-1} animal $unit^{-1}$
Transportation to Storage (Pumping)	1.19E-04	kWh day^{-1} animal $unit^{-1}$
Storage Agitation	5.47E-03	kWh day^{-1} animal $unit^{-1}$
Irrigation	9.32E-03	kWh day^{-1} animal $unit^{-1}$
Solid Liquid Separation	4.66E-05	kWh day^{-1} animal $unit^{-1}$

Table B8: Manure Management Diesel Emissions – Aguirre-Villegas and Larson [10]

Process (Permitted Facility >1000 Cows)	Value	Units
Collection (Skid Steer or Vacuum*)	107.00	g CO2-eq day^{-1} animal $unit^{-1}$
Land Application (Tanker Injection)	806.00	g CO2-eq day^{-1} animal $unit^{-1}$
Land Application (Manure Broadcasting)	520.00	g CO2-eq day^{-1} animal $unit^{-1}$
**Diesel powered vacuum collection approximated as skid-steer collection in current study*		

EcoInvent LCI Data

Life Cycle Inventory (LCI) data obtained through the EcoInvent database (version 3.9.1) [73] were accessed using the software openLCA 1.11.0 [74]. LCI data from EcoInvent are proprietary and cannot be published openly. The names of the various inventories used for the LCA in this study are listed in the table below, so that EcoInvent license holders may find the exact inventory data used in the analysis.

Table B9: Inventory Names for LCI Data Obtained from EcoInvent for RNG Upgrading

Consumable or Process	Inventory Name in EcoInvent
NG Boiler (<100 kW)	heat production, natural gas, at boiler condensing modulating <100kW | heat, central or small-scale, natural gas | Cutoff, U
NG Boiler (>100 kW)	heat production, natural gas, at boiler condensing modulating >100kW | heat, district or industrial, natural gas | Cutoff, U
RNG Pipeline Transport	transport, pipeline, long distance, natural gas | transport, pipeline, long distance, natural gas | Cutoff, U
Iron (II) Chloride	iron(II) chloride production | iron(II) chloride | Cutoff, U
Calcium Hydroxide	lime production, hydrated, loose weight | lime, hydrated, loose weight | Cutoff, U
Monoethanolamine (MEA)	market for monoethanolamine | monoethanolamine | Cutoff, U

Tap Water	tap water production, underground water without treatment | tap water | Cutoff, U
Wastewater (to be treated)	market for wastewater, average | wastewater, average | Cutoff, U

Complete-Mix Anaerobic Digester (CMAD) Energy Consumption

CMAD digester mixing and pumping energy (0.8532 kWh AU^{-1} day^{-1}) was estimated based on previous work from Gooch and Labatut [116], with calculations explained below:

Table B10: Parameters for CMAD – Gooch and Labatut [116]

Parameters	**Value**	**Units**	**Notes**
Total Parasitic Load	92	MWh/period	
Total WCEs	1900	WCEs	1800 lactating + 200 dry
Total Manure Contribution	1,759,370	gal/month	
Total Imported Co-Substrate	617,950	gal/month	
Days per Sampling Period	30	days	

From Gooch and Labatut [116] the assumed contribution to mixing and pumping is proportional to the fluid contribution, thus the manure contribution to the parasitic load, $F_{PL,M}$, is calculated with Equation B1:

$$F_{PL,M} = \frac{1{,}759{,}370}{(1{,}759{,}370+617{,}950)} = 74\% \quad \text{(Eq. B1)}$$

The parasitic load for CMAD mixing and pumping per sampling period for liquid manure, PL_M, is calculated with Equation B2:

$$PL_M = 74\% \times 92 \ \frac{\text{MWh}}{\text{period}} = 68 \ \frac{\text{MWh}}{\text{period}} \quad \text{(Eq. B2)}$$

And the specific parasitic load for mixing and pumping per day per animal unit, PL_s, is calculated using the days per reporting period and an animal unit conversion multiplier of 1.4 [116] with Equation B3:

$$PL_s \frac{kWh}{AU \times day} = \frac{PL_M \times 1000}{30} \times \frac{1}{1900 \times 1.4} = 0.8532 \frac{kWh}{AU \times day} \quad \text{(Eq. B3)}$$

Regional Data

Typical Average Mass (TAM)

Results for manure management scenarios and emissions reductions are based on Holstein cows (TAM 680 kg) [2,156], which made up 79.9% of the U.S. dairy herd in 2020 [96]. The analysis also considers the impact of increasing Jersey and mixed breed populations by incorporating TAM variability in the Monte Carlo uncertainty analysis based on the data in Table B11 below. Holstein cows are assumed to consistently weigh 680 kg while Jersey cows range between 362.8 and 544.2 kg [156]. The low, average, and high weight of cross-bred cow was estimated by taking the average of a Holstein cow and the lower, average, and upper mass of a Jersey cow, respectively. The low, average, and high weighted TAM for the U.S. dairy herd (used as the Monte Carlo distribution for TAM) was then calculated using the percentage of Holstein, Jersey, and Cross Breed cows in the U.S herd in 2020.

Table B11: Potential TAM Range for U.S. Dairy Herd

Breed	**% of US Herd in 2020** [96]	**Weight Low** [156]	**Weight Average**	**Weight High** [156]
Holstein	80%	680.3	680.3	680.3
Jersey	8%	362.8	453.5	544.2
Cross Breed	12%	521.5	566.9	612.2
U.S. Herd Weighted TAM		635.8	648.5	661.2

VS excretion rates per WCE for each state were determined using state-level VS excretion data for milking dairy cows from the EPA [2] and VS excretion rates for non-milking dairy cows on feed (constant) obtained from the CARB GREET model [95] and Equation B4:

$$VS_{WCE,i} = 0.85\left(\frac{TAM_L}{1000}\right)VS_{L,i} + 0.15\left(\frac{TAM_{NL}}{1000}\right)VS_{NL} \quad \text{(Eq. B4)}$$

Where TAM_L is the typical average mass of a lactating Holstein dairy cow (680 kg) [2,156], TAM_{NL} is the typical average mass of a non-lactating or "dry" Holstein dairy cow (684 kg) [95], $VS_{L,i}$ is the VS excretion per 1000 kg animal mass for lactating cows in state i (table B12 below), and VS_{NL} is the VS excretion per 1000 kg animal mass for non-lactating dairy cows (5.56 kg VS/1000 kg mass/day) [95]. Regional VS excretion rates were derived using a weighted average of state-level data, weighted by each state's share of cows in a region.

State-Level VS Excretion Data

Table B12: State-level VS and N Excretion Data for Lactating Dairy Cows in Each State [2]

State	Region	Number of Cows Included in Status Quo Adoption Case (Regional %)	Number of Cows Included in Opportunity Adoption Case (Regional %)	kg VS/1000 kg animal mass/day	kg N/1000 kg animal mass/day
Alabama	Southeast			9.13	0.55
Arizona	Southwest	35,280 (24%)	75,800 (22%)	11.78	0.65
Arkansas	Southeast			8.28	0.50
California	California	309,091 (100%)	515,909 (100%)	11.53	0.64
Colorado	Southwest			12.25	0.67
Connecticut	Northeast			11.32	0.63
Delaware	Northeast			9.98	0.58
Florida	Southeast	31,500 (100%)	54,250 (100%)	10.71	0.61
Georgia	Southeast			11.19	0.64
Idaho	Northwest	45,500 (39%)	112,000 (50%)	11.96	0.66
Illinois	Midwest			10.87	0.61
Indiana	Midwest			11.51	0.64
Iowa	Midwest			11.80	0.65
Kansas	Southwest			11.51	0.64

Kentucky	Southeast			10.49	0.60
Louisiana	Southeast			8.45	0.51
Maine	Northeast			11.00	0.62
Maryland	Northeast			10.68	0.60
Massachusetts	Northeast			10.38	0.59
Michigan	Midwest	70,000 (56%)	111,580 (38%)	12.55	0.68
Minnesota	Midwest	17,500 (14%)	50,260 (17%)	11.22	0.63
Mississippi	Southeast			9.54	0.56
Missouri	Midwest			8.70	0.52
Montana	Northwest			10.76	0.61
Nebraska	Midwest			11.83	0.66
Nevada	Southwest			11.81	0.65
New Hampshire	Northeast			10.79	0.61
New Jersey	Northeast			10.35	0.59
New Mexico	Southwest	0 (0%)	65,757 (19%)	11.83	0.66
New York	Northeast	42,000 (80%)	110,040 (83%)	11.76	0.65
North Carolina	Southeast			11.18	0.64
North Dakota	Midwest			10.97	0.62
Ohio	Midwest			11.04	0.62
Oklahoma	Southwest			9.67	0.56
Oregon	Northwest			10.72	0.61
Pennsylvania	Northeast	10,500 (20%)	21,840 (17%)	10.81	0.61
Rhode Island	Northeast			10.95	0.62
South Carolina	Southeast			10.30	0.60
South Dakota	Midwest			11.34	0.63
Tennessee	Southeast			10.05	0.59
Texas	Southwest	114,720 (76%)	207,362 (59%)	11.90	0.66
Utah	Southwest			11.37	0.64
Vermont	Northeast			10.81	0.61
Virginia	Southeast			10.72	0.62
Washington	Northwest	70,000 (61%)	109,900 (50%)	11.71	0.65
West Virginia	Southeast			8.86	0.53
Wisconsin	Midwest	38,500 (31%)	129,063 (44%)	11.73	0.65
Wyoming	Northwest			11.96	0.66

Table B13: Weighted Regional VS and N Excretion Rates for Lactating Dairy Cows

Status Quo Adoption Case		
Region	**kg VS/1000 kg mass/day**	**kg N/1000 kg mass/day**
Northeast	11.57	0.64
Midwest	12.12	0.67
Southeast	10.71	0.61
Southwest	11.87	0.66
California	11.53	0.64
Northwest	11.84	0.65
Opportunity Adoption Case		
Region	**kg VS/1000 kg mass/day**	**kg N/1000 kg mass/day**
Northeast	11.60	0.65
Midwest	11.96	0.66
Southeast	10.71	0.61
Southwest	11.86	0.66
California	11.53	0.64
Northwest	11.84	0.65

Monthly Average Ambient Temperatures

For each state (except for California), monthly average ambient temperatures were obtained from NOAA [101] with regional averages estimated by taking the average of each state in a given region. For California, monthly average ambient temperatures were obtained by taking the average of the monthly average ambient temperatures for the counties in the San Joaquin Valley where >90% of the CA dairy industry is located. Included counties and the name of the weather station representing each county are provided in the table below.

Table B14: Counties Included in CA Temperature Data

Location (County)	**Location of Weather Station**
Fresno	FRESNO
Kern	BAKERSFIELD
Kings	HANFORD
Madera	MADERA
Merced	MERCED
San Joaquin	STOCKTON
Stanislaus	MODESTO
Tulare	VISALIA

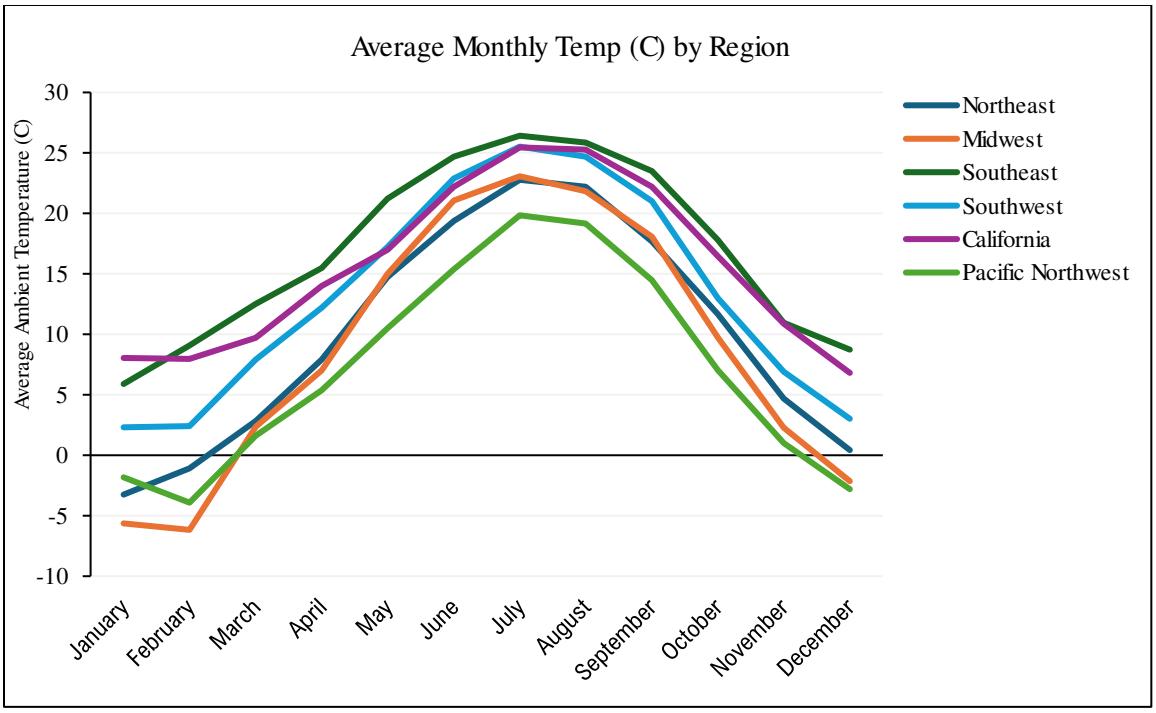

Figure B8: Monthly Average Ambient Temperatures for Each Dairy Region

Regional Cleanout Schedules

Assumed regional cleanout schedules for settling basins, ambient anaerobic lagoon, and effluent ponds are presented in the Tables B15-B17:

Table B15: Percentage of Settling Basin Emptied in Each Month for Scenarios with Settling Basins (Northwest, California, and Southwest)

Month	% of Settling Basin Emptied
January	0%
February	0%
March	0%
April	0%
May	0%
June	100%
July	0%
August	0%
September	0%
October	0%
November	0%
December	100%

Table B16: Percentage of Ambient Lagoon Volume Emptied per Month for Each Region (for baseline scenarios, volume is removed straight from the lagoon, and for AD scenarios the volume is removed from the effluent pond)

Month	Northwest	California	Southwest	Southeast
January	0%	0%	10%	0%
February	0%	0%	10%	0%
March	0%	0%	10%	0%
April	90%	0%	10%	0%
May	0%	40%	20%	40%
June	0%	50%	20%	50%
July	0%	67%	20%	67%
August	0%	0%	20%	0%
September	0%	0%	20%	0%
October	90%	50%	20%	50%
November	0%	67%	10%	67%
December	0%	100%	5%	100%

Table B17: Percentage of Liquid/Slurry Storage Emptied per Month for Each Region

Month	Northwest	Midwest	Northeast	Southwest
January	0%	0%	0%	10%
February	0%	0%	0%	10%
March	0%	0%	0%	10%
April	90%	70%	0%	10%
May	0%	0%	0%	20%
June	0%	30%	100%	20%
July	0%	40%	0%	20%
August	0%	30%	0%	20%
September	0%	30%	0%	20%
October	90%	90%	100%	20%
November	0%	0%	0%	10%
December	0%	0%	0%	5%

Regional Methods of Land Application

For each region, the percentages of total manure land applied via broadcasting, irrigation, and tanker injection were defined based on expert opinion and discussion from the Manure Technology Team (MTT). The regional methods of land application are presented in Table B18 below:

Table B18: Regional Manure Land Application Methods (Informed Assumptions)

Region	% of Manure Broadcasted	% of Manure Irrigated	% of Manure Injected
Northwest	10%	80%	10%
California	10%	90%	0%
Midwest	10%	0%	90%
Northeast	10%	0%	90%
Southwest	0%	100%	0%
Southeast	10%	90%	0%

Solid-Liquid Separation Technologies

Table B19: VS Removal Efficiency of Different Solid-Liquid Separation Technologies

Type of Solids Separation	VS Removed	VS Sent Downstream	Reference
Gravity	0.45	0.55	CARB GREET [95]
Stationary Screen	0.3	0.7	Williams et al. [103]
Vibrating Screen	0.15	0.85	CARB GREET [95]
Screw Press	0.25	0.75	CARB GREET [95]
Centrifuge	0.7	0.3	CARB GREET [95]
Roller Drum	0.25	0.75	CARB GREET [95]
Belt Press/Screen	0.5	0.5	CARB GREET [95]
Settling Basin	0.5	0.5	Chastain & Henry [108]

Non-Anaerobic Storage Systems

Table B20: Temperature Dependent Methane Conversion Factor (MCF) for Solid Storage [95]

Ave. Reporting Period Temperature (C)	MCF	Climate Classification
26 - 28	0.05	Warm
15 - 25	0.04	Temperate
10 - 14	0.02	Cool

With the temperature-dependent MCF factor, monthly GHG emissions from solid storage of separated solids and manure that falls on the open lot and is harrowed, stacked, and stored are calculated by Equation B5:

$$CO2_{e,SS,i} = VS_{SS,i} \times MCF_i \times B_0 \times 0.68 \times 27 \quad \text{(Eq. B5)}$$

where $CO2_{eq,SS,i}$ is the total GHG emissions from solid storage (SS) in kg CO_2-eq in month i, $VS_{SS,i}$ is the total mass of VS (in kg) sent to solid storage in month i, MCF_i is the temperature-dependent MCF factor for solid storage (from Table B20) in month i, B_0 is the maximum specific methane formation for raw manure (0.24 m^3 CH_4 kg VS $added^{-1}$) [95], 0.68 is the conversion factor for m^3 CH_4 to kg CH_4 [95], and 27 is the GWP-100 value for non-fossil methane from the IPCC 6th Assessment Report (AR6).

Liquid/Slurry Storage Systems

Methane emissions from liquid/slurry manure storages were calculated with a monthly timestep, where the total VS in the liquid/slurry storage is calculated by Equation B6:

$$VS_{in\ storage,\ i} = VS_{to\ storage,\ i} + \left(VS_{residual,\ i-1} \times (1 - \omega_{i-1})\right) \quad \text{(Eq. S6)}$$

where $VS_{to\ storage,\ i}$ is the total mass of VS (in kg) collected and sent to the liquid/slurry storage system in month i, ω_i is the percentage of the total storage volume that is agitated and emptied at the end of the previous month, and $VS_{residual,\ i-1}$ is the total residual VS that carries over from the previous month calculated with Equation B7:

$$VS_{residual,i} = VS_{in\ storage,i} \times (1 - f_i) \quad \text{(Eq. B7)}$$

where f_i is the temperature dependent Arrhenius factor for month i. The Arrhenius factor uses the monthly average temperature to determine the fraction of VS that are biological available to degrade [95], calculated with Equation B8:

$$f_i = \min\left(\exp\left[\frac{E(T_2 - T_1)}{RT_1T_2}\right], 0.95\right) \quad \text{(Eq. B8)}$$

where E is the activation energy, $T_2$is the monthly average ambient temperature in Kelvin, T_1 is the bioassay temperature, and $R = 1.987\ \left[\frac{cal}{K*mol}\right]$ is the ideal gas constant. The values for activation energy and T_1 used by the CARB GREET model and the 2006 IPCC model are from Mangino et al. [157] defined as $E = 15{,}175\ \left[\frac{cal}{mol}\right]$ and $T_1 = 303.16\ [K]$. The 2019 update to the 2006 IPCC model recommends that studies use the updated values from Petersen et al. [158] defined as $E = 19{,}347\ \left[\frac{cal}{mol}\right]$ and $T_1 = 308.16\ [K]$. These two sets of values were used to define the parameter distributions for E and T1 in the Monte Carlo analysis. Model results for specific scenarios and for the regional and national emissions reduction estimates use the average of these two values with $E = 17{,}261\ \left[\frac{cal}{mol}\right]$ and $T_1 = 305.66\ [K]$.

Finally, the monthly GHG emissions from liquid/slurry storages are calculated by Equation B9:

$$CO2_{e,LS,i} = VS_{in\ storage,\ i} \times f_i \times B_0 \times 0.68 \times 27 \quad \text{(Eq. B9)}$$

where $CO2_{eq,LS,i}$ is the total GHG emissions from liquid/slurry storage (LS) in kg CO_2-eq in month i, $VS_{in\ storage,i}$ is the total mass of VS (in kg) sent to solid storage in month i, f_i is the temperature-dependent Arrhenius factor for month i, B_0 is the maximum specific methane formation for raw manure (0.24 m^3 CH_4 kg VS $added^{-1}$) [95], 0.68 is the conversion factor for m^3 CH_4 to kg CH_4 [95], and 27 is the GWP-100 value for non-fossil methane from the IPCC 6th

Assessment Report (AR6). The methodology for calculating GHG emissions from liquid/slurry storages outlined in Equations B6-B9 is aligned with existing IPCC models [102].

Uncovered Ambient Lagoon Storages

GHG emissions from uncovered ambient lagoons were determined though a robust VS mass balance approach tracking both degradable and non-degradable VS through the system. The degradable portion of VS entering the lagoon system was determined by Equation B10:

$$F_D = \frac{B_0}{\delta} = \frac{0.2613}{0.505} = 51.70\% \text{ or } 0.5170 \left[\frac{kg\ VS_{degradable}}{kg\ VS_{added}}\right] \quad \text{(Eq. B10)}$$

where B_0 is the maximum specific methane formation for manure separated liquid from Labatut et al. [104] equal to $0.2613 \left[\frac{m3\ CH4}{kg\ VS\ added}\right]$ and δ is the measured biogas formation per kg of VS destroyed from Summer & Williams [105] equal to $0.505 \left[\frac{m3\ CH4}{kg\ VS\ destroyed}\right]$.

For uncovered anaerobic lagoons, the total quantities of degradable and non-degradable VS in the lagoon in each month are determined by the mass balance between VS entering the lagoon from manure collection via flushing, the VS destroyed through biogas formation, and the VS exiting the lagoon via irrigation water. The following equations were used to quantify the mass of degradable and non-degradable VS in the lagoon in each month:

$$VS_{D,\,i} = (VS_{added,i} \times F_D) + VS_{D,carryover,\,i-1} \quad \text{(Eq. B11)}$$

$$VS_{ND,\,i} = (VS_{added,i} \times (1 - F_D)) + VS_{ND,carryover,\,i-1} \quad \text{(Eq. B12)}$$

Degradable VS destroyed through biogas formation was determined by Equation B13:

$$VS_{D,destroyed,\,i} = VS_{D,\,i} \times f_i \quad \text{(Eq. S13)}$$

where, f_i is the monthly temperature-dependent Arrhenius factor (Eq. S8). The portion of degradable VS that does not degrade (due to sub-optimal temperature) is considered residual VS and remains in the system, calculated by Equation B14:

$$VS_{D,residual,\,i} = VS_{D,\,i} - VS_{D,destroyed,\,i} \quad \text{(Eq. B14)}$$

$$VS_{ND,residual,\,i} = VS_{ND,\,i} \quad \text{(Eq. B15)}$$

As the non-degradable VS does not have the potential to produce biogas, all non-degradable VS remains in the system (Eq. B15) until removal via irrigation water. Total residual VS is calculated by Equation B16, while the fraction of residual VS that is degradable in month i, $FR_{D,i}$, and non-degradable in month i, $FR_{ND,i}$, are determined by Equations B17 and B18:

$$VS_{Total\ residual,\,i} = VS_{D,residual,\,i} + VS_{ND,residual,\,i} \quad \text{(Eq. B16)}$$

$$FR_{D,i} = \frac{VS_{D,residual,\,i}}{VS_{Total\ residual,\,i}} \quad \text{(Eq. B17)}$$

$$FR_{ND,i} = \frac{VS_{ND,residual,\,i}}{VS_{Total\ residual,\,i}} \quad \text{(Eq. B18)}$$

Finally, non-degradable and degradable VS carryover to the following month were determined by Equations B19-B21.

$$VS_{removed,i} = (V_i \times \omega_i) \times VS_{draw-down}\ \left[\frac{mg\ VS}{L}\right] \quad \text{(Eq. B19)}$$

$$VS_{D,\,removed,i} = VS_{removed,\,i} \times FR_{D,i} \quad \text{(Eq. B20)}$$

$$VS_{ND,\,removed,i} = VS_{removed,\,i} \times FR_{ND,i} \quad \text{(Eq. B21)}$$

where $VS_{draw-down}\left[\frac{mg\ VS}{L}\right]$ is the average VS concentration in lagoon effluent. For CA, $VS_{draw-down} = 3{,}178$ (Summer & Williams [105]; Meyer et al. [106]). For other regions,

$VS_{draw-down} = 4{,}227$ (Leytem et al. [107]). For cases with settling basin, this is multiplied by the VS removal eff. of the settling basin – set to 50% (Chastain et al. [108]). Lagoon volume for each month, V_i, was estimated by assuming a ratio of total solids to volatile solids of 0.71 (Labatut et al. [104]) and assuming 2% total suspended solids. Finally, carryover of degradable and non-degradable VS into the following month are calculated by Equations B22 and B23:

$$VS_{D,carryover,\,i} = VS_{D,residual,\,i} - VS_{D,\,removed,i} \quad \text{(Eq. B22)}$$

$$VS_{ND,carryover,\,i} = VS_{ND,residual,\,i} - VS_{ND,\,removed,i} \quad \text{(Eq. B23)}$$

GHG emissions from methane formation in the lagoon are calculated by Equation B24:

$$CO2_{e,Lagoon,i} = VS_{destoyed,\,i} \times \delta \times 0.68 \times 27 \quad \text{(Eq. B24)}$$

where δ is the measured biogas formation per kg of VS destroyed from Summer & Williams [105] equal to $0.505\ \left[\frac{m3\ CH4}{kg\ VS\ destroyed}\right]$, 0.68 is the conversion factor for m^3 CH_4 to kg CH_4 [95], and 27 is the GWP-100 value for non-fossil methane from the IPCC 6th Assessment Report (AR6).

Covered Ambient Lagoon Digesters

GHG emissions from covered lagoon digesters were determined with a very similar approach to uncovered lagoon storages, with a few small distinctions. Due to the installation of a cover to capture biogas, a constant lagoon volume must be maintained, accomplished through the installation of an effluent pond. In the case of a covered lagoon digester, all irrigation and flush water is removed from the effluent pond. Thus, the volume to the effluent pond in each month is equal to the volume sent to the lagoon each month, Equation B25:

$$Volume_{to\ lagoon,i} = Volume_{to\ EP,i} \quad \text{(Eq. B25)}$$

The inflow of VS to the effluent pond is determined by Equation B26:

$$VS_{to\ EP,i} = Volume_{to\ EP,i} \times VS_{draw-down} \quad \text{(Eq. B26)}$$

The total VS in the effluent pond in each month is the balance of VS inflow from the digester and removal through irrigation. The effluent pond was assumed to be agitated prior to irrigation, meaning the percentage of volume emptied is equal to the percentage of total VS emptied. Thus, the GHG emissions from methane formation in the effluent pond are calculated by Equations B27 and B28:

$$VS_{in\ EP,\,i} = VS_{to\ EP,\,i} + \left(VS_{in\ EP,\,i-1} \times (1 - f_{i-1}) \times (1 - \omega_{i-1})\right) \quad \text{(Eq. B27)}$$

$$CO2_{e,EP,i} = (VS_{in\ EP,\,i} \times f_i \times B_0 \times 0.68 \times 27) \times (1 - \eta_{cap}) \quad \text{(Eq. B28)}$$

Covered lagoons were assumed to have a biogas capture efficiency, η_{cap}, of 95%, with the remaining 5% leaked to the atmosphere [95].

Settling Basins

GHG emissions from settling basins are calculated with the same segregated mass balance approach used for uncovered ambient lagoons with total VS to the settling basin determined with Equation B29:

$$VS_{to\ SB,i} = VS_{ex} \times F_{collected} \times \eta_{SB} \quad \text{(Eq. B29)}$$

where VS_{ex} is the total VS excreted (in kg), $F_{collected}$ is the percentage of manure collected via flushing, and η_{SB} is the VS removal efficiency of settling basins, equal to 50%. Additionally, settling basins were assumed to be agitated prior to cleanout, meaning the percentage of the

settling basin emptied in each month (Table B12) resulted in an equivalent percentage of total VS removal. Carryover of residual VS to the following month was calculated by Equation B30:

$$VS_{removed,i} = \left(VS_{Total\ residual,\ i-1} \times (1 - \omega_{i-1})\right) \quad \text{(Eq. B30)}$$

Complete-Mix Anaerobic Digesters (CMAD)

Engineered anaerobic digesters were assumed to be held at a constant temperature of 36°C [86,109,110,159]. A sensible heat input was required to maintain this constant temperature, calculated by Equation B31:

$$Q_{required} = \left(m \times C_p \times (T_{reactor} - T_{amb})\right) \times \left(1 + (Q_{loss} - Q_{rec})\right) \quad \text{(Eq. B31)}$$

where the total mass to the digester per day, m, was estimated assuming a contribution of 35 gallons of manure/liquid per WCE per day and a density of 8.4 lbs per gallon [160]. The specific heat capacity of manure, C_p, was assumed to equal the specific heat capacity of water, the sensible heat loss, Q_{loss}, was assumed to be 59% based on the work of Pain et al. [161], and the heat recycle rate was approximated as 50%. In combined heat and power scenarios, heat generated in the CHP unit was assumed to heat the digester, with supplemental heat provided by a natural gas boiler. Biogas formation and GHG emissions from CMAD were calculated by Equations B32 and B33:

$$CH_4 = \eta_{CMAD} \times B_o \times VS_{input} \quad \text{(Eq. B32)}$$

where $B_0 = 0.24\ \left[\frac{m3\ CH4}{kg\ VS}\right]$, and the biogas conversion efficiency of the CMAD reactor, $\eta_{mesophilic}$, was assumed to equal 85%. The CMAD was assumed to capture 98% of the biogas, with 2% leaked to the atmosphere [95]. Unconverted VS was assumed to flow to liquid/slurry storage with total mass of VS to storage quantified by Equation B33:

$$VS_{to\ storage} = (1 - \eta_{mesophilic}) \times VS_{input} \quad \text{(Eq. S33)}$$

The conversion efficiency of the CMAD is dependent on the reactor temperature, retention time, VS loading rate, and complexity of the reactor and biogas capture system [110,112]. A sensitivity analysis was performed to explore the impact of the CMAD efficiency on the total annual emissions reduction potential per region for the Status Quo and Opportunity adoption cases. Results are shown in Figure B9.

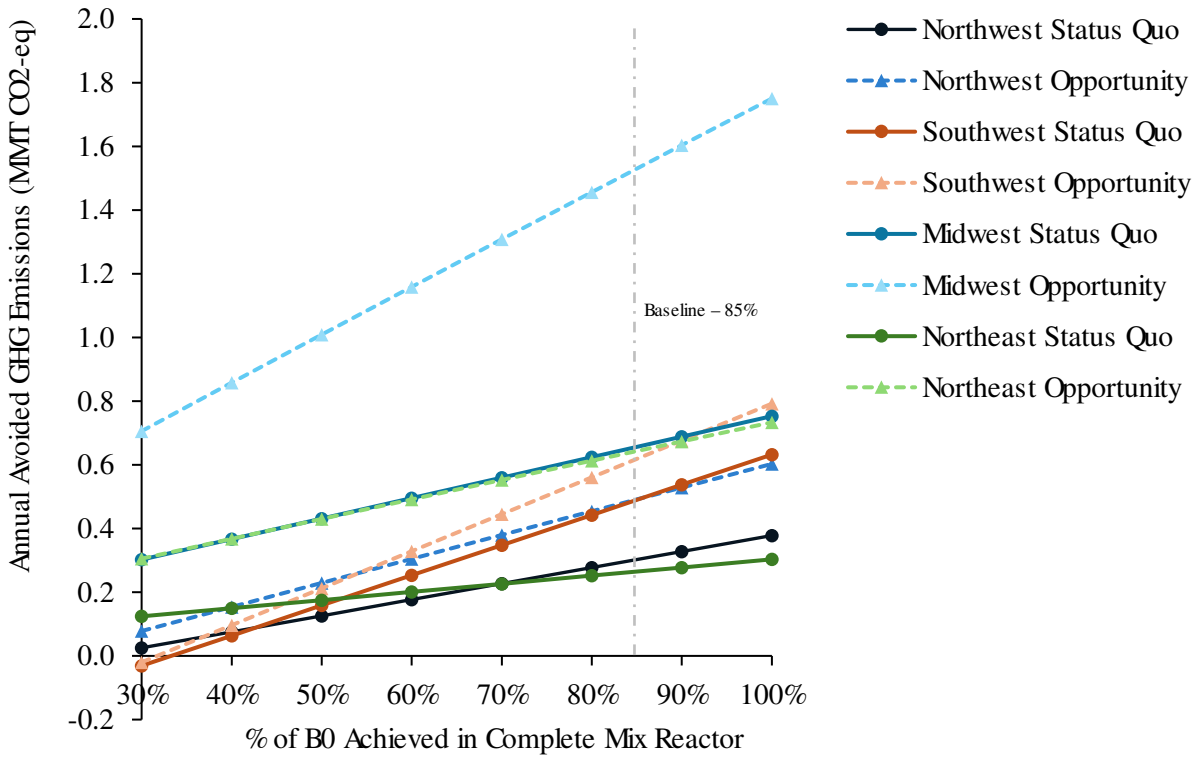

Figure B9: Impact of the conversion efficiency (% of the maximum biogas potential achieved) of engineered CMAD on the annual GHG emissions reduction potential by region for the Status Quo and Opportunity adoption cases. California is excluded as there are no scenarios in California which use CMAD.

N_2O Accounting

The modeling approach follows the mass balance of Nitrogen in the system. The mass balance considers N losses on the dry lot, in the barn/parlor, settling basins, anaerobic lagoons (covered and uncovered), CMAD systems, and liquid slurry storage (w/ and w/out natural crust cover), as well as losses resulting from solid liquid separation (SLS). Nitrogen losses are then translated to N_2O emission using the appropriate emissions factors (EF4 and EF5). Nitrogen excretion per WCE per year in state i was determined by Equation B34, using state-level N excretion rates for dairy cows in the U.S. (shown in Tables B12 and B13) obtained from the EPA [2]:

$$N_{EX,yr_i}\left[\frac{kg\ N}{WCE*yr}\right] = N_{EX,day_i}\left[\frac{kg\ N}{1000\ kg\ animal\ mass*day}\right] * \frac{TAM\left[\frac{kg}{WCE}\right]}{1000} * 365\left[\frac{days}{year}\right] \quad \text{(Eq. B34)}$$

The N losses considered in this analysis include:

- Direct N_2O emissions from the manure management system
- Indirect N_2O formation from the volatilization of manure N to NH_3 and NO_x
- Indirect N_2O formation from N leaching from the manure management system

Table B21: N2O Emissions Factors, Units, and Variable Name

Emissions Factor/Parameter	Units	Short Name
Direct N2O Emissions Factor	kg N2O-N per kg N excreted	EF_3
Nitrogen Loss Fractions due to Volatilization of NH3 and NOx	% of N excreted lost to volatilization	$Frac_{gas}$
Emissions Factor for N2O from N Volatilization	kg N2O-N/(kg NH3-N + NOx-N volatilized)	EF_4
Nitrogen Loss Fractions due to Leaching	% of N lost to leaching	$Frac_{leach}$
Emissions Factor for N2O from N Leaching	kg N2O-N/(kg N leached and runoff)	EF_5
N Removal from Soid Liquid Separation	% of N removed by SLS	N_{rem_SLS}

Nitrogen Removal from Solid-Liquid Separation

For standard screw press Gooch et al. [162] reported an average recovery of 44, 16, and 17% of the total input of dry matter, nitrogen and phosphorous. Work conducted by Fournel et al. [117] resulted in 35, 13 and 19% of the total input as dry matter, total nitrogen and total phosphorus. Moller et al. [163] reported 25, 1.5 and 16% and Wu [118] reported 50, 24 and 14% as dry matter, total nitrogen and total phosphorus. Zhang et al. [119] report an average TS removal of 40% and nitrogen removal of 16% for slope screen separators. This study assumes 15% of N is removed in the separation of course fibers with no N_2O emissions until land application (broadcasting).

Table B22: Emissions Factors for Different Manure Management Systems

Emissions Factor	**Open Lot**	**Barn/ Parlor**	**Settling Basin**	**Ambient Lagoon**	**Effluent Pond**	**Complete-Mix Digester[1]**	**Liquid/Slurry w/Natural Crust Cover**	**Liquid/Slurry Uncovered**
EF_3	0.02	0	0.005	0	0	0.0006	0.005	0
$Frac_{gas}$	0.3	0.155	0.3	0.35	0.35	0.00*	0.3	0.48
EF_4	0.01	0.01	0.01	0.01	0.01	0.01	0.01	0.01
$Frac_{leach}$	0.035	0	0	0	0	0.00*	0	0
EF_5	0.011	0.011	0.011	0.011	0.011	0.011	0.011	0.011
References and Notes	IPCC: Table 10.21, Table 10.22, Table 11.3	USDA: GHG Accounting Methods (2023 draft out for public comment)	IPCC: Treated as liquid/slurry with crust Table 10.21, Table 10.22, Table 11.3	IPCC: Table 10.21, Table 10.22, Table 11.3	IPCC: Table 10.21, Table 10.22, Table 11.3	*Indirect emissions determined from long term storage of digestate as liquid/slurry (see right)	IPCC: Table 10.21, Table 10.22, Table 11.3	IPCC: Table 10.21, Table 10.22, Table 11.3

Notes:
[1]Indirect N_2O emissions for anaerobic digestion (from NH_3 and NO_x volatilization and leaching during storage of digestate) are accounted for in the long-term storage module assuming storage as Liquid/Slurry Uncovered.

Direct N2O Emissions

Direct N2O emissions were calculated with Equation B35 (Eq. 10.25 2019 Refinement to the 2006 IPCC Guidelines for National GHG Inventories [102]) with the appropriate emissions factor from table B20.

$$kg\ N2O\ = N_{EX} \times F_{collected}\ \times\ EF_3\ \times \frac{44}{28}\quad \text{(Eq. B35)}$$

Indirect N2O Emissions

Indirect N2O emissions from volatilization, $N2O_{vol}$, and from leaching, $N2O_{leach}$, from the manure management system were calculated with Equations B36 and B37 obtained from the 2019 Refinement to the 2006 IPCC Guidelines for National GHG Inventories [102] from the IPCC:

$$N2O_{vol}\ = N_{EX} \times F_{collected}\ \times\ Frac_{gas}\ \times EF_4 \times\ \frac{44}{28};\ \text{where } EF_4 = 0.01\quad \text{(Eq. B36)}$$

$$N2O_{leach}\ = N_{EX} \times F_{collected}\ \times\ Frac_{leach}\ \times EF_5 \times\ \frac{44}{28};\ \text{where } EF_5 = 0.011\quad \text{(Eq. B37)}$$

N2O Emissions from Land Application of Residual Manure Solids

Total land applied nitrogen was determined to be the balance of nitrogen collected and nitrogen losses throughout the system to direct and indirect emissions. The total amount of manure nitrogen land applied was determined for each scenario with Equation B38, with indirect N2O emissions calculated with Equation B39:

$$N_{LA} = N_{EX} * F_{collected}\ - \sum N_{losses}\quad \text{(Eq. B38)}$$

$$N2O_{land-application}\ = \Big((N_{LA} \times \%_{broadcast}\ \times\ EF_{broadcast}) + \big(N_{LA} \times \%_{injected} \times EF_{injected}\big)\Big) + \big(N_{LA} \times \%_{irrigated} \times\ EF_{irrigated}\big) \times\ \frac{44}{28}\quad \text{(Eq. B39)}$$

where $EF_{broadcast} = 0$ for both raw and digested manure, $EF_{injected} = 0.02$ for raw manure and 0.01 for digested manure, $EF_{irrigated} = 0.01$ for both raw and digested manure and the percentage of manure land applied through each method was based on the region, with regional values specified in Table B16.

N2O Emissions from Raw Liquid Dairy Manure vs. Digested Liquid Dairy Manure

Midwest and Northeast

In the Midwest and Northeast base case, the assumptions are a scrape system (in some cases followed by coarse fiber separation), long-term storage, and ground application (not irrigation application) of liquid dairy manure slurries (LDMS). In the anaerobic digestion case, the scrape system is followed by a CMAD and separation of coarse fiber from digestate before long-term storage.

Rationale for Assuming Injection as the Application Method for Comparing N_2O Emissions from Raw (R) and Anaerobically Digested (AD) LDMS

The underlying assumptions are the following:

1. Large ammonia volatilization losses occur when either RLDMS or ADLDMS are broadcast without immediate incorporation via tillage
    a. These ammonia volatilization losses are generally greater from ADLDMS than RLDMS because of higher ammonium content and higher pH [164]
    b. The lower solids content and viscosity of ADLDMS results in faster infiltration into the soil; that helps lower ammonia volatilization losses, but higher ammonium content and higher pH are the overriding factors [165]

2. Immediate Injection almost eliminates ammonia volatilization losses from both RLDMS and ADLDMS [165]
3. A dairy that implements AD is well managed, has been injecting RLDMS in order to prevent large ammonia volatilization losses, and will inject ADLDMS to prevent potentially even larger ammonia volatilization losses (assumptions based on professional judgement)

An example extension guideline regarding fraction of ammonium (NH_4) retained (not lost as NH3) from various manures vs. injection method and length of time to incorporation is in Table B23 (em8954.pdf (oregonstate.edu). Note that as the percent solids in liquid manure increases, the fraction of ammonium retained with a given application practice decreases. This is because with increasing solids content there generally is higher viscosity and slower and less infiltration and overall contact of LDM with the soil to help lower ammonia volatilization. For the Midwest and Northeast cases, coarse fiber is separated from the LDM, in which case the Thin slurry column in Table B23 (below) is likely applicable in most cases. The Lagoon Water column is applicable in cases discussed later in which LDM is applied in irrigation systems.

Table B23: Example extension guideline regarding fraction of ammonium (NH_4) retained (not lost as NH3) from various manures vs. injection method and length of time to incorporation

Table 1. Estimated fraction of manure ammonium-N retained after application.
Use the appropriate value from this table in Worksheet Step 3, "PAN from NH_4-N."

	Manure type and dry matter (DM) content					
Time to incorporation[a]	Lagoon water (< 1% DM)	Thin slurry (1–5 % DM)	Thick slurry (5–10% DM)	Solid (> 10% DM)	Compost	Solid poultry (> 10% DM)
	----------Fraction of manure NH_4-N retained[b]----------					
Immediate incorporation (1 hr)	0.95	0.95	0.95	0.95	1.00	0.95
Incorporation 1 day after	0.95	0.70	0.60	0.50	1.00	0.70
Incorporation 2 days after	0.95	0.60	0.45	0.30	1.00	0.50
Incorporation 7 days after	0.95	0.55	0.40	0.20	1.00	0.40
Directed application methods:						
Subsurface injection		0.95	0.95			
Surface band (partial incorporation)		0.85	0.70			
Surface band (no incorporation)		0.75	0.60			

[a] Tillage with harrow, cultivator, plow, etc. to incorporate manure, or overhead sprinkler irrigation (0.5 inch) after manure application.

[b]Ammonium-N retention estimates for lagoon water, slurry, solid manure, and compost apply to all livestock manures except solid poultry.

Injection Generally Results in a Tradeoff between Ammonia Volatilization and N_2O Emissions

As indicated above, injection of both RLDMS and ADLDMS greatly lowers ammonia volatilization compared with broadcast application without tillage incorporation. In contrast, compared with broadcasting, injection of LDM generally increases N_2O. The main reason is that the injection zone has a much higher moisture content and higher concentration of water-soluble carbon, both of which generally persist for a significant period of time (Figure B10). The higher moisture content slows movement of oxygen from the atmosphere into the injection zone, resulting in low oxygen conditions that are conducive to denitrification, especially with the elevated level of water-soluble carbon that serves as an energy source for denitrification. The elevated level of water-soluble carbon also stimulates general microbial activity in the retention zone and associated oxygen consumption. The injection zone is also high in ammonium. The

ammonium diffuses to the outer portion of injection zone where there is enough oxygen to support conversion of ammonium to nitrate and then the nitrate diffuses into the low-oxygen zone where it is partially converted to N_2O via denitrification [166]. In contrast to the above, a factor that can lower N_2O from injected LDM slurry (equally applicable to both RLDMS and ADLDMS) is that N_2O has a longer path to the soil surface, providing more opportunity for N_2O to convert to N_2 before arriving at the soil surface [167]; this is important with very high soil moisture levels and very low oxygen levels that are common in LDM slurry injection zones.

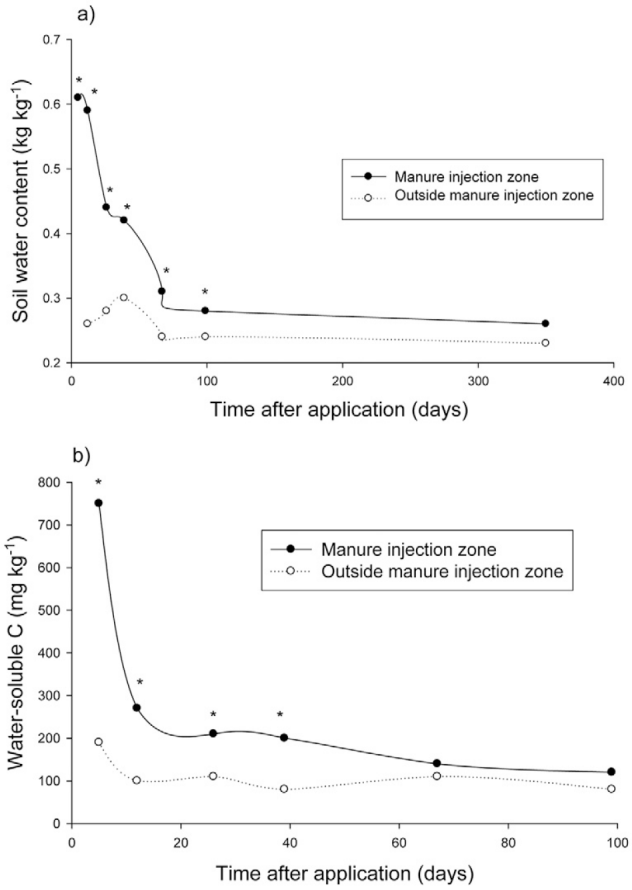

Figure B10: Dell et al. [168] after Comfort et al. [166]

In recent northeastern United States studies reported in the Table B24, broadcast and injected LDM (not anaerobically digested) were compared, each over a period of three years. The crop was corn. All three studies were conducted on silt loam soils with good internal drainage. In all three cases, injection instead of broadcasting resulted in more than a 2X increase in N_2O. The average N_2O emission factor for broadcast and injection was 1.0 and 2.1%, respectively. The N rate for the injected applications averaged 160 lb N/Ac and (160 lb N/Ac) x 0.021 x (1.57 lb N_2O/lb N_2O-N) x (298 lb CO_2/lb N_2O) x (12 lb C/44 lb CO_2) = 429 lb C_e/Ac = 0.21 tons C_e/Ac. This is close to the 0.2 tons C/Ac that Dell et al. [168] estimated as the increase in soil C sequestration by switching the silage corn portion of an alfalfa/silage corn rotation from conventional-till to no-till and illustrates the relative impact of injecting liquid dairy manure.

Table B24: Literature Values for N2O Emissions Factors for Land Application of Manure

Literature Study	**State**	**Texture**	**Broadcast**	**Injected**
			N_2O Emission Factor (%)	
Duncan et al., 2017	PA	Silt Loam	0.8	1.8
Ponce de Leon et al., 2021	PA	Silt Loam	0.6	1.5
Dittmer et al., 2020	VT	Silt Loam	1.5	3.1

The N_2O emission factors in Table B24 should be considered on the conservative side. For example, Herr et al. [169] compared surface application/tillage incorporation within 2 hours (INC) and injection (INJ) of cattle slurry on a “silty loamy” soil in Germany, Table B24 [169]. INJ plus several nitrification inhibitors was also compared. Applications were made in the spring of 2015 (150 lb N/Ac) and 2016 (170 lb N/Ac). The N_2O emission factors are presented in Table B25 and are much higher in the first than the second year. The first year was extraordinarily warm and dry. The second year is more representative of typical spring temperature and moisture and the INJ treatment in the second year was 2.4X higher than the INC treatment. The second-year N_2O emission factor for INJ of 4.4% can be translated to tons C_e/Ac as follows: (170 lb

N/Ac) x 0.044 x (1.57 lb N_2O/lb N_2O-N) x (298 lb CO_2/lb N_2O) x (12 lb C/44 lb CO_2) = 954 lb C_e/Ac = 0.48 tons C_e/Ac. These data further illustrate that large increases in N_2O can occur when liquid cattle manure slurries are injected rather than applied on the soil surface and incorporated with tillage immediately.

Table B25: N2O Emissions Factors

Treatment	N_2O Emission [kg N_2O-N ha^{-1} yr^{-1}]			EF [% of N Applied]		
	1st Year	2nd Year	Mean	1st Year	2nd Year	Mean
CON	2.3 [b]	3.3 [c]	2.8			
INC	2.1 [b]	6.7 [b,c]	4.4	0.0	1.8	0.9
INC + DMPP&DMPSA	n.d.	5.4 [b,c]	5.4	n.d.	1.1	1.1
INJ	16.2 [a]	11.5 [a]	13.9	8.4	4.4	6.4
INJ + DMPP	12.8 [a]	5.5 [b,c]	9.2	6.3	1.2	3.8
INJ + DMPSA	12.4 [a]	8.4 [b]	10.4	6.1	2.7	4.4
INJ + DMPP&DMPSA	9.6 [a]	4.9 [b,c]	7.3	4.4	0.9	2.7
INJ + nitrapyrin	12.8 [a]	7.9 [b]	10.4	6.3	2.4	4.4
INJ + DCD	11.0 [a]	4.4 [b,c]	7.7	5.2	0.6	2.9
INJ + TZ&MP	13.4 [a]	n.d.	13.4	6.7	n.d.	6.7

n.d. not determined.

N_2O Emissions from Injected ADLDMS vs. Injected RLDMS

Anaerobic digestion converts part of the volatile solids to methane. This reduces the level of water-soluble carbon, thereby decreasing the energy source for denitrification. Less water-soluble carbon also reduces microbial activity in general and associated oxygen consumption, resulting in slower depletion of oxygen levels in the application zone. These factors generally result in less denitrification-based N_2O, even though anaerobic digestion results in higher ammonium levels that potentially could be converted to nitrate and then converted to N_2O, if oxygen levels are sufficiently low and water-soluble carbon levels are sufficiently high [170]. Also, the lower viscosity of ADLDMS is predicted to enable ADLDMS to expand into a larger injection zone and thereby reduce concentrations of the band constituents according to a model

by Frey et al. [171]**.** In some cases, N_2O has been higher from injected anaerobically digested liquid manure than from injected raw liquid manure. This was observed by Moller and Stinner [172] in a case where moisture levels in the injection zone were below field capacity, too low for denitrification; in that case, the interpretation was that N_2O was mainly nitrification based and the higher ammonium levels in digestate resulted in higher N_2O. In a three-year study with corn on a loam soil in Ontario, the average N_2O emission factor was 2.2% for injected RLDMS and 1.5% for ADLDM, a 32% reduction in N_2O with ADLDMS [173]. In a review of strategies for reducing N_2O, VanderZaag et al. [170] concluded that overall, there is consistent evidence that anaerobic digestion reduces N_2O emissions from liquid manure by up to 70%. For the Midwest and Northeast regions, we assume direct N_2O emission factors of 2.0% for injected RLDM and 1.0% for injected ADLDMS. Based on the previous discussion of ammonia volatilization from injected LDM, we assume very low ammonia volatilization from both injected RLDMS and injected ADLDMS, and therefore, very low indirect N_2O from both. For the current level of assessment, zero indirect N_2O from volatilized ammonia seems like a reasonable assumption.

The coarse fiber separated from AD digestate is much lower in ammoniacal N, labile carbon, and water content and generally is broadcast rather than injected. These factors result in much lower N_2O emission factors for separated coarse fiber than the digestate. For example, averaged over four years, the N_2O emission factor was 0.07% for solids separated with a screw press and broadcast applied and 0.95% for injected digestate, both from beef cattle manure [174]. N_2O from raw separated coarse fiber may be somewhat higher than from digested separated coarse fiber due to more ammonium and labile carbon, but still relatively low. Based on these findings, we assume zero direct and indirect N_2O from both raw and AD broadcast separated coarse fiber.

California and Southeast

In both California and the Southeast, the base case is a flush system followed by either coarse fiber separation or a settling basin, followed by an ambient lagoon, effluent pond, and land application of dilute lagoon water via irrigation (flood in California and sprinkler in the Southeast). In some cases, the irrigated lagoon water is further diluted with irrigation water. The only difference in the anaerobic digestion case is that the ambient lagoon is covered, and methane is captured. We assume that covering the ambient lagoon has no significant effect on the properties of the liquid dairy manure that is land applied, and no significant effect on either direct or indirect N_2O emissions following land application. The direct N_2O emission factor for flood-irrigated dairy lagoon water ranged from 0.8% to 1.3% in a review of N_2O emissions for California agriculture [175]. Comparable N_2O emission data for sprinkler-irrigated dairy lagoon water were not found. In this assessment we assume an N_2O emission factor of 1.0 for flood- and sprinkler-irrigated dairy lagoon water.

Regarding indirect N_2O from volatilized ammonia, ammonia volatilization from land-applied lagoon water is small in general (Table B23) and therefore, indirect N_2O is small. The amount of water (actual lagoon water and/or blended fresh irrigation water) applied with ammoniacal N results in significant movement of ammoniacal N into the soil; the interaction of lagoon water with the soil results in low ammonia volatilization from sprinkler-applied lagoon water [176]. Chastain [177] did a combined analysis of available studies on ammonia volatilization from lagoon water enroute from sprinklers to the soil surface and found that those ammonia losses are small. There is a dearth of information regarding ammonia volatilization from flood-irrigated LDM in California but based on the low concentrations of ammoniacal N in lagoon water, especially when mixed with irrigation water, we assume that ammonia

volatilization from flood-irrigated lagoon water in California is low (10% or less) [178]. For the current level of assessment, we assume zero indirect N_2O from lagoon water applied in irrigation systems.

Southwest and Northwest

The predominant practice in the Southwest and Northwest is flush systems with sprinkler-irrigated lagoon water. It is recommended that the direct and indirect N_2O emission factors for California and Southeast (discussed above) also be used for the predominant practice in the Southwest and Northwest. In western Oregon and western Washington, only part of the LDM is sprinkler irrigated; for this portion, the indirect and direct N_2O emission factors for California and the Southeast are recommended. The rest of the LDM produced in western Oregon and western Washington is produced as a slurry that is injected; in these cases, the direct and indirect N_2O emission factors for the Midwest and Northeast are recommended.

Summary

A summary of the first-approximation estimates for the scenarios addressed above is provided in Table B26. The injected dairy manure slurry scenario is projected to result in AD having a significant impact on N_2O from land application. The other two scenarios are projected to result in AD not having a significant impact on N_2O from land application. The first two scenarios are predominantly applicable in the Midwest and Northeast and the last scenario is predominantly applicable in California and the Southeast, Southwest, and Northwest (except for western Oregon and Washington as discussed in the previous paragraph).

Table B26: First-Approximation Estimates of Anaerobic Digestion Effects on N2O from Land-Applied Dairy manure

Direct N_2O Emission Factor (%)[1]					
Injected		Broadcast		Irrigation-Applied	
Dairy Manure Slurry		Separated Coarse Fiber		Dairy Lagoon Water	
Raw	AD	Raw	AD	Raw	AD
2.0	1.0	~0	~0	1.0	1.0
[1]Indirect N2O from volatilized ammonia assumed zero for all cases					

Regional Adoption Projects

Forecasting AD adoption by dairy farms is complicated by existing farm practices and evolving farm dynamics. At the farm level, there is much variability in manure conveyance, animal housing, bedding material and existing infrastructure that impact adoption. While milk production has grown, the number of farms has decreased and the total U.S. herd size is constant, driven by increasing milk production per cow. The cow population currently participating in anaerobic digesters (or digesters that are actively under construction) was a key input to the economic modeling. The team utilized the current USDA Ag Star database [179] summarized in Table B27 to inform regional adoption estimates.

Table B27: Number of Cows Currently Associated with Digesters in the U.S. (2023) [179]

Region	**Number of Cows in Digesters from Farms with <2,500 Cows**	**Number of Cows in Digesters from Farms with >2,500 Cows**	**Total Cows in Digesters in the U.S. as of 2023**
Northwest	8,800	93,500	102,300
California	40,181	726,661	766,842
Midwest	35,460	190,912	226,372
Northeast	62,817	30,203	93,020
Southwest	2,250	184,659	186,909
Southeast	500	10,809	11,309

Adoption estimates considered two cases. The Status Quo Case was based on potential adoption of anaerobic digesters over the next six years predicated on economics for producing

renewable natural gas for sale into the California Low Carbon Fuel Standard (LCFS) market, the value generated from the U.S. EPA Renewable Fuel Standard D3 RINs plus gas sales. A high-level economic analysis was performed (presented in the attached excel spreadsheet) with results suggesting a minimum equivalent farm size of ~3,500 mature cows necessary to support investment in an AD system for manure management. USDA National Agricultural Statistics Data (NASS) [94] were used as a basis for estimating the total number of potential mature cows on farms with 2,500 or more mature cows (NASS categories of 2,500-4,999 and 5,000+ mature cows). The economic analysis incorporated RNG production estimates (Newtrient, LLC), LCFS and RIN value (Eco Engineers), rCNG value (Henry Hub), CI score (CARB), capital and operating input estimates (Newtrient, LLC), the number of cows currently participating in digester programs (US EPA AgSTAR), public announcements made by food companies expanding dairy processing capacity (Southwest Region), USDA National Agricultural Statistics Service (NASS) [94] data and outreach to digester developers. NASS data was foundational in our evaluation. The most recent NASS data available when the analysis was conducted was 2017.

The Opportunity Case expanded the number of cows to include the NASS category of 1,000-2,499 mature cows and assumes future program(s) (e.g., EPA RFS eRIN Program) will provide an incentive for electricity production on farms with 1000-2,499 mature cows. The economic analysis suggested a minimum equivalent farm size of 1,750 cows to support investment in an on-farm AD system.

Where the average number of cows per farm falls short of the threshold (3,500 for RNG and 1,750 for CHP) for a given region, we made the simplifying assumption that cows could be grouped using a virtual pipeline to achieve the total number of cows predicted for each region. A

virtual pipeline allows distribution of natural gas to consumers via an injection point into a commercial natural gas pipeline. The renewable natural gas is transported by tanker truck from a project site to the injection point.

To simplify, the top ten milk producing states were considered in the adoption analysis (California, Wisconsin, Idaho, New York, Texas, Michigan, Pennsylvania, Minnesota, New Mexico, and Washington). In addition, Florida was considered for the Southeast region and Arizona for the Southwest Region. Recognizing there is a great deal of variability in these estimates, we used a combination of expert opinion and NASS data [94].

Two important terms are used throughout the discussion of adoption projections, "mature cows", and "participating cows." The minimum equivalent farm sizes determined in the economic analysis are based on the metric of "mature cows" meaning 100% of manure is utilized in AD systems. In scenarios where less than 100% of manure is collected (open lot scenarios), the total number of cows required to meet economic feasibility is increased to account for non-collected portions, providing the total number of "participating cows."

Northwest

Status Quo Case: 115,500 mature cows were assumed for the Status Quo Case with contributions from Idaho and Washington of 45,500 and 70,000 mature cows, respectively. As a frame of reference, there are 573,911 cows on farms in the 2,500+ (USDA NASS) categories and approximately 93,500 of these are already associated with digesters. Our baseline assumes 50% of the cows are housed in confined operations (25% Scenario 2A and 25% Scenario 2C) and 50% of the cows are housed in open lots converted to scrape systems (equally split between Scenarios 1A and 1B). All these cows are associated with AD Scenario 5C.

Opportunity Case: An additional 66,500 mature cows (in addition to the 115,000 from the Status Quo Case) were assumed for the Opportunity Case with contributions from Idaho and Washington of 26,250 and 40,250 mature cows, respectively. The actual number of participating cows is larger in this category due to the prevalence of open lot dairies where less than 100% of the manure is collected as liquid. The corresponding participating cows for WA are 39,900 and 66,500 cows for Idaho. We assumed 60% of the participating cows are associated with Western Washington Dairies in the 1000-2,499 category (USDA NASS) and split equally between Scenarios 2A and 2C). We assumed the balance of the cows for this estimate are from Idaho or Eastern Washington, housed in open lot dairies and likely from the 2500+ category (USDA NASS), adopting vacuuming of feed lanes (split equally between Scenarios 1A and 1B). The additional cows added under the Opportunity Case are associated with AD Scenarios 4A and 5A

California

Status Quo Case: 238,000 mature cows were assumed for the Status Quo Case. Though tremendous farm to farm variability exists, we assumed 77% of the excreted manure was captured for digestion, therefore, the total number of participating cows equals 309,091. There are 808,500 mature cows in the 2,500+ category (USDA NASS) with approximately 727,000 cows in the 2500+ demographic associated with digesters [179]. This suggests a limited opportunity for additional adoption under current economic and policy conditions; however, we considered the potential for cluster systems due to dairy density coupled with funding through the Dairy Digester Development and Research Program in developing this estimate. We assumed an equal split between Scenarios 3B and 3C for the baseline with AD scenario 6D applying to both cases.

Opportunity Case: An additional 159,250 mature cows equating to 206,818 participating cows (in addition to the 309,091 participating cows from the Status Quo Case) were assumed for the Opportunity Case. There are approximately 638,000 mature cows in the 1000–2,499 category (USDA NASS) with only about 40,000 currently associated with digesters (AgSTAR). We assumed a baseline with 50% to Scenario 3B and 50% to Scenario 3C with AD Scenario 6C applying to both cases.

Midwest

Status Quo Case : 126,000 mature cows were assumed for the Status Quo Case (mature cows are the same as participating cows because 100% of manure is assumed to be collected). There are 374,000 mature cows in the 2,500+ category (USDA NASS) between these three states. Based on the AgSTAR database, there are approximately 210,000 cows in the 2500+ category (AgSTAR) associated with digesters. By difference, there are approximately 164,000 cows in the 2500+ demographic with potential for adoption. Most Midwest dairies are confined scrape operations and are well positioned to adopt AD systems. We assumed 67% of the participating cows are aligned with baseline Scenario 2C and the balance with Scenario 2B. All cows are associated with AD Scenario 5D.

Opportunity Case: An additional 164,903 mature cows (in addition to the 126,000 from the Status Quo Case) were assumed for the Opportunity Case with mature cows the same as participating cows. There are approximately 330,000 mature cows in the 1000–2,499 category (USDA NASS) and only 35,000 cows in this category are currently associated with digesters (AgSTAR). We assumed the baseline 2C for 67% of the additional cows and Scenario 2B for the balance with the AD adoption of Scenario 5B applied to all additional cows in the Opportunity case.

Northeast

Status Quo Case: 52,500 mature cows were assumed for the Status Quo Case (mature cows are the same as participating cows because 100% of manure is assumed to be collected). There are approximately 88,000 mature cows in the 2,500+ category (USDA NASS) and approximately 30,200 cows in the category are associated with digesters (AgSTAR). This results in approximately 58,000 mature cows in the 2500+ demographic with potential for adoption. Though this estimate is aggressive, due to combination of confined operations with continued consolidation, we believe this outcome is possible. The baseline scenario 2C was applied to 67% of the cows and 2B to the balance. AD Scenario 5D applies to 100% of the cows.

Opportunity Case: An additional 79,380 mature cows (in addition to the 52,500 from the Status Quo Case) were assumed for the Opportunity Case with mature cows the same as participating cows due to 100% manure collection for AD. There are 204,612 mature cows in the 1000–2,499 category (USDA NASS) and approximately 63,000 cows in this category are associated with digesters (AgSTAR) leaving approximately 142,000 cows available for AD adoption. We assumed approximately 55% adoption for a total addition (to the Status Quo Case) of 79,380 cows. The baseline scenario 2C applies to approximately 67% of the cows and 2B to the balance. The AD Scenario 5D applies to 52,000 cows and adoption scenario 5B applies to 79,380 of the cows.

Southwest

Status Quo Case: Most of the cows in the SW are housed in open lot dairy configurations that are not conducive to comprehensive manure collection. Four new cheese plants are planned for the region and will drive the addition of several large confined dairy operations. Based on expert opinion, it was assumed that 150,000 cows could adopt anaerobic digestion with

approximately 105,000 being driven by new confined dairies to meet the cheese plant demand (baseline Scenario 2A) and an additional 50,000 mature cows driven by open lot to scrape conversion equally divided between Scenarios 1A and 1B). AD Scenario 5C applies to 100% of the cows. Mature cows equal participating cows because 100% of the manure is collected.

Opportunity Case: The opportunity case is driven by economics predicated on 1000–2,499 participating mature cows. Due to the predominance of open lot dairies in the SW, we expanded the pool of potential farms to include all sizes of dairies with more than 1,000 cows and considered the potential for several manure collection variations distributed across scenarios 1A, 1B (25% each) and Scenario 1C (50%). In total, we assumed 79,567 additional mature cows equating to 198,918 participating cows with AD Scenario 4A plus the Status Quo case of 150,000 cows all under AD Scenario 5C.

Southeast

Status Quo Case: 31,500 mature cows were assumed for the Status Quo Case (mature cows are the same as participating cows because 100% of manure is assumed to be collected). 54,563 cows are in the 2,500+ category (USDA NASS) and 10,809 cows in this category (AgSTAR) are associated with digester projects. This is an aggressive estimate but does not consider other states in the SE with dairies in the 2,500+ category. If other SE states such as Georgia, North Carolina, and Virginia were considered, this would add 35,600 additional cows in the 2500+ category. The baseline Scenario 3A and AD Scenario 6B were applied to all cows in the Status Quo Case.

Opportunity Case: An additional 22,750 mature cows (in addition to the 31,500 from the Status Quo Case) were assumed for the Opportunity Case with mature cows the same as participating cows. There are 44,670 cows in the 1000-2,499 category (USDA NASS). We

assumed approximately 50% of these cows adopt anaerobic digestion for a total addition (to the Status Quo Case) of 22,750 with a baseline Scenario of 3A and AD Scenario of 6A.

Table B28: Summary of Anaerobic Digestion Adoption Estimates by State and Region

Region	State	Total Cows Status Quo	Total Cows Opportunity
Northwest	Washington	70,000	109,900
	Idaho	45,500	112,000
California	California	309,091	515,909
Southwest	Arizona	35,280	75,800
	New Mexico	0	65,757
	Texas	114,720	207,362
Midwest	Michigan	70,000	111,580
	Minnesota	17,500	50,260
	Wisconsin	38,500	129,063
Southeast	Florida	31,500	54,250
Northeast	New York	42,000	110,040
	Pennsylvania	10,500	21,840

Table B29: Status Quo Baseline and Adoption Scenario Breakout by Number of Cows

Region	Status Quo Baseline Scenario Breakout [number of cows]									Status Quo Adoption Scenario Breakout [number of cows]				
	1A	1B	2A	2B	2C	3A	3B	3C	Total	5C	5D	6B	6D	Total
Northwest	28,875	28,875	28,875		28,875				115,500	115,500				115,500
California							154,545	154,545	309,091				309,091	309,091
Southwest	22,500	22,500	105,000						150,000	150,000				150,000
Midwest				41,580	84,420				126,000		126,000			126,000
Northeast				17,325	35,175				52,500		52,500			52,500
Southeast						31,500			31,500			31,500		31,500

Table B30: Status Quo Baseline and Adoption Scenario Breakout by Total GHG Emissions (kt CO2-eq/yr); kt: kilotonnes

Region	Status Quo Baseline Scenario Breakout [kt CO2-eq/yr]									Status Quo Adoption Scenario Breakout [kt CO2-eq/yr]					Emissions Reduction	
	1A	1B	2A	2B	2C	3A	3B	3C	Total	5C	5D	6B	6D	Total	kt CO2-eq per year	%
Northwest	75	76	117		166				434	146				146	287	66.3%
California							874	1,165	2,039				590	590	1,448	71.0%
Southwest	59	63	578						700	226				226	474	67.7%
Midwest				197	532				729		169			169	560	76.9%
Northeast				83	225				308		65			65	242	78.8%
Southeast						199			199			56		56	142	71.6%
National									4,407					1,253	3,154	71.6%

Table B31: Opportunity Baseline and Adoption Scenario Breakout by Number of Cows

Region	Opportunity Baseline Scenario Breakout [number of cows]									
	1A	**1B**	**1C**	**2A**	**2B**	**2C**	**3A**	**3B**	**3C**	**Total**
Northwest	62,125	62,125		48,825		48,825				221,900
California								257,955	257,955	515,909
Southwest	72,230	72,230	99,459	105,000						348,918
Midwest					95,998	194,905				290,903
Northeast					43,520	88,360				131,880
Southeast							54,250			54,250
Region	**Opportunity Adoption Scenario Breakout [number of cows]**									
	4A	**5A**	**5B**	**5C**	**5D**	**6A**	**6B**	**6C**	**6D**	**Total**
Northwest	66,500	39,900		115,500						221,900
California								206,818	309,091	515,909
Southwest	198,918			150,000						348,918
Midwest			164,903		126,000					290,903
Northeast			79,380		52,500					131,880
Southeast						22,750	31,500			54,250

Table B32: Opportunity Baseline and Adoption Scenario Breakout by Total GHG Emissions

Region	Opportunity Baseline Scenario Breakout [kt CO2-eq/yr]									
	1A	1B	1C	2A	2B	2C	3A	3B	3C	Total
Northwest	161	163	0	198	0	280	0	0	0	803
California	0	0	0	0	0	0	0	1,459	1,944	3,403
Southwest	191	202	458	578	0	0	0	0	0	1,428
Midwest	0	0	0	0	454	1,229	0	0	0	1,683
Northeast	0	0	0	0	208	564	0	0	0	773
Southeast	0	0	0	0	0	0	342	0	0	342
National										8,431

Region	Opportunity Adoption Scenario Breakout [kt CO2-eq/yr]										Emissions Reduction	
	4A	5A	5B	5C	5D	6A	6B	6C	6D	Total	kt CO2-eq per year	%
Northwest	126	47	0	146	0	0	0	0	0	319	483	60.2%
California	0	0	0	0	0	0	0	442	590	1,033	2,370	69.6%
Southwest	371	0	0	226	0	0	0	0	0	597	831	58.2%
Midwest	0	0	208	0	169	0	0	0	0	377	1,306	77.6%
Northeast	0	0	125	0	65	0	0	0	0	190	583	75.4%
Southeast	0	0	0	0	0	43	56	0	0	99	243	71.0%
National										2,616	5,816	69.0%

Social Policy Impact and Adoption

Social policy can have a major impact on rates of adoption. The use of anaerobic digestion to treat manure, mitigate methane emissions from manure storage, and produce renewable biogas need not be restricted only to larger dairies. Public policy in Germany has supported the construction and operation of approximately 10,000 anaerobic digestion facilities, more than any other location in the world [180,181]. The majority of these are farm based, with energy crops including silage maize, cereal silages, and sugar beets in order of importance contributing slightly more than half of the feedstocks used, and the rest consisting of animal manures, predominantly liquid slurries from dairy farms. Larger farms (by German standards), and cooperative arrangements among nearby farms have supported the majority of these installations. Recent policies there seek to increase participation by smaller farms, especially including very small, owner-operated livestock farms, a traditional and valued feature of the nation's landscape. These recent policies seek to discourage crop-based systems and rely more on manures and by-products [180]. Forty percent of support is reserved for smaller farms under these regulations, demonstrating that the installation of AD systems to reduce manure emissions and capture renewable natural gas is a function of both economic constraints and public policy choices and values [180].

Carbon Intensity Scores

The Low Carbon Fuel Standard (LCFS) is a key part of California's emissions reduction efforts under Assembly Bill 32. It offers benefits such as diversifying fuel sources, reducing petroleum dependence, and enhancing air quality. Similar programs are being adopted in regions like Oregon, Washington, and British Columbia. The LCFS employs carbon intensity scores (CI scores, in g CO2-eq MJ^{-1}) determined through cradle-to-grave life cycle assessments for

participant fuels. These scores are compared to petroleum-based fuels to calculate credits that encourage the use of low-carbon fuels. CI scores for each baseline and AD scenario combination are presented in Figure B11 on a per MJ basis.

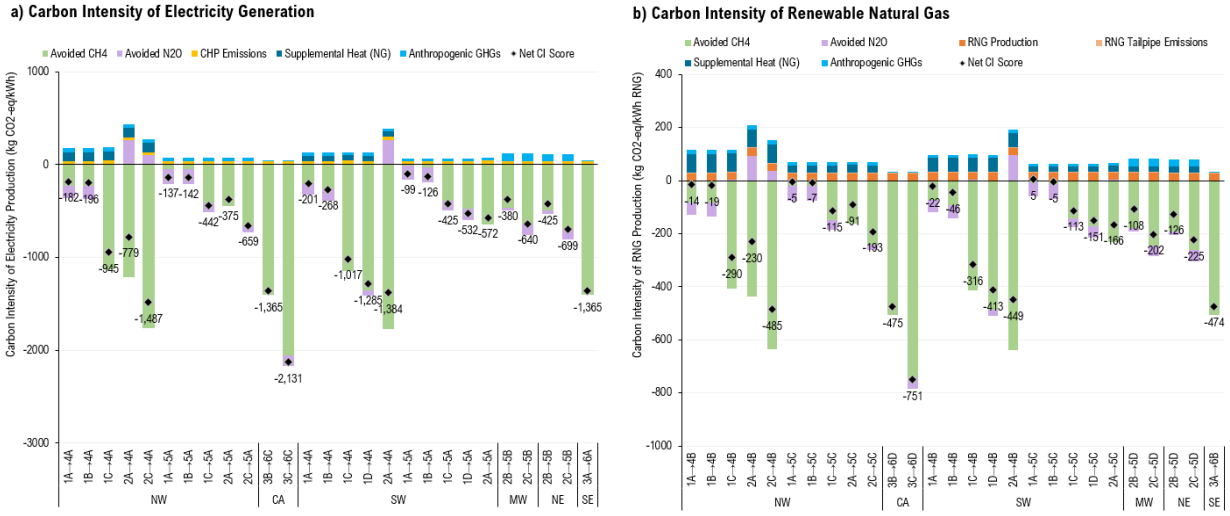

Figure B11: Carbon Intensity (CI) scores for electricity produced through combined heat and power (a) and renewable natural gas (b) produced from anaerobic digestion of dairy manure.

As illustrated in Figure B11, the combined heat and power pathway results in negative CI scores for every possible baseline to AD scenario. CI scores for electricity from manure biogas range from -99 gCO_2-eq MJ^{-1} in Southwest (1A→5B) to -2,131 gCO_2-eq MJ^{-1} in California (3C→6C) highlighting the potential of biogas from manure in the LCFS or similar programs. In a future scenario with regulated carbon pricing, a CI score of -2,131 gCO_2-eq MJ^{-1} would result in a subsidy of roughly $0.38 per kWh assuming a future carbon market value of $50 per tonne CO_2-eq. A subsidy this large could provide a mechanism to overcome the economic barriers preventing adoption of anaerobic digestion with combined heat and power systems. For the RNG pathway, all but 1 potential adoption pathways result in negative CI scores per MJ of RNG used in CNG passenger vehicles and buses. The 1A→5C pathway in the Southwest has the only positive CI score of 5 gCO_2-eq MJ^{-1} which still represents a 94.4% reduction relative to the 2023

benchmark for diesel fuel of 89.15 gCO_2-eq MJ^{-1} and generation of credits in the LCFS program [95]. The 3C→6D pathway in California has the largest negative CI score of -751 gCO_2-eq MJ^{-1} representing a 942% reduction relative to the 2023 petroleum diesel benchmark in the LCFS [95]. In general, a higher percentage of manure collection results in maximum energy recovery and a more favorable (larger negative) CI score for either biogas-use pathway. These favorable GHG outcomes can lead to adoption by smaller dairy units, especially if supported by favorable policy initiatives.

Model Validation – Comparison to IPCC [102] Methane Conversion Factor (MCF) Values

Model validation for critical calculations was performed by comparing the resulting MCF values for lagoon and liquid/slurry storages across the dairy regions with temperature dependent MCF values for manure storages from the IPCC [102] (Table 10.17 (Updated in 2019) under Chapter 10: Emissions from Livestock and Manure Management). MCF values for lagoon and liquid/slurry systems were determined as the actual methane formation in m^3 CH_4 divided by the maximum potential methane formation (total VS loading multiplied by B_0 for dairy manure). The comparison of calculated MCF values with IPCC estimates illustrates the model's ability to accurately estimate methane formation considering VS loading, system cleanout schedules, and monthly temperature for the two main long-term storage configurations considered in the analysis. To validate with IPCC estimates for ambient lagoons, the model was harmonized with IPCC assumptions by adjusting lagoon cleanout schedules to have a 12-month retention time, and using activation energy and bioassay temperatures from Mangino et al. [157] to estimate the monthly Arrhenius factor. These model validation results are presented in Table B33.

Table B33: Calculated MCF for Uncovered Lagoon Scenarios vs. IPCC MCF Values

Region	Climate Zone (Based on Annual Ave. Temp)	Scenario	Retention Time	Calculated MCF	IPCC MCF (Table 10.17) [102]
Northwest	Cool Temperate, Moist/Dry	1A - 1C	12 months	66.5%	60% - 67%
California	Warm Temperate to Tropical, Dry	3B - 3C	12 months	81.1%	76% - 80%
Southwest	Warm Temperate, Dry	1A - 1D	12 months	76.3%	76.0%
Southeast	Tropical Moist	3A	12 months	80.9%	80.0%

For Liquid/Slurry systems, calculated MCF values within the model were compared to IPCC values for Liquid/Slurry with a 6-month retention time from Table 10.17 in Chapter 10 of the 2019 Refinement to the 2006 Guidelines for National Greenhouse Gas Inventories [102]. The selected IPCC climate region based on the annual average ambient temperature for each dairy region. To harmonize with IPCC assumptions, activation energy and bioassay temperature values from Petersen et al. [158] were used. The results from this model validation effort are presented in Table B34.

Table B34: Calculated MCF for Liquid/Slurry Storage Scenarios vs. IPCC MCF Values

Region	Climate Zone	Scenario	Retention Time	Calculated MCF	IPCC MCF (Table 10.17) [102]
Northwest	Cool Temperate, Moist/Dry	2A and 2C	6 months	26.8%	21% - 26%
Midwest	Warm Temperate, Moist	2B – 2C	6 months	36.3%	37.0%
Northeast	Cool/Warm Temperate, Moist	2B – 2C	6 months	33.0%	21% - 37%
Southwest	Warm Temperate, Dry	2A	6 months	41.4%	41.0%

The results in Tables B33 and B34 demonstrate the model's ability to recreate IPCC MCF values for lagoon systems and liquid slurry storages when retention times and Arrhenius factor calculations are harmonized with IPCC assumptions. Furthermore, the results suggest that IPCC accounting protocols were successfully implemented into the modeling framework, setting a robust foundation to explore the impacts of differences in regional cleanout schedules, reduced VS loading through solid-liquid separation, anaerobic digestion, and biogas capture.

Manure Technology Team

The Manure Technology Team (MTT) is a panel of experts assembled by the Innovation Center for U.S. Dairy [93] with representatives from key dairy regions. All members of the manure technology team are listed below:

Table B35: Manure Technology Team Members

Name	Affiliation	Email
Jim Wallace	Sustain RNG, LLC	jim.wallace@jwallaceconsult.com
April B. Leytem	USDA ARS, Kimberly, ID	april.leytem@usda.gov
Robert B. Williams	California Biomass Collaborative, University of California, Davis	rbwilliams@ucdavis.edu
Stephen R. Kaffka	California Biomass Collaborative, University of California, Davis	srkaffka@ucdavis.edu
C. Alan Rotz	USDA ARS, University Park, PA	al.rotz@usda.gov
Mark Stoermann	Newtrient, LLC	mstoerm@newtrient.com
Robert Hagevoort	New Mexico State University	dairydoc@nmsu.edu

Sensitivity Analysis Results

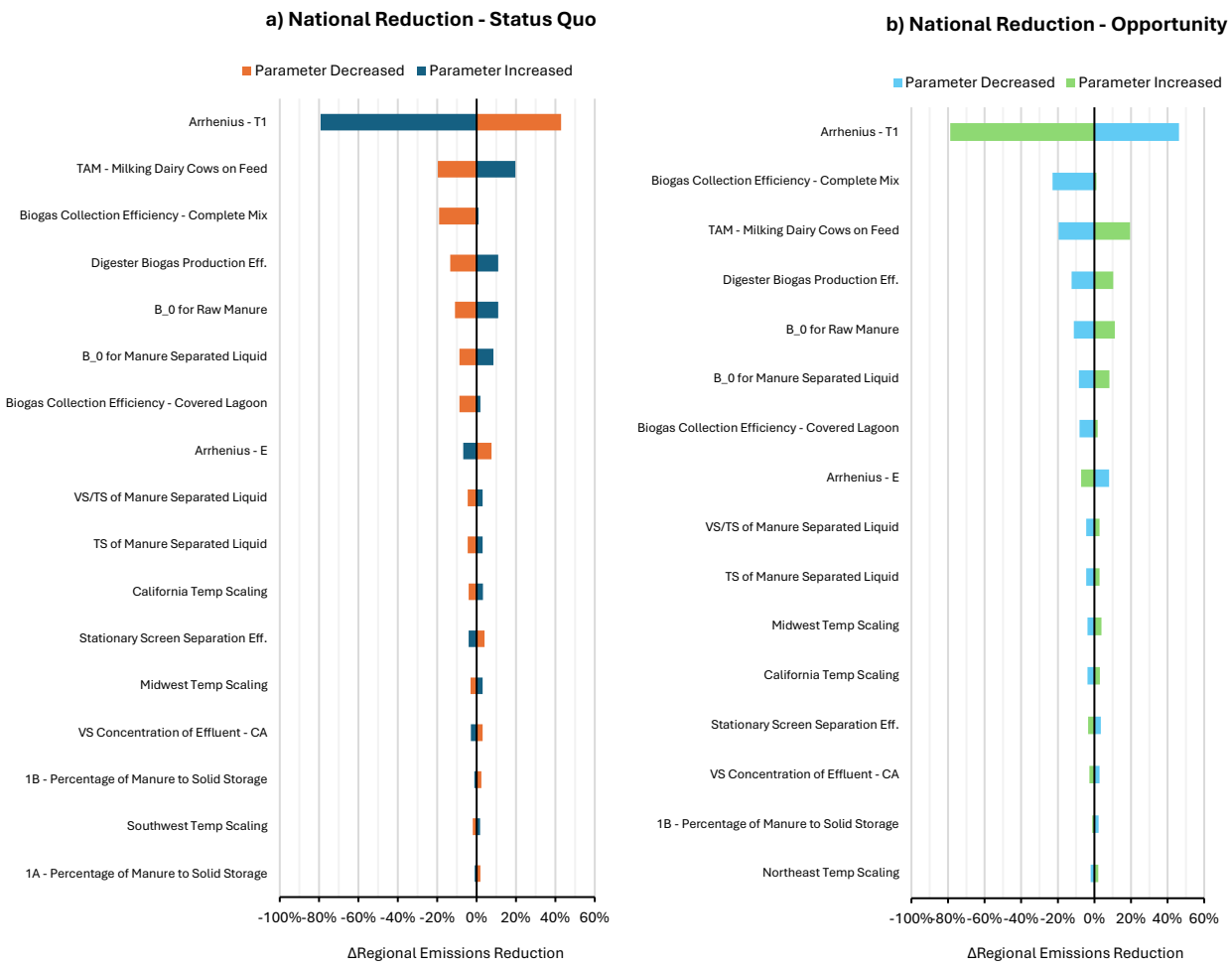

Figure B12: National Emissions Reduction Sensitivity Analysis Results for the Status Quo Case (a) and Opportunity Case (b). Input variables were adjusted by ±20% and national emissions reduction potentials were recorded.

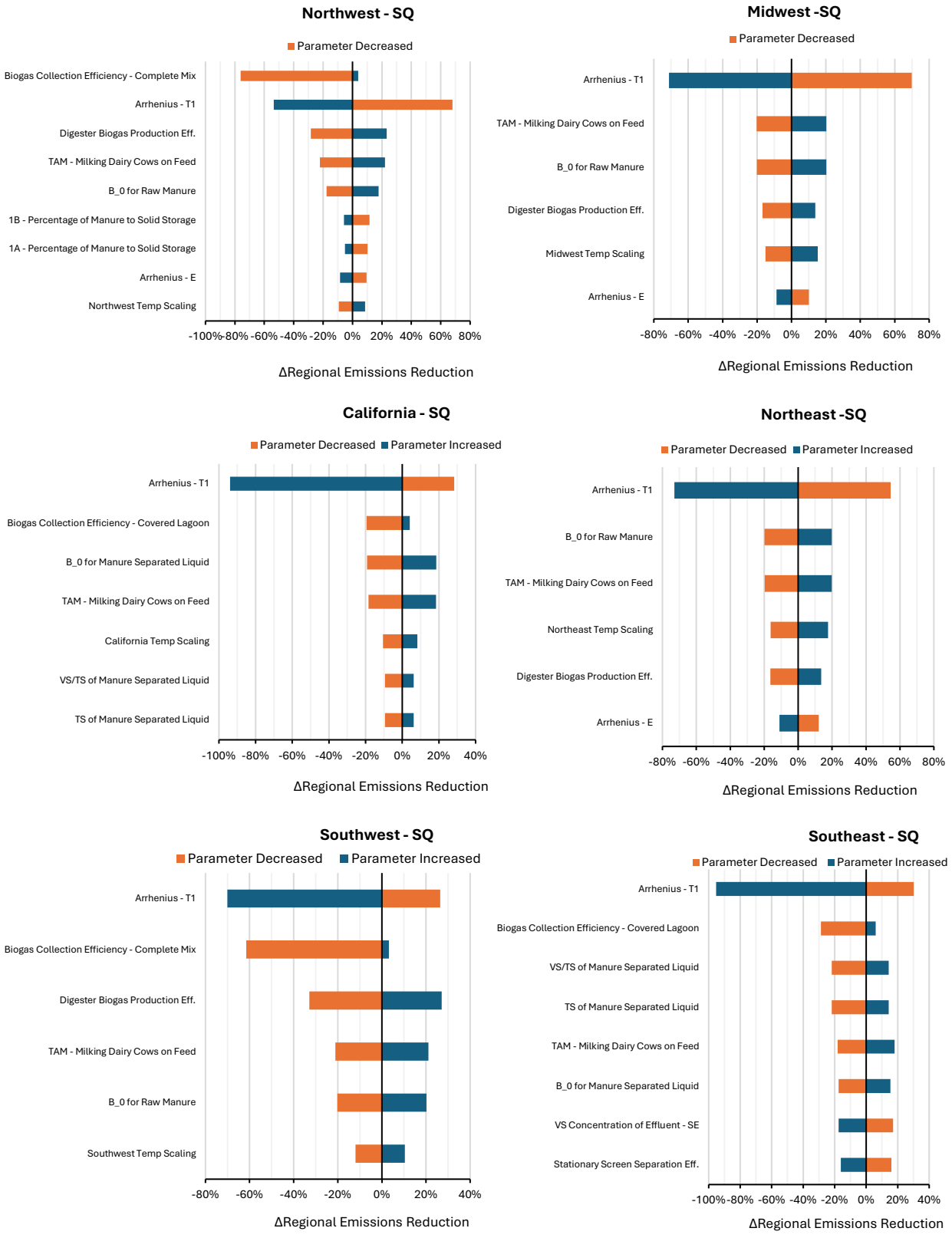

Figure B13: Regional Sensitivity Analysis Results for the Status Quo Case (Input variables were adjusted by ±20% and regional emissions reduction potentials were recorded). Only variables whose alteration led to >10% change in regional emissions reduction potentials are shown.

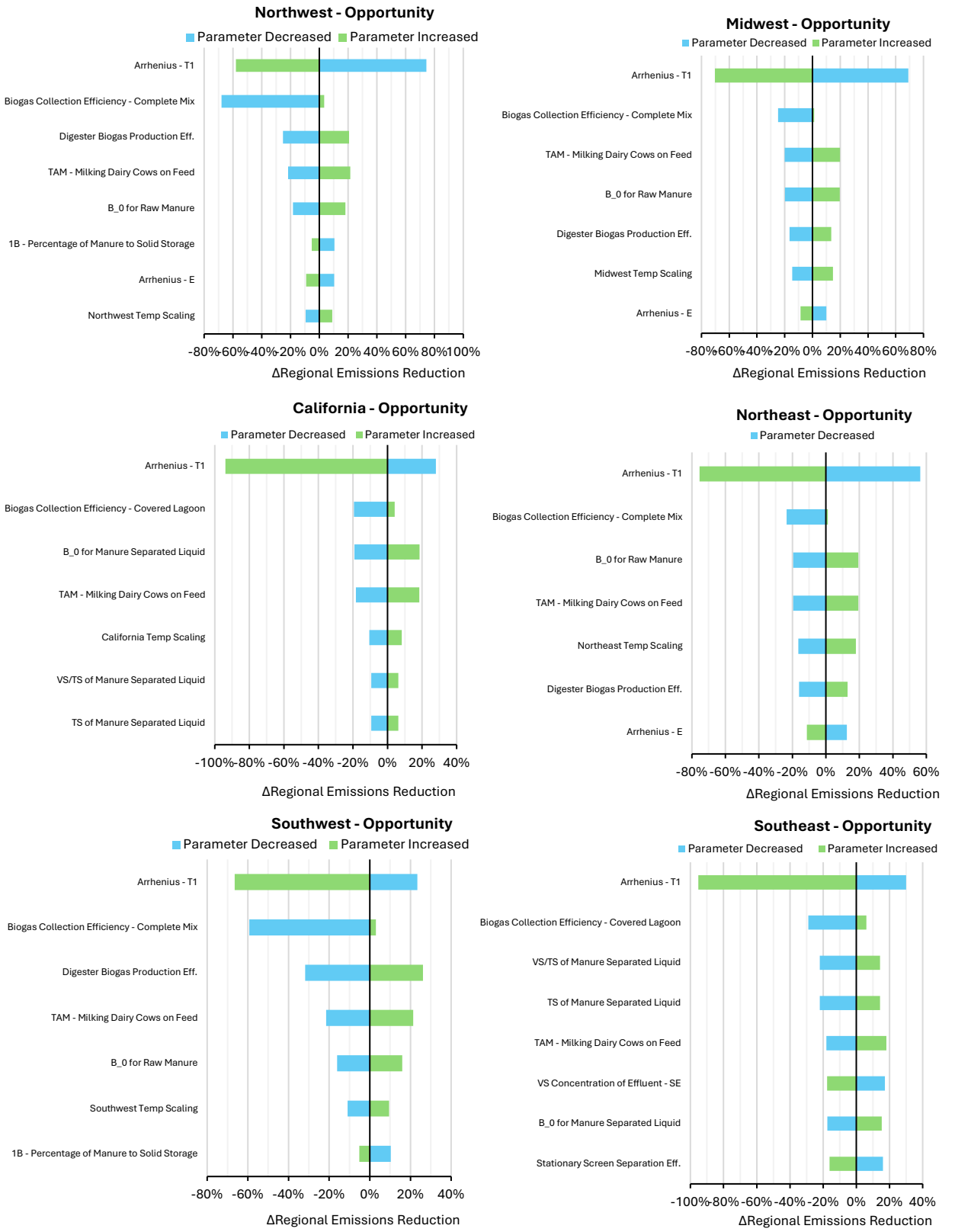

Figure B14: Regional Sensitivity Analysis Results for the Opportunity Case (Input variables were adjusted by ±20% and regional emissions reduction potentials were recorded). Only variables whose alteration led to >10% change in regional emissions reduction potentials are shown.

Monte Carlo Analysis of Uncertainty

Table B36: Monte Carlo Variable Distributions

Parameter	Min.	Mean (Baseline)	Max.	Units	Distribution Type and Justifications
Arrhenius Factor Activation Energy	15175	NA	19347	calories/mol	**Uniform:** two cited values are commonly used for activation energy including 15,175 (Mangino et al. [157]) and 19,347 (Petersen et al. [158]). The uniform distribution ensures neither value is favored in simulations.
Arrhenius Factor Bioassay Temperature (T1)	303.16	NA	308.16	Kelvin	**Uniform:** two cited values are commonly used for T1 including 303.15 K (Mangino et al. [157]) and 308.16 K (Petersen et al. [158]). The uniform distribution ensures neither value is favored in simulations.
B_0 for Manure Separated Liquid	0.18	0.24	0.30	m3 CH4/kg VS added	**Triangular:** 0.24 m3 CH4/kg VS added is used by the IPCC [102], LCFS program [95] (CARB-GREET model), and many other studies. The selected distribution allows for a 25% increase or decrease from this number.
B_0 for Raw Manure	0.20	0.26	0.33	m3 CH4/kg VS added	**Triangular:** 0.26 m3 CH4/kg VS added is the value reported by Labatut et al. [104] The selected distribution allows for a 25% increase or decrease from this number.
Biogas Collection Efficiency - Covered Lagoon	90%	95%	99%	% of gas collected by the lining	**Triangular:** The LCFS program [95] and CARB-GREET model assume a 95% biogas collection efficiency. Minimum and maximum collection efficiency selected based on expert opinion.
Biogas Collection Efficiency - Complete Mix	95%	98%	99%	% of gas collected by CMAD	**Triangular:** The LCFS program [95] and CARB-GREET model assume a 98% biogas collection efficiency from engineered digesters. The low end of 95% equates to performance a covered lagoon, maximum of 99%.
Digester Biogas Production Eff.	75%	85%	95%	% of B_0 achieved in CMAD	**Triangular:** Assumed baseline for highly-engineered complete mix systems is 85%. The distribution allows a 10% increase or decrease from this assumption.
TAM - Milking Dairy Cows on Feed	635.8	648.5	661.2	(TAM) kg/animal	**Triangular:** Captures mix of U.S. dairy herd in 2020 (80% Holstein, 8% Jersey, 12% mixed) [96] where minimum assumes low-end of Jersey weight (362 kg) and maximum assumes high-end of Jersey weight (544 kg). See Table B11 for more information.

VS Concentration of Effluent - NW	3593	4227	4861	mg VS/L	**Triangular:** Chosen distribution allows 15% increase or decrease from measured value of 4227 mg VS/L from Leytem et al. [107]
VS Concentration of Effluent – CA, SW, SE	2701	3178	3655	mg VS/L	**Triangular:** Chosen distribution allows 15% increase or decrease from measured value of 3178 mg VS/L from Summers & Williams [105]
1A - Percentage of Manure to Solid Storage	85%	90%	92%	% of Manure to Solid Storage	**Triangular:** Realistic range based on expert opinion.
1B - Percentage of Manure to Solid Storage	85%	90%	92%	% of Manure to Solid Storage	**Triangular:** Realistic range based on expert opinion.
Stationary Screen Separation Eff.	20%	30%	40%	% of VS removed	**Triangular:** Realistic range based on expert opinion and data from Williams et al. [103]
TS of Manure Separated Liquid	1.5%	2.25%	3.0%	% TSS	**Triangular:** Realistic range based on expert opinion and data from Summers and Williams [105] and Williams et al. [103]
VS/TS Ratio of Manure Separated Liquid	0.71	0.78	0.85	ratio of VS/TS	**Triangular:** Realistic range based on expert opinion and data from Summers and Williams [105] and Williams et al. [103]
NW Temp Scaling Factor	0.9	1	1.1	scaling factor	**Triangular:** Enables possibility of a ±10% change in the monthly average regional temperature used in MCF and Arrhenius Factor calculations.
MW Temp Scaling Factor	0.9	1	1.1	scaling factor	
CA Temp Scaling Factor	0.9	1	1.1	scaling factor	
NE Temp Scaling Factor	0.9	1	1.1	scaling factor	
SW Temp Scaling Factor	0.9	1	1.1	scaling factor	
SE Temp Scaling Factor	0.9	1	1.1	scaling factor	

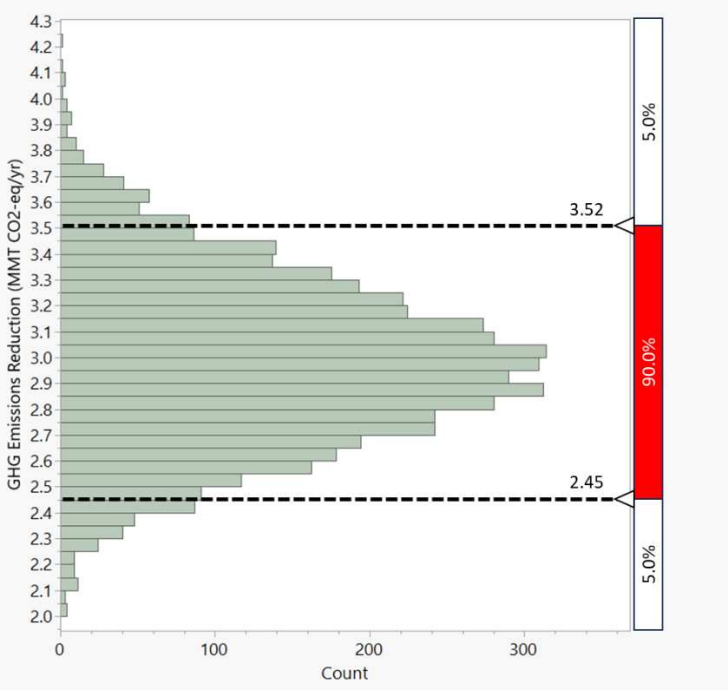

Figure B15: Monte Carlo Analysis Results – National Emissions Reduction Potential for the Status Quo Adoption Case and the uncertainty bound encompassing 90% of the simulation outcomes.

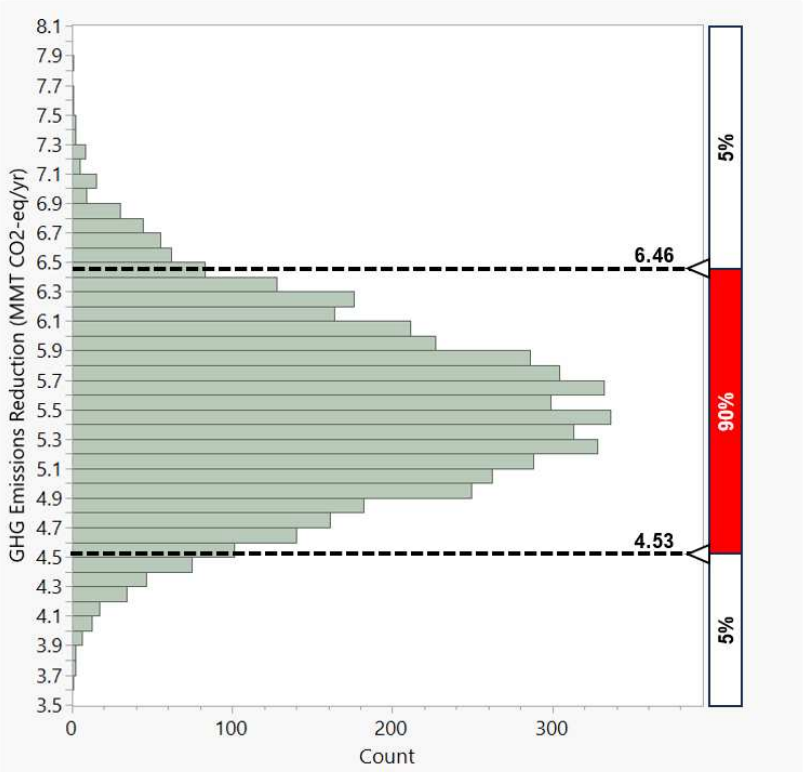

Figure B16: Monte Carlo Analysis Results – National Emissions Reduction Potential for the Opportunity Adoption Case and the uncertainty bound encompassing 90% of the simulation outcomes.

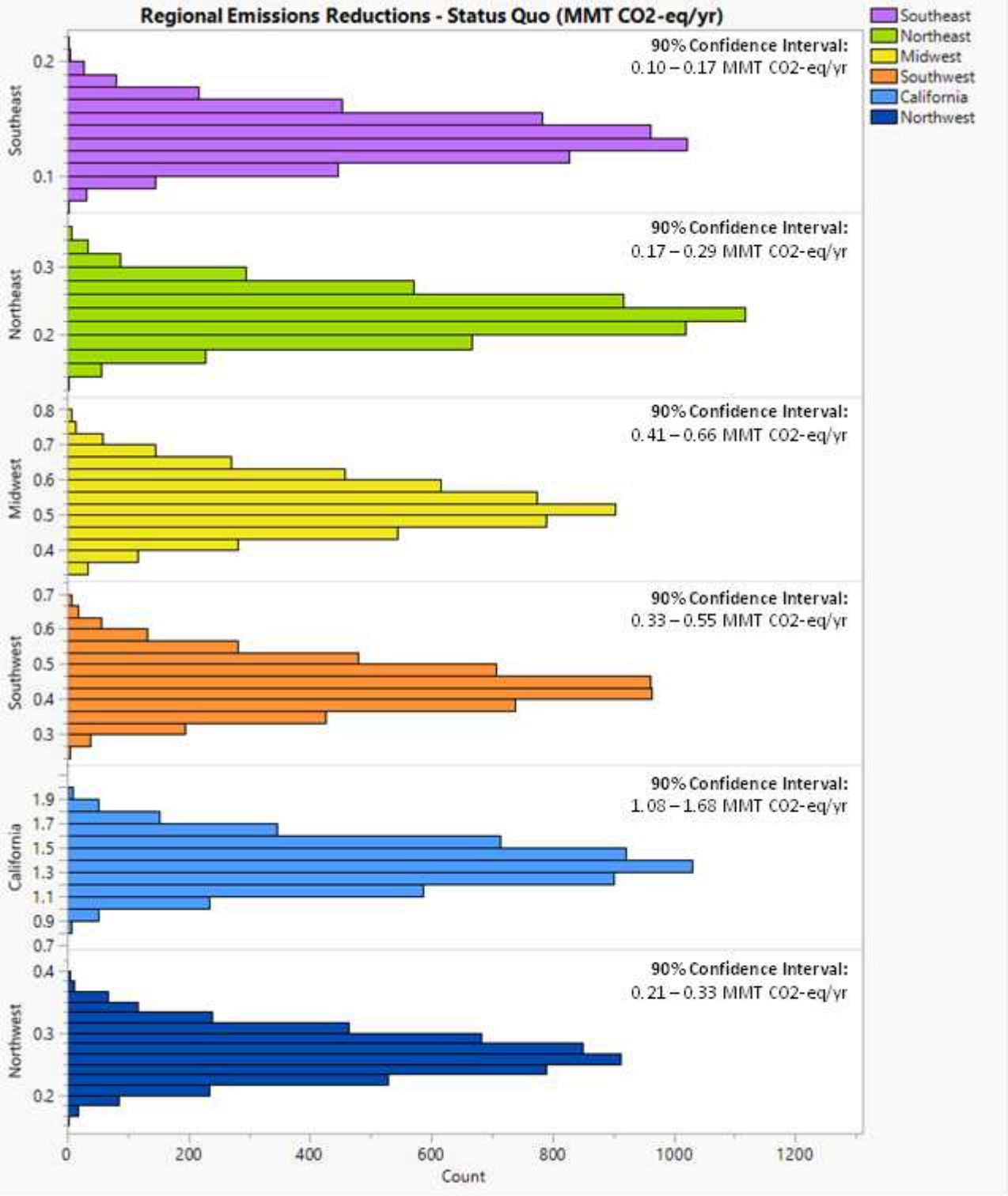

Figure B17: Monte Carlo Analysis Results – Regional Emissions Reduction Potential in MMT CO2-eq/yr for the Status Quo Adoption Case and the uncertainty bound encompassing 90% of the simulation outcomes.

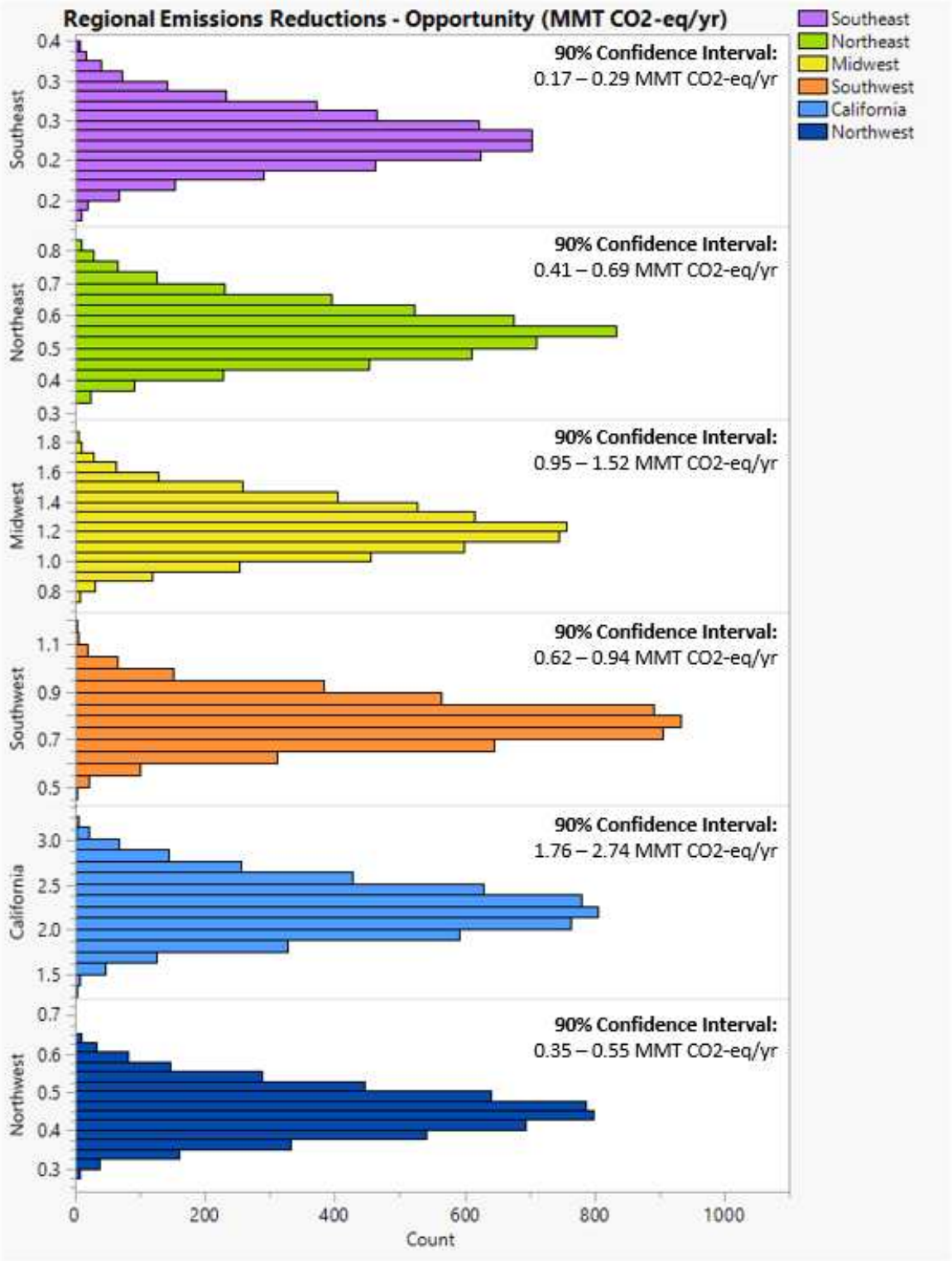

Figure B18: Monte Carlo Analysis Results – Regional Emissions Reduction Potential in MMT CO2-eq/yr for the Opportunity Adoption Case and the uncertainty bound encompassing 90% of the simulation outcomes.

Nitrogen Mass Balance

The nitrogen balance for each of the modeled scenarios is presented in Table B37 and Figure B19. The numbers in Table B37 provide the total mass of nitrogen excreted per WCE in kg N per year per WCE, the mass of N lost to direct and indirect N2O emissions, and the total residual N from the system that is land applied through manure broadcasting, irrigation, or injection.

Table B37: Nitrogen Balance of Modeled Scenarios. All units are kg N/yr.

Region	Scenario	kg N Generated	Direct and Indirect Nitrogen Losses to N2O (kg N lost to N2O)						kg N Land Applied		
		Manure Excretion	Open Lot/ Dry Lot	Barn/ Parlor	Settling Basin	Ambient Lagoon	CMAD	Liquid/ Slurry	Broadcasting	Irrigation	Injection
Northwest	1A	162.18	51.82	2.51	0.00	4.08	0.00	0.00	96.96	6.06	0.76
	1B	162.18	51.82	2.51	4.18	3.33	0.00	0.00	94.77	4.95	0.62
	1C	162.18	34.54	10.06	0.00	16.31	0.00	0.00	74.02	24.23	3.03
	2A	162.18	0.00	25.14	0.00	0.00	0.00	55.91	26.61	48.46	6.06
	2C	162.18	0.00	25.14	0.00	0.00	0.00	41.80	9.52	76.20	9.52
	4A	162.18	34.54	10.06	0.00	0.00	0.03	22.35	73.40	19.37	2.42
	4B	162.18	34.54	10.06	0.00	0.00	0.03	22.35	73.40	19.37	2.42
	5A	162.18	0.00	25.14	0.00	0.00	0.08	55.88	26.60	48.43	6.05
	5C	162.18	0.00	25.14	0.00	0.00	0.08	55.88	26.60	48.43	6.05
California	3B	159.00	12.98	18.98	0.00	30.78	0.00	0.00	44.82	51.44	0.00
	3C	159.00	12.98	18.98	31.55	25.17	0.00	0.00	28.26	42.06	0.00
	6C	159.00	12.98	18.98	0.00	30.78	0.00	0.00	44.82	51.44	0.00
	6D	159.00	12.98	18.98	0.00	30.78	0.00	0.00	44.82	51.44	0.00
Midwest	2B	165.61	0.00	25.67	0.00	0.00	0.00	57.10	27.18	0.00	55.67
	2C	165.61	0.00	25.67	0.00	0.00	0.00	42.68	9.73	0.00	87.53
	5B	165.61	0.00	25.67	0.00	0.00	0.08	57.06	27.16	0.00	55.64
	5D	165.61	0.00	25.67	0.00	0.00	0.08	57.06	27.16	0.00	55.64
Northeast	2B	160.00	0.00	24.80	0.00	0.00	0.00	55.16	26.26	0.00	53.78
	2C	160.00	0.00	24.80	0.00	0.00	0.00	41.24	9.40	0.00	84.57
	5B	160.00	0.00	24.80	0.00	0.00	0.08	55.13	26.24	0.00	53.75
	5D	160.00	0.00	24.80	0.00	0.00	0.08	55.13	26.24	0.00	53.75
Southwest	1A	163.53	52.25	2.53	0.00	4.11	0.00	0.00	97.00	7.63	0.00
	1B	163.53	52.25	2.53	4.21	3.36	0.00	0.00	94.93	6.24	0.00
	1C	163.53	34.83	10.14	0.00	16.44	0.00	0.00	71.58	30.54	0.00
	1D	163.53	34.83	10.14	16.86	13.45	0.00	0.00	63.29	24.97	0.00
	2A	163.53	0.00	25.35	0.00	0.00	0.00	56.38	20.73	61.08	0.00
	4A	163.53	34.83	10.14	0.00	0.00	0.03	22.54	71.57	24.42	0.00
	4B	163.53	34.83	10.14	0.00	0.00	0.03	22.54	71.57	24.42	0.00
	5A	163.53	0.00	25.35	0.00	0.00	0.08	56.34	20.71	61.04	0.00
	5C	163.53	0.00	25.35	0.00	0.00	0.08	56.34	20.71	61.04	0.00
Southeast	3A	152.00	0.00	23.56	0.00	0.00	0.00	38.21	26.36	63.87	0.00
	6A	152.00	0.00	23.56	0.00	38.21	0.00	0.00	26.36	63.87	0.00
	6B	152.00	0.00	23.56	0.00	38.21	0.00	0.00	26.36	63.87	0.00

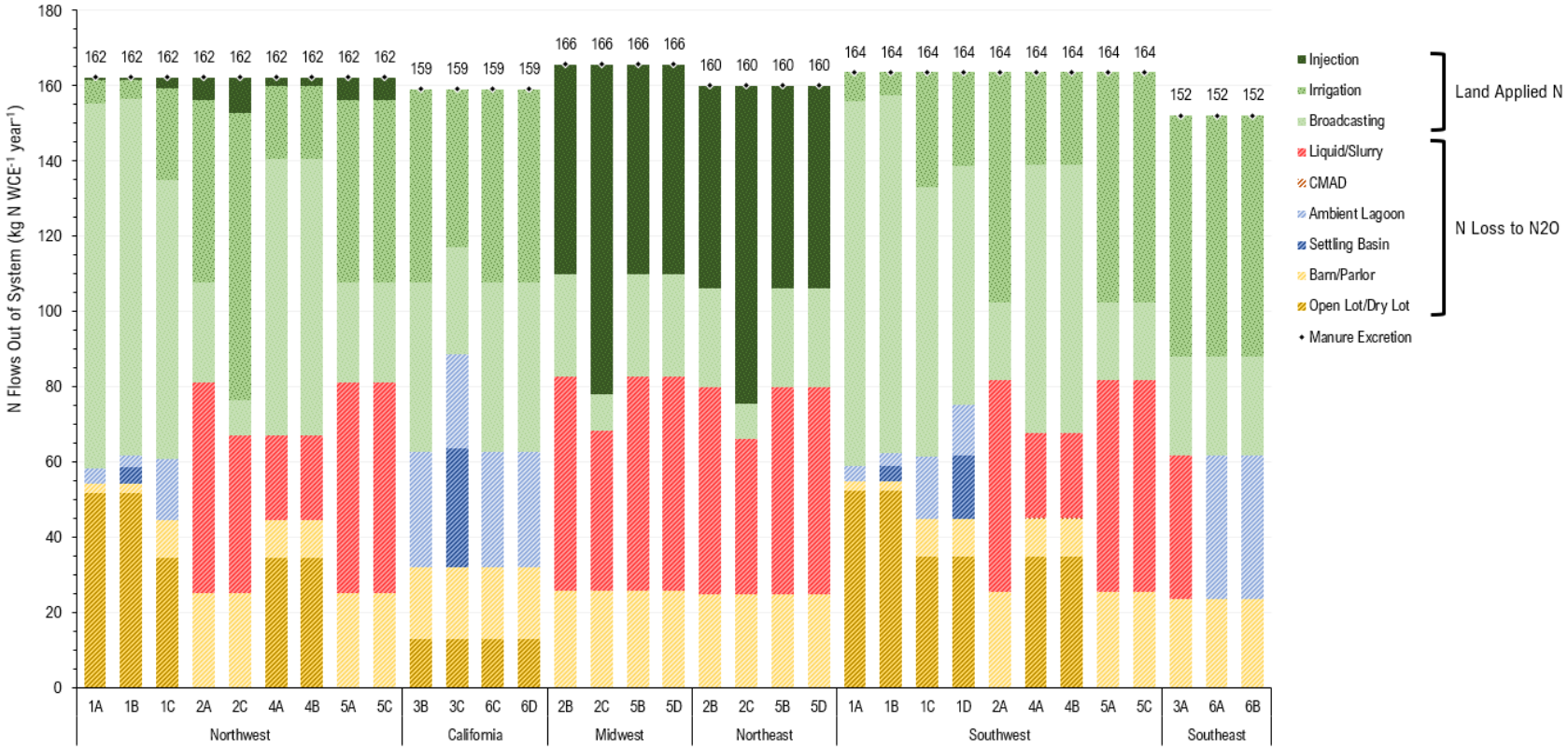

Figure B19: Nitrogen Balance for all Modeled Scenarios. Values show the loss of Nitrogen from the system due to losses from direct and indirect N2O emissions and land application.

Glossary of Manure Management Systems and Terms

Open Lot: An open area where dairy cattle are kept, without a roof or enclosed structure. Manure accumulates on the ground and is periodically removed. In the context of this study, 90% of manure falls on the open lot and is harrowed and stacked in non-anaerobic storage and 10% is flushed from the milking parlor to subsequent treatment or storage systems.

Open Lot w/ Manure on Concrete: Similar to an open lot, but with a concrete floor where manure is collected. This setup facilitates easier manure scraping or washing. In the context of this study, 60% of manure falls on the open lot and is harrowed and stacked in non-anaerobic storage while 40% is vacuumed to subsequent treatment or storage systems.

Confined Scrape: A system where dairy cattle are housed in an enclosed area with solid flooring. Manure is mechanically scraped and collected for management or treatment. For the large-scale dairies considered in this assessment, a diesel-powered skid steer is used for manure scraping.

Confined Flush: An enclosed housing system with channels or pipes to flush manure with water into a collection or treatment area, often used in barns with slatted floors.

Vacuum: A method of manure collection using vacuum systems to suck up manure from floors, which is particularly useful in barns or confined areas for liquid manure management.

Stationary Screen: A device used to separate solid and liquid components of manure by screening out larger solid particles from the liquid fraction.

Screw Press: A type of mechanical separator that uses a screw mechanism to press out liquid from manure, effectively separating the solid and liquid fractions.

Settling Basin: A containment area where manure-laden water is allowed to stand, letting solid particles settle to the bottom, thereby separating them from the liquid portion.

Solid Storage: The practice of storing raw manure or separated solids in specific facilities to manage odor and facilitate easier fertilizer application.

Ambient Anaerobic Lagoon: A large, open-air pond designed to treat manure through anaerobic digestion at ambient temperature conditions, reducing pathogens and stabilizing organic matter.

Covered Lagoon Digester: An anaerobic lagoon with a flexible or rigid cover that captures biogas produced during digestion, improving energy recovery, and reducing odor and GHG emissions.

Effluent Pond: A storage pond to manage overflow from covered lagoon digesters that may or may not have a cover for biogas collection.

Complete Mix Anaerobic Digester: A controlled, enclosed system where manure is continuously or regularly mixed, promoting uniform anaerobic digestion of organic matter to produce biogas.

Mesophilic Temperature Range: The temperature range, typically between 20°C to 45°C (68°F to 113°F), under which mesophilic microorganisms optimally digest organic matter in an anaerobic environment.

Liquid/Slurry Systems: Systems designed to handle manure in liquid or semi-liquid form, allowing for easier transport and application as fertilizer through irrigation or other methods. Liquid/slurry systems are often shallower than anaerobic lagoons

Digestate: The residual material remaining after the anaerobic digestion of manure, containing stabilized organic matter, nutrients, and is used as a soil amendment or fertilizer.

Manure Broadcasting: A method of manure application where manure is spread over the surface of the field, either in solid or liquid form, without immediate incorporation into the soil.

Manure Injection: A technique where manure is directly injected into the soil at a certain depth, minimizing odor and reducing ammonia volatilization and nutrient runoff.

Irrigation: The application of manure-laden water to crops through irrigation systems, providing both water and nutrients to the soil in an efficient manner.

Renewable Natural Gas (RNG): RNG is upgraded biogas with similar quality to fossil natural gas, used interchangeably for fuel or in natural gas infrastructure.

Combined Heat and Power (CHP): CHP generates electricity and useful heat simultaneously from one energy source, such as biogas, enhancing energy use efficiency.

Biogas Upgrading: This process cleans biogas by removing impurities to increase its methane content, making it suitable for energy use or as vehicle fuel.

APPENDIX C: SUPPORTING INFORMATION FOR CHAPTER 4

Land Coverage and Property Listing for Different Land Types

Table C1: The top four states and respective land type coverage for barren land, forest land, shrub land, and grassland/herbaceous land according to Wentland et al. [143].

Barren Land		
Rank	State	Coverage (1000-acres)
1	California	4,934
2	Utah	4525
3	Nevada	2465
4	Arizona	1962
Forest Land		
Rank	State	Coverage (1000-acres)
1	California	22,097
2	Oregon	22024
3	Montana	19212
4	Colorado	18459
Shrub Land		
Rank	State	Coverage (1000-acres)
1	Texas	95,919
2	New Mexico	62400
3	Nevada	58935
4	Arizona	57839
Grassland/Herbaceous		
Rank	State	Coverage (1000-acres)
1	Texas	82,000
2	Montana	46000
3	South Dakota	23000
4	Kansas	18000

Table C2: Property listings for barren land from Zillow.com [142]

Location	**City**	**Acreage**	**Price**	**$/acre**
California	Essex	10	$19,900	$1,990
	Vidal	80	$45,000	$563
	Amboy	20	$20,000	$1,000
	Needles	10	$7,000	$700
	Brawley	160	$240,000	$1,500
Utah	Wendover	160	$65,000	$406
	Wendover	640	$350,000	$547
	Milford	40.88	$30,000	$734
	Milford	120	$49,900	$416
	Beryl	20	$26,500	$1,325
Nevada	Valmy	59.06	$13,000	$220
	Winnemucca	629.36	$87,500	$139

	Winnemucca	57.8	$25,000	$433
	Winnemucca	640	$110,000	$172
	Gerlach	160	$39,000	$244
Arizona	Dateland	85	$49,500	$582
	Dateland	80	$79,900	$999
	Dateland	37.89	$22,500	$594
	Dateland	15	$30,000	$2,000
	Dateland	40.1	$39,500	$985
Maximum				$2,000
Minimum				$139
Average				$777

Table C3: Property listings for forest land from Zillow.com [142]

Location	**City**	**Acreage**	**Price**	**$/acre**
California	Salyer	71.2	$165,000	$2,317
	Crescent City	128	$399,000	$3,117
	Callahan	160	$899,995	$5,625
	Burnt Ranch	40	$200,000	$5,000
	Kneeland	45	$250,000	$5,556
Oregon	Brookings	20	$250,000	$12,500
	Riddle	1247.57	$12,495,000	$10,015
	Ashland	30.83	$199,000	$6,455
	Tiller	160	$340,000	$2,125
	Eagle Point	278.99	$799,000	$2,864
Montana	Eureka	160	$650,000	$4,063
	Marion	640	$2,176,000	$3,400
	Alberton	2549	$4,500,000	$1,765
	Marion	40	$375,000	$9,375
	Libby	35.92	$750,000	$20,880
Colorado	Black Hawk	19.28	$289,000	$14,990
	Dumont	78.35	$479,000	$6,114
	Black Hawk	3.82	$58,900	$15,419
	Idaho Springs	69.44	$630,000	$9,073
	Evergreen	643	$9,000,000	$13,997
Maximum				$20,880
Minimum				$1,765
Average				$7,732

Table C4: Property listings for shrub land from Zillow.com [142]

Location	City	Acreage	Price	$/acre
Texas	Van Horn	19.23	$50,000	$2,600
	Van Horn	330	$525,000	$1,591
	Van Horn	10.5	$28,000	$2,667
	Fort Stockton	40	$248,000	$6,200
	Terlingua	195	$235,000	$1,205
New Mexico	Roswell	120	$60,000	$500
	Roswell	318	$777,777	$2,446
	Hagerman	40	$62,500	$1,563
	Tinnie	27	$250,000	$9,259
	Santa Rosa	166.02	$125,000	$753
Nevada	Alamo	847	$1,500,000	$1,771
	Pioche	160	$395,000	$2,469
	Bunkerville	80	$550,000	$6,875
	Overton	80	$105,000	$1,313
	Moapa	20	$200,000	$10,000
Arizona	Elfrida	2.51	$4,500	$1,793
	Elfrida	20	$31,950	$1,598
	Douglas	38.64	$55,900	$1,447
	Douglas	1.94	$3,995	$2,059
	Douglas	5.11	$35,000	$6,849
Maximum				$10,000
Minimum				$500
Average				$3,248

Table C5: Property listings for grassland/herbaceous land from Zillow.com [142]

Location	City	Acreage	Price	$/acre
Texas	Hereford	27.14	$198,000	$7,296
	Miami	12	$90,000	$7,500
	Miami	93	$465,000	$5,000
	McLean	649.19	$945,000	$1,456
	Panhandle	10.34	$39,900	$3,859
Montana	Miles City	40	$79,000	$1,975
	Miles City	117.37	$167,000	$1,423
	Ekalaka	7.84	$54,500	$6,952
	Baker	57.94	$180,000	$3,107
	Mile City	117	$167,000	$1,427
South Dakota	Fort Pierre	3.83	$38,500	$10,052
	Pierre	41.47	$290,000	$6,993
	Fort Pierre	5.95	$80,000	$13,445
	Scenic	44.14	$140,000	$3,172
	Hermosa	480	$1,368,000	$2,850
Kansas	Oberlin	158.53	$384,000	$2,422
	Gove	153	$229,500	$1,500
	Bogue	158.27	$227,000	$1,434
	Alexander	160	$242,500	$1,516
	Ludell	418	$501,600	$1,200
Maximum				$13,445
Minimum				$1,200
Average				$4,229

Criteria Rankings from the Expert Survey

Table C6:Sustainability criteria rankings and confidence levels from the expert survey

Expert	**Jason Quinn**	**Ryan Davis**	**Braden Limb**	**David Quiroz**	**Jack Smith**	**Peter Chen**	**Bruno Klein**	**Peter Valdez**	**Jonah Greene**	**Average**	**Final Rank**
Affiliation	**CSU**	**NREL**	**CSU**	**CSU**	**CSU**	**CSU**	**NREL**	**PNNL**	**CSU**		
Cost (Minimum Fuel Selling Price)	1	1	1	2	2	3	2	1	2	1.70	2
High Value Land Use	4	6	3	4	4	4	4	4	3	4.00	4
Water Footprint	3	4	4	3	3	2	3	3	4	3.20	3
Acidification	10	12	12	7	7	12	7	6	8	9.00	10
Carcinogenics	9	7	8	8	9	8	10	9	12	8.90	9
Ecotoxicity	11	5	9	10	6	11	6	10	7	8.30	8
Eutrophication	5	10	6	6	5	10	8	7	6	7.00	5
Fossil Fuel Depletion	7	3	5	12	13	13	5	5	5	7.60	6
Global Warming Potential	2	2	2	1	1	1	1	2	1	1.40	1
Non-Carcinogenics	13	8	13	11	10	9	13	12	13	11.30	13
Ozone Depletion	8	11	11	9	11	6	9	13	9	9.70	11
Photochemical Smog Formation	12	13	10	7	12	5	11	11	10	10.10	12
Respiratory Effects (PM 2.5)	6	9	7	5	8	7	12	8	11	8.10	7
Confidence Level	High	Medium	Medium	High	Medium	Medium	Medium	Medium	Medium		

Criteria Rankings for Pre-Made Sustainability Themes

Table C7:Sustainability criteria rankings for the pre-made sustainability themes. The color indicates the level of influence used for calculating weighting factors under the geometric mean method (green: direct influence, yellow: indirect influence, light orange: peripheral influence, dark orange: marginal influence).

Rank:	Human Health	Terrestrial Biodiversity	Aquatic Biodiversity	Economic Viability	Food and Water Supply	Energy Supply	Global Impacts
1	Carcinogenics	Ecotoxicity	Acidification	Cost	High Value Land Use	Fossil Fuel Depletion	Global Warming Potential
2	Non-Carcinogenics	Global Warming Potential	Eutrophication	High Value Land Use	Water Footprint	Global Warming Potential	Ozone Depletion
3	Respiratory Effects	Eutrophication	Global Warming Potential	Water Footprint	Global Warming Potential	Water Footprint	Acidification
4	Smog Formation	Acidification	Ecotoxicity	Fossil Fuel Depletion	Eutrophication	High Value Land Use	Ecotoxicity
5	Ozone Depletion	Ozone Depletion	Water Footprint	Global Warming Potential	Acidification	Eutrophication	Respiratory Effects
6	Global Warming Potential	Water Footprint	Ozone Depletion	Eutrophication	Ecotoxicity	Acidification	Carcinogenics
7	Water Footprint	Smog Formation	Smog Formation	Acidification	Ozone Depletion	Ecotoxicity	Non-Carcinogenics
8	High Value Land Use	Respiratory Effects	Respiratory Effects	Ecotoxicity	Smog Formation	Ozone Depletion	Smog Formation
9	Acidification	Carcinogenics	Carcinogenics	Ozone Depletion	Respiratory Effects	Smog Formation	Water Footprint
10	Eutrophication	Non-Carcinogenics	Non-Carcinogenics	Smog Formation	Carcinogenics	Respiratory Effects	Eutrophication
11	Ecotoxicity	High Value Land Use	High Value Land Use	Respiratory Effects	Non-Carcinogenics	Carcinogenics	Fossil Fuel Depletion
12	Fossil Fuel Depletion	Fossil Fuel Depletion	Fossil Fuel Depletion	Carcinogenics	Fossil Fuel Depletion	Non-Carcinogenics	High Value Land Use
13	Cost	Cost	Cost	Non-Carcinogenics	Cost	Cost	Cost

Discussion on Mid-Point vs. End-Point Metrics

The distinction between midpoint and endpoint metrics in LCA plays a significant role in evaluating environmental impacts, with tools like the TRACI relying heavily on midpoint indicators [45]. Understanding the trade-offs between these approaches is crucial for addressing uncertainty, scientific consensus, and the representation of environmental effects.

Midpoint metrics quantify impacts at an intermediate stage in the cause-effect chain, focusing on measurable processes like global warming potential (GWP), eutrophication, and acidification. These metrics are based on well-established scientific models and provide a reliable way to track direct environmental stressors [45]. The relationships between emissions and midpoint impacts, such as CO_2 and GWP, are well-supported by data and widely accepted within the scientific community [45]. This makes midpoint metrics a critical part of LCA because they involve less uncertainty than endpoint metrics, which aim to assess the ultimate damage caused by those emissions.

One of the key reasons TRACI focuses on midpoint metrics is to reduce the subjectivity that often accompanies endpoint metrics. Endpoints attempt to quantify final outcomes, like species loss or human health impacts, which require extensive modeling and assumptions. Moving from a stressor like nitrogen runoff to an endpoint like ecosystem collapse introduces more uncertainty, as multiple factors—including geographic and temporal variability—affect the outcome. These complex modeling processes introduce significant challenges, making endpoint metrics less reliable for objective assessments [45].

In TRACI, using midpoint metrics enables more transparent, reproducible assessments, which are essential for regulatory purposes. For example, indicators such as acidification potential, based on sulfur dioxide (SO_2) and nitrogen oxides (NOx) emissions, provide actionable

insights without attempting to predict longer-term damage to ecosystems. This focus on scientifically grounded, measurable impacts avoids the need for subjective decisions about which environmental damages should be prioritized. Midpoints allow decision-makers to focus on mitigating specific environmental stressors without becoming entangled in the uncertainties that come with endpoint models [45].

Another challenge with endpoint metrics is the requirement to make value-based decisions about how to weigh different types of damage. Value-based decisions introduce personal bias into the assessment, as stakeholders may have different values and priorities [45,138]. In contrast, midpoint metrics sidestep many of these subjective decisions, focusing on quantifiable indicators like emissions and chemical concentrations that are more universally agreed upon.

Transitioning from midpoint to endpoint metrics is difficult not only because of the added complexity but also because of the inherent uncertainty in linking short-term environmental stressors to long-term outcomes [138]. While increased smog can be linked directly to NOx emissions, predicting how this smog will ultimately affect human health, agriculture, or ecosystems involves significant assumptions and uncertainties. Determining the relative importance of different types of environmental harm—such as human health versus ecological damage—can also lead to inconsistent results, as different stakeholders might prioritize these impacts differently.

The importance of using midpoint metrics in TRACI lies in their ability to provide clear, objective insights into environmental impacts while avoiding the pitfalls of personal bias and subjective decision-making. Focusing on midpoints ensures that the evaluation remains rooted in scientific consensus and quantifiable data, making it suitable for policy development and

regulatory assessments. However, it is also essential to recognize that focusing solely on midpoint metrics can oversimplify the broader environmental consequences of a given action, as they do not capture the full extent of potential harm to ecosystems or human health [138].

The discussion of midpoint versus endpoint metrics reveals the complexity inherent in assessing environmental impacts, particularly when balancing scientific rigor with practical decision-making. Midpoint metrics, as used in TRACI, are favored for their lower uncertainty, higher scientific consensus, and greater focus on measurable environmental stressors like GWP and acidification. These metrics avoid the subjective value judgments required for endpoint metrics, which attempt to predict long-term outcomes like ecosystem damage or human health impacts. The significant challenges of moving from midpoint to endpoint metrics—such as increased uncertainty, the introduction of personal bias, and the difficulty of quantifying final damage—highlight why midpoint metrics remain a cornerstone in LCA, especially in tools designed for decision support.

This preference for midpoint metrics is evident in the design of the ECO-STEPS tool, which leverages the objectivity and reliability of midpoint data to inform decision-making about engineered climate solutions. By focusing on midpoint indicators from TEA and LCA, such as those generated by TRACI, ECO-STEPS avoids the pitfalls associated with endpoint assessments, where uncertainty compounds and subjective value judgments influence the results. The tool uses midpoint metrics to compare sustainability across competing technologies, such as algae-based renewable diesel, soybean biodiesel, and corn ethanol, allowing stakeholders to evaluate environmental and economic trade-offs with greater confidence and transparency.

In summary, ECO-STEPS relies on midpoint metrics not only for their robustness and lower uncertainty but also because they facilitate more inclusive and transparent decision-

making. By avoiding the complexity and biases of endpoint metrics, ECO-STEPS enables stakeholders to balance environmental, economic, and resource considerations while navigating the trade-offs inherent in pursuing sustainable climate solutions. This approach ensures that the decision-making process is grounded in reliable data, making it a valuable tool for advancing long-term sustainability goals.